

N7625157



NASA CR-144963

# TECHNICAL AND ECONOMIC ASSESSMENT OF SPAN-DISTRIBUTED LOADING CARGO AIRCRAFT CONCEPTS

Final Report

June 1976

(NASA-CR-144963) TECHNICAL AND ECONOMIC ASSESSMENT OF SPAN-DISTRIBUTED LOADING CARGO AIRCRAFT CONCEPTS FINAL REPORT (BOEING COMMERCIAL AIRPLANE CO., SEATTLE) 218 P HC \$7.75

N76-25157

UNCLAS 42200

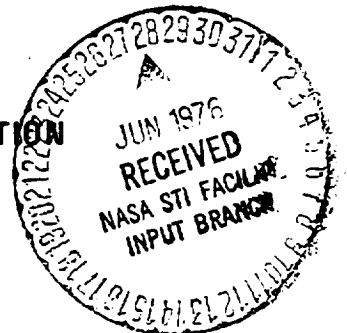
CSCD 010 63/05

Prepared under contract NAS1-13963 by Preliminary Design Department

Boeing Commercial Airplane Company  
P.O. Box 3707  
Seattle, Washington 98124

REPRODUCED BY: **NTIS**  
U.S. Department of Commerce  
National Technical Information Service  
Springfield, Virginia 22161

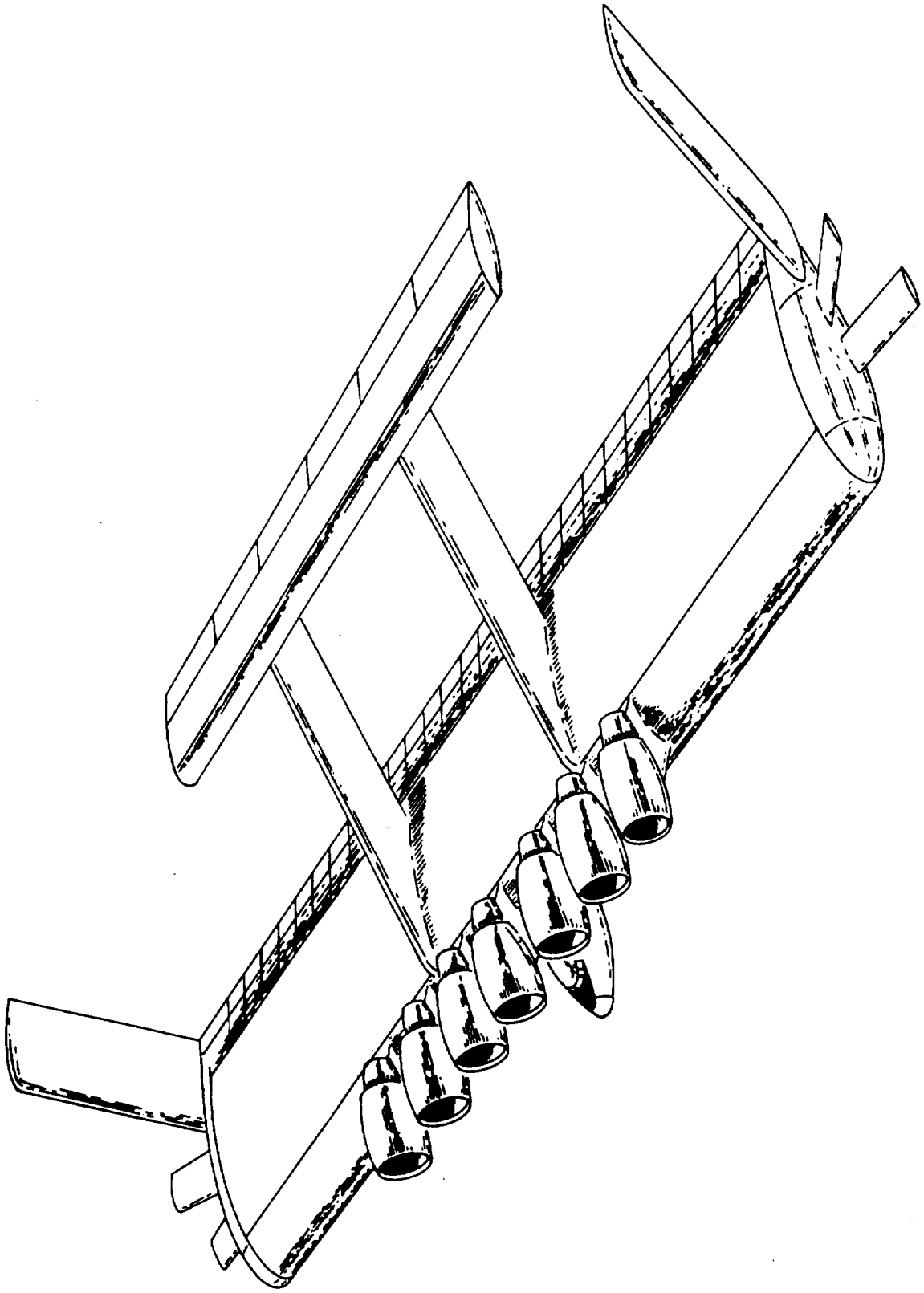
Langley Research Center  
NATIONAL AERONAUTICS AND SPACE ADMINISTRATION  
Hampton, Virginia 23665

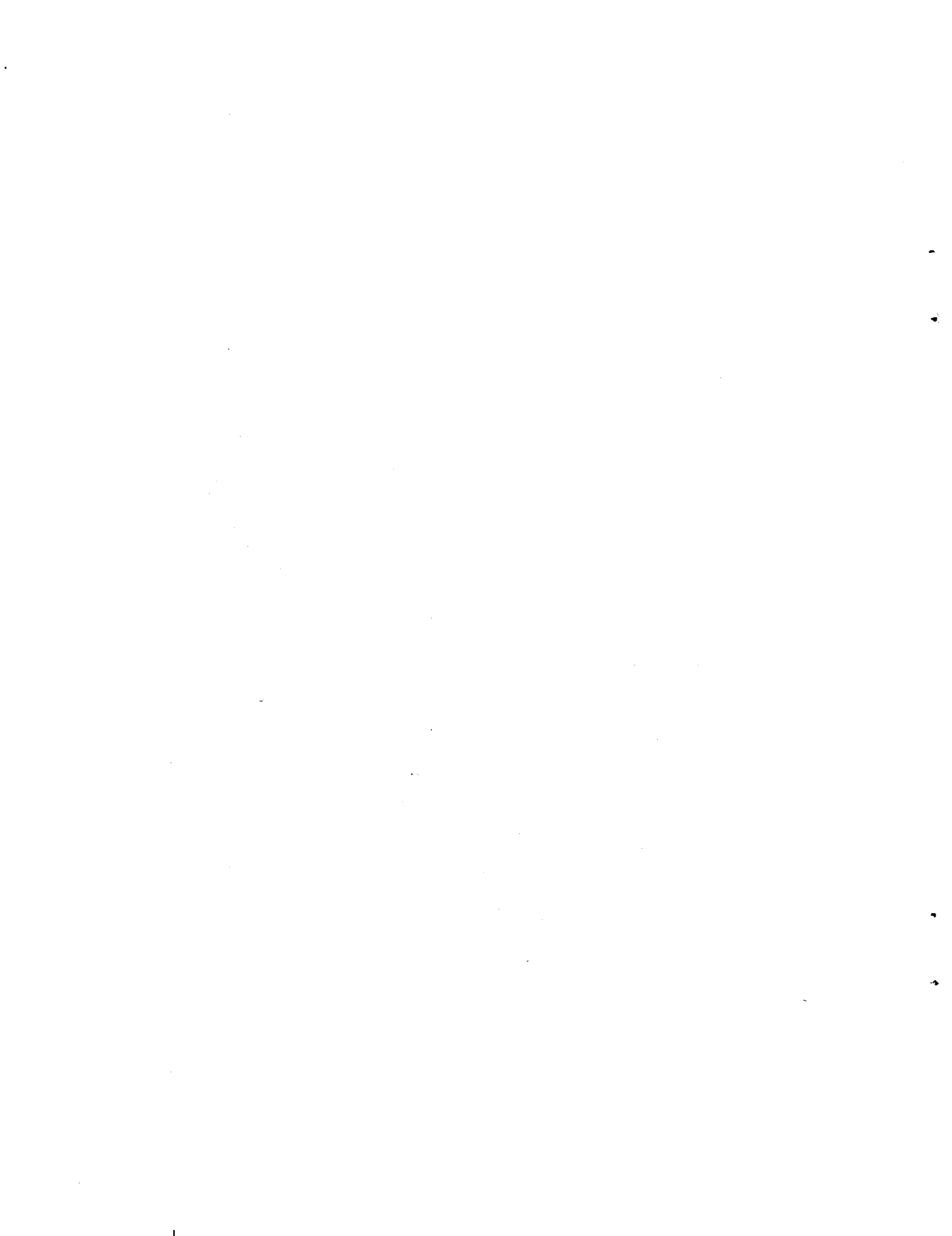




1. Report No. <b>NASA CR-144963</b>	2. Government Accession No.	3. Recipient's Catalog No.	
4. Title and Subtitle <b>TECHNICAL AND ECONOMIC ASSESSMENT OF SPAN-DISTRIBUTED LOADING CARGO AIRCRAFT CONCEPTS</b>		5. Report Date <b>June 1976</b>	6. Performing Organization Code
		8. Performing Organization Report No. <b>D6-75776</b>	10. Work Unit No.
7. Author(s) <b>David H. Whitlow and P.C. Whitener Preliminary Design Department</b>		11. Contract or Grant No. <b>NAS1-13963</b>	13. Type of Report and Period Covered <b>Contractor Report</b>
9. Performing Organization Name and Address <b>Boeing Commercial Airplane Company P.O. Box 3707 Seattle, Washington 98124</b>		14. Sponsoring Agency Code	
		12. Sponsoring Agency Name and Address <b>National Aeronautics and Space Administration Langley Research Center Hampton, Virginia 23665</b>	
15. Supplementary Notes <b>Technical Monitor, Allen H. Whitehead, Jr. ASD NASA Langley Research Center Hampton, Virginia 23665</b>			
16. Abstract <p>A preliminary design study of the performance and economics resulting from the application of the distributed load concept to large freighter aircraft was made. The study was limited to configurations having the payload entirely contained in unswept wings of constant chord with conventional tail surfaces supported from the wing by twin booms. A parametric study based on current technology (1980 production) showed that increases in chord (with accompanying decreases in thickness ratio) had a similar effect on the economics as increases in span (and hence aspect ratio). Increases in both span and chord or airplane size had the largest and most favorable effect.</p> <p>At 600,000 lbs payload a configuration was selected and refined to incorporate advanced technology that could be in production by 1990 and compared with a reference conventional airplane having similar technology. Although the distributed load airplane was only slightly superior in economics at this size, the effects of size and preliminary assessment of promising technical options (such as sweepback) and further cost saving concepts (simplified production techniques) indicates that further study is warranted.</p>			
17. Key Words (Suggested by Author(s))		18. Distribution Statement	
19. Security Classif. (of this report) <b>Unclassified</b>	20. Security Classif. (of this page) <b>Unclassified</b>	21. No. of Pages <b>217</b>	22. Price*







# CONTENTS

	<u>Page</u>
SUMMARY . . . . .	1
INTRODUCTION . . . . .	7
ABBREVIATIONS AND SYMBOLS . . . . .	9
GUIDELINES . . . . .	15
Mission Constraints . . . . .	15
Throughput Capacity . . . . .	15
Mission Range . . . . .	15
Payload . . . . .	15
Speed . . . . .	15
Configuration Constraints . . . . .	15
Design Approaches . . . . .	15
Propulsion System . . . . .	15
Terminal Area Operation . . . . .	16
Configuration Matrix . . . . .	16
Technology Status . . . . .	16
Pressurization . . . . .	16
Economics . . . . .	16
Reference Configuration . . . . .	16
CONTRACTOR TASKS . . . . .	17
Introduction . . . . .	17
Parametric Study . . . . .	17
Parametric Study Approach . . . . .	17
Configuration Constraints . . . . .	18
Baseline Airplane Definition . . . . .	19
Parametric Study Geometry Trades . . . . .	19
Configuration Matrix . . . . .	19
Parametric Study Results . . . . .	20
Airplane Characteristics . . . . .	20
Performance Comparisons . . . . .	20
Economic Comparisons . . . . .	21
Parametric Sensitivity Studies . . . . .	22
Design Payload . . . . .	22
Design Payload Density . . . . .	23
Effect of Throughput . . . . .	24
Design Range Sensitivity . . . . .	24
Fuel Economy . . . . .	25
Selected Configuration Study . . . . .	25
Selected Configuration Definition . . . . .	26
Selection Rationale . . . . .	26.

## CONTENTS (Concluded)

	<u>Page</u>
Consideration of Intangibles . . . . .	27
Selected Configuration . . . . .	28
Principal Design Features . . . . .	29
Technology Definition and Analysis . . . . .	29
Aerodynamic Design . . . . .	29
Propulsion and Noise . . . . .	33
Loads Analysis . . . . .	35
Structural Design . . . . .	36
Weight and Balance . . . . .	37
Pressurization Effects on Design . . . . .	40
Performance Characteristics . . . . .	40
Reference Configuration Study . . . . .	41
Reference Configuration Definition . . . . .	41
Reference Configuration Technology Definition and Analysis . . . . .	41
Concept Comparison . . . . .	42
Technical Comparison . . . . .	42
Aerodynamic Performance . . . . .	42
Structural and Payload Efficiencies . . . . .	43
Takeoff and Landing Performance . . . . .	43
Fuel Consumption . . . . .	43
Economic Comparison . . . . .	43
Sensitivities . . . . .	44
Effect of Airplane Size . . . . .	45
Other Effects . . . . .	46
Areas for Further Refinement and Study . . . . .	46
Revised Straight Wing Airplane Configuration Restricted to 8- by 8-ft Container Size . . . . .	46
Prop-Fan Propulsion Installation . . . . .	46
Wing Weight Reduction . . . . .	46
The Use of Composites . . . . .	47
Optimum Sized Airplanes . . . . .	47
Thick Airfoil Technology . . . . .	47
Laminar Flow Control . . . . .	47
Overwing Engine Installation . . . . .	48
Control and Guidance Research . . . . .	48
 CONCLUSIONS . . . . .	 49
 APPENDIX A -- Parametric Data Base . . . . .	 175
 APPENDIX B -- Pricing and Costing Methodology . . . . .	 206
 APPENDIX C -- Economic Analysis Methods . . . . .	 214
 REFERENCES . . . . .	 217



## FIGURES

<u>No.</u>		<u>Page</u>
1	Wing Section Utilization . . . . .	51
2	Parametric Study Payloads . . . . .	52
3	Economic Comparison, Selected Versus Reference Configuration . . . . .	53
4	Cost Breakdown Comparison, Selected Versus Reference Configurations . . . . .	54
5	Distributed Load and Conventional Freighter Comparative Economics . . . . .	55
6	Effect of Airplane Size on Economics . . . . .	56
7	Wing Weight Distribution (Structure Plus Integral Items) . . . . .	57
8	General Arrangement, Parametric Baseline Airplane 759-163A . . . . .	58
9	Tail Boom Installation . . . . .	59
10	Leading Edge Structure . . . . .	60
11	Wing Section Utilization . . . . .	61
12	Geometry Constraints . . . . .	62
13	Parametric Study—Configuration Geometry . . . . .	63
14	Parametric Study Payloads . . . . .	64
15	Wing Loading Results . . . . .	65
16	Aerodynamic Efficiency . . . . .	66
17	Empty Weight Fraction . . . . .	67
18	Payload Weight Fraction . . . . .	68
19	Productivity/Gross Weight . . . . .	69
20	Fleet Size Versus Payload . . . . .	70
21	Effect of Payload on Economics—89.9 m (295 ft) Span Parametric Configuration . . . . .	71
22	Effect of Payload on Economics—121.9 m (400 ft) Span Parametric Configuration . . . . .	72
23	Effect of Payload and Payload Density on Economics—152.4 m (500 ft) Span Parametric Configurations . . . . .	73
24	Effect of Payload Density on Economics—89.9 m (295 ft) Span Parametric Configurations . . . . .	74
25	Effect of Payload Density on Economics—121.9 m (400 ft) Span Parametric Configurations . . . . .	75
26	Effect of Airplane Size on Economics . . . . .	76
27	Effect of Airplane Size and Geometry on Economics—Constant Design Net Containerized Density = $80.1 \text{ kg/m}^2$ ( $5 \text{ lb/ft}^2$ ) . . . . .	77
28	Effect of Airplane Size and Geometry on Economics—Constant Design Net Containerized Density = $120.1 \text{ kg/m}^3$ ( $7.5 \text{ lb/ft}^3$ ) . . . . .	78
29	Effect of Airplane Size and Geometry on Economics—Constant Design Net Containerized Density = $160.185 \text{ kg/m}^3$ ( $10 \text{ lb/ft}^3$ ) . . . . .	79
30	Effect of Airplane Size and Geometry on Economics—Constant Design Net Containerized Density = $200.2 \text{ kg/m}^3$ ( $12.5 \text{ lb/ft}^3$ ) . . . . .	80
31	Design NCD Versus DOC Plus AIC . . . . .	81
32	Effect of Throughput . . . . .	82
33	Design Range Sensitivity—3 Bays . . . . .	83
34	Design Range Sensitivity—4 Bays . . . . .	84
35	Block Fuel Versus Gross Payload . . . . .	85

## FIGURES (Continued)

<u>No.</u>	<u>Page</u>
36	87
37	89
38	91
39	93
40	97
41	101
42	103
43	105
44	107
45	109
46	111
47	112
48	113
49	114
50	115
51	116
52	117
53	118
54	119
55	120
56	121
57	122
58	123
59	124
60	125
61	126
62	127
63	128
64	129
65	130
66	131
67	132
68	133
69	134
70	135
71	136
72	137
73	138
74	139
75	140
76	141

## FIGURES (Concluded)

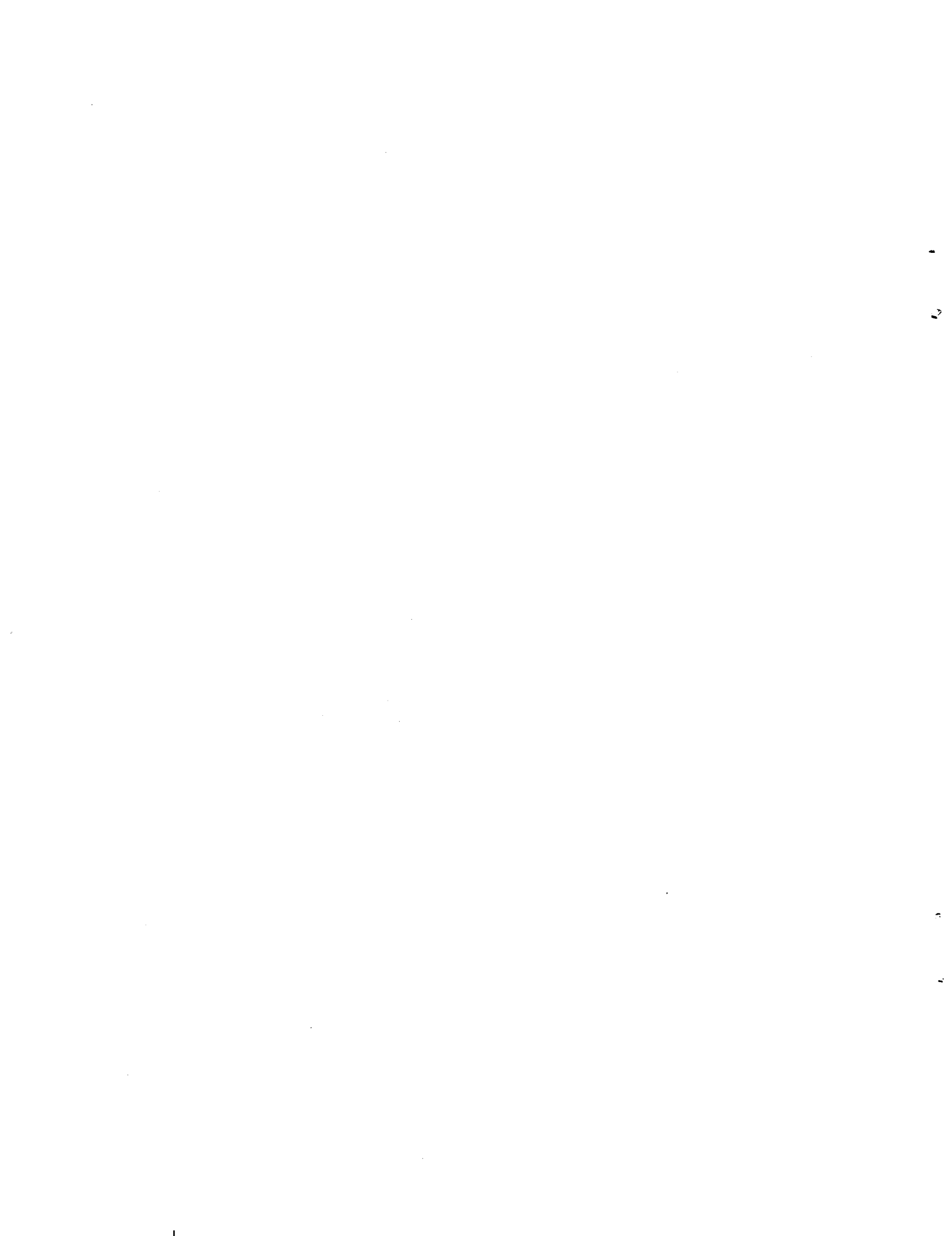
<u>No.</u>		<u>Page</u>
77	Reference Configuration Loading Diagram . . . . .	143
78	Drag Polar, Reference Configuration . . . . .	144
79	Reference Configuration Performance . . . . .	145
80	Weight Distribution Comparisons . . . . .	146
81	Economic Comparison, Selected Versus Reference Configuration . . . . .	147
82	Cost Breakdown Comparison, Selected Versus Reference Configurations . . . . .	148
83	Economic Sensitivity Comparisons, Selected Versus Reference Configurations . . . . .	149
84	Distributed Load and Conventional Freighter Comparative Economics . . . . .	150
85	Effect of Airplane Size on Economics . . . . .	151
86	Aerodynamic Thumbprint Program Flow Chart . . . . .	186
87	Airplane Matching Technique . . . . .	187
88	Cruise Drag Characteristics . . . . .	188
89	Form Drag Characteristics . . . . .	189
90	Drag Divergence Mach Number Versus Thickness Ratio . . . . .	190
91	Drag Creep Characteristics . . . . .	191
92	Untrimmed Cruise Polars—Model 759-165A . . . . .	192
93	Cruise Trim Drag Versus c.g. Location $C_L$ —Model 759-165A . . . . .	193
94	Cruise Polar Shape and Compressibility Drag, Model 759-165A . . . . .	194
95	Climbout L/D Versus $C_L$ , Model 759-165A . . . . .	195
96	Approach L/D Versus $C_L$ , Model 759-165A . . . . .	196
97	Geometric Relationships . . . . .	197
98	Weight Scalars, Model 759-163A, Propulsion Items . . . . .	198
99	Weight Scalars, Model 759-163A . . . . .	199
100	Relative Structure Part Card Release Versus Structure Weight . . . . .	210
101	Span-Distributed Loading Cargo Aircraft Study—Cost Savings Attributed to Part Commonality . . . . .	211
102	Sample Program Schedule . . . . .	212



## TABLES

<u>No.</u>		<u>Page</u>
1	Distributed Load Freighter Comparison With Reference Configuration . . . . .	152
2	Geometric and Aerodynamic Characteristics . . . . .	153
3	Payload Characteristics--Parametric Study Airplanes . . . . .	155
4	Economic Characteristics--Parametric Study Airplanes . . . . .	157
5	DLF Selected Configuration--1990 Aerodynamic Technology Development . . . . .	159
6	Parasite Drag Summary . . . . .	160
7	1990 Engine Technology Gains . . . . .	161
8	Selected Configuration Weight Statement . . . . .	163
9	1990 Technology Items Utilized . . . . .	165
10	Selected Configuration, Minimum Structural Requirements . . . . .	166
11	Pressurization Impact, Selected Configuration . . . . .	166
12	Performance Summary, Selected Configuration . . . . .	167
13	Reference Configuration Weight Statement . . . . .	169
14	1990 Technology Items Utilized . . . . .	171
15	1990 Advanced Aerodynamic Technology . . . . .	172
16	Distributed Load Freighter Comparison With Reference Configuration . . . . .	173
17	Parasite Drag Summary--Model 759-165A . . . . .	200
18	Weight Estimating Techniques . . . . .	201
19	Parametric Group Weight Statements . . . . .	203
20	Model 759-163A, Potential Configurations . . . . .	205
21	Distributed Load Freighter Price Analysis . . . . .	213
22	Direct Operating Cost Formulas for Dedicated International Airfreighters . . . . .	214

**PRECEDING PAGE BLANK NOT FILMED**



## SUMMARY

This document presents the analyses and results of a study of the span-distributed load design concept as applied to large freighter aircraft. The study is limited to unswept wings of constant chord with tail surfaces supported by twin booms extending aft from the wing rear spar. The choice of the unswept configuration is the result of the contractor having a more extensive data base on this type rather than any preference for this configuration over swept tailless designs, which are also being studied concurrently by the contractor.

A parametric study of a range of distributed load configurations of this general type was made to determine the best choice of size and geometry for optimum economics versus payload weight. The wing cross sections shown on figure 1 were chosen to provide a logical relationship between the interior cargo arrangement and the exterior airfoil contours. As thickness-to-chord ratio is decreased the wing chord is increased, to maintain a bay height suitable for a 2.4-meter-square (8-ft-square) cross section containers in all bays and a 3.25-m (128-in.) height in the center bays (sufficient for an M-60 tank in military versions). Each of these four cross sections was then combined at two different wing spans (89.9 m (295 ft) and 121.92 m (400 ft)) plus a single three-bay configuration with 192.4-m (500-ft) span to furnish a matrix of parametric study configurations. At each combination of chord and span the gross weight and number of engines were varied thus producing the payload and payload density variations shown in figure 2.

It was found that increasing design payload and, hence, airplane size had both the greatest and the most favorable effect on the economics.

Increasing either the span or the chord to increase the payload produced approximately the same effect. At constant payload the savings in fuel costs of a long-span, short-chord airplane (i.e., one with high aspect ratio) were balanced by the effects of the increase in speed or productivity of a shorter span, longer chord (and lower thickness-to-chord ratio) airplane. Although the economics did not appear to be very sensitive to configuration effects, the optimum configurations occurred at a nearly constant aspect ratio of about 4 to 5. As the airplane size and payload increased, the thickness-to-chord ratio for best economics decreased, since the physical thickness of the wing was constrained by the interior height of the cargo bay and the chord was increased with increases in the number of cargo bays.

Parametric sensitivity studies showed that little economics penalty would be paid by designing to somewhat lower payload densities than the specified  $160.18 \text{ kg/m}^3$  ( $10 \text{ lb/ft}^3$ ) to hedge against possible errors in the payload density predictions. The choice of optimum design was also little influenced by overall system productivity. Design range studies showed

that it was more economical to design for somewhat shorter ranges than the longest expected routes (offload payload for the longest ranges). Fuel economy trades showed that distributed-load airplanes sized for a net payload of 272 155 kg (600 000 lb) are similar to the 747-200. At much larger sizes, they are considerably better than the 747-200.

Following the parametric study, a configuration with the best economics was selected for a net payload of 272 155 kg (600 000 lb) at  $160.18 \text{ kg/m}^3$  ( $10 \text{ lb/ft}^3$ ) net payload density as specified by the statement of work. This was a four-bay airplane with a wing span of 83.8 m (275 ft) and 21.5% thickness-to-chord ratio. The selected airplane was refined to incorporate improvements discovered after the parametric study was initiated. Since the parametric study was done using present-day technology (1980 production), the selected airplane was also revised to incorporate the improvements associated with 1990 technology. Some of the improvements in technology that are being included in the design of the selected configuration are improved airfoil characteristics, improved aluminum and titanium alloys, composite control surfaces, carbon brakes, and more advanced powerplants with lower specific fuel consumption. A full-time load alleviation system has also been assumed. A conventional configuration was also designed around 1990 technology to use as a reference airplane to compare with the selected distributed load configuration.

On table 1 is tabulated a comparison of the characteristics of the selected and reference configurations. The 757 500-kg (1 670 000-lb) distributed-load airplane delivers the same payload per pound of takeoff gross weight (PL/TOGW = 0.417) as the 467 200-kg (1 030 000-lb) conventional airplane. The saving in structural weight of the distributed load design (OEW-GW = 0.3195 compared with 0.3848) is just balanced by the increased fuel weight. The distributed-load airplane is considerably less expensive to produce for its size, costing \$304/kg (\$137.90/lb) of empty weight compared with \$355/kg (\$161.20/lb) for the conventional airplane.

These differences show up in the economic comparisons on figure 3. The more costly but fuel-efficient advanced conventional design has slightly lower direct operating costs (DOC) out to the design point range 5556 km (3000 nmi) and more significant improvement at longer ranges. However when ownership costs to the operator are more fully considered by adding a 12% annual airplane investment cost,\* the distributed-load airplane is better than the conventional airplane out to 8519 km (4600 nmi) range. Figure 4 shows the breakdown in costs of the two and helps explain the reason for these differences. In computing DOC the lower cost of the distributed-load airplane is reflected in the lower depreciation which does not quite compensate for the higher fuel costs. When airplane investment is added, the lower cost of the distributed load freighter (DLF) more than makes up for the fuel cost in the total DOC plus airplane investment cost.

Aircraft size is an important consideration in comparing distributed-load with conventional designs, as can be seen in figure 5. Although the economics of the conventional design are not expected to improve with size over this reference airplane, the parametric study showed that distributed-load airplanes improve considerably with size. The 272 155-kg (600 000-lb) net

---

\*Airplane Investment Cost is allocated per ton mile by taking 12% of the airplane price and dividing it by the airplane yearly productivity in ton miles at 65% load factor.



payload or 322 050-kg (701 000-lb) gross payload used in this study for the selected configuration results in a selected design that is too small to fully exploit the distributed load advantages. On figure 6 are shown cost component breakdowns of two particular airplanes from the parametric study (at constant-design net containerized density) at two payload levels. The strong effect of size on the economics and the reasons for it can be seen by comparing these two airplanes. The first airplane was 89.9-m (295-ft) span, four-bay design carrying 322 050-kg (701 000-lb) gross payload and the second is a 121.92-m (400-ft) span, five-bay airplane carrying 544 311 kg (1 200 000 lb) of gross payload. The most significant saving is in fuel cost due to the higher aerodynamic efficiency of the larger design. The higher aspect ratio (5.04 compared with 4.34) and the thinner wing ( $t/c = 0.19$  compared with 0.215) and the hence higher speed reduce the fuel cost to the level of advanced conventional designs while still retaining the lower investment costs characteristic of the DLF.

Significant economic gains are possible using distributed load airfreighters of very large sizes. At the study baseline net payload design level of 272 155 kg (600 000 lb), the selected DLF design exhibits only about a 5% saving in total costs\* per ton-mile over the reference advanced conventional design. However, the parametric study, where airplane size was varied, indicated that a distributed-load airplane carrying 453 592 kg (1 000 000 lb) net payload would result in a total cost amounting to 75% to 80% that of the reference conventional design. The distributed-load carrying this payload would have a takeoff gross weight of over 1 134 000 kg (2 500 000 lb), and a wing span of 121.92 m (400 ft).

The contractor is studying the application of these very large airplanes. Although the marketing studies are in the very preliminary stage and much more extensive work needs to be done, certain early conclusions can be cited. Ultimately, these huge aircraft would be used almost entirely in intercontinental airfreight and the most likely system configuration would be to connect a small number of worldwide hub cities. Practical networks, each connecting as few as 10 cities, appear feasible. In this hub-and-spoke concept, the cargo would be delivered from the origin to the hub city by supplementary transportation, either by surface vehicles or short-range airfreight. With this type of system the cost of widening the runways for these giant aircraft will be restricted to the hub cities. Providing two widened runways at each of ten hubs adds only 0.5% of the total cost,\* a negligible impact on total system economics.

These early studies indicate that the distributed-load concept is promising and will improve as the technology and marketing data are further refined. The effort to reduce structural weight in the wing (fig. 7) has been successful, with bending material, shear material, and ribs contributing only 25.8% of the wing weight. The other wing components are now prime candidates for study of further refinement in their design. The group of items relating to airplane control at the present time weigh 27.6% of the wing weight, actually more than the basic structure of the wing. Detail design in this area could provide some very important weight reductions.

The successful application of distributed-load concepts will require careful scrutiny of every item in the weight statement if maximum benefits are to be realized.

---

\*DOC plus Airplane Investment Cost

In addition to weight savings in the detailed design, there are many technical and marketing study areas that should be and are being pursued. Internal contractor studies of tailless, swept-wing designs indicate that they will be superior to the straight-wing designs covered in this study. They will cruise at higher Mach number and thus increase productivity, and they have better L/D ratio, which will also save fuel. When sweepback is applied to designs much larger than the configuration selected for this study, the compounding of favorable size and sweepback effects will produce a step gain in economics.

In CONTRACTOR TASKS, AREAS FOR FURTHER REFINEMENT AND STUDY, a number of study possibilities is presented; all of these offer potential improvements in the performance and economics of distributed-load aircraft. Revising the wing cross sections to contain only containers of 2.44 x 2.44 meters (8 x 8 ft) instead of also carrying an M-60 tank in the center bay, could benefit commercial economics. Prop-fan technology seems particularly attractive and applicable in the speed regime of the DLF. More extensive use of composites should be studied. Study and development of thick airfoils and laminar flow technology will improve aerodynamics and thus contribute gains. The nacelle-wing integration problem of overwing engines needs to be further explored. Control and guidance research of the unique control problems, such as touchdown and dispersion, needs to be advanced. The need for all of these studies is further confirmation that the DLF studies are in their early stages and preliminary assessment of the effect of these study areas indicates that the DLF concept will improve with development.

### STUDY CONCLUSIONS

1. DLF economics continually improves with size while conventional airplane peaks at about 450 000 kg (1 million lb) gross weight.
2. DLF has slightly better economics (5% lower DOC + AIC) at the study payload size than the most advanced conventional air freighter (1990 technology) at its optimum size and the DLF improves to 25% better than the optimum conventional when the DLF size is doubled.
  - At approximately 272 000 kg (600 000 lb) net payload the lower production cost of the DLF approximately balances the lower fuel cost of the advanced conventional freighter.
  - At 544 311 kg (1 200 000 lb) net payload the fuel cost of the DLF equals the fuel cost of the advanced conventional freighter.
3. Based on optimum economics, the optimum thickness ratio for the DLF varies with size:

<u>NET PAYLOAD kg (lb)</u>	<u>THICKNESS RATIO</u>	<u>NO. OF CARGO BAYS</u>
272 155 (600 000)	0.24 to 0.215	3 or 4
408 233 (900 000)	0.215 to 0.19	4 or 5
544 311 (1 200 000)	0.19 to 0.16	5 or 6
680 389 (1 500 000)	0.16 to 0.14	7

4. Distributed-load freighter concept has potential for further improvement in:

- Sweep
- Reduced cargo bay height requirement
- Optimum payload size
- Weight reduction



## INTRODUCTION

The study was carried on by the Boeing Commercial Airplane Company under contract to NASA Langley (Contract NAS1-13963). The purpose of the study was to enumerate and quantify the benefits of the span-distributed loading concept as applied to future commercial air cargo operations. The contractor has conducted the necessary engineering analysis and design studies to evaluate the technical feasibility and demonstrate the potential economic advantages of span-distributed loading concepts for air cargo.

The NASA study is an extension of earlier Boeing preliminary design studies. The parametric study uses the data previously generated at Boeing except for the addition of one more design (the 152.4 m (500-ft) span airplane). These data, which assumed present technology levels (production 1980), allow the selection of the most economic combination of wing geometry and aircraft size for any desired weight of payload).

The study recognized the desirability of comparing any resulting selected distributed-load design with an advanced conventional design at the same technology level. Further, the technology of both types should incorporate the best features that can be predicted for commitment to production by 1985 for actual production by 1990. Accordingly, the selected design (CONTRACTOR TASKS, SELECTED CONFIGURATION STUDY) and the reference conventional design (CONTRACTOR TASKS, REFERENCE CONFIGURATION STUDY) were developed for comparison with a common set of technology ground rules.

The data presented in this document include the parametric study, the sensitivity studies, the engineering analyses of the selected and reference configurations, and the economic comparisons of both. The parametric study covered a range of payloads from 180 000 to 800 000 kg (400 000 to 1 800 000 lb) with payload densities from 80 to 240 kg/m<sup>3</sup> (5 to 15 lb/ft<sup>3</sup>) and airplane gross weights from 0.535 to 1.53 million kilograms (1.18 to 3.37 million pounds). The selected distributed load configuration was chosen primarily on the basis of good economics combined with favorable characteristics relative to such intangibles as minimum runway width, growth potential, development risks, and potential improvement.

**PRECEDING PAGE BLANK NOT FILMED**



## ABBREVIATIONS AND SYMBOLS

A/C	aircraft
AIC	airplane investment cost
Ail	aileron
Alt	altitude
A/P	airplane
APR	automatic performance reserve
APU	auxiliary power unit
$AR_W$	aspect ratio--wing
$AR_H$	aspect ratio--horizontal tail
ARAS	Arctic Resource Aircraft System
ATA	Air Transport Association
$A_{wet}$	wetted areas
b	span or wingspan
$b_w$	wingspan
$b_{TE}$	span--trailing edge
$b_V$	vertical tail span
BF	block fuel
BL	buttock line
blk	block
BPR	bypass ratio
BS	body station
$\bar{c}$	mean aerodynamic wing chord
$C_d$	drag coefficient

**PRECEDING PAGE BLANK NOT FILMED**

$C_{d_p}$	profile drag coefficient
$C_{d_{subcrit}}$	drag coefficient below critical Mach number
$C_{d_w}$	drag coefficient – wing
$C_f$	skin friction drag coefficient
c.g.	center of gravity
$C_H$	chord horizontal tail
$C_L$	lift coefficient
$C_L$	centerline
cm	centimeters
$C_m$	pitching moment coefficient
$C_m$	pitching moment coefficient angle of attack
CRAF	Civil Reserve Air Fleet
$c_{TE}$	chord – trailing edge
$c_v$	chord vertical tail
$c_w$	chord – wing
DAF	dedicated air freighter
def	deflection
deg	degrees
dia	diameter
DLF	distributed load freighter
DOC	direct operating cost
ECS	environmental control system
f	equivalent flat plate drag area
ft	feet



ft <sup>2</sup>	square feet
ft <sup>3</sup>	cubic feet
FPR	fan pressure ratio
g	acceleration of gravity
gal	gallons
GTM	gross ton miles
GW	gross weight
hr	hour
HSAS	hard stability augmentation system
hyd	hydraulic
in.	inch
in-lb	inch-pound
inbd	inboard
int	international
IOC	indirect operating cost
keas	knots estimated air speed
kg	kilograms
km	kilometers
kn	knot
lb	pound
lb/ft <sup>2</sup>	pounds divided by square feet
lb/ft <sup>3</sup>	pounds divided by cubic feet
L/D	lift divided by drag ratio
(L/D) <sub>max</sub>	maximum lift to drag ratio

LEMAC	leading edge of the mean aerodynamic chord-body station
LF	load factor
ldg	landing
$L_{ref}$	reference length
M	Mach
m	meters
MAC	mean aerodynamic chord
$M_{cruise}$	cruise Mach number
$M_{DD}$	Mach number at drag divergence
misc	miscellaneous
MLF	multimission large freighter
$M_{mo}$	maximum operating Mach number
MTOGW	maximum takeoff gross weight
MZFW	maximum zero fuel weight
N	Newton
NASA	National Aeronautics and Space Administration
NCD	net containerized density or
NPD	net payload density
nmi	nautical miles
OEW	operating empty weight
OPR	overall pressure ratio
PL	payload
psia	pounds per square inch absolute
q	dynamic pressure

ref	reference
$R_e$	Reynolds number
RTM's	revenue ton miles
ROI	return on investment
$S_W$	wing area
$S_{ref}$	reference wing area
SAS	stability augmentation system
sec	seconds
sec	section
SFC	specific fuel consumption
SL	sea level
SLST	sea level static thrust
$S_{TE_{proj}}$	trailing edge projected area
std	standard
t	airfoil thickness
t/c	airfoil thickness divided by chord
T	thrust
TE	trailing edge
TIT	turbine inlet temperature
TOC	total operating cost
TOFL	takeoff field length
TOGW	takeoff gross weight
TSLS	thrust–sea level static
V	velocity, speed

$V_c$	cruise speed
$V_{app}$	approach speed
$V_B$	maximum gust intensity speed
$V_{mo}$	maximum operating speed
$\bar{V}_H$	horizontal tail volume
VOL	volume
W	weight
W/S	wing loading—weight divided by wing area
WCP	wing chord plane
$\delta$	surface deflection angle
$\delta_a$	aileron deflection
$\delta_{TE}$	trailing edge deflection
$\phi$	roll angle
$\eta$	spanwise wing coordinate—percent semispan
$\Delta$	change in specific parameter
$\Lambda$	wing sweep

## **GUIDELINES**

### **MISSION CONSTRAINTS**

The span-distributed loading concepts generated in this study are considered to be available for introduction into service by 1990. For the purpose of this study, these large-capacity airplanes are assumed to provide carrier service between major "gateway" centers, i.e., dedicated air cargo distribution centers serving major city pairs worldwide.

### **THROUGHPUT CAPACITY**

The available dedicated market that could be served by 1990 by a fleet of span-distributed load transports is assumed to be 118 billion ton-kilometers (67 billion revenue ton-statute-miles) per year.

### **MISSION RANGE**

Design mission range in this study is approximately 3000 nautical miles.

### **PAYLOAD**

Payload weight is varied between 180 000 and 800 000 kg (400 000 and 1 800 000 lb) with values of net payload densities from 80 to 240 kg/m<sup>3</sup> (5 to 15 lb/ft<sup>3</sup>). The comparison between a conventional and distributed-load design is made at a net payload of 272 155 kg at 160.185 kg/m<sup>3</sup> (600 000 lb at 10 lb/ft<sup>3</sup>) net payload density. The payload is assumed to be containerized or assembled hardware and nonbulk. The cargo volume in the wing section accommodates parallel rows of 2.44- by 2.44-meter (8- by 8-foot) cargo containers or suitable assembled cargo appropriate to a higher ceiling height.

### **SPEED**

To provide increased productivity, the subsonic design Mach number is as high as practical, commensurate with configuration constraints and economic considerations.

### **CONFIGURATION CONSTRAINTS**

#### **DESIGN APPROACHES**

Only the all-fuel-and-payload-in-the-wing payload distribution concept is studied. The design comprises a high-thickness-ratio airfoil section with constant cross section, unswept wings, and tail assembly.

#### **PROPULSION SYSTEM**

The study configurations employ turbofan engines.

## TERMINAL AREA OPERATION

The configurations are capable of operating in and out of 12 000-foot runways.

## CONFIGURATION MATRIX

The matrix of configuration variables considered includes wing loading, aspect ratio, and thickness ratio.

## TECHNOLOGY STATUS

The configuration designs include those elements of advanced technology that may be ready for production application by 1990.

## PRESSURIZATION

The cargo hold is analyzed both unpressurized and for a minimum cargo hold pressure of  $68\,948\text{ N/m}^2$  (10 psi) absolute at any flight altitude.

## ECONOMICS

The 1967 Air Transport Association equations for international passenger transports updated to 1 January 1975 experience and corrected for expected differences due to carrying air cargo instead of passengers is used to calculate direct operating cost in cents per ton mile. Manufacturing and development costs are estimated by in-house methods. For revenue estimating purposes, the production number of airplanes corresponds to 118 billion ton-kilometers (67 billion ton-miles) throughput at the appropriate range at 65% load factor. The rules for computing direct operating cost and return on investment are given in Appendix C.

Economic variables considered are shown as follows:

<u>ITEM</u>	<u>NOMINAL VALUE</u>	<u>ADDITIONAL VALUES</u>
Fuel price	\$0.37 per gal	\$0.25, 0.75 per gal
Maintenance	Updated ATA costs (see table 22)	0.75 and 1.25 times nom. val.
Crew size	3-man	2-man
Purchase price	Contractor's est.	0.75 and 1.25 times nom. val.

## REFERENCE CONFIGURATION

The reference configuration is a fuselage-loaded cargo airplane. The reference airplane has the same degree of advanced technology elements and approximately the same design range as the study configuration.

# CONTRACTOR TASKS

## INTRODUCTION

The parametric study is the first contractor task. It is a wing geometry and sizing exercise to determine the combinations of wing span, chord, and thickness ratio that result in the most favorable configuration characteristics to warrant further study and refinement. The parametric study approach shows the design background and configuration constraints, chooses a baseline airplane, and defines the configuration matrix for the study. The parametric study results then show the resulting airplane characteristics, performance, and economics. The sensitivity of these parametric study airplanes to design payload density, throughput level, design range, and fuel economy is also presented.

From the results and conclusions of the parametric study a configuration is selected and analyzed in **SELECTED CONFIGURATION STUDY**. The rationale for the selection is shown first, followed by a detailed definition of the configuration. Next, the 1990 technology is defined and then applied to the selected configuration. The resulting performance of this airplane is shown in **PERFORMANCE CHARACTERISTICS**.

The same technical cycle is repeated for a reference conventional airplane in **REFERENCE CONFIGURATION STUDY** but in somewhat less detail than for the selected distributed-load configuration. Then the configuration and the 1990 technology are defined and the technology applications are analyzed.

Finally, two concepts are compared in **CONCEPT COMPARISON**. A technical assessment of their relative performance, productivity, and fuel consumption is shown. Economic comparisons are shown including sensitivities to economic assumptions and the effect of airplane size.

Areas for further refinement and study are discussed and study conclusions are stated.

## PARAMETRIC STUDY

### PARAMETRIC STUDY APPROACH

The projected growth of aircargo of 11% to 16% per year results in a market size by 1990 that could support much larger aircraft than are in use today. The economics of conventional aircraft with separate wing, body, and tail components improves with size but appears to reach an optimum at a gross weight of around 450 000 kg (1 000 000 lb). Aircraft larger than this have decreasing efficiencies, because the slight improvements in aerodynamics with size are more than offset by the progressively increasing wing weights caused by the large wing root bending moments.

It has been appreciated for some time that placing all of the payload and fuel in the wing and distributing these loads along the span would result in a much lighter and more efficient airplane. However, the opportunity to exploit this principle for commercial cargo airplanes requires airplanes sufficiently large that a cargo of standard commercial containers with a

cross section of 2.44 by 2.44 meters (8 by 8 feet) could be placed entirely within the wing. Preliminary Boeing studies indicated that distributed-load commercial freight airplanes of 0.68 million kg (1.5 million lb) gross weight and above could be configured with the cargo completely in the wings and could compete with large advanced conventional freight airplane designs. On figure 8 is shown the typical configuration that evolved from these design studies. This configuration will serve as the baseline for the parametric study.

### Configuration Constraints

The normal preliminary design process requires the design of a baseline airplane on which considerable detailed technical analysis can be expended to assure a technical depth sufficient for a credible study. It is desirable to pick a baseline design that is as near to the expected final design as preliminary judgments will permit. The constraints imposed on the design must be consistent with system objectives, since they have a critical effect on study results.

The configuration constraints and the rationale for their application to the baseline design and the airplanes of the parametric study are as follows:

*Straight-Wing Concept (Unpressurized).*—The Boeing data base is on straight-wing, unpressurized, distributed-load airplanes. The constant-chord design of the wing and horizontal tail helps to reduce airplane construction costs by simplifying engineering and tooling and by promoting commonality of parts used throughout the airplane.

*Fully Distributed Load.*—This is interpreted as having the entire payload contained within the wing contours and distributed from tip to tip.

*Container and M-60 Tank Capability.*—To accommodate standard commercial containers of 2.44 by 2.44 by 6.2 meters (8 x 8 x 20 feet)\* requires 2.54-meter (100-inch) inside height at the corners for the containers and 3.25-meter (128-inch) height at the center for the M-60 tank. M-60 tank must be able to straddle two adjacent cargo lanes.

*Advanced Wing Section (High  $t/c$ ).*—Baseline has 0.215 thickness ratio wing section with drag divergence  $M = 0.64$ , as indicated by preliminary wind tunnel tests.

*Fly by Wire, Hard SAS, Active Controls.*—Boeing experience with flight critical stability augmentation systems (SST program) indicated the feasibility of balancing the airplane to a static longitudinal instability level corresponding to unaugmented-time-to-double-amplitude as low as 2 seconds.

*Performance Requirements.*—Design range is 5232 km (2825 nmi); takeoff field length is 3658 m (12 000 ft).

\*The dimensions given here will apply throughout this document when “standard containers” are discussed.



## Baseline Airplane Definition

Using these constraints and background, the airplane chosen as the baseline is shown on the general arrangement drawing, figure 8. The wing cross section contains four unpressurized cargo compartments or bays, each at least large enough to house standard containers. The resulting chord of the 0.215-thickness-ratio airfoils is 20.73 m (68 ft), which, with the 89.92-m (295-foot) span, yields an aspect ratio of 4.34. Seven engines having a sea-level static thrust of 264 223 (59 400 lb) each are used. They are located above the wing to permit short, light landing gears and to keep the cargo floors close to the ground. The horizontal tail is sized for a static stability level corresponding to an unaugmented divergence time to double amplitude of 2 seconds. The tail is supported by two tail booms (fig. 9) with diagonal cables to take out the side loads from the vertical tails mounted at the horizontal tail tips. There are 18 landing gears arranged in pairs, one forward (fig. 10) and one aft of the main wing box at nine spanwise stations. Each gear is steerable for crosswind conditions and has a long oleo stroke to adjust for runway contour variations.

## Parametric Study Geometry Trades

Since the distributed-load airplane wings are loaded tip-to-tip with cargo containers, the cargo volume is a function of the number of container bays and the wing span. Figure 11 shows the relationship between number of container bays, thickness ratio, and wing chord. The cargo compartment cross section constraints were to provide vertical ceiling height in the fore and aft corners to accommodate standard containers and provide 3.25 meters of height in a double-lane center bay to accommodate M-60 tanks. The latter requirement was aimed at providing a space envelope compatible with either Civil Reserve Air Fleet (CRAF) or dedicated military uses. A thickness ratio was selected at each integral number of container bays to efficiently use the wing internal volume. Airfoil sections were scaled to meet the geometric constraints by means of a simple computer program that linearly scaled airfoil ordinates from the 0.215 thickness ratio baseline. Design lift coefficient and camber were held fixed during the scaling process.

Since the choice of thickness ratio determined the number of cargo bays and wing chord, there are implicit relationships between payload weight and volume and airplane geometry. Figure 12 shows these effects at a constant net payload density of  $160 \text{ kg/m}^3$  ( $10 \text{ lb/ft}^3$ ). Particularly apparent is that aspect ratio is a fallout rather than an input variable. For example, at 272 155 kg (600 000 lb) net payload capacity, the 0.24 thickness ratio, three-bay airplane has an aspect ratio of 6.2, while the 0.14 thickness ratio, seven-bay configuration has an aspect ratio of only 1.5. Only at the very large payloads and airplane gross weights do the low-thickness-ratio airfoils have reasonable aspect ratios. Doubling the payload to 544 000 kg (1 200 000 lb) still yields an aspect ratio of under three for the seven-bay ( $t/c = 0.14$ ) airplane.

## Configuration Matrix

Figure 13 shows the configurations chosen for the parametric study analysis. Those showing some configuration details were analyzed as individual designs and checked for many practical design considerations (such as landing gear arrangement and retraction, tail boom attachments, wing structural design, engine placement and mounting, and tail sizing and

design). The characteristics of the airplanes shown in block outlines were designs whose characteristics were interpolated into or extrapolated from the other configurations. For every configuration of the matrix a group weight statement (30 items) was made and the weight component trends checked for consistency.

For each configuration shown, the allowable gross weight and resulting empty weight to meet a takeoff field length of 3566 m (11 000 ft) and cruise thrust requirements were determined for varying numbers of engines. The payloads and payload densities that can be carried at 5232 km (2825 nmi) design range by these combinations of span, thickness ratio, and numbers of engines are shown on figure 14.

## PARAMETRIC STUDY RESULTS

The approach used to obtain a variation of payload density (the fixed span and thickness ratio (or number of bays)) for each of the nine basic study configurations of figure 12 was to vary the takeoff gross weight of each. The airplane-engine matching program ("thumbprint") described in appendix A permits specifying an integral number of engines and solving for the maximum takeoff gross weight that meets either cruise or takeoff field length thrust requirements. Built-in internal scaling rules then allow for determining the airplane empty weight, the fuel weight needed, and the payload weight that can be carried at the required range. Since payload volume is fixed for each configuration, payload density is obtained as a function of the number of engines while empty weight, fuel weight, takeoff gross weight, and wing loading are fallouts from the basic calculations.

### Airplane Characteristics

On table 2 are shown the resulting geometric and aerodynamic characteristics of all the airplanes analyzed for the parametric study. For each set of the independent input variables of span, thickness ratio, and number of engines, the airplane, payload, and economic characteristics are derived. The range of payloads and payload densities covered is shown on figure 14. Similarly, the range of takeoff wing loadings is a derived characteristic and is shown on figure 15 with lines of constant design net containerized density equalling  $160.185 \text{ kg/m}^3$  ( $10 \text{ lb/ft}^3$ ), cross-plotted for each wing span.

### Performance Comparisons

The trends in aerodynamic, structural, and overall airplane efficiencies are summarized below.

*Aerodynamic Efficiency.*—At constant span (89.92 m (295 ft)), the L/D ratio varies with Mach number as shown in figure 16. The thicker airfoil configurations have better L/D at low Mach number but L/D decreases more rapidly with increasing Mach number. The parametric study airplanes were flown at the speed affording the best M (L/D) from the lower set of curves. The actual cruise L/D used (as tabulated on table 2) decreases slightly with thickness ratio, but the Mach number increases more rapidly than the L/D decreases. The net effect is to increase cruise efficiency as measured by M (L/D) or range factor with decreasing thickness ratio. Comparisons at constant span are misleading, however, in that a seven-bay airplane is a much larger airplane than a three- or four-bay airplane, having about twice the payload capacity and gross weight. Comparing airplanes of similar capacity, say a

three-bay airplane of 152.4-m (500-ft) span with a five-bay airplane of 89.92 m (295 ft) span, shows the range factor to be superior for the three-bay version: 19 308 km versus 17 029 km or 10 426 nmi versus 9681 nmi.\*

*Structural Efficiency.*—The structural efficiencies as measured by the ratio (OEW/TOGW) are very good (0.28 to 0.30 for airplanes with constant net payload density) compared to conventional airplanes and do not vary greatly between these configurations. Figure 17 shows that the empty weight fraction increases slightly with span and indicates that the five-bay configuration has the lowest weight fraction at a given span. As originally designed, however, the five-bay configuration had a poorer weight fraction than the faired data would indicate, since the wing rib weights of the five-bay configuration were higher than the other configurations due to the chordwise position of the landing gears. In the three-, four-, and five-bay designs, the landing gear loads were taken out at the fore and aft spars at either end of the cargo bays. Since the five-bay design had the greatest distance between the spars, the chordwise bending moments reacting the landing gear loads in that design required stronger and heavier ribs. A tentative solution that would reduce these rib weights was examined. It consisted of moving the forward landing gears one bay aft and the rear landing gears one bay forward as in the seven-bay design, thus reducing the distance between the gears and the resulting rib loads and weights. Although there was not sufficient time or budget to prove the feasibility of this solution, the faired data were used instead of the calculated five-bay rib weights.

*Airplane Efficiencies.*—The increasing aerodynamic efficiency with increasing size is reflected in the payload weight fraction as shown on figure 18. Increases in span or chord (and hence gross payload) at constant-payload density show gains in payload weight fraction, with the impact of span being the greater. Productivity/gross weight ratios (fig. 19) show that increases in chord, because of the associated increases in Mach number, are more effective than increased span on this parameter. However, economic considerations are more important in comparing configurations than these purely technical characteristics, as will be shown in the next section on economic results.

### **Economic Comparisons**

A detailed tabulation of the payload characteristics of the parametric study airplanes is shown on table 3. The maximum gross payloads and their densities are shown first, followed by net payloads and the corresponding net payload densities. Since the economic comparisons will be made with each airplane carrying 65% of the maximum gross payload (65% weight load factor), the net payloads at an NPD of  $160 \text{ kg/m}^3$  ( $10 \text{ lb/ft}^3$ ) are also shown. The volume load factor shown in the fraction of usable gross volume that is used when loaded with  $160 \text{ kg/m}^3$  ( $10 \text{ lb/ft}^3$ ) NPD at 65% of the maximum gross payload weight. The airplane prices are based on a fleet size (fig. 20) carrying this payload 5232 km (2825 nmi) to produce 118 billion revenue ton-kilometers (67 billion revenue ton-statute miles) per year.

\*Interpolated values of range factor at a net payload density of  $160 \text{ kg/m}^3$  ( $10 \text{ lb/ft}^3$ )

The economic characteristics of the parametric study airplanes are shown on table 4. The economic criteria are direct operating cost (DOC) and DOC plus airplane investment cost (AIC). For those airplanes with similar production costs per pound of airframe weight, the economic trends as measured by DOC are followed closely by DOC plus AIC. As explained more fully in the section entitled **SELECTED CONFIGURATION DEFINITION, SELECTION RATIONALE**, DOC plus AIC is a better measure of airplane economics, particularly when used as a comparison with dissimilar airplanes such as the reference conventional airplane and the span-distributed selected configuration. For this reason, DOC plus AIC will be used to show the trends on plotted curves although both criteria are tabulated.

The effect of payload on economics is shown in the next three figures: for airplanes of 89.92-m (295-ft) span on figure 21, for those of 121.92-m (400-ft) on figure 22, and for the 152.4-m (500-ft) span airplane on figure 23. These same data have been crossplotted by spotting in each curve having a fixed number of cargo bays the payload weights corresponding to particular cargo densities of 80, 120, 160, and 200 kg/m<sup>3</sup> (5, 7.5, 10, and 12.5 lb/ft<sup>3</sup>). Lines of constant design cargo density can then be obtained by connecting the appropriate points on the curves having various numbers of cargo bays. Figure 24 for the 89.92-m (295-ft) span, figure 25 for the 121.92-m (400-ft) span, and figure 23 for the 152.4-m (500-ft) span airplanes show the resulting lines of constant payload density. The lowest costs occur at design payload density of 160 kg/m<sup>3</sup> (10 lb/ft<sup>3</sup>), and a gross payload of 521 631 kg (1 500 000 lb). Designing for 120 or 200 kg/m<sup>3</sup> (7.5 or 12.5 lb/ft<sup>3</sup>) adds less than 0.17 cents/Tkm at 89.92 m (295 ft) span. At 121.92-m (400 ft) span, the cost differences attributed to payload density are even less for payloads in excess of 450 000 kg (1 000 000 lb). It is also obvious that the larger the airplane or payload, the better the economics. At a constant design payload density of 160 kg/m<sup>3</sup> (10 lb/ft<sup>3</sup>), an envelope of optimum airplane configurations derived from figures 24 and 25 can be found and are shown on figure 26.

## PARAMETRIC SENSITIVITY STUDIES

### Design Payload

By collecting the previous economics curves at one payload density and at the three wing spans and plotting the data versus wing span, the effect of size or design payload level can be shown. Figure 29 shows the result at a design NPD of 160 kg/m<sup>3</sup> (10 lb/ft<sup>3</sup>). At a particular payload level the wingspan required at any particular number of cargo bays to carry a specific payload can be spotted and cross-plotted (shown as dashed lines). Note that at 272 155 kg (600 000 lb) the choice on the basis of minimum cost is clearly between the three-bay and the four-bay designs with the optimum falling midway between at a fictitious 3.5 bays. On figure 28 is shown the results of the same technique at a design payload density of 120 kg/m<sup>3</sup> (7.5 lb/ft<sup>3</sup>). The minimum cost occurs at a four-bay design with a wingspan of 103.63 m (340 ft). Both of these "optimum" airplanes have an aspect ratio of approximately 5.

At the higher payload level of 408 233 kg (900 000 lb) net payload level, the optimum aspect ratio appears to be about 4, the six-bay\* configuration having a 106.68-m (350-ft) span at

\*Interpolated

120 kg/m<sup>3</sup> (7.5 lb/ft<sup>3</sup>) density and the five-bay configuration having a 97.54-m (320-ft) span at 160 kg/m<sup>3</sup> (10 lb/ft<sup>3</sup>) density. Above this payload level there is insufficient information generated by this study to allow any rational fairing of the data.

A greater range of wing spans (both larger and smaller) at the larger chords (five-, six-, and seven-bay) would be required to deduce a reasonable pattern of optimum configuration growth for the parametric study. Since the addition of the tip fins on the selected configuration would change the effective aspect ratio, the whole parametric study would have to be redone with tip fins. Either extending the parametric study or revising it for the effect of tip devices is beyond the scope of this study.

### Design Payload Density

Studies of airfreight payload density trends at Boeing and elsewhere show net payload densities from 80 to 320 kg/m<sup>3</sup> (5 to 20 lb/ft<sup>3</sup>) with averages between 128 and 160 kg/m<sup>3</sup> (8 and 10 lb/ft<sup>3</sup>). These averages are vulnerable to accuracy problems in predicting the patterns that will actually prevail 15 to 30 years hence, particularly with an expected change in the class of goods that will utilize airfreight. In order to capture a share of the freight market that will justify the large expansion in airfreight capability associated with fleets of giant distributed-load airplanes, the basic reason for shipping by airfreight must change from the present emergency basis to a regular shipment basis. This means that many categories of goods not now shipped by airfreight must be captured by this new mode. Predicting the density of these new commodities is hazardous. Therefore, the new airfreight system should be designed to be relatively insensitive to cargo density to hedge against these uncertainties.

Fortunately, the economic data collected for the parametric study (table 4) can be cross-plotted to show the effects of changing design density and thus indicate how best to design the system to minimize the risks of cargo density prediction. At constant design net containerized density (NCD) costs\* versus wing span can be plotted at constant number of cargo bays as shown in figure 27. This shows that bigger is better, since either more bays or more span will improve the economics. By plotting lines of constant payload, a distinct optimization pattern emerges. At 80 kg/m<sup>3</sup> (5 lb/ft<sup>3</sup>) design NCD, the minimum cost\* equals 5.25¢/Tkm (7.65¢/gross ton-mile (GTM)) occurs for an interpolated six-bay airplane with a 103.63-m (340-ft) span when carrying 272 155 kg (600 000 lb) of 160 kg/m<sup>3</sup> (10 lb/ft<sup>3</sup>) cargo. On the next figure (29) the minimum cost (4.91¢/Tkm (7.16¢/GTM)) occurs for a four-bay airplane at about 115.8 m (380 ft) wingspan when carrying the same payload and a design NCD of 120 kg/m<sup>3</sup> (7.5 lb/ft<sup>3</sup>). Figure 29 shows that for a design NCD of 160 kg/m<sup>3</sup> (10 lb/ft<sup>3</sup>), the minimum cost is 4.84¢/Tkm (7.06¢/GTM) for a three-bay airplane with about a 111.25-m (365-ft) span. Figure 30 suggests that at 200 kg/m<sup>3</sup> (12.5 lb/ft<sup>3</sup>), the highest cargo density considered, a two-bay airplane would probably be optimum.

To put the above effects in perspective, suppose the real market had an average NCD of 160 kg/m<sup>3</sup> (10 lb/ft<sup>3</sup>). These effects are summarized on figure 31, which shows the effect of airplanes designed for different densities but carrying a particular density 160 kg/m<sup>3</sup> (10 lb/ft<sup>3</sup>).

\*DOC plus AIC

If a four-bay configuration had been designed to carry  $120 \text{ kg/m}^3$  ( $7.5 \text{ lb/ft}^3$ ) cargo density, figure 31 shows that no economic penalty would result from carrying  $120 \text{ kg/m}^3$  ( $10 \text{ lb/ft}^3$ )  $120 \text{ kg/m}^3$  ( $7.5 \text{ lb/ft}^3$ ) cargo density (DOC plus investment cost =  $4.94\text{¢/Tkm}$  ( $7.2\text{¢/GTM}$ ) for either case). If the four-bay configuration was designed for  $200 \text{ kg/m}^3$  ( $12.5 \text{ lb/ft}^3$ ) the cost when carrying  $160 \text{ kg/m}^3$  ( $10 \text{ lb/ft}^3$ ) cargo would be  $5.38\text{¢/Tkm}$  ( $7.85\text{¢/GTM}$ ) or  $0.45\text{¢/Tkm}$  ( $0.65\text{¢}$ ) greater than one designed for  $160 \text{ kg/m}^3$  ( $10 \text{ lb/ft}^3$ ) density. The three-bay designed for  $120 \text{ kg/m}^3$  ( $7.5 \text{ lb/ft}^3$ ) density pays a penalty  $5.18 - 4.94 = 0.24\text{¢/Tkm}$  over the four-bay designed for  $120 \text{ kg/m}^3$  ( $7.5 \text{ lb/ft}^3$ ) and also carrying  $160 \text{ kg/m}^3$  ( $10 \text{ lb/ft}^3$ ) density cargo. The four-bay configuration designed for the lower density of  $120 \text{ kg/m}^3$  ( $7.5 \text{ lb/ft}^3$ ) is therefore the more flexible design in that it pays no penalty in economics for a range of cargo densities from  $120$  to  $160 \text{ kg/m}^3$  ( $7.5$  to  $10 \text{ lb/ft}^3$ ).

Note that the sensitivity is low and hence extra volume can be a relatively inexpensive insurance on errors in predicting the air cargo density.

### Effect of Throughput

The parametric study economics assumed a constant fleet productivity of throughput of 118 billion revenue ton-kilometers (67 billion revenue ton-statute miles)\* per year at 5232 km (2825 nmi) range. The airplane prices used in the economics are based on the production of just enough airplanes of each configuration geometry to produce this throughput at 65% gross payload load factor. Since the choice of the selected configuration depends on the relative economic performance based on this assumption, it is appropriate to check the effect of throughput level on the economics of representative parametric configurations.

Accordingly, three configurations having approximately the same payload (about 362 874 kg (800 000 lb)) were analyzed at three different throughput levels and the results are shown on figure 32. The four-bay configuration has the superior economics compared to the others at half (59 billion Tkm or 33.5 billion RTM's) and at double (236 billion Tkm or 134 billion RTM's) the original throughput, but the relative margin over the others changes with throughput. At low throughput, the four- and five-bay airplanes change very little relatively, whereas the seven-bay improves with throughput, but never equals the others. The conclusion reached is that the effect of a variation in throughput is insufficient to affect the parametric study results.

### Design Range Sensitivity

The choice of design range, like that of design payload density, has certain risks since it involves predicting airborne commodity flow patterns 15 to 30 years in the future. It is clear, however, that any airfreighter intended for international routes should be reasonably economical at ranges between 5556 km (3000 nmi) for the North Atlantic routes and 10 000 km (5500 nmi) for the North Pacific routes. The buildup of international airfreight is

\*Boeing internal studies erroneously used ton statute miles instead of ton nautical miles as specified in the Statement of Work. However, this does not change the relative economics between configurations, as is shown by the above analysis.

expected to follow that of passenger traffic, starting in the Atlantic and later developing in the Pacific. The present generation of international commercial airplanes (747 and DC-10) has design ranges appropriate to Pacific routes in the original passenger versions, but these airplanes can only carry full cargo loads at ranges corresponding to Atlantic routes in the airfreighter models. Internal Boeing studies intended to compare airfreight configurations have recently used an arbitrary 7408 km (4000 nmi) as the design range.

Since the choice of configuration to carry 272 155 kg (600 000 lb) net payload has been narrowed down to be either the three-bay or four-bay configuration, a design range sensitivity study has been made of these two configurations. Design ranges of 3704, 5232, and 11 112 km (200, 2825, and 6000 nmi) were considered and the economic effects are shown on figure 33 for the three-bay and on figure 34 for the four-bay configuration. These curves show that either airplane pays the greatest economic penalty for flying at ranges less than the design range, whereas much less penalty is paid for flying considerably further than the design range. For example, a four-bay configuration designed for 3704 km (2000 nmi) can be flown as far as 8334 km (4500 nmi) before one designed for 11 112 km (6000 nmi) is superior. The envelope of design ranges, shown as the dashed line for both configurations, crosses at 6482 km (3500 nmi). The four-bay is superior below this range and the three-bay is superior at longer ranges. Since the differences are slight at all ranges and the four-bay configuration is expected to improve more than the three-bay when tip devices are added to each, there is little to choose between the two in range sensitivity.

### Fuel Economy

Block fuel versus gross payload at 5232 km (2825 nmi) range has been plotted and is shown on figure 35 for the 89.92-m (295-ft) and 121.32-m (400-ft) span airplanes. Radial lines from the origin are plotted at constant payload delivered per pound of fuel consumed. Increasing the gross payload, the number of cargo bays, or the span improves the fuel economy relative to the 89.92-m (295-ft) span, three-bay airplane. At 317 968 kg (701 000 lb) gross payload (272 155 kg (600 000 lb) net payload) carrying 160 kg/m<sup>3</sup> (10 lb/ft<sup>3</sup>) NDC cargo, the four-bay, 89.92-m (295-ft)-span, distributed-load airplane uses slightly more fuel per pound of payload delivered than the 747-200F, but the larger distributed-load airplanes are considerably better than the 747. It is expected that the improved technology being incorporated in the selected configuration will also improve the fuel consumption of the distributed load airplane relative to the conventional airplanes.

## SELECTED CONFIGURATION STUDY

The results of the parametric study indicate that the choice of configuration geometry, particularly the thickness ratio or number of cargo bays, depends on the size of payload desired. Since the study guidelines (see GUIDELINES, PAYLOAD) are interpreted to require the evaluation to be made at 272 155 kg (600 000 lb) net payload at a density of 160 kg/m<sup>3</sup> (10 lb/ft<sup>3</sup>), the selected configuration will be chosen to match these requirements. The rationale leading to the choice of configuration is presented, followed by the detailed definition of the selected configuration. This section will define the 1990 technology and present the technical analyses of the chosen airplane.

## SELECTED CONFIGURATION DEFINITION

### Selection Rationale

The objective of producing a new airfreight system using very large airplanes based on the distributed-load principle will be to provide a superior service expediting the flow of goods and the bonds of trade between nations around the world. The service will basically offer time savings of weeks over other transport modes on international routes at a price consistent with the value of goods that are candidates for this class of service.

The rationale used to select the best airplane design from the parametric study must compare the same factors that ultimately determine the economic justification for the system, i.e., the service must be offered at a price that will produce the demand from shippers to pay the system costs and reasonable returns on investment to the manufacturer and operator.

The burden of the selection criteria is that it must reflect this complex, real-world, supply-and-demand relationship in a simple, straightforward, practical technique. Direct operating cost plus airplane investment cost (including taxes) to the operator at constant total fleet productivity is the primary basis for comparison for this study. The rationale for this choice and the detailed assumptions involved will be explained in the following paragraphs.

Direct operating cost has been the traditional criterion for comparing airplane designs for some good reasons, but it also suffers from significant deficiencies as a standard for economic performance. On the positive side, DOC can be predicted with reasonable reliability from extrapolation of the trends from the extensive airline operating cost records. Correlation of these trends is continuous and the DOC coefficients are revised every year. Even the form of the equation is varied if additional data and/or better regression analyses indicate the desirability of making a change (e.g., different equations are used for high-bypass engines than for low-bypass engines).

The application of these data to a new generation of advanced airfreighter airplanes has acceptable risks and is probably conservative for the following reasons: high-bypass engine technology and its associated maintenance patterns have matured sufficiently so that no great change in trends is anticipated. Advances in engine technology, such as significantly higher pressure ratios, do imply higher maintenance costs, but the resolution of this effect is beyond the scope of this study. Historical high-bypass ratio maintenance cost trends are used in economic analysis, hence the effect of the engine 1990 technology is shown at assumed present levels of engine maintenance costs. Airframe maintenance costs are expected to decrease relative to previous trends because the basic airframe of these distributed load designs is simpler, cheaper, and designed for longer life than previous generations of aircraft.

The special failing of DOC is that it does not sufficiently account for airplane first cost, since the only factor related to first cost is depreciation. Using 14 years' straight-line depreciation to a salvage value of 10% of the original price results in an effective 6.43% depreciation per year. A reasonable return on investment of 12% per year (including taxes and not including depreciation per CAB guidelines) to the operator was used to attract the capital to finance this project. Depreciation accounts for only a third of those costs associated with buying the airplane fleet. Comparing airplane design on the basis of DOC alone tends to



result in the high-first-cost, low-operating-cost airplanes to be chosen, whereas using DOC plus AIC results in the most economic airplanes in an overall sense to be the winners.

Although the total transportation cost is the sum of DOC plus return on investment cost plus indirect operating cost, the airplane related costs are almost entirely in the DOC plus ROI. The indirect operating costs, although important in assessing the supply-demand problem, have very little bearing on comparing airplanes, since IOC is chiefly the cost of handling the cargo and running the ground system. The investment cost of the new ground system for these huge airplanes is expected to be substantial at a small number of large hub airports from which these airplanes will operate. The investment cost per airport is more related to the actual throughput per day at a particular airport rather than the characteristics of the airplanes that supply the throughput. Hence, an airport and ground system study would contribute little to understanding the basic economic trades between airplane configurations. The increased efficiency of these specialized ground systems, however, is expected to reduce the IOC's almost as much as the DLF will reduce the DOC's.

The fleet size or number of airplanes expected to be built has a significant effect on the comparison. Since airplane price decreases with increasing production, so does the resulting operating and investment costs and ultimately the cost of the service to the shipper. The total market for the service (the demand) increases with decreasing cost until the market is saturated, i.e., until building more airplanes will not lower the costs enough to generate the additional demand required to justify the additional airplanes. At the other end of the supply-demand spectrum, building too few airplanes results in such a high cost for the service that insufficient market is found to warrant building the airplane. At some point between these extremes is the production level where there is a maximum difference between the costs of supplying the service and the price the demand will bear. Since there are considerable risks associated both with predicting the demand and predicting the total system costs, it is prudent to design the system for the productivity level where maximum profit potential exists. In addition, it is desirable to compare airplane fleets of varying size and design at the same constant fleet productivity level rather than at a fixed number of airplanes. Comparing at constant fleet size or number of airplanes implicitly assumes that the market will vary with the size of the airplane; however, this assumption cannot be supported as a logical way to compare airplane designs.

In exploring this market, Boeing has concluded that the 118 billion ton kms (67 billion revenue ton-statute-mile) annual total fleet productivity by 1990 specified in this contract is a reasonable level at which to compare distributed-load airplane systems. It is approximately midway between upper and lower levels of market size predicted by different assumptions. It results in reasonable fleet sizes for efficient production and the projected total transportation costs should include a reasonable margin for profit.

### Consideration of Intangibles

The formal measurement of DOC plus AIC as the economic figure of merit must be biased by a number of intangibles that are not practical to measure within the scope of this study. From the parametric study economic results, the choice of a configuration to carry a 272 155 kg (600 000-lb) net payload at 160 kg/m<sup>3</sup> (10 lb/ft<sup>3</sup>) cargo density 318 000 kg (701 050 lb) gross payload could be either the three-bay, 112-m (366-ft) span, or four-bay,

84.73-m (278-ft) span configuration. The three-bay configuration is slightly superior in DOC plus AIC at the design point, but the four-bay is less sensitive to excursions in payload density or range from the design point. Therefore, consideration of the following intangibles is needed to make the decision on which configuration should be chosen for more extensive analysis.

*Minimum Runway Width.*—The expected use of these large aircraft would be in the inter-continental airfreight, where a small number of worldwide hub cities would be connected by this service. Although the difference in wingspan of the four-bay configuration over the three-bay configuration is 30.48 m (100 ft) and clearly an advantage for the four-bay, it is not expected to be a critical factor in the ultimate economics in the application of either airplane. Even with 40 hub cities having two widened runways each, the saving of airport costs of the four-bay over the three-bay configuration is of the order of 1% of DOC plus AIC.

*Good Payload Growth Potential.*—At 272 155 kg (600 000 lb) net payload at 160 kg/m<sup>3</sup> (10 lb/ft<sup>3</sup> NCD, the three-bay configuration has a DOC plus AIC equal to 4.84¢/Tkm (7.06¢/GTM), while the four-bay version has 4.94¢/Tkm (7.20¢/GTM) for a 65% load factor at 5232 km (2825 nmi). At 408 233 kg (900 000 lb) net payload, the three-bay version has 4.66¢/Tkm (6.79¢/GTM), while the four-bay has 4.27¢/Tkm (6.23¢/GTM). At this payload the three-bay configuration has a 164.9-m (541-ft) span, while the four-bay version has a 125-m (410-ft) span. Increasing payload and size produces significant advantages for the four-bay configuration.

*Minimum Aerodynamic Risks.*—Boeing has tested the 0.215 thickness ratio airfoil used on the four-bay configurations but has not tested the 0.24 thickness ratio airfoils used with the three-bay configurations. Although the 0.215 thickness ratio airfoil had very good high-speed characteristics (drag divergence Mach number = 0.64 with reasonable drag creep with Mach number), the thicker three-bay airfoil is moving yet further away from conventional airplane wing thicknesses and therefore represents considerable technical risk at this time.

*Greater Impact From Improvement.*—The selected configuration will be equipped with wing-tip aerodynamic devices (winglets) that will be designed to increase the effective aspect ratio. These are particularly effective at low aspect ratio and are therefore expected to improve the performance of the lower-aspect ratio, four-bay configuration more than the higher aspect ratio, three-bay configuration.

### **Selected Configuration**

The airplane chosen as the study “selected configuration” is shown on the general arrangement drawing, figure 36. Its airframe is the same as the parametric study baseline airplane, with the wingspan reduced by 6.1 m (20 ft) to match the payload specified in the study guidelines. The wing airfoil section and cargo space envelope were sized to be compatible with CRAF and dedicated military uses (M-60 tank headroom and width); however, the cargo volume used in this study is based on standard 2.44- by 2.44- by 6.1-m (8- by 8- by 20-ft) containers. Gross volume of the 52 containers is 1885 m<sup>3</sup> (66 560 ft<sup>3</sup>) and the design mission range is 5556 km (3000 nmi).

Vertical surfaces have been moved from the horizontal tail to the wingtips. The wingtip fins are all-movable and include split trailing edge surfaces to serve as a drag device during "engine-out" situations prior to liftoff. Winglets also are added at the wingtips to improve effective aspect ratio. Horizontal tail size is based on the same criteria used for the parametric study airplanes.

### **Principal Design Features**

Weight and performance evaluation of the selected configuration considers that 1990 materials and propulsion technology are incorporated in the design. Low cost and lightweight construction techniques suitable for large distributed-load airplanes are important elements of the concept. Figures 37 through 40 show the wing structure, a large percentage of which is constructed from honeycomb sandwich panels, using riveting and bonding at the splices and joints. Important features are noted on the drawings.

Figure 41 shows the landing gear assembly that is used in all twenty locations on the airplane. The steering system provides angles greater than  $90^\circ$  in either direction. Powered wheels and high-angle steering provide unusually flexible ground maneuver capability and accommodate crosswind takeoffs and landings.

An advanced engine installation concept is described in figure 42. The overwing location requires a nonstandard engine support but lends itself to a novel quick-engine change concept, as shown on the drawing. The airplane has been designed to make use of the air cushion effect to permit takeoff and landings to be made without rotation prior to liftoff or touch-down. The overwing engine is the only practical location to permit the wing to be placed low enough to the ground to achieve the proper air cushion. The air cushion effect, is, of course, very sensitive to flap position; when the flaps are fully down, high lift and low drag are achieved. As the flaps are retracted in ground effect, at some point a negative lift will be achieved, which is useful in braking. It is expected that ground effects improve the low-speed aerodynamics to some extent.

Space allocation for subsystems is depicted by figure 43. Access for installation and maintenance is unusually good due to the large size of the airplane and the absence of small closed areas. Long straight raceways make it possible to bench-assemble long wire bundles and hydraulic tubing subassemblies prior to installation. Schematics of the hydraulic power and fuel supply systems are shown by figures 44 and 45. Reliability through redundancy and conventional sizing of the APU's and pumps is a feature of these systems.

## **TECHNOLOGY DEFINITION AND ANALYSIS**

### **Aerodynamic Design**

The criteria used to establish which aerodynamic technology improvements to employ for the current study are:

1. The concept must be one for which some degree of improvement has already been demonstrated or is clearly obtainable.
2. A clear physical understanding of the improvement phenomenon must exist.

3. The implications of introducing the concept, with respect to weight, structure, and complexity, must be obtainable in a timely manner to ensure proper comparison between DLF concepts and the conventional freighter reference configuration.

The technology advances chosen for this study include reductions in drag due to roughness and interference, improved airfoils, tip fins, and fully active control systems. The introduction of laminar flow control systems is expected to provide substantial gains in aerodynamic performance but has not been included in the current study. A study of substantial magnitude would be required to establish the compromises required to implement LFC systems on both the selected DLF airplane and the conventional reference configuration. This study is not possible within the scope of the present effort and criterion 3 above could not be satisfied. Reference 1 indicates that moderate reductions in friction drag are obtainable with compliant skins. However, the current lack of understanding of the drag reduction mechanisms and of the required surface characteristics violate criterion 2 and no improvement is assumed.

The selected DLF configuration is the four-bay, 89.92-meter- (295-foot)-span parametric configuration updated to 1990 technology with a 6.096-m (20-ft) span reduction to obtain a NPD of  $160 \text{ kg/m}^3$  ( $10 \text{ lb/ft}^3$ ). The aerodynamic technology levels employed to establish performance and economics are based on recent Boeing advanced technology studies (references 1 and 2) and extrapolated in-house IR&D program results.

Table 5 summarizes the gains in M (L/D) resulting from the drag reductions shown. The overall M (L/D) is increased 23.5%. The 1980 base levels characterized by the four-bay, 89.92-meter (295-foot)-span configuration characteristics are shown for reference. It should be noted that the gains indicated do not include the penalties resulting from reduced span; however, these have been included in formulating the drag polars.

The 1% increase in M (L/D) for reduced roughness, excrescence and interference drag is due to a 33% reduction in the drag of these items. Approximately two-thirds of this reduction is forecast to result from reduced interference drag. The application of advanced aerodynamic configuration analysis tools such as the contractor's internal potential flow programs have already demonstrated that wing-nacelle-strut interference effects can be all but eliminated by proper contouring and fairing. The placement of engines above the wing leading edge are deemed to represent a more difficult installation problem and a smaller reduction is predicted. The remaining gains due to reduced roughness and excrescence drag are predicted to result from improved installation of antennae, scoops and other protuberances, plus anticipated improvements in surface conditions.

Form drag for the 0.215 thickness ratio thick airfoils used on the 1975 base DLF configuration is approximately double that of current 0.15 thickness ratio thick airfoils. Renewed research on thick airfoils is currently underway at NASA (reference 5) and promises gains in overall airfoil performance. Based on these studies and current trends with thickness ratio, a 4% decrease in form drag is predicted. The resulting increase in M (L/D) is 0.5%.

Thick airfoil studies conducted under Boeing IR&D indicate increases of 0.02 in critical Mach number for the base airplane. Another 0.02 increase in Mach number (for 1990) is predicted with further airfoil development. The total Mach number improvement of 0.04 is equivalent to a 6% increase in M (L/D).

The selected configuration takes advantage of tip fins for reduced drag due to lift. Due to its low aspect ratio wing, tip fins are partially effective. Figure 46 gives induced drag factors for various fin combinations including that used for the selected configuration. However, the selected configuration does show a 34.5% reduction in drag due to lift with an attendant 16% increase in L/D relative to the same configuration without tip fins.

The resulting selected configuration drag summary is presented in table 6 and figure 47. The procedures used are similar to those outlined in the PARAMETRIC DATA BASE section of the Appendix except that wing-nacelle-strut interference was included.

The low-speed aerodynamic characteristics are presented in figure 48. Lift-drag ratio as a function of second-segment lift coefficient is presented for both the 1980 base configuration and the selected configuration. The L/D improvement shown results from the technology advances noted above and from an increase in flap span from 61% wing span to full span. The low-speed aerodynamic analysis was made without regard to ground effects. It is expected that ground effects improve the low-speed aerodynamics to some extent.

*Stability and Control Analysis.*—The selected configuration was also evaluated on the basis of aerodynamic stability, control, and maneuver criteria. The elevator was sized for longitudinal trim requirements at approach. Horizontal tail size was established on the basis of unaugmented longitudinal stability such that the time to double amplitude of the longitudinal motion is not less than two seconds ( $t_2 = 2$  sec). This two-second criterion is based on Boeing SST experience and is representative of stability augmentation system capability in the projected operational time period of the DLF airplane. Minimum dynamic stability ( $t_2 = 6$  sec) is provided by a flight-critical or hardened stability augmentation system (HSAS).

The all-moving wingtip vertical surfaces were sized by lateral maneuverability requirements on final approach. These vertical surfaces both deflect the trailing edge in or out in this mode of operation to act as side force generators. These surfaces are also used for directional control and lateral/directional stability augmentation. In this second mode of operation the surfaces deflect independently, with the trailing edges moving only outboard. The vertical fins incorporate split trailing edge drag devices for critical engine-out directional trim at takeoff.

Roll control is provided by wing trailing-edge control surfaces and roll authority supplemented by spoilers in flight regimes requiring maximum roll acceleration (e.g., wind gust on landing approach).

*Longitudinal Stability and Control.*—Longitudinal stability philosophy and criteria are shown in figure 49. The horizontal tail is sized for a static margin that will produce an unaugmented longitudinal response corresponding to time-to-double-amplitude of not less than 2 seconds. A flight-critical (hard) SAS will provide a longitudinal stability level such that time-to-double-amplitude is equal to or greater than 6 seconds. A handling quality SAS will provide satisfactory handling qualities characteristics; however, these two longitudinal SAS systems may be integrated as a common system.

Figure 50 presents a summary of the horizontal tail sizing criteria. Allowable forward and aft center-of-gravity locations are shown as a function of tail volume coefficients as established by approach trim and stability requirements. Allowable aft c.g.'s are shown: (1) for the unaugmented airplane, (2) for stability augmented by a handling-qualities SAS, and (3) for stability augmented by a hard SAS. The static neutral point and maneuver point are shown as references for the allowable centers of gravity. Superimposed upon the allowable c.g. variation are the forward and aft c.g. limits established for the airplane loading range. This figure illustrates the reduction in tail size permitted by utilization of HSAS. It also demonstrates that the unaugmented airplane cannot be balanced at the aft c.g. by increasing horizontal tail size.

*Lateral-Directional Stability and Control.*—The lateral control system was evaluated relative to landing approach wind gust criteria. A roll-attitude hold-flight control system was employed to minimize roll excursions on final approach introduced by a 20-ft/sec asymmetric wind gust. Flight control system gain levels were established on the basis of 1980-1990 state-of-the-art flight controls technology to minimize roll excursion and to provide adequate separation between structural mode frequencies and the control frequency. Figure 51 presents maximum bank angle excursion as a function of roll attitude gain. Shown also is the bank angle for wingtip-ground strike. This figure illustrates that a small increase in flight controls technology capability over that of current transport aircraft should result in satisfactory attitude hold characteristics.

Takeoff engine-out directional trim capability is provided by split trailing edge devices on the wingtip-mounted vertical surfaces in conjunction with an automatic performance reserve (APR) system. Figure 52 presents surface trailing edge deflections required to trim the most critical engine-out as a function of the percent of power maintained on the opposite outboard engine. These data are based on a 32% vertical tail chord trailing edge device and 10% thrust increase on the remaining two engines on the failed engine wing provided by the APR system.

Lateral flight path control for landing approach runway alignment is provided by deflection of the split rudders at the trailing edge of both wingtip-mounted vertical fins and by deflection of the vertical fins themselves. Figure 53 demonstrates that the airplane lateral control system does not provide lateral capability required to satisfy localizer beam offset criteria for either the Category I or Category II decision heights. However, addition of two 111.5-m<sup>2</sup> (1200-ft<sup>2</sup>) side-force generators to supplement the translational capability of the lateral control system enables the airplane to meet the Category II minimum decision height criteria.

The DLF selected configuration requires a lateral-directional SAS because of unaugmented airplane Dutch roll mode instability. The inherent low directional stability produced by the wingtip location of the vertical fins (and the resultant relationship of  $C_{l\beta}$  to  $C_{n\beta}$ ), combined with the close coupling of the directional control surfaces, places increased demands on the lateral-directional SAS. A lateral-directional stability evaluation was performed to determine the capability of a conventional yaw damper (yaw rate feedback to rudder) to satisfy stability criteria. Results of the evaluation indicate that the MIL-F8785B Dutch roll frequency and damping criteria (reference 5) can be met at a yaw damper gain sufficiently low to avoid control surface saturation in the presence of a 37-km/sec (20-kn), 90° design crosswind gust. The special mode was found to be stable at the required gain level. The roll time constant

exceeds the maximum allowable for the MIL-F criteria (reference 5); however, the roll response criteria may not be appropriate for airplanes of the DLF weight and inertia class due to the restricted flight regime of the cargo transport mode of operation. A conventional yaw damper implemented through the all-moving vertical surfaces will satisfy lateral-directional stability criteria, provided that adequate separation can be maintained between control frequency and structural bending mode frequencies.

## Propulsion and Noise

*Propulsion Engine Selection Rationale.*—The criteria established for the distributed-load-concept airplane were that the propulsion system should reflect 1990 technology and the engine should match the airplane design mission.

In order to accomplish these objectives properly for both the conventional reference airplane and the distributed-load freighter (DLF) airplane, an extensive study, beyond the scope of this contract, would be required. Therefore, it was necessary to conduct an abbreviated study to establish a 1990 technology engine. The engine selection rationale used for this study involves the following steps:

1. Conduct parametric engine cycle studies.
2. Select engine overall pressure ratio and turbine inlet temperature technology.
3. Conduct an airplane mission sensitivity study.
4. Select fan pressure ratio and resultant bypass ratio for the mission.

This process is indicated schematically on figure 54 and will be discussed below.

The Boeing Company continually conducts independent studies of the engine component efficiency level trends and engine technology projections. Results of these studies and coordination with the engine manufacturers provide a data bank whereby Boeing predictions are made for component efficiency levels expected in the future. With these data, an engine parametric cycle study was conducted with variables of overall pressure ratio (OPR), turbine inlet temperature (TIT), fan pressure ratio (FPR), and bypass ratio (BPR). This parametric study provided the basis for establishing trend data showing the effects on engine SFC, diameter, and weight of varying OPR and TIT. The trend data were prepared at constant cruise thrust for a constant BPR. These data are shown on figure 55.

The trend data of figure 55 are judged to be valid for the range of airplane Mach numbers considered and are used to establish the overall pressure ratio and turbine inlet temperature for the 1990 engine. These data show that if SFC alone is considered, the selection would go to the lowest TIT and the highest OPR. However, the data also show this particular selection would result in the highest engine weight and engine diameter with higher nacelle drag. While the later effect is significant, previous studies indicate that the effects of OPR and TIT on weight and SFC are considerably more important, so that emphasis is usually placed on higher values of OPR and TIT. However, technology development at any given

time generally tends to place upper limits on both of these parameters. Of particular importance in relation to OPR selection are internal aerodynamic design and sealing techniques. Turbine temperature levels are influenced primarily by advancements in high-temperature materials and cooling techniques. The final selection of an overall pressure ratio of 40 and a standard day-cruise turbine inlet temperature of 1528 K (2750°F) for this 1990 engine was based on assessment of the probable technology limits for the 1990 time period. This level is considered to be approximately 111°C higher than current commercial engines. The data on figure 55 indicate that this selection reduces SFC and weight and provides a reasonable compromise between SFC, weight, and fan diameter.

After the cycle overall pressure ratio and turbine inlet temperature have been selected, it is necessary to establish the proper fan pressure ratio and the resulting bypass ratio. Fan pressure ratio selection is influenced by the airplane mission. The objective is to select a fan pressure ratio that will provide the best economics for the airplane. An in-depth airplane trade study is generally required to determine the optimum fan pressure ratio. However, due to the limited effort allocated for this contract, a study of this type was not undertaken. Therefore, a simplified approach was necessary to establish a proper fan pressure ratio. Utilizing the previously indicated component efficiencies, OPR and TIT, engine performance data were computed at several values of fan pressure ratio for the two Mach numbers associated with the reference airplane and the DLF selected airplane. These engine data were used to show the trends of engine weight, SFC, and diameter as a function of fan pressure ratio and are shown in figure 56. For constant cruise thrust, it can be seen that as fan pressure ratio decreases, engine weight and diameter increases while SFC decreases. These trends were considered in selecting the proper fan pressure ratio. Using DOC plus AIC as a figure of merit, airplane sensitivity factors (due to weight, drag, and SFC) were obtained for the DLF airplane for a 7408 km (4000 nmi) mission. Using these data and the engine trend data, a curve was developed showing the percent changes in DOC plus AIC as a function of fan pressure ratio, which is shown on figure 57. On the basis of economics, a fan pressure ratio of 1.6 is optimum for the direct-drive fan over the Mach number range considered. The optimum value is somewhat lower for a geared fan which has a significant weight advantage. However, consultations with engine manufacturers have indicated that other considerations (e.g., overall market requirements) may exert influence toward a higher fan pressure ratio. Also, related noise studies have shown that overall engine noise levels do not improve below a fan pressure ratio of about 1.6. Thus, a geared fan with FPR = 1.6 was finally selected.

At a 1.6-fan-pressure ratio, it was necessary to establish the bypass ratio that would produce minimum SFC. Engine performance data were computed and it was established that a bypass ratio of 9.5 satisfied this requirement. The engine cycle is thereby established as:

FPR = 1.6 (geared fan)  
OPR = 40  
ST. DAY CR. TIT = 1528 K  
BPR = 9.5



The projected engine technology gains for the 1990 engine relative to current technology level turbofans are shown on table 7. The higher compression ratio and turbine inlet temperature of the advanced cycle will tend to increase maintenance costs over the 1980 levels. An additional increment in maintenance costs must also be added due to the gearbox for the gear-driven fan. For this study, current engine maintenance levels were assumed; however, resolution of maintenance costs remains for future studies.

With the above cycle established and the aerodynamic component efficiencies, cooling effectiveness, and metal temperature capability established from the parametric study, an engine cycle computer program was run to establish a resultant performance package, including engine weight and physical size. Figure 56 shows the engine data development process. At this point, the performance data is for an uninstalled engine with 100% inlet recovery and ideal exhaust nozzles. Adjustments to the weight data were made to allow for the anticipated usage of composite materials, advanced lightweight metals, and other materials in the 1990 time period. This engine will also have a gear-driven fan based on lowest engine weight. The 1990 engine has the following characteristics:

M = 0.74 @ 9144 m (30 000 ft)	
Cycle as noted above	
Maximum cruise net thrust	58 672 N (13 190 lb)
Maximum cruise SFC kg/hr/kg (lb/hr/lb)	0.4988
Engine weight	3312 kg (7301 lb)
Engine length	2.53 m (99.8 in.)
Fan diameter	2.63 m (103.4 in.)
LP turbine diameter	1.25 m (49.3 in.)
SLS takeoff thrust	226 858 N (51 000 lb)

This estimated 1990 technology data was compared to recent 1990 engine data submitted by the engine manufacturers. Only slight differences were apparent as to the selection of FPR, OPR, and BPR.

Installation correction factors were determined for this engine to account for the effects on performance of the flight installation covering inlet, fan duct, exhaust nozzle, horsepower extraction, and airbleed. Estimated installed thrust and fuel consumption data are shown on figures 58 through 60 for takeoff, climb, and maximum cruise conditions. These data were used as the basis for the DLF studies and were scaled as appropriate to provide the engine size required for the airplane.

### Loads Analysis

Span-loaded airplanes are designed to balance the inertia forces with the external forces. During 1-g flight, this balance is limited by the requirements for a low drag-span-lift distribution and for variations in the payload distribution. However, during maneuver and gust loads, the active control system can be used to fine-tune the lift distribution to minimize a measured bending moment. These considerations lead to the possibility that the once-per-flight loads may comprise a large proportion of the ultimate design loads, which would be early fatigue damage. To prevent this, ground rules were developed relating the minimum-design-loads envelope to the 1-g loads. Ultimate design loads were at least three times the 1-g

loads for any flight condition and at least 2.5 times the 1-g loads for any ground taxi condition. In addition to these minimum requirements, the usual flight and ground design conditions were considered. The 2.5-g flight maneuver loads and the gust loads were reduced by the active control system so they were not critical.

Design criteria were established to define payload variations and a flight envelope. Three payload distributions were used as representative of the spectrum of distributions that would result from loading requirements. The payload shear curves for these distributions are shown in figure 61. The structural design speed-altitude envelope is shown in figure 62.

Since the minimum design loads envelope is sensitive to the 1-g lift distribution, a preliminary trade study was conducted to determine the relation between L/D and wing-bending moment. Only the uniform payload (P/L 1) was considered for this trade study; however, the results were applied to all three of the payload distributions. Because the winglets extend beyond the payload compartment, the lift distribution for maximum L/D gives rather large bending moments. Lift-to-drag ratio and bending moment changes due to perturbations to the lift distribution were determined. The results showed that for a small reduction in L/D from  $L/D_{max}$ , a substantial reduction in bending moment could be achieved. The lift distribution for  $L/D_{max}$  and the selected lift distribution, along with the resulting bending moments, are shown on figure 63.

Landing gear reactions were calculated for taxi load factors of 1 g and 1.67 g considering a flat runway, a crown with 0.75% slope, and a dip with 0.375% slope. A two-stage oleo air curve was developed to give a good load distribution while maintaining a minimum stroke (fig. 64). The same air curve was used for all gears. The gears were designed so that the reactions were all equal for a 1.67-g taxi on a flat runway with the maximum payload uniformly distributed over the span. The reactions for the most critical payload distribution (P/L 2) are shown on figure 65.

The design load envelopes that result from the above considerations are shown on figure 66.

### Structural Design

Wing structural material was determined based on the design loads discussed above, selected material and construction techniques, and minimum gauge constraints.

Advanced technology aluminum was selected over advanced composites on the basis of cost. Because the configuration concept leads to low structural loads, bonded honeycomb construction for skins, ribs, spars, and intercostals is both weight- and cost-effective. The advanced technology aluminum yield and ultimate allowables were estimated to be 8% higher than current allowables. This estimate was based on a review of research activities. No improvement in buckling allowables below yield levels was assumed, since no improvement in the modulus of elasticity is anticipated. Type 7075 material was used for the upper panel H/C skins, upper surface intercostals, and ribs. Type 2024 was used for the lower panel H/C skins and lower surface intercostals. Figure 67 gives the tension, compression, and shear allowables.

Minimum gauge requirements for aluminum honeycomb primary structure were established based on considerations of manufacturing, maintenance, hail, lightning, and bird strike.

Minimum face sheets of 0.03 cm (0.012 in.) are a handling requirement for honeycomb panels. In addition, the inner face sheet gauge cannot be less than 25% of the outer face sheet. In order to allow walking on the upper surface, a minimum gauge of 0.081 cm (0.032 in.) is required for the outer face sheet, which in the lower wing surfaces is 0.041 cm (0.016 in.) minimum gauge. In areas exposed to damage from tires, two layers of fiberglass are required over the outer face sheet.

Considerations of hail damage to the leading edge result in a minimum outer face sheet of 0.091 cm (0.036 in.). Lightning protection of bonded aluminum structure can be achieved with a minimum outer face sheet of 0.041 cm (0.016 in.), provided that all of the exterior skins are adequately joined together electrically. Bird hazard is aggravated on the selected configuration because the wing leading edges carry fuel and present large, flat, strike areas and because portions of the leading edge are in the vicinity of engine exhaust. The honeycomb core in the leading edge was designed so that the fuel tank would not be penetrated by the impact of a 1.81-kg (4-lb) bird at the maximum cruise speed. This leads to a 256 kg/m<sup>3</sup> (16 lb/ft<sup>3</sup>) core tapered from a maximum of 15 cm (6 in.) thick at the leading edge to between 4.45 and 5.08 cm (1.75 and 2 in.) thick at the front spar. The minimum gauge requirements are shown in figure 68.

The total bending material was determined based on design loads, allowables for the selected honeycomb construction, and minimum gauge limitations. In addition, to achieve simplicity in the structure, constant skin gauges were maintained from the airplane centerline to  $n = 0.527$ , and again from  $n = 0.527$  to the wingtip. The spar chord and intercostal material was varied as required to meet the design load conditions. Figure 69 presents the skin material and total bending material of the upper surface and lower surfaces.

Spar shear material was determined from the design shear envelope shown in figure 66. Front and rear spar webs of 0.061 cm (0.024 in.) thickness (inner plus outer face sheets) is adequate for all areas except in the vicinity of the outboard gear where 0.10-cm (0.04-in.) webs are required.

The upper and lower ribs were considered to be one structural unit tied together at the spars by vertical stiffening members and by two tension rods between the bays. The joints between the ribs and the vertical stiffeners at the spars were considered rigid. The tie rods supported tension loads only. The ribs were assumed to share the loads with the effective upper and lower surface skins. The required cap areas and web gauges for a typical rib are shown in figure 70. See figures 37 and 38 for detail design.

## Weight and Balance

Table 8 is the weight and balance statement for the selected configuration. Column 1 shows the weights as initially calculated. Column 2 lists the incremental weights necessary to correct to 1990 technology levels with the resulting, uncycled airplane weights shown in column 3. Column 4 is the final, cycled 1990 airplane with balance shown in the last column. Column 1 is identified as an advanced baseline because some advanced technology materials and systems were incorporated in the airplane initially.

The specific items of advanced technology utilized for this study are listed in table 9. The weight impacts shown were determined, for the most part, by relying on definitions and allowances developed in past studies. Weight analysis techniques used are described in the PARAMETRIC DATA BASE discussion in the Appendix.

The loadability diagram is shown in figure 71. Tolerances and allowances used in constructing this grid are discussed in the Appendix. The floor center is at 38.2% MAC, the fuel volume center is at 40.1% MAC, and the c.g. range halfway between maximum zero fuel weight and maximum taxi weight is 34.8% to 40.3% MAC. The payload volume and the fuel volume are each split roughly equal about their respective centers. This allows great flexibility in positioning the airplane longitudinal center of gravity.

The "available" limits shown are those set by stability and control. The actual loading range may possibly expand to these limits, if structural limitations are not exceeded.

The preliminary weight statement for the selected configuration was estimated in the study cycle based on the ultimate design loads envelope. These loads reflect a load alleviation system designed to reduce net values. Weight data was generated incrementally in three phases:

1. Structural weight needed to satisfy minimum requirements described in table 10
2. Structural weight due to strength requirements
3. Structural weight required to provide pressurization of the cargo compartment

A unit weight for the basic aluminum honeycomb panel was generated considering the criteria of:

1. Minimum gauge face sheets of 0.03 cm (0.012 in.) each, representing a practical handling gauge during manufacturing processes
2. Honeycomb core with wall thickness of 0.00254 cm (0.0001 in.) thickness and cell cross section of 0.476 cm (3/16 in.)
3. Reticulating adhesive of 5 mil thickness per glue line
4. Material primers and finishes of standard aircraft quality

This represents a practical minimum-weight honeycomb panel which must be added to cover design considerations based on experimental tests, current production honeycomb experience, and advanced engineering design.

Additional design criteria applied to the honeycomb configuration are as follows:

1. Exposed face sheets are increased to 0.041 cm (0.016 in.) thickness to prevent damage from corrosive pitting. This applies primarily to the lower wing surface.
2. The outer face sheets on the wing upper surface must be incremented to 0.081 cm (0.032 in.) to provide walk-on capability for ground service and maintenance.
3. Leading edge outer face sheets were increased to 0.091 cm (0.036 in.) to prevent damage from hail strike.
4. The inner skins of the leading edge, the fuel tank end bulkheads, and the front spar were increased for fuel hydrostatic head pressure with gauge increases to 0.041 cm (0.016 in.) at the upper surface and 0.051 cm (0.020 in.) at the lower surface. It is assumed that the fuel vent system is adequate to prevent pressurization of the fuel cavity during the filling operation.
5. The leading-edge fuel cells require protection to prevent penetration of the fuel cavity on impact with flying birds. The criterion used was the assumed impact of the airplane at design cruise speed of 518.56 km/hr (280 KEAS) with a 1.81-kg (4-lb) bird flying at 111 km/hr (60 KEAS). Both inner and outer face sheets require 0.091 cm (0.036 in.) thickness. The core must be increased to 256 kg/m<sup>3</sup> (16 lb/ft<sup>3</sup>) density and increased to 15.24 cm (6 in.) maximum depth at leading edge and tapered to 3.81 cm (1.5 in.) at the front spar location.

These increments are tabulated in figure 72 with a typical wing section showing zones affected by each criterion.

Additional unit weight increments were calculated for the following items:

1. Moisture sealant drip coat for square-edge panels
2. Spanwise "T" and plate splice joints with additional doublers (1.2 times skin thickness) and adhesives
3. Spanwise spar chords and associated installation hardware
4. Dense-core beef-up for the spanwise intercostals and chordwise ribs
5. Rib corner attachments and reinforcements
6. Laminated attachment chords for ribs and intercostals

These developed unit weights were applied to the specific structural cross sectional arrangement drawing of the selected configuration to complete an integrated design, which accounts for the special criteria. An additional factor of 8% over the theoretical value was applied to the basic honeycomb panel weight for nonoptimum weight not accounted for.

Additional weight increments for strength design were evaluated by the methods discussed in the Appendix. To reiterate this analytical procedure:

1. Net aeroelastic loads were generated employing an assumed load-alleviating system.
2. Geometry of the selected configuration was provided and advanced technology honeycomb allowables were used in the analysis.
3. Required strength-designed bending and shear material section areas were generated.

The required areas were distributed in the structural analysis to provide relatively constant honeycomb panels with variable spanwise stiffeners.

The strength-designed weight increments for bending and shear material were evaluated from these areas by removal of all areas considered by the special criteria tabulated in figure 68. It is noted that only face sheets are assumed to carry bending and shear loads in honeycomb panels.

Strength-sized interspar ribs were manually sized. Incremental weights for the strength-sized ribs consist of skin shear and rib chord material requirements above the basic aluminum honeycomb panel with assumed minimum chord areas.

### **Pressurization Effects on Design**

The upper and lower surfaces, spar panels, tension ties, and ribs were sized to determine strength requirements for pressure considering three factors on pressure alone and one and one-half factors on pressure acting with design loads. The results for  $68\,948\text{ N/m}^2$  (10 psia) are presented.

The skin panels were assumed to be simply supported at ribs and intercostals, while the spar webs were simply assumed to be supported at ribs and spar caps. The upper surface skin gauge was increased by 0.048 cm (0.018 in.) inboard of station 0.527. In the lower surface, the increases were 0.061 cm (0.024 in.) inboard and 0.041 cm (0.016 in.) outboard. The spar webs were increased by 0.013 cm (0.005 in.) all along the span.

The most significant changes that result from pressurization occur in the ribs. A typical rib redesigned for 10 psia pressure is shown in figure 73.

The impact of pressurization on the selected configuration weight is summarized by table 11. The major penalties are in the interspar rib face sheets and rib chords. Significant increases are also required in the cover material face sheets and core.

The total pressurization penalty shown is relatively small for large flat panels, when compared to conventional construction due to the inherent structural characteristics of honeycomb panels.

## **PERFORMANCE CHARACTERISTICS**

The flight profile and associated time, fuel, and distance are based on 1967 ATA international mission rules. A Boeing computer program described in the Appendix, is used to compute

the performance. The missions are calculated for a design range of 5556 km (3000 nmi) and a gross payload of 31 615 kg (697 800 lb), corresponding to an NPD of 160 kg/m<sup>3</sup> (10 lb/ft<sup>3</sup>). Aerodynamic, propulsion, structures, and weights technologies correspond to the 1990 time period and are established as indicated above in Technology Definition and Analysis. The engines are sized by the thrust required at cruise for minimum takeoff gross weight. This results in a takeoff field length of 2134 m (7000 ft), well below the 3658 m (12 000 ft) specified in the contract guidelines. The corresponding range factor is 24 071 km (13 000 nmi). The resultant performance is summarized in table 12. The takeoff gross weight is 0.759 million kg (1.674 million lb) with an operating empty weight fraction of 0.3145.

Payload, block fuel, and block time are presented as a function of range in figure 74. The 65% loading curve is presented for use in the economic studies presented below.

Figure 75 presents FAR Part 25 takeoff field length as a function of takeoff gross weight. Data are presented for sea level standard day conditions.

## REFERENCE CONFIGURATION STUDY

### REFERENCE CONFIGURATION DEFINITION

The reference configuration was chosen from the dedicated air freighter (DAF) studies currently being performed in the Boeing Preliminary Design group. Figure 76 shows a three-view drawing of the fuselage-loaded airplane, which is an outgrowth of those studies. Developed as an intercontinental air freighter with a wide (double lobe) fuselage, it offers several advantages to the operator. All cargo is carried on one deck level, with loading accomplished through a nose door with a sill height of 215.38 cm (84 in.) above ground using a kneeling landing gear. The cargo compartment was sized for 2.44- by 3.098-m (8- by 10-ft) containers and military cargo, but for this study the cargo volume is equivalent to thirty-two 2.44- by 2.44- by 6.096-m (8- by 8- by 20-ft) containers. The double-lobe fuselage shape is adaptable to pressurization if this becomes a requirement.

Because of the more conventional geometric configuration of the reference airplane, the flight control system requirements differ from those of the DLF selected configuration. Low-speed control and takeoff-rotation requirements establish the minimum horizontal tail size of the reference configuration. The minimum tail size, as established by control requirements, satisfies the unaugmented longitudinal stability criterion of time-to-double-amplitude of 6 seconds, permitting use of a handling-qualities SAS to meet handling-qualities criteria. There is therefore little advantage in decreasing horizontal tail size to meet the relaxed stability criterion of time-to-double-amplitude of 2 seconds with the consequent necessity of hard SAS implementation. Analyses of the lateral-directional stability characteristics of the reference configuration demonstrate satisfactory Dutch roll frequency and damping and spiral stability so that no requirement exists for a lateral-directional stability augmentation system.

### REFERENCE CONFIGURATION TECHNOLOGY DEFINITION AND ANALYSIS

Table 13 is the weight and balance statement for the reference configuration. The reference configuration baseline, the incremental weights necessary to correct the baseline to 1990

technology, and the 1990 uncycled reference airplane are shown by columns 1, 2, and 3, respectively. Column 4 is the final, cycled 1990 airplane with balance shown in the last column. The advanced technology items utilized and the associated weight impact are listed in table 14.

The reference configuration loadability diagram is shown in figure 77. Tolerances and allowances used were similar to those used for the selected configuration.

The same criteria and rationale used to develop the 1990 technology levels for the DLF selected configuration were applied to obtain the reference configuration levels. The results for the two configurations are compared in table 15. The most noteworthy differences are in the M (L/D) improvement shown for tip fins and active controls.

The gain in aerodynamic efficiency, M (L/D), due to tip fins, for the DLF selected configuration is 16%, while that of the reference configuration is only 4%.

The 2% increase in reference configuration M (L/D) due to tip fins results from an 8% aft shift in c.g. to approximately 40% plus a reduction in tail size compatible with reduced stability. It is assumed that an appropriate shift in wing and landing gear location can be accomplished. The 2% gain is evenly distributed due to reduced trim drag and tail size.

The resulting 1990 reference configuration drag polar is presented in figure 78. The procedures used are outlined in the Appendix, PARAMETRIC DATA BASE.

## CONCEPT COMPARISON

### TECHNICAL COMPARISON

The flight profile, mission rules, and procedures used to establish reference configuration performance are identical to those used for the DLF performance. The gross payload, corresponding to an NPD of  $160 \text{ kg/m}^3$  ( $10 \text{ lb/ft}^3$ ), is 194 773 kg (429 000 lb). The takeoff gross weight is 467 200 kg (1.03 million lb). Payload, block fuel, and block time are presented as a function of range for the reference configuration in figure 79. The 65% loading curve is presented for use in the economic comparisons. Though somewhat smaller than the DLF selected configuration, the results can be normalized for comparison. Table 16 presents the technical comparison of the selected and reference configurations.

#### Aerodynamic Performance

The reference airplane exhibits superior aerodynamic performance over the selected configuration. It cruises at higher Mach number ( $M = 0.78$  versus  $M = 0.68$ ) at higher aerodynamic efficiency ( $L/D = 21.9$  versus  $16.6$ ) and airplane cruise efficiency (range factor  $RF = 34\,818$  compared with  $24\,076$ ). The cruise altitude is higher ( $10\,058 \text{ m}$  versus  $8534 \text{ m}$  ( $30\,000 \text{ ft}$  versus  $24\,800 \text{ ft}$ )). The airplanes have similar wing spans; the DLF having only 10% longer span but almost twice the wing area.



## Structural and Payload Efficiencies

The structural efficiency of the distributed-load configuration selected is considerably better than that of the reference conventional airplane (OEW/TOGW = 0.3145 versus 0.3848). This saving in structural weight fraction is barely offset by the increase in fuel weight fraction for the DLF to yield nearly identical payload to gross weight fractions (DLF PL/TOGW = 0.4171 versus 0.4169 for the reference configuration).

Figure 80 presents the OEW, payload, and fuel weight fractions as a function of MTOW for the selected and reference configurations. An additional breakdown of structure and wing weight is included to show the weight fraction effects of combining the functions of the wing and body of a conventional configuration in a span-loaded wing.

## Takeoff and Landing Performance

The lower cruise L/D of the DLF dictates a higher installed thrust-weight ratio ( $T/W = 0.227$  for the DLF versus  $T/W = 0.203$  for the reference airplane). This higher thrust, when coupled with the lower wing loading  $439$  versus  $591 \text{ kg/m}^2$  ( $90$  versus  $121 \text{ lb/ft}^2$ ), yields a much shorter takeoff field length for the DLF ( $2134$  versus  $3566 \text{ m}$  ( $7000$  versus  $11700 \text{ ft}$ )). The takeoff noise level of the DLF will, therefore, be much lower and the airplane will have to carry much less sound suppression material. The over-the-wing engine exhaust will also contribute to a reduced noise level for the DLF. These noise considerations could have important economic consequences, since round-the-clock operations are envisioned and night curfew laws could have a restrictive effect.

## Fuel Consumption

Distributed load designs at the selected airplane size will burn more fuel than the reference conventional airplane. The block fuel to payload ratio is 60% better ( $0.5512$  versus  $0.3843$ ) for the reference airplane than for this size DLF. Airplane productivity relative to gross weight favors the conventional airplane ( $M(PL/GW) = 0.3235$  to  $0.2836$ ), but relative to empty weight, the selected DLF would be clearly superior. ( $(PL/OEW) M = 0.902$  for the DLF versus  $0.841$  for the conventional airplane.)

The conclusion to this technical comparison is that the reference airplane delivers more payload per pound of fuel, but the selected airplane delivers more payload per pound of airplane purchased. Further, since the DLF is considerably cheaper per pound of empty weight ( $\$304/\text{kg}$  ( $\$137.9/\text{lb}$ ) compared with  $\$355/\text{kg}$  ( $\$161.20/\text{lb}$ )), the DLF has an even greater advantage in airplane first cost per pound of payload delivered ( $104$  versus  $148.8$ ). The ultimate economics will therefore depend on the relative weight-of-fuel cost versus airplane cost in the final accounting.

## ECONOMIC COMPARISON

A comparison of the selected and reference configuration's operating economics versus range is shown in figure 81. This comparison shows the importance of including investment costs along with DOC in assessing and comparing airplanes. In terms of DOC alone, the reference

configuration shows superior economics except at ranges below about 1389 km (750 nmi). At the 5556 km (3000 nmi) design range, the difference in DOC between the two configurations is 0.096¢/Tkm (0.14¢/GTM) or 2.7%, and at 11 112 km (6000 nmi), the difference is 0.80¢/Tkm (1.17¢/GTM) or 16.9%.

However, the addition of airplane investment cost to account more fully for airplane price alters the comparison significantly. The selected configuration is shown to have better DOC plus AIC than the reference configuration up to 8519 km (4600 nmi), past which the reference configuration economics are better. The improvement in the selected configuration with respect to the reference configuration using DOC plus AIC is due to the lower production cost design of the selected configuration. At the 5556 km (3000 nmi) design range the selected configuration DOC plus investment cost of 0.25¢/Tkm (0.37¢/GTM), or 5.4% lower than for the reference airplane. At 11 112 km (6000 nmi), the reference configuration DOC plus AIC is 0.51¢/Tkm (0.75¢/GTM), or 7.6% lower than the selected configuration. The better economics at long ranges for the reference configuration is due to its aerodynamic efficiency. The reference airplane range factor is 34 818 as compared to 24 076 for the selected configuration.

To gain more insight into the economic differences between the two airplanes, figure 82 shows a cost breakdown comparison at the 5556-km (3000-nmi) design range. This breakdown shows the main differences to be fuel cost (which favors the reference airplane) and those costs that are a direct function of airplane price, e.g., insurance, depreciation, and investment cost (which favors the selected configuration). Crew cost also favors the selected configuration due to these costs being distributed over a larger payload. Maintenance costs are nearly equal.

### Sensitivities

The cost sensitivity to range has already been presented on figure 81. The DOC plus AIC for both airplanes decreases with increasing range and the curves are approximately parallel out to 5556 km (3000 nmi). Past this point the costs increase with range, with the selected configuration cost increasing more rapidly than for the reference configuration. The DOC plus investment cost for the two airplanes is equal at 8519 km (4600 nmi).

Additional cost sensitivity comparisons are presented on figure 83. DOC plus AIC data for both airplanes are shown at 5556 km (3000 nmi) range. The shaded bars show the selected configuration costs and the unshaded bars show the reference airplane data. The base data are shown in the bars at the far left. The sensitivity to changes in fuel price is shown in the next two sets of bars. Due to the greater fuel efficiency of the reference configuration, the reference airplane benefits most from an increase in fuel price and the selected configuration benefits most from fuel price decreases. The DOC plus AIC for the two airplanes would be equal at a fuel price of 59¢/gallon. The approximate doubling in fuel price from 37¢/gallon to 75¢/gallon causes a 35% increase in DOC plus AIC for the selected configuration and a 25% increase for the reference configuration.

Since the cost of maintaining the two airplanes is approximately equal, as shown on the previous figure, the sensitivities to changes in maintenance cost level are also approximately

the same when measured in absolute terms. The percentage change in DOC plus AIC for changes in maintenance costs is slightly more for the selected configuration, since the maintenance cost is a larger percentage of the total DOC plus AIC for this airplane. A change from three to two crewmembers benefits the reference configuration more than the selected configuration since crew cost for the base case is a larger percentage of the total cost for the reference airplane.

The sensitivity to airplane price shows that decreases in price favor the reference airplane and price increases do less harm to the selected configuration. Because price directly affects a larger portion of DOC plus AIC than any of the other parameters shown, a percentage change in price has greater influence on DOC plus AIC than a similar percentage change in any one of the other parameters.

The next two sets of bars show sensitivity to aircraft utilization. The base case utilization is based on airplane availability of 17.5 hours per day, 341 days per year, and 5% airplane backup. The bars show the effect of changing utilization to 15 and 20 available hours per day. The increased utilization aids the reference configuration relatively and decreased utilization does less harm to the selected configuration.

### Effect of Airplane Size

The economic comparisons just presented are critically dependent on the assumed distributed-load airplane size. The selected configuration was arbitrarily selected to yield a nominal payload capability of about 272 155 kg (600 000 lb) of revenue payload at 160 kg/m<sup>3</sup> (10 lb/ft<sup>3</sup>) net density. The actual gross payload is 316 517 kg (697 800 lb).\* The maximum gross payload of the reference configuration is 194 682 kg (429 200 lb). From previous Boeing studies of conventional design airplanes it appears that this payload is very nearly optimum for this type of design in attaining minimum DOC plus AIC. Increases in payload would cause poorer economics. However, the economics of the distributed-load airplanes were shown to improve very substantially in the parametric study as maximum payload capability is increased. These trends are presented in figure 84. Figure 85 shows a comparison of two airplanes from the parametric study with equal design densities but different payload capabilities. The increase in size from 317 515 kg (700 000 lb) to 544 310 kg (1 200 000 lb) maximum gross payload capability yields a decrease in DOC plus AIC of 0.823¢/Tkm (1.2¢/GTM), due primarily to greater aerodynamic efficiency, which shows up in fuel savings.

Airplanes with larger payload capability would not directly serve many marginal cities as airfreighters do today. They would be utilized in a hub-and-spoke concept, flying only between a limited number of large transportation centers. These centers would be fed by smaller aircraft as well as by surface modes. Such a concept has the potential to cut the airplane DOC plus AIC as well as the indirect operating costs through the use of very large airplanes.

\*The actual payloads are slightly different from the nominal because the thumbprint computer program is recycled to a finite closure tolerance. The actual net payload at this gross payload would be the gross payload minus the tare weight of 52 standard containers:

$$\text{Net payload} = 316\,517 \text{ kg} - 521\,871 \text{ kg} \text{ (697\,800 lb - 52 (1920 lb))} = 271\,225 \text{ kg} \text{ (597\,600 lb)}$$

$$\text{Net payload density} = \frac{271\,225}{52 \times 32.28} = 161.58 \text{ kg/m}^3$$

$$\left( \frac{597\,600}{52 \times 1190} = 10.087 \text{ lb/ft}^3 \right)$$

## **Other Effects**

An additional factor that has not been addressed in this study is the effect of wing sweep on the distributed load designs. Preliminary Boeing studies indicate that the increased airplane speed and productivity resulting from sweeping the wings offer significant decreases in DOC plus AIC. Corresponding decreases are not possible for the conventional airplane design, since it already incorporates wing sweep.

## **AREAS FOR FURTHER REFINEMENT AND STUDY**

### **REVISED STRAIGHT-WING AIRPLANE CONFIGURATION RESTRICTED TO STANDARD CONTAINER SIZE**

The data base for performing this contract was built around a four-bay wing cross section that would contain an M-60 tank in the center bays. The fore and aft extreme bays were higher than necessary to carry standard size containers for three- and four-bay configurations. The NASA contract work statement calls for the use of 2.44- by 2.44-m (8- by 8-ft) containers. There is an unknown penalty caused by the height requirements to carry the M-60 tank. A configuration should be developed keeping exactly the same planform and container volume as the DLF selected configuration but reducing the t/c to 18.5% in order to precisely enclose four 2.44- by 2.44-m (8- by 8-ft) containers side by side in the airfoil. The data base available from the parametric studies and other work done during the contract should enable the contractor to perform this additional work efficiently.

### **PROP-FAN PROPULSION INSTALLATION**

Span-distributed-load aircraft require relatively thick airfoils to contain the payload, resulting in low cruise Mach numbers. Current prop-fan studies planned for cruise speeds above Mach 0.8 may not reveal the particular advantages of prop-fans when applied to cargo type aircraft with optimum aerodynamic cruise performance between Mach 0.6 and 0.75 at relatively low altitudes. The current NASA contract dealing with span-distributed-load designs provides a logical base for application of the prop-fan concept to aircraft that operate at low cruise speeds and that do not involve passenger reaction effects. Studies should be conducted to determine the relationship between airplane economics and wing thickness for an optimum power plant.

### **WING WEIGHT REDUCTION**

An examination of figure 7 shows that the effort to reduce basic structural weight in the wing has been successful, with the bending and shear materials and ribs contributing only 25.8% of the wing weight. The other components in the wing are prime candidates for further refinement in the design. The bird-strike penalty is considered to be excessive but could not be studied further under the present contract. The group of items relating to airplane control at the present time weigh 27.6% of the wing weight, more than the basic structure of the wing. Detail design in this area could provide some very important weight reductions. The successful application of distributed-load concepts will require careful scrutiny of every item in the weight statement if the full benefits are to be realized.

## **THE USE OF COMPOSITES**

The use of composites on distributed-load aircraft will result in a considerably different optimization compared to conventional aircraft with large bending moments at the wing root. The distributed-load aircraft tends to have constant cross sections that will allow long lengths of composites without joints and, when joints are used, will result in small loads in the joints.

The primary unsolved problem in the use of composites in a conventional structure is in joints, especially for highly loaded joint design. In addition, much of the benefit of the composites is lost in the joint design. With a distributed load configuration with few and lightly loaded joints, much of the potential benefit of composites can actually be realized. The current contract calls for the use of 1990 technology that would normally involve the use of composites, but the data base available is insufficient to properly assess the value of composites in the design within budget constraints.

## **OPTIMUM SIZED AIRPLANE**

The parametric study showed that the economics improved strongly with increases in airplane size at the selected throughput of 118 billion Tkm (67 billion RTM) per year. A rationale should be developed to select an airplane size based on the current data base that would assess the tangible and intangible factors to develop an optimum sized airplane configuration for a throughput of this magnitude.

## **THICK AIRFOIL TECHNOLOGY**

The 0.215 thickness ratio airfoil used on the DLF selected configuration suffers a substantial penalty due to form drag, the form factor being double that of similar 0.15 thickness ratio airfoils. While technology advances for thick airfoils are anticipated to result in some drag reductions of approximately 4%, this amounts to only 0.5% in cruise M (L/D). Thus, in order to have meaningful impact, the form drag reductions would have to be appreciably greater. It is, therefore, recommended that alternate airfoils, such as blunt-based airfoils with some degree of base bleed (which offer the possibility of both form drag and Mach number improvements), be investigated and the system trades established.

## **LAMINAR FLOW CONTROL**

The studies performed in reference 1 indicate that cycled gains in M (L/D) as high as 25% can be attained by applying laminar flow control to the wing and surfaces of the study airplanes. These gains were accompanied by reductions in takeoff gross weight in the order of 17% and fuel savings as high as 28%. Laminar flow control thus appears to offer the greatest single return of any of the technology concepts presented for distributed-load freighters. The implication of these gains with respect to power requirements, structural/weight implications (especially regarding the honeycomb skins of the DLF), configuration impact, and cost are not known. It is recommended that a study be performed to investigate the benefit and trades resulting from application of laminar flow control to the wing and horizontal tail of the distributed load-freighter.

## OVERWING ENGINE INSTALLATION

As noted previously, the installation of engines over the leading edge of the DLF wing is expected to result in a more severe interference problem than for under-the-wing installations. Since this arrangement is favored by the design of the DLF, the details of this installation should be established. It is proposed that test data of past installations of this type be examined with the aim of confirming the present interference levels. A subsequent program to minimize adverse interference by appropriate local contouring and/or acceleration bodies can be accomplished by application of a Boeing Potential Flow Program. A simplified wind tunnel program should then be performed to confirm the results. Some recent data suggest a reduction in induced drag due to upper surface blowing. The implications of these gains relative to the selected DLF configuration should be established and a study (concurrent with the interference study) should be performed to indicate any potential benefit.

## CONTROL AND GUIDANCE RESEARCH

The DLF airplane will have a large wingspan, unconventional configuration, and a very limited range of acceptable bank and pitch attitudes at touchdown. Work done to date indicates that an SAS control law can be synthesized to stabilize the lateral dynamic characteristics and that with the use of side-force generators, lateral maneuverability for touchdown positioning comparable to current large airplanes will be provided.

What remains to be done is to demonstrate that the lateral SAS synthesis is compatible with the structural mode characteristics of a representative airplane and to investigate the guidance system requirements to achieve acceptable touchdown position and attitude dispersions in the presence of realistic guidance system noise, offsets, etc., with realistic wind shear and turbulence.

Analysis and simulation of the airframe, control system, and guidance system (including the effects of failure cases, guidance noise, and atmospheric conditions) are required to establish the feasibility and the ground and airborne system requirements for this class of airplane.

## CONCLUSIONS

1. DLF economics continually improves with size while conventional airplane peaks at about 450 000 kg (1 million lb) gross weight.
2. DLF has slightly better economics (5% lower DOC + AIC) at the study payload size than the most advanced conventional air freighter (1990 technology) at its optimum size and the DLF improves to 25% better than the optimum conventional when the DLF size is doubled.
  - At approximately 272 000 kg (600 000 lb) net payload the lower production cost of the DLF approximately balances the lower fuel cost of the advanced conventional freighter.
  - At 544 311 kg (1 200 000 lb) net payload the fuel cost of the DLF equals the fuel cost of the advanced conventional freighter.
3. Based on optimum economics, the optimum thickness ratio for the DLF varies with size:

<u>NET PAYLOAD kg (lb)</u>	<u>THICKNESS RATIO</u>	<u>NO. OF CARGO BAYS</u>
272 155 (600 000)	0.24 to 0.215	3 or 4
408 233 (900 000)	0.215 to 0.19	4 or 5
544 311 (1 200 000)	0.19 to 0.16	5 or 6
680 389 (1 500 000)	0.16 to 0.14	7

4. Distributed-load freighter concept has potential for further improvement in:
  - Sweep
  - Optimum payload size
  - Reduced cargo bay height requirement
  - Weight reduction

## EXHIBIT

to the extent that the same are not otherwise provided for in the above schedule of assets and liabilities.

The above schedule of assets and liabilities is based on the best information available to the undersigned at the time of the filing of this report, and is subject to change as more information becomes available.

The undersigned hereby certifies that the above schedule of assets and liabilities is true and correct to the best of his knowledge and belief, and that the same are not otherwise provided for in the above schedule of assets and liabilities.

Witness my hand and the seal of the above-named corporation this 1st day of January, 1964.

\_\_\_\_\_  
 Secretary

ASSETS	LIABILITIES	NET ASSETS
Cash	Accounts Payable	100,000.00
Accounts Receivable	Notes Payable	200,000.00
Inventory	Other Liabilities	300,000.00
Fixed Assets		400,000.00

The above schedule of assets and liabilities is based on the best information available to the undersigned at the time of the filing of this report, and is subject to change as more information becomes available.



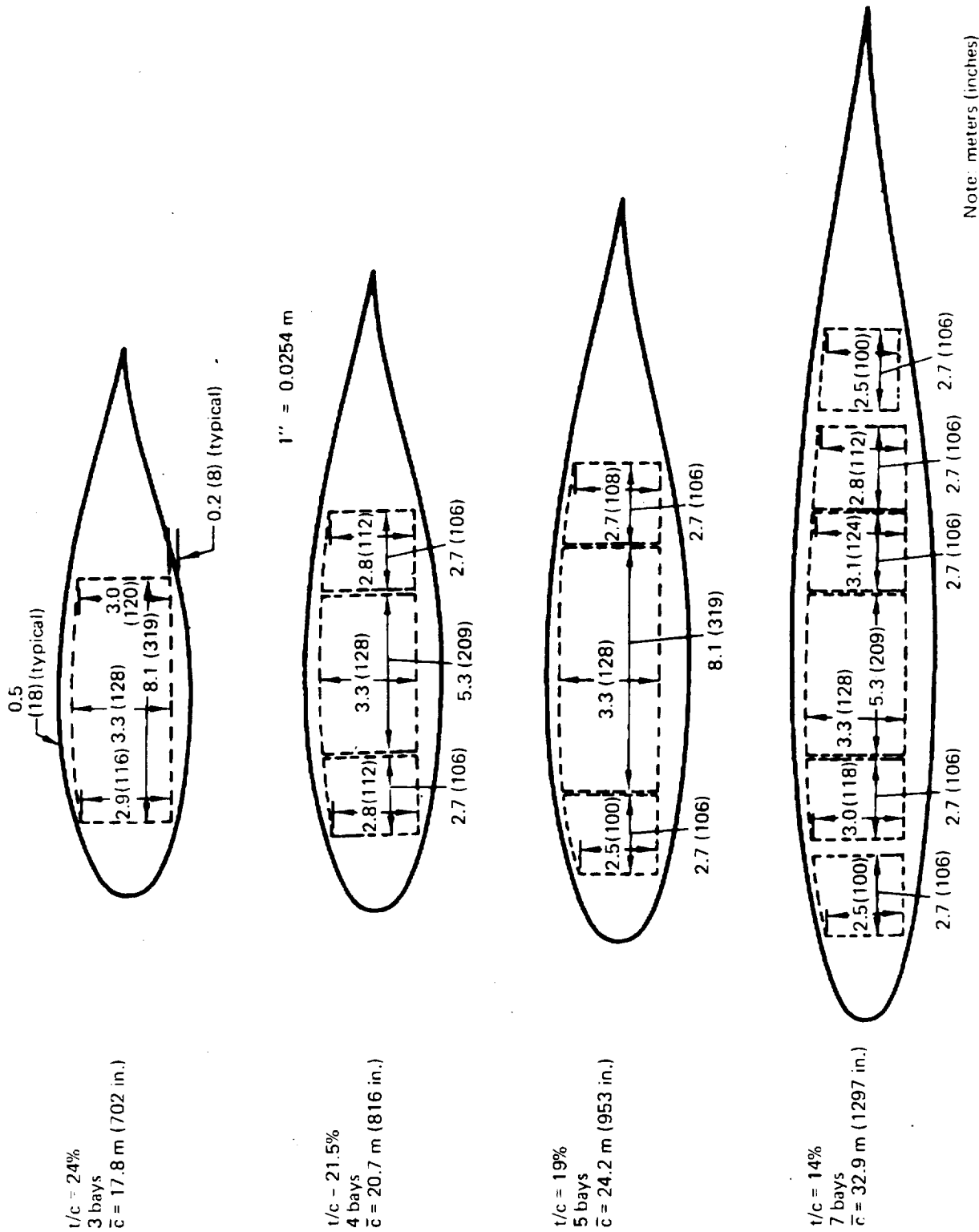


Figure 1.—Wing Section Utilization

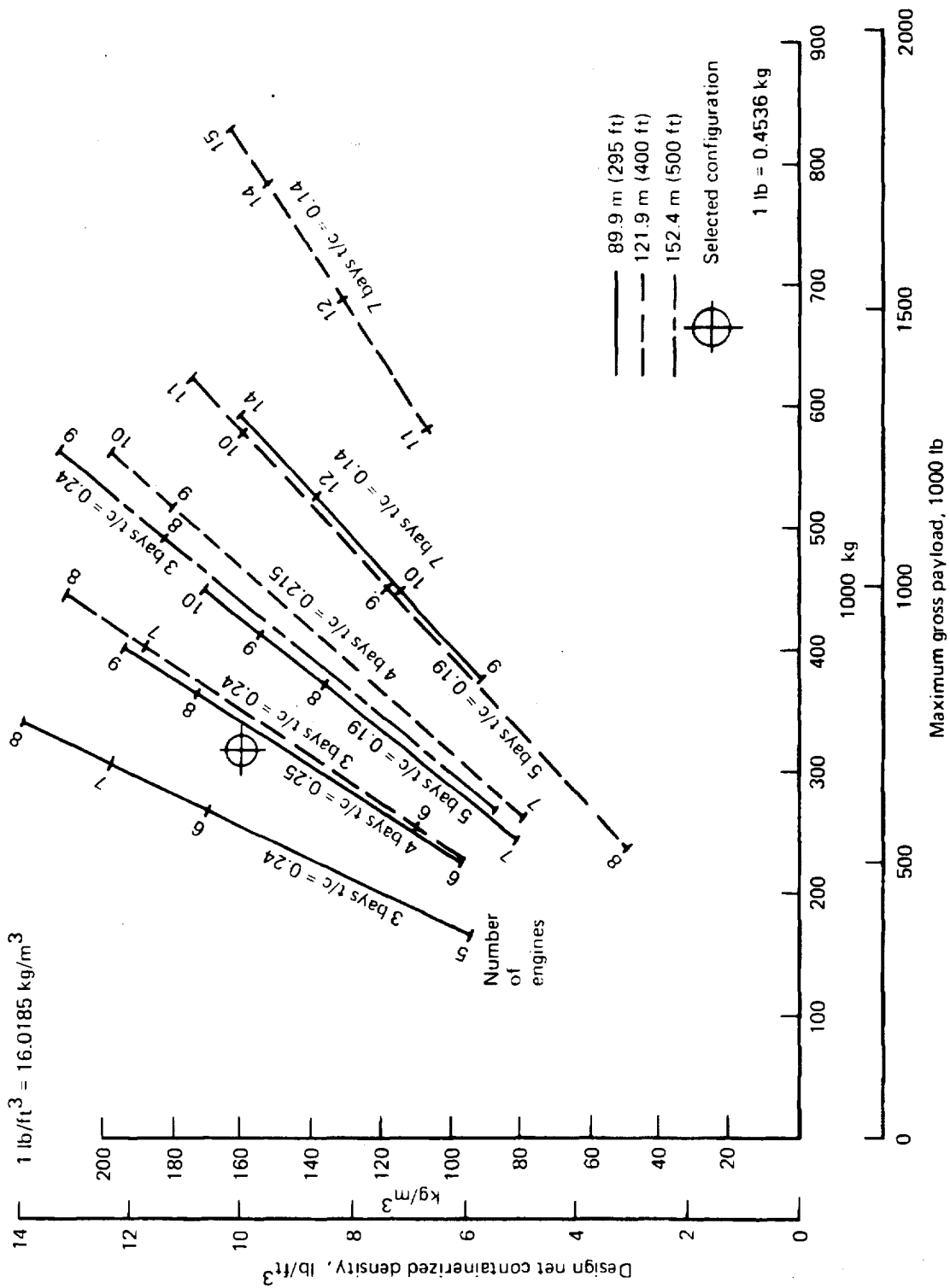


Figure 2.—Parametric Study Payloads

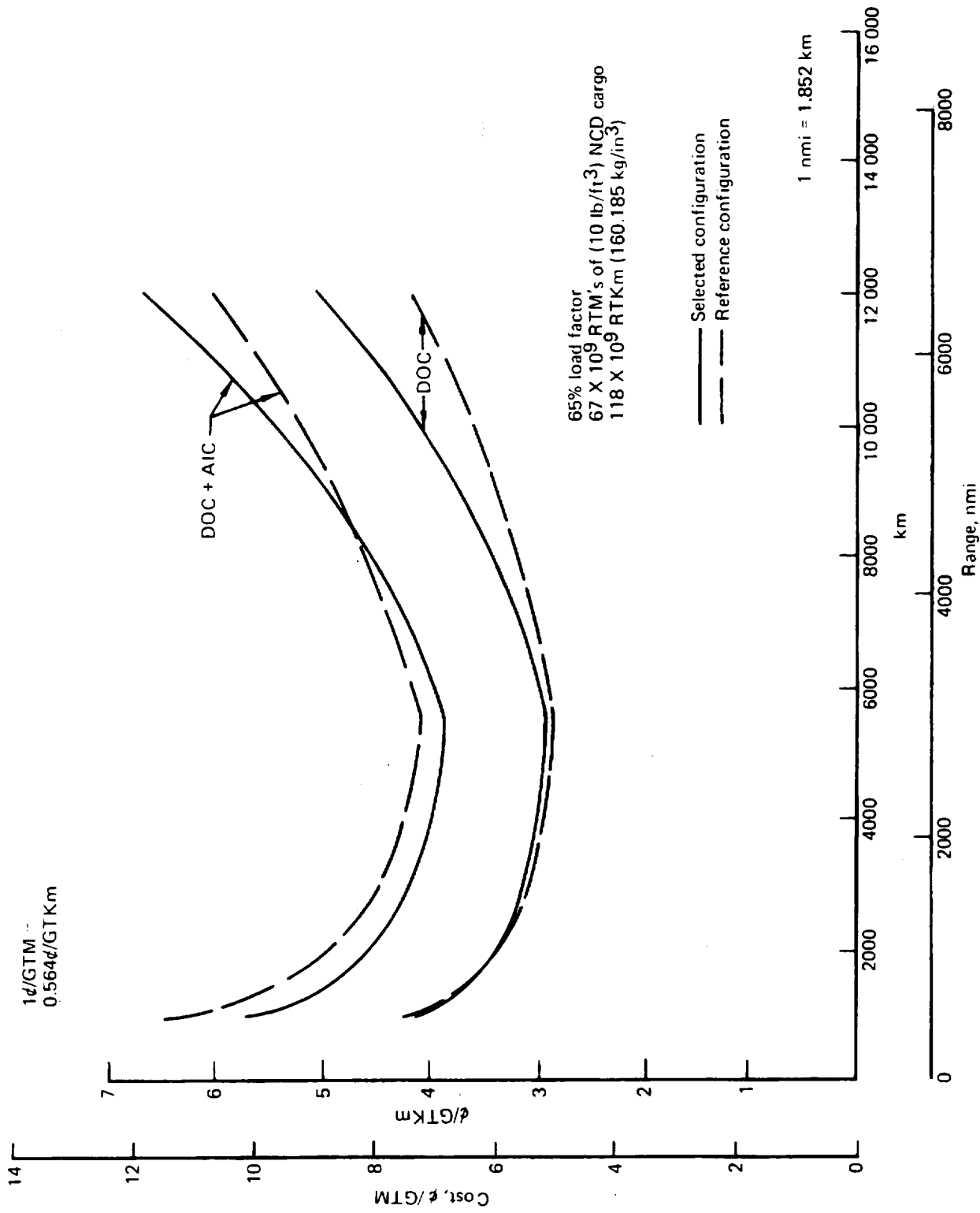


Figure 3.—Economic Comparison Selected Versus Reference Configuration

1990 Technology

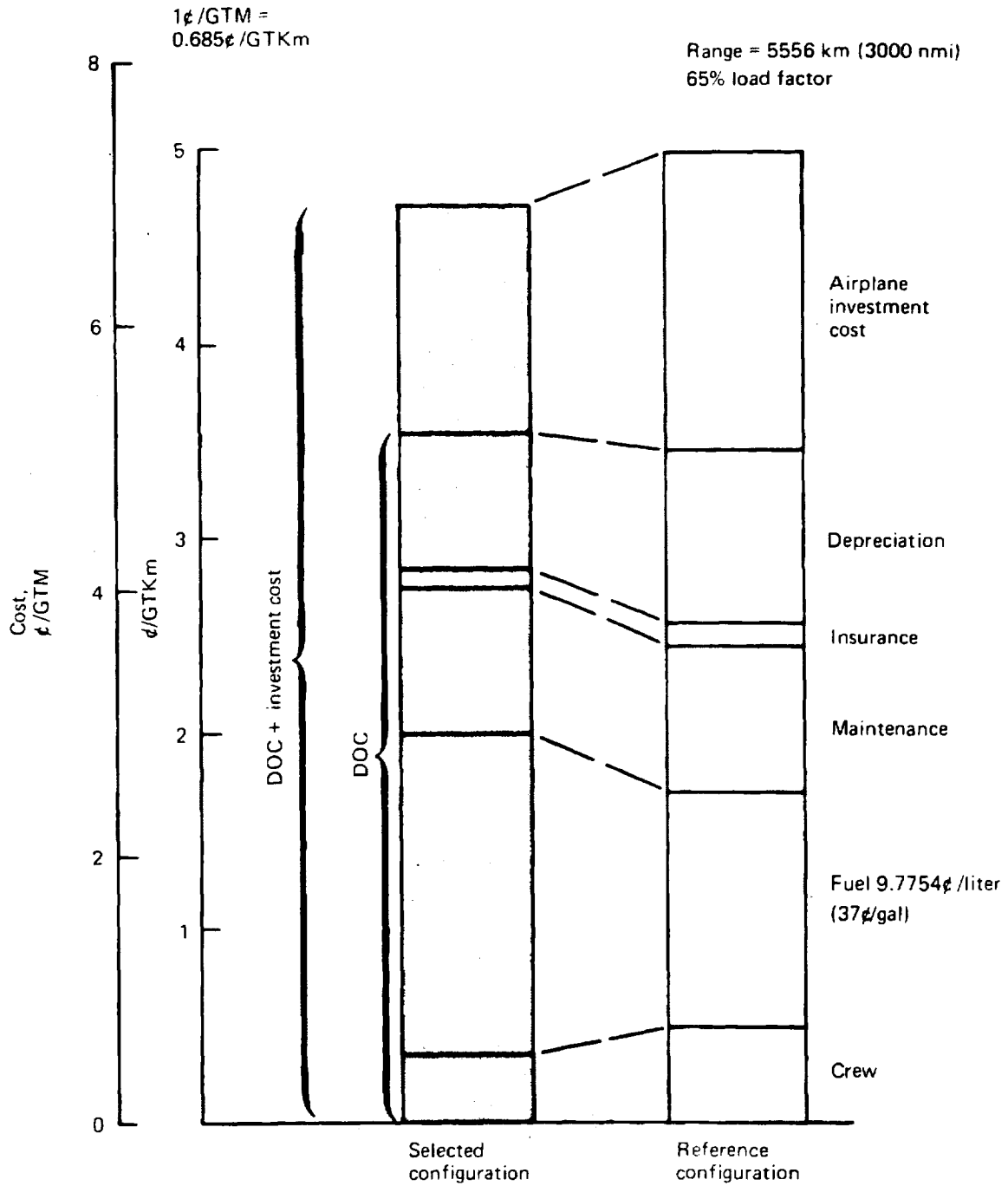


Figure 4.—Cost Breakdown Comparison Selected Versus Reference Configurations

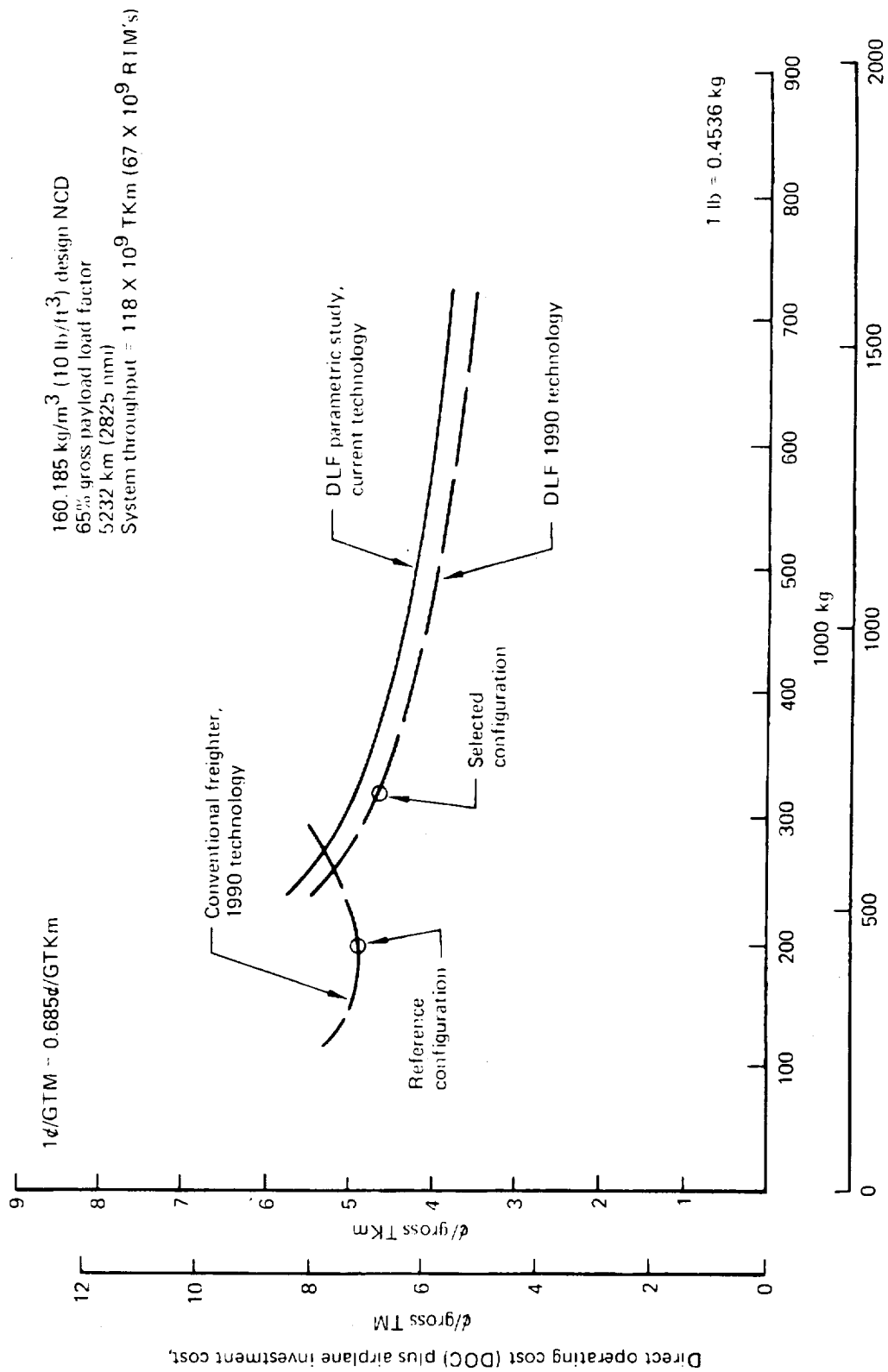


Figure 5.—Distributed Load and Conventional Freighter Comparative Economics

Parametric Study  
1980 Technology

Range = 5232 km (2825 nmi)  
65% load factor  
NCD = 148.97 kg/m<sup>3</sup> (9.3 lb/ft<sup>3</sup>)

1  $d$ /GTM =  
0.685 $d$ /GTKm

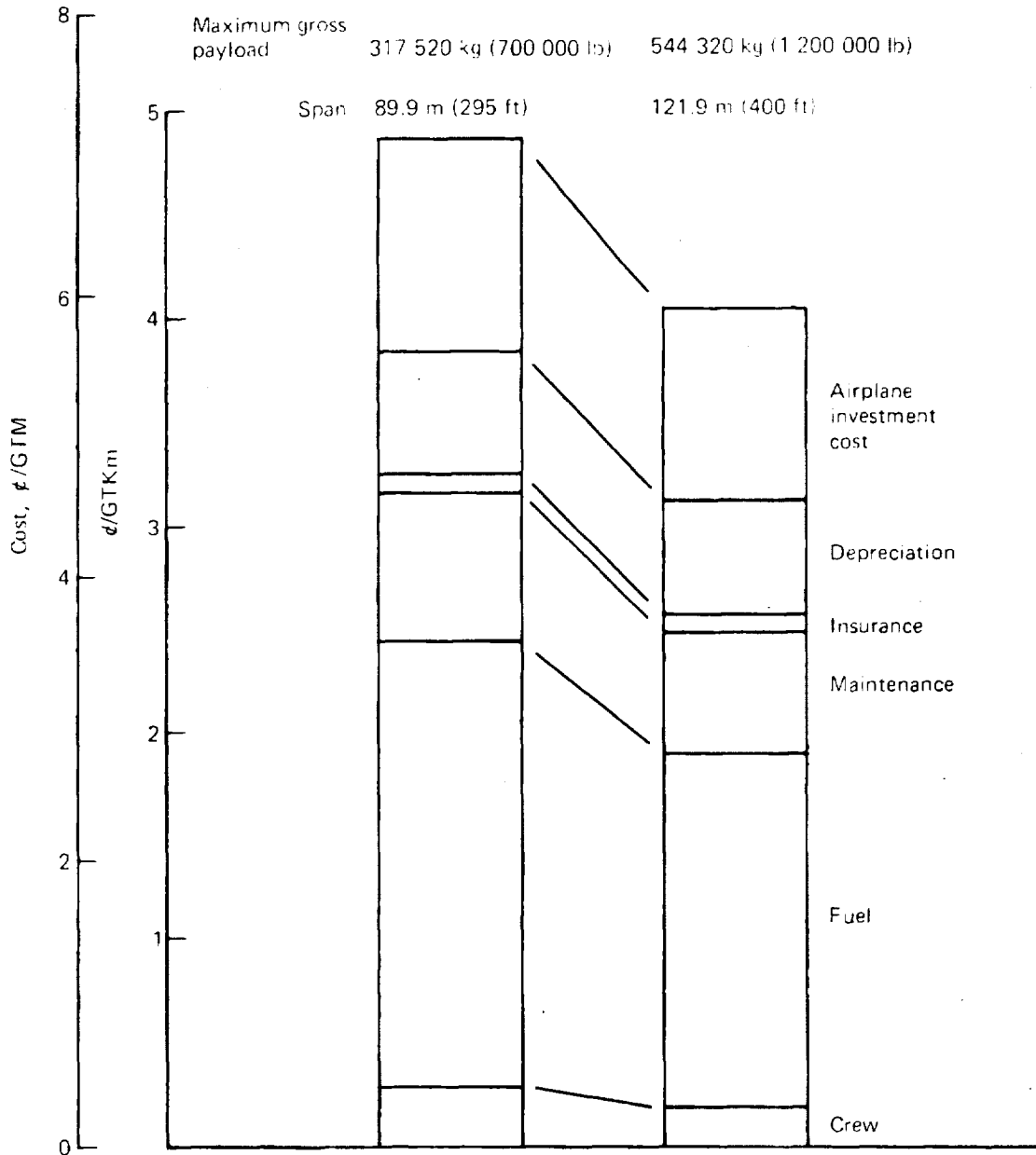
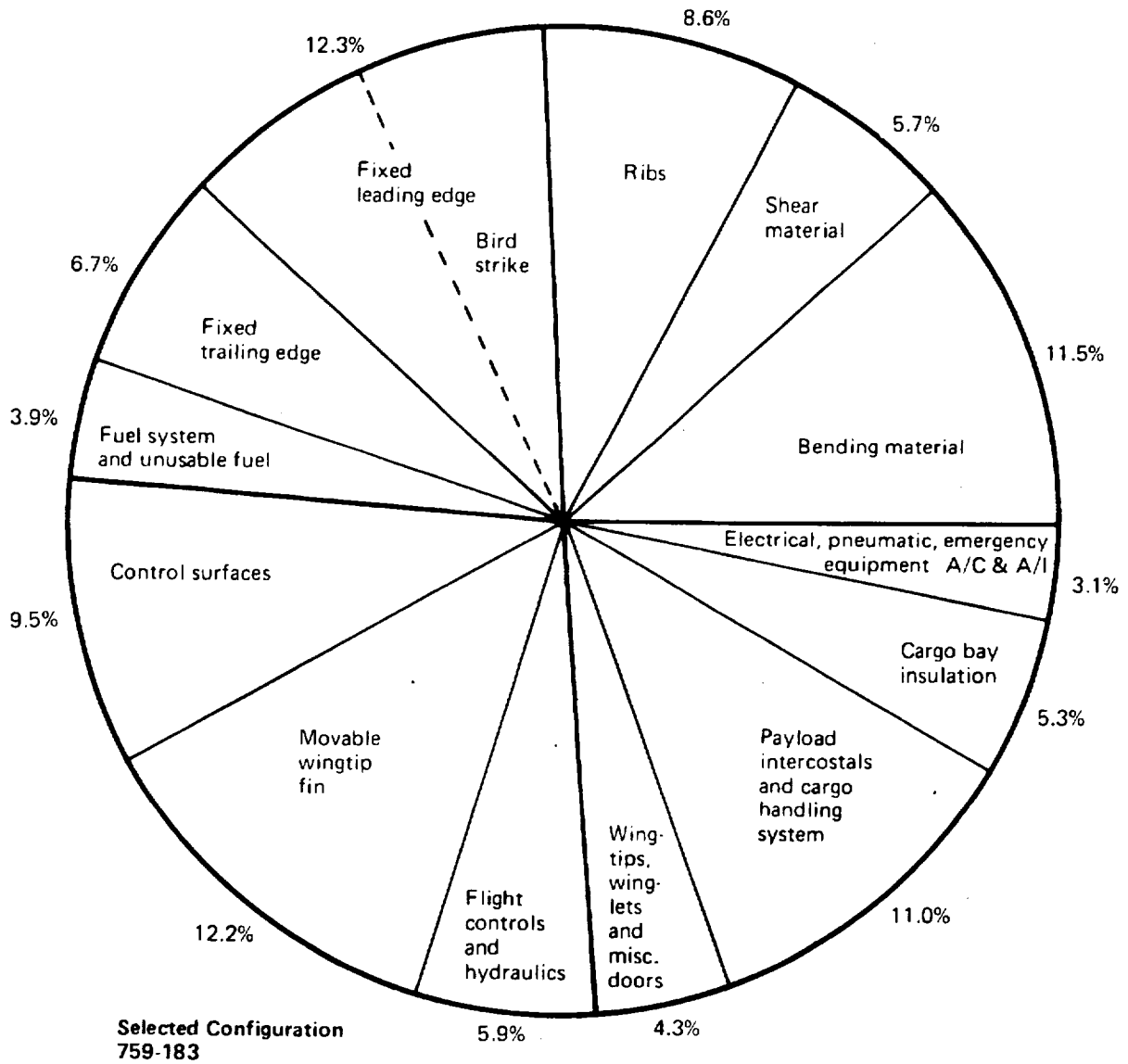
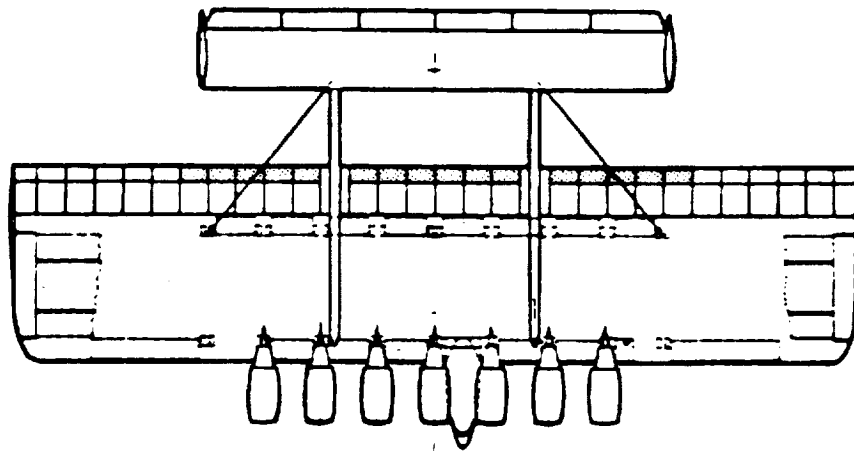


Figure 6.—Effect of Airplane Size on Economics




Wing area = 1730 m<sup>2</sup> (18 620 ft<sup>2</sup> (53% OEW)  
 Basic wing structure - 78 210 kg (172 420 lb)  
 Wing and contents = 127 434 kg (280 940 lb)

Figure 7.—Wing Weight Distribution (Structure Plus Integral Items)



Maximum gross weight 806 501 kg (1 778 000 lb)  
 Wing span 89.9 m (295 ft)  
 Wing area 1856 m<sup>2</sup> (19 980 sq ft)  
 MAC 20.7 m (816 in.)

 T.E. flap area

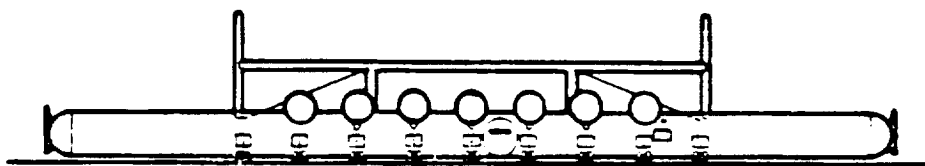
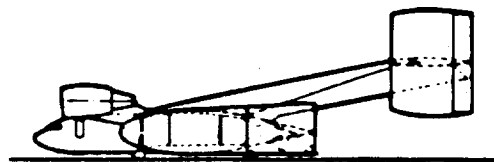


Figure 8.—General Arrangement, Parametric Baseline Airplane 759-163A



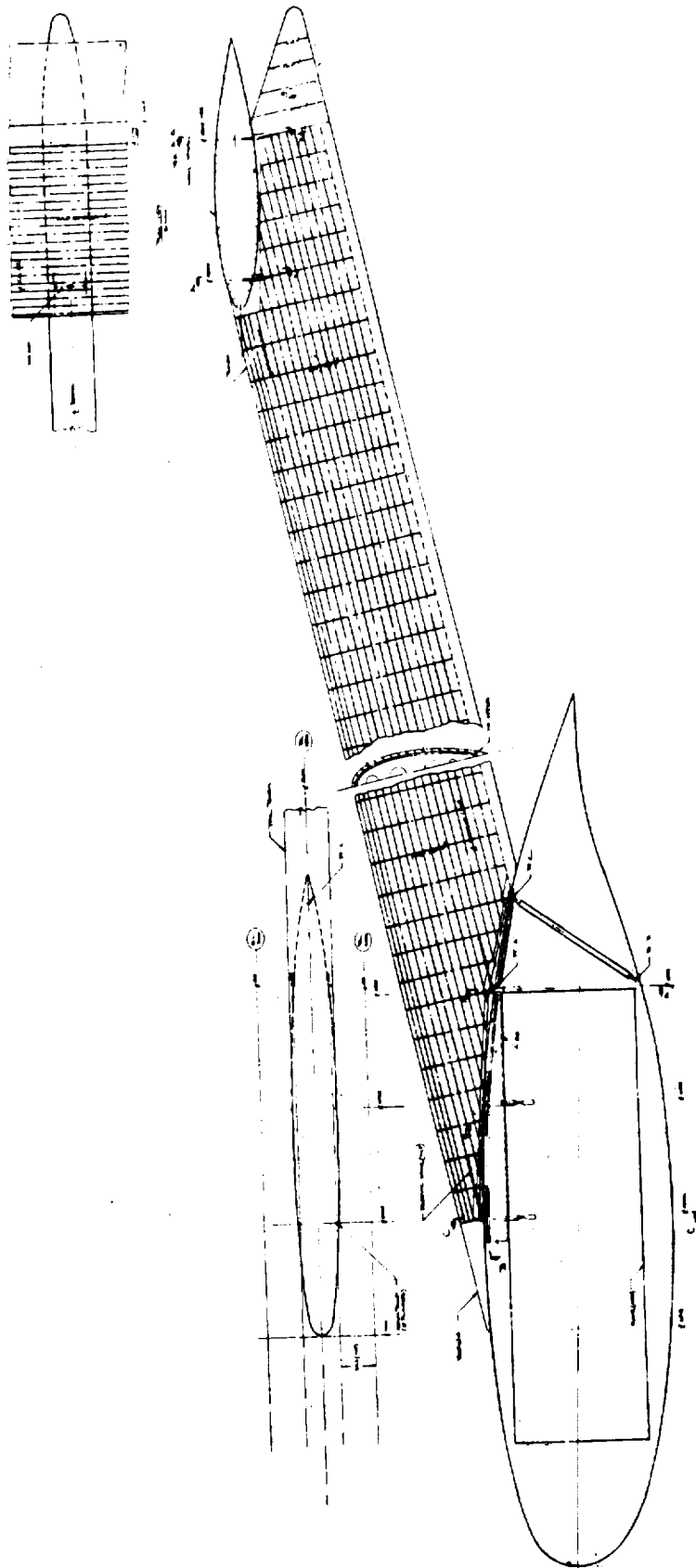
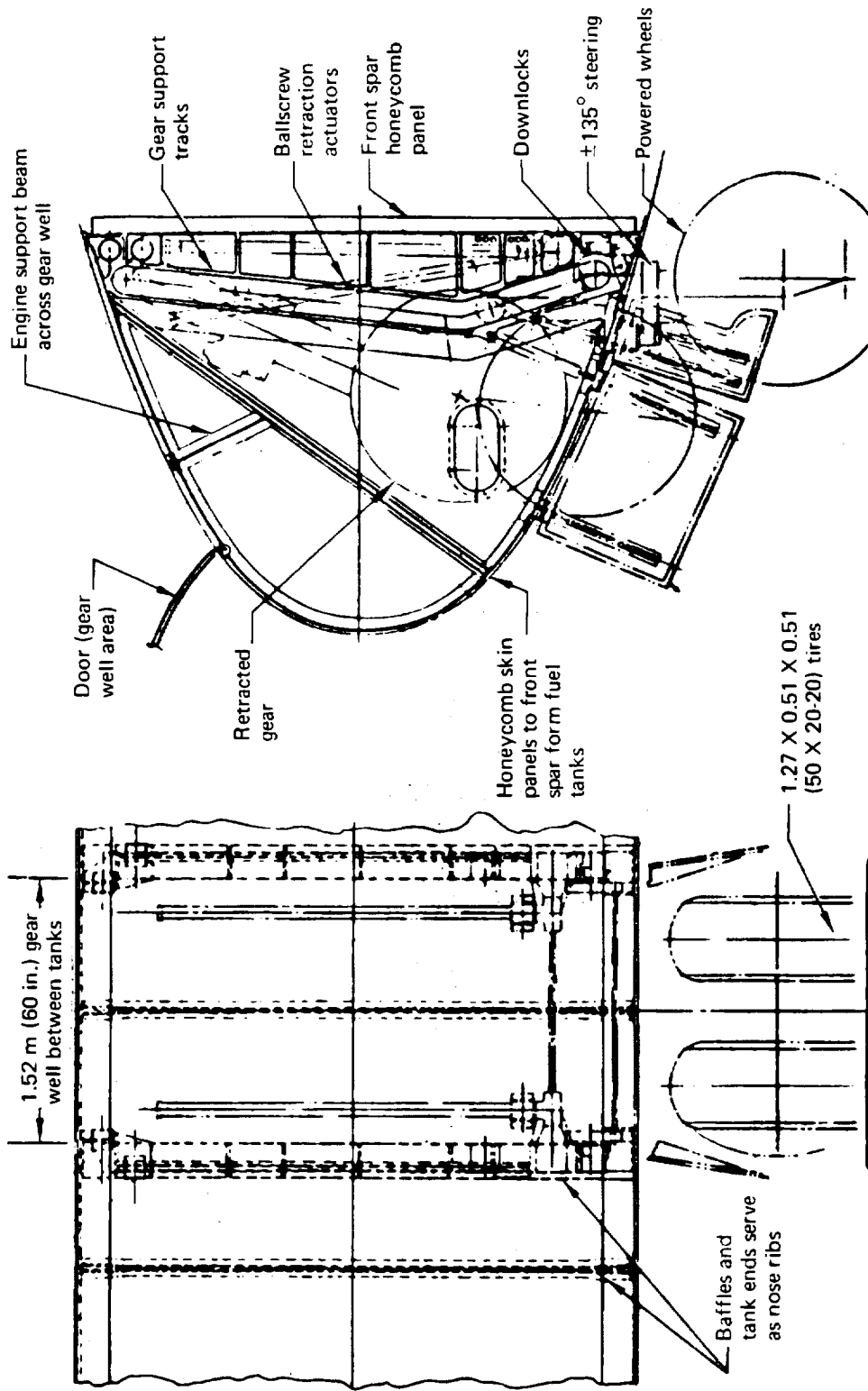
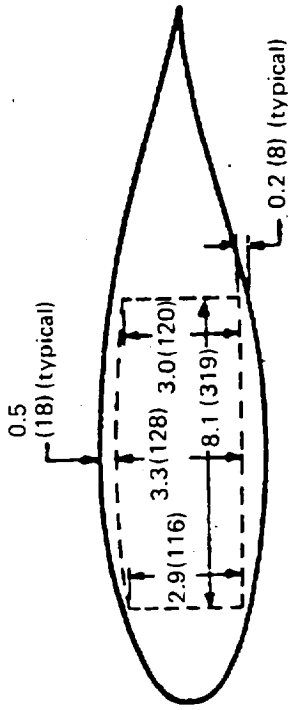


Figure 9.—Tail Boom Installation



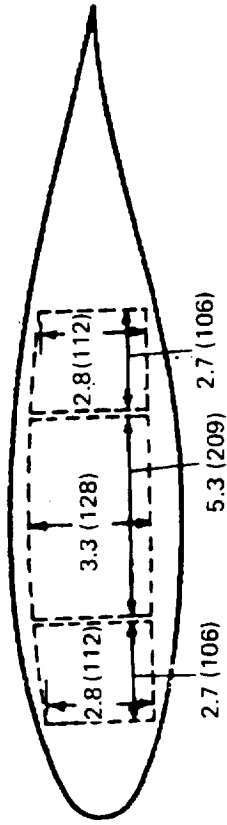
Note: meters (inches)

Figure 10.—Leading Edge Structure

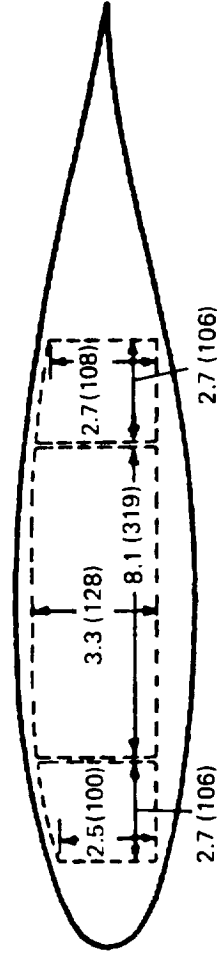


t/c = 24%  
 3 bays  
 $\bar{c} = 17.8 \text{ m (702 in.)}$

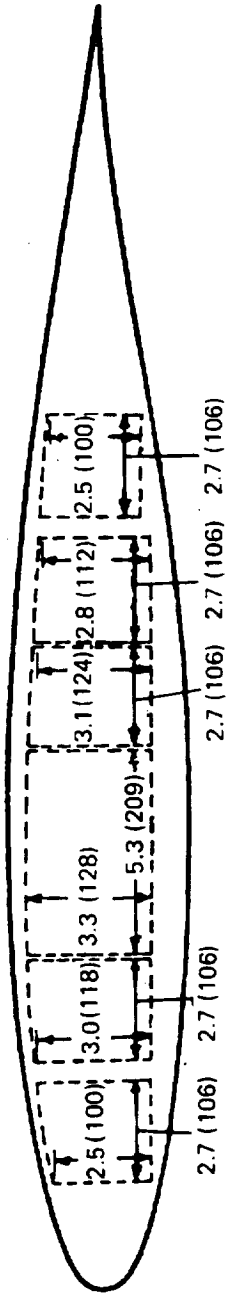
1" = 0.0254 m



t/c = 21.5%  
 4 bays  
 $\bar{c} = 20.7 \text{ m (816 in.)}$



t/c = 19%  
 5 bays  
 $\bar{c} = 24.2 \text{ m (953 in.)}$



t/c = 14%  
 7 bays  
 $\bar{c} = 32.9 \text{ m (1297 in.)}$

Note: meters (inches)

Figure 11.—Wing Section Utilization

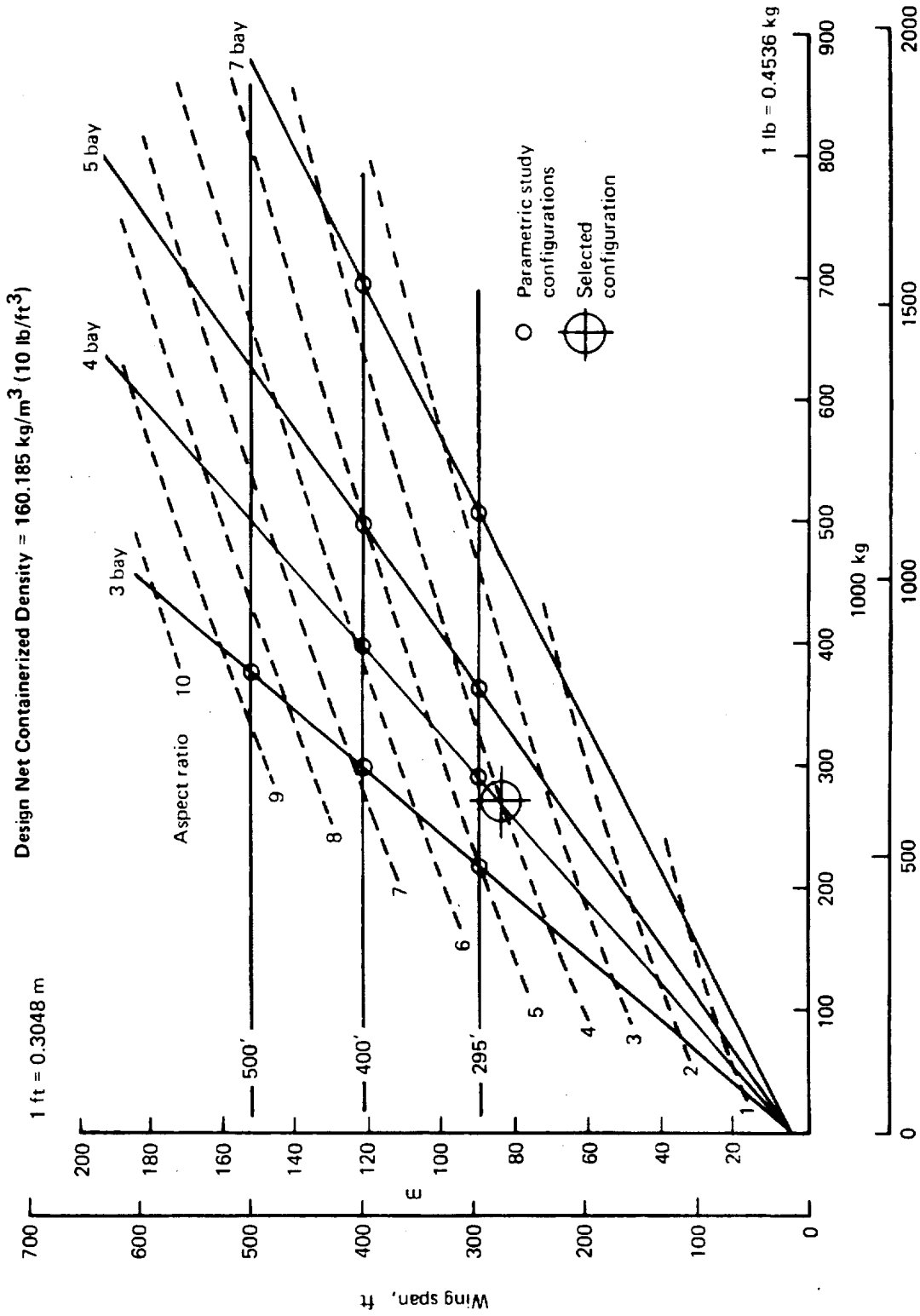


Figure 12.—Geometry Constraints

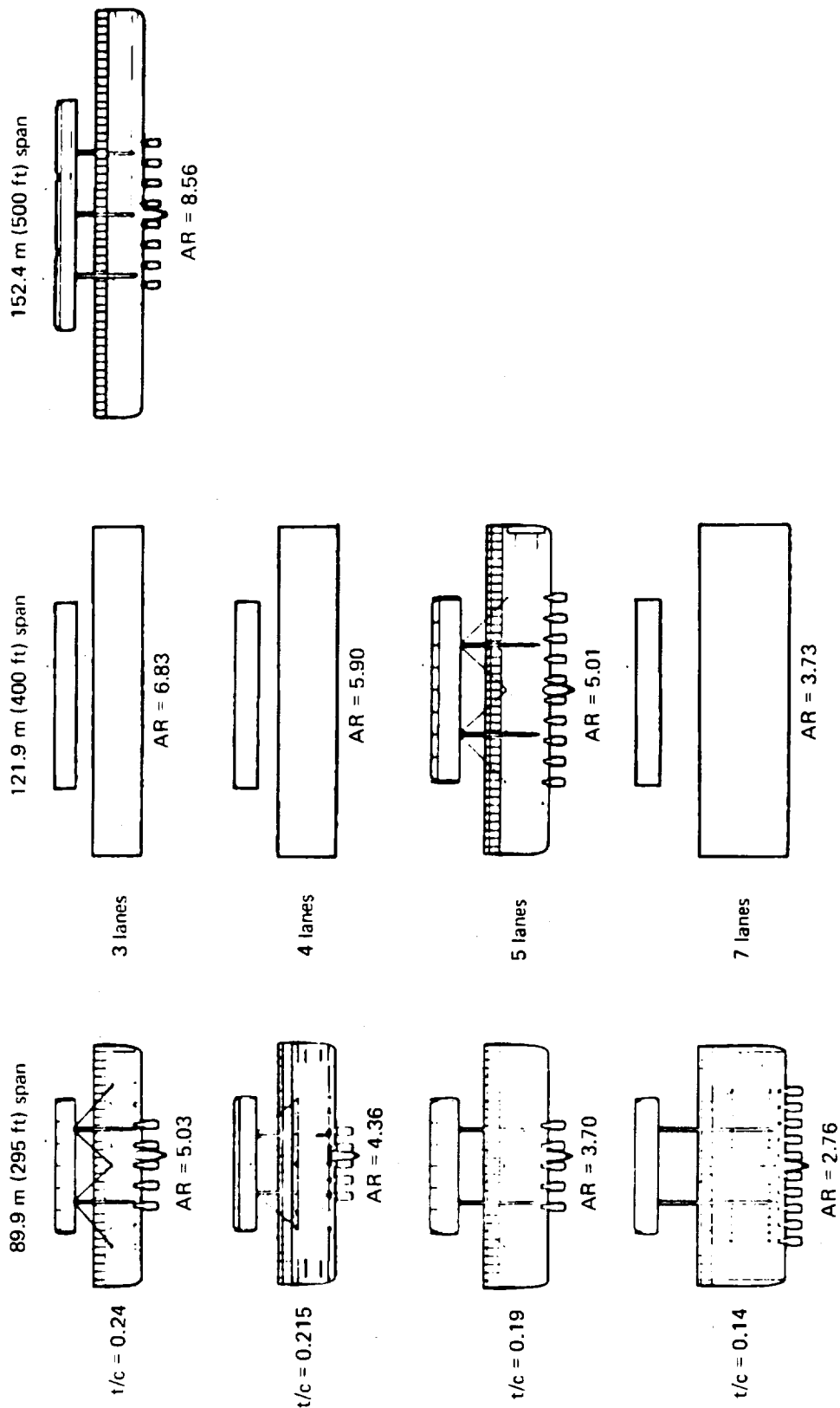


Figure 13.—Parametric Study—Configuration Geometry

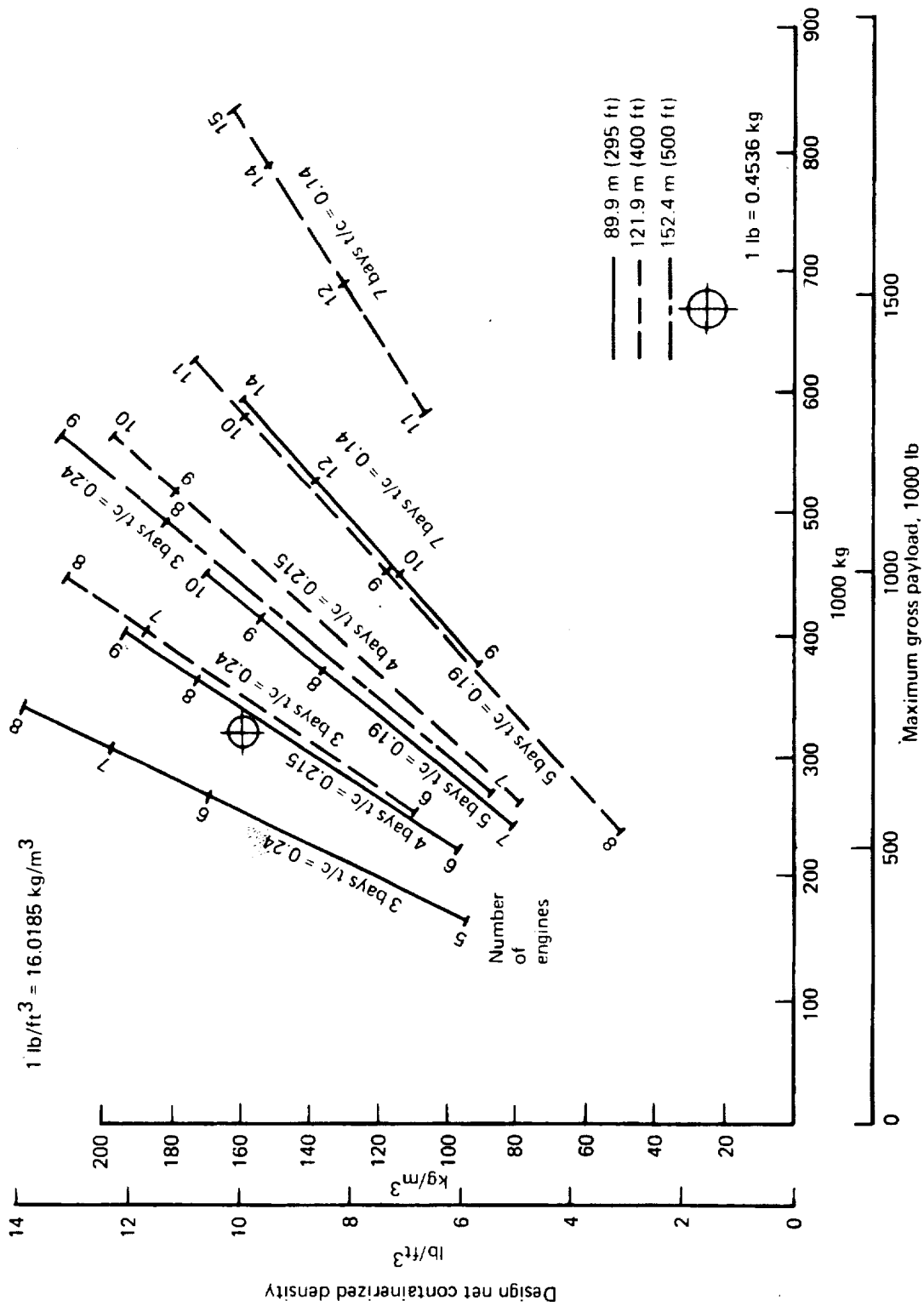


Figure 14.—Parametric Study Payloads

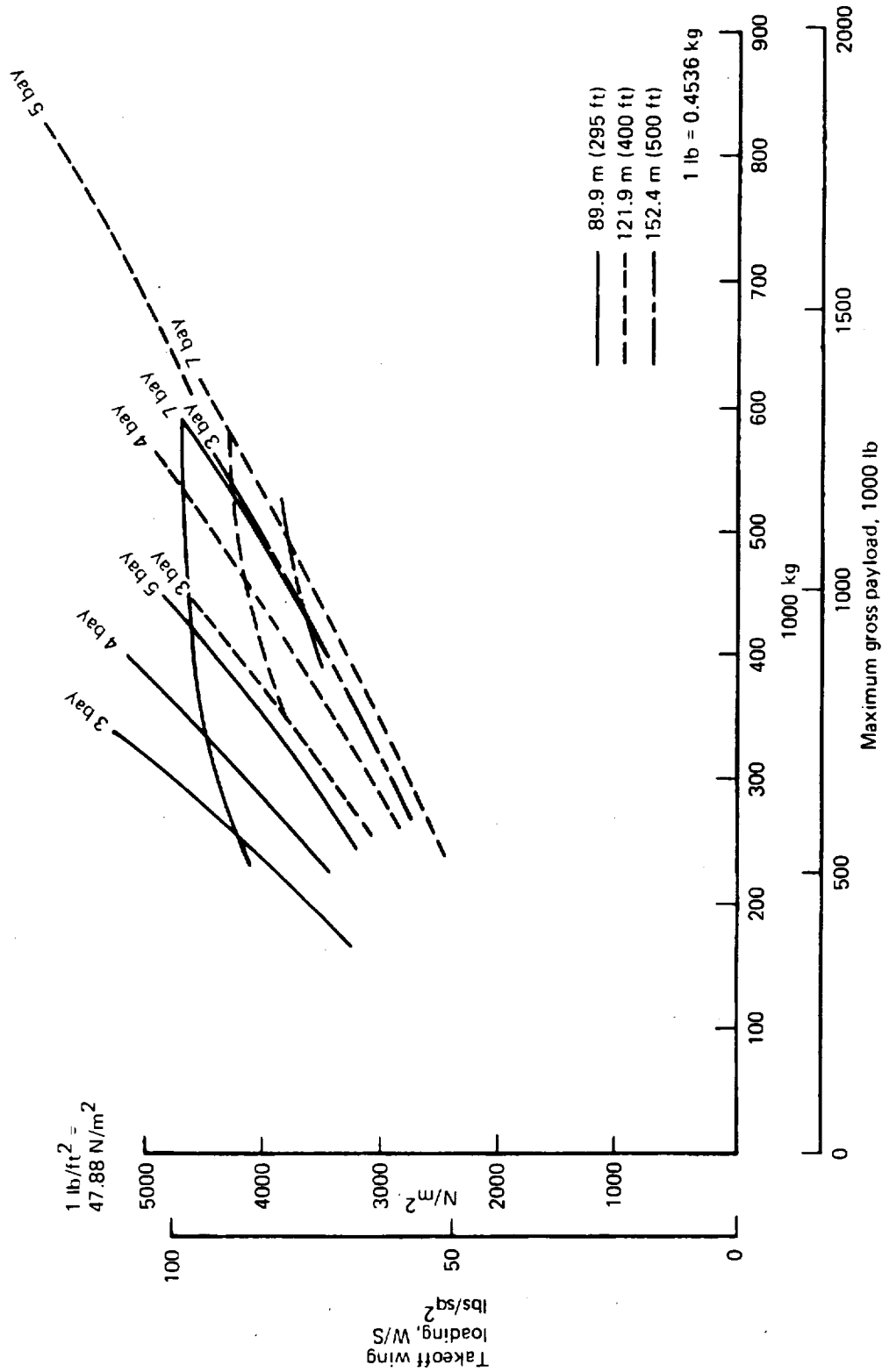


Figure 15.—Wing Loading Results

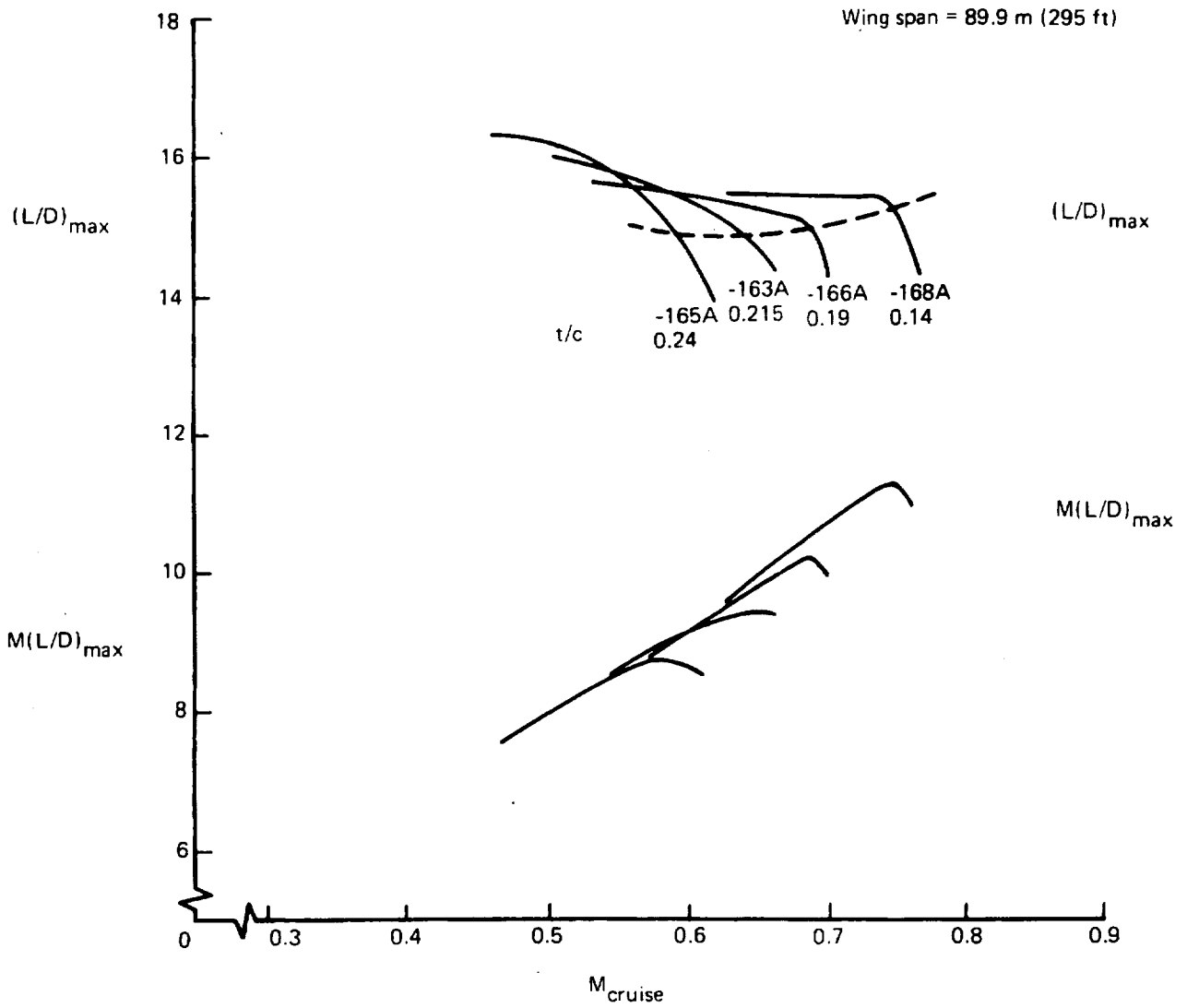


Figure 16.—Aerodynamic Efficiency



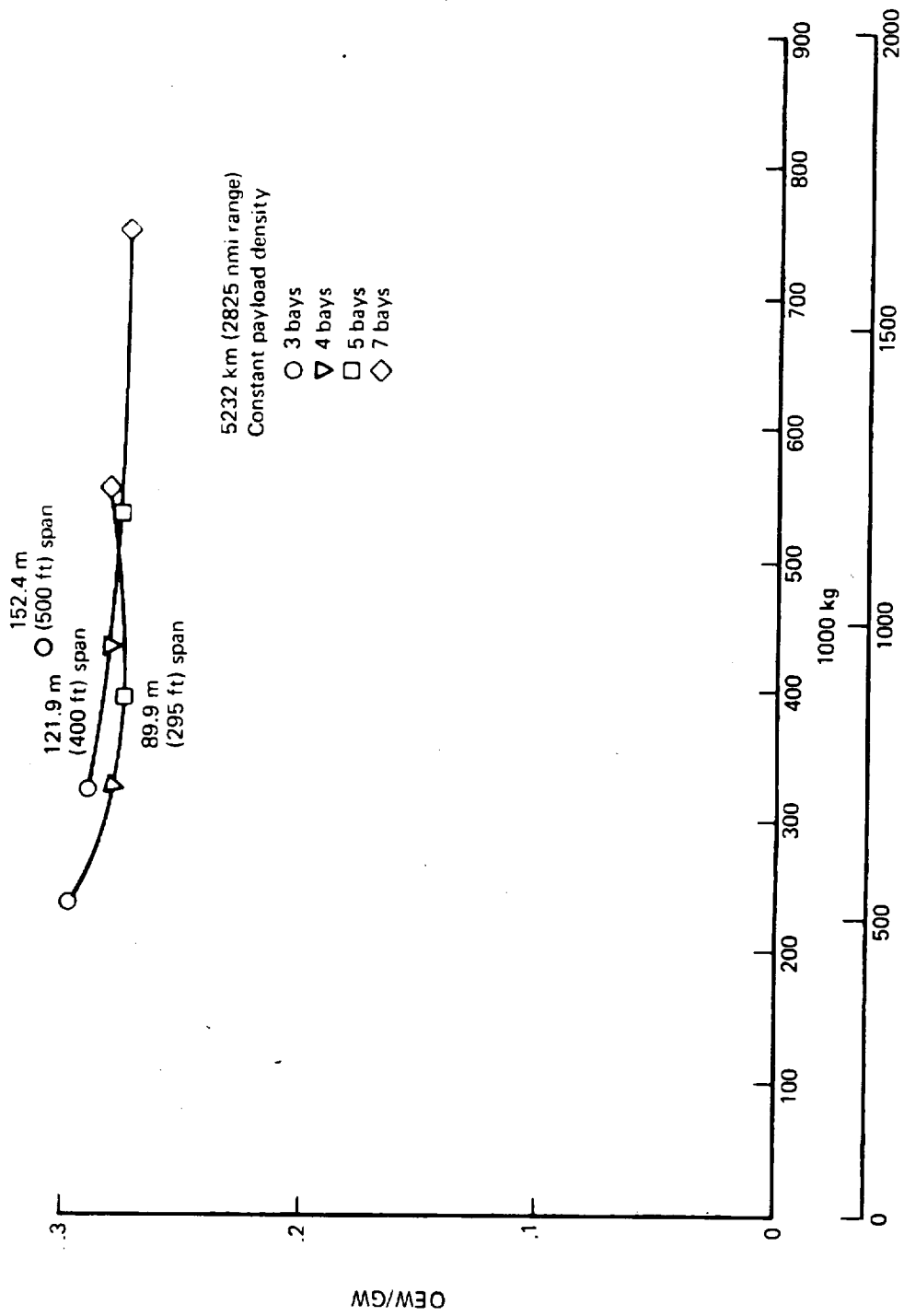


Figure 17.—Empty Weight Fraction

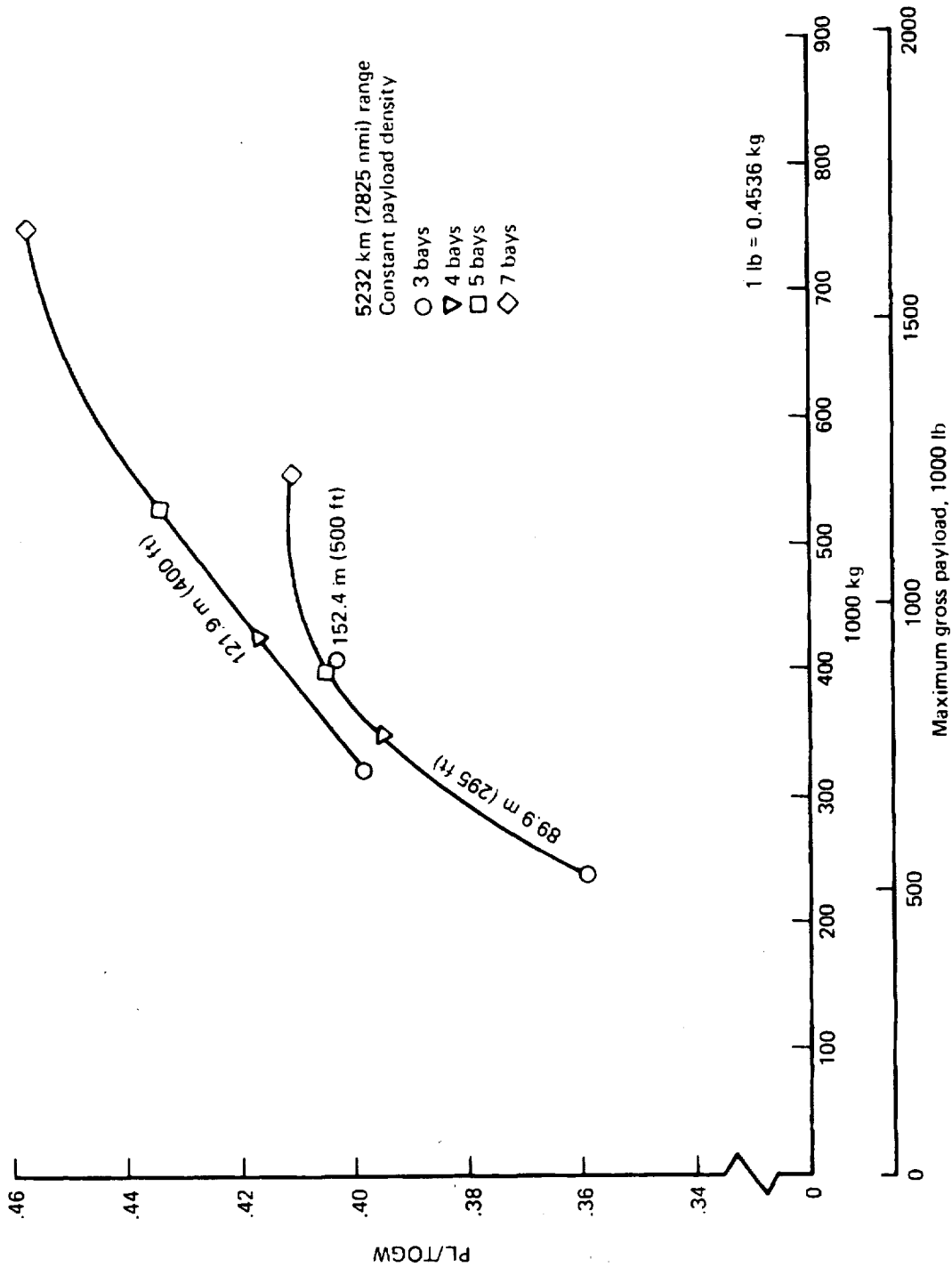


Figure 18.—Payload Weight Fraction

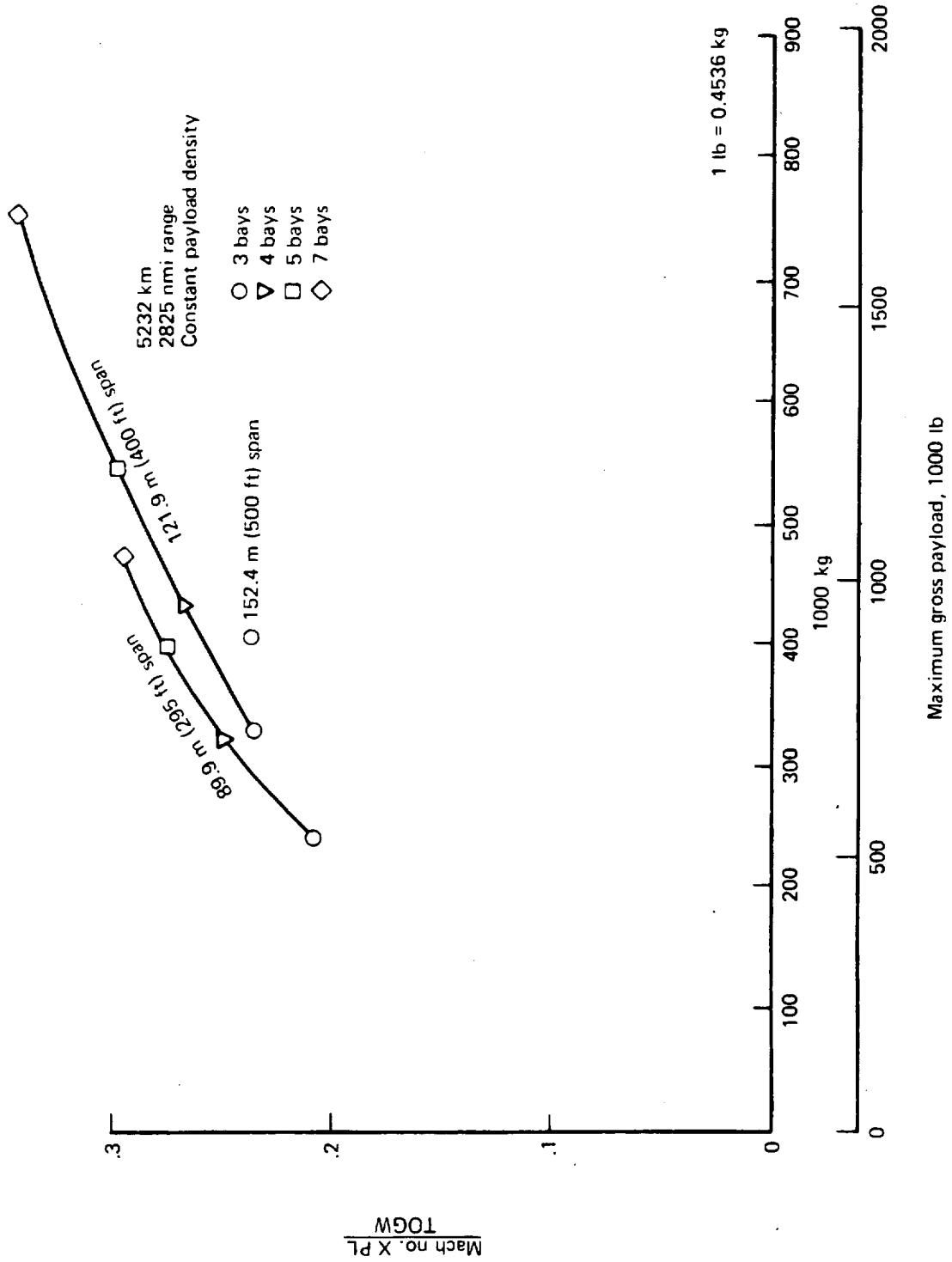


Figure 19.—Productivity/Gross Weight

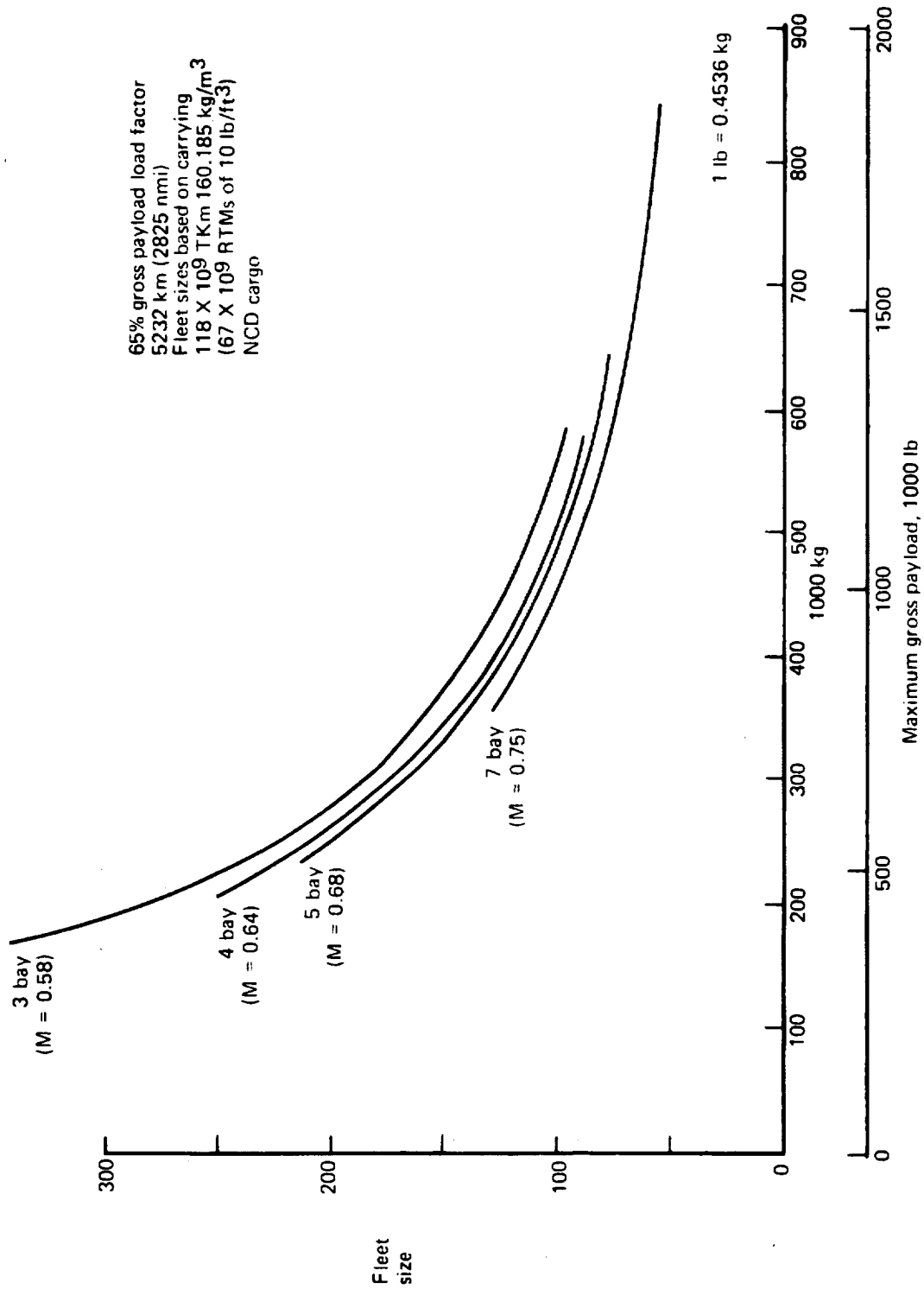


Figure 20.—Fleet Size Versus Payload

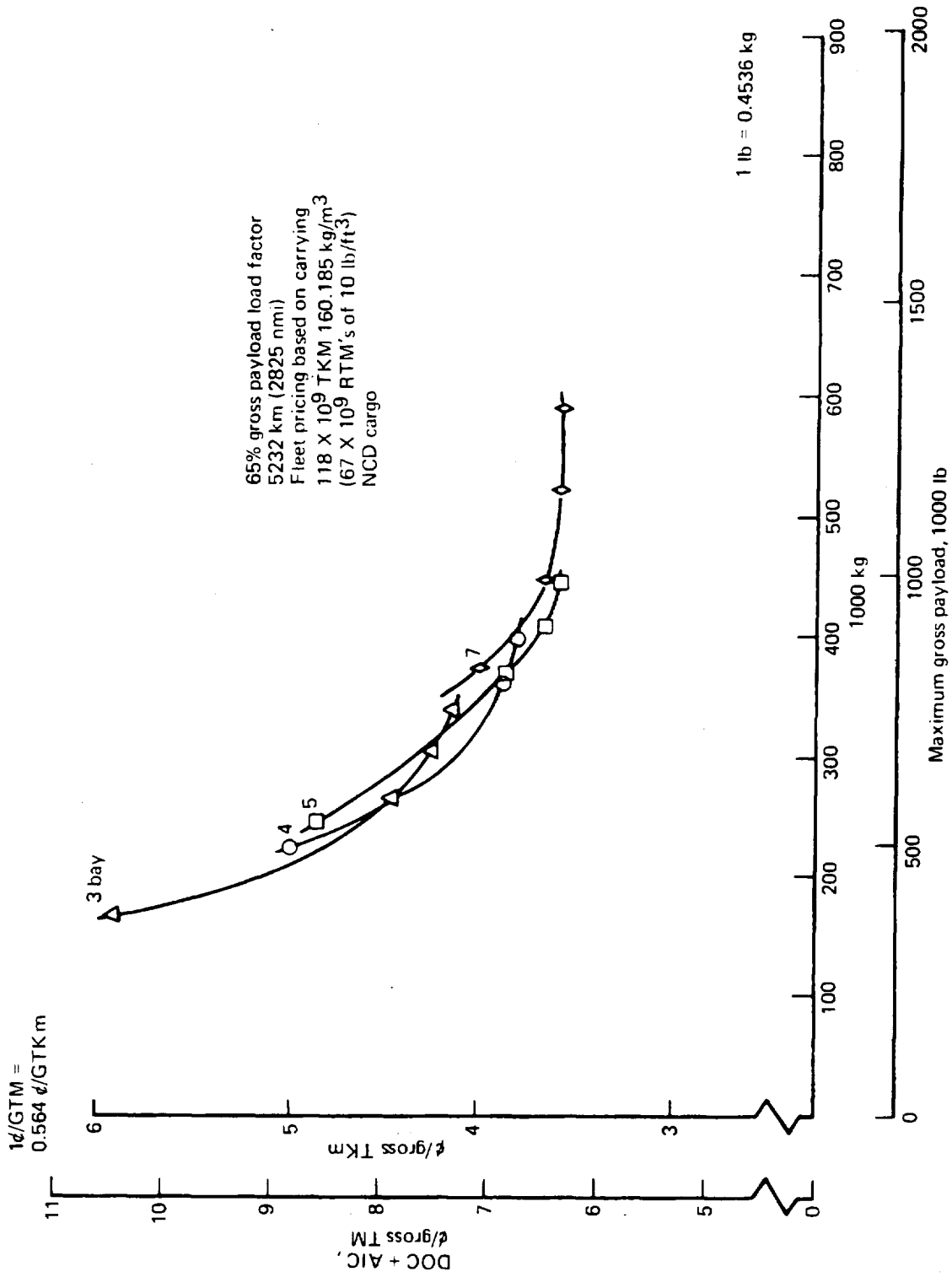


Figure 21.—Effect of Payload on Economics—89.9 m (295 ft) Span Parametric Configurations

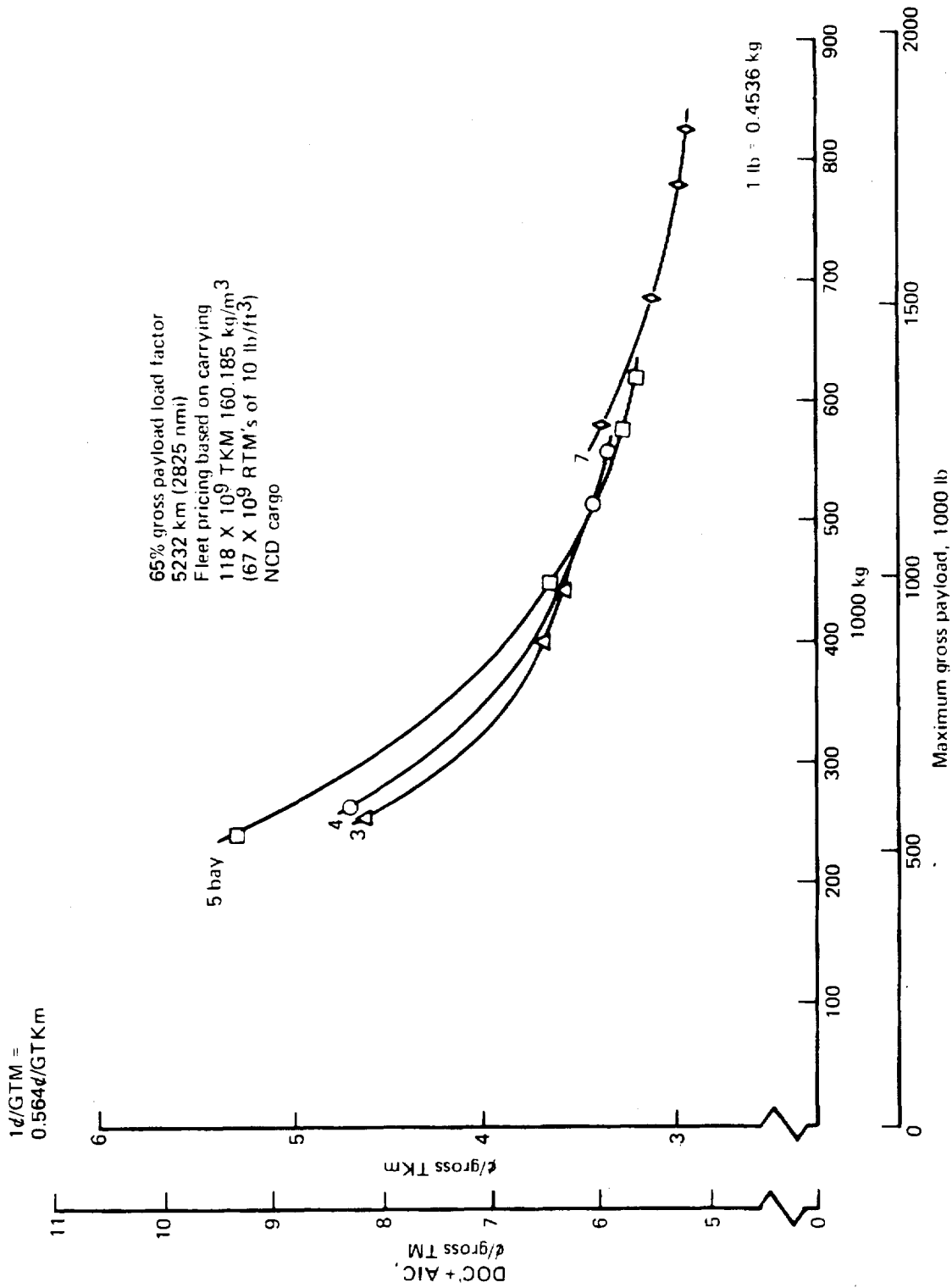
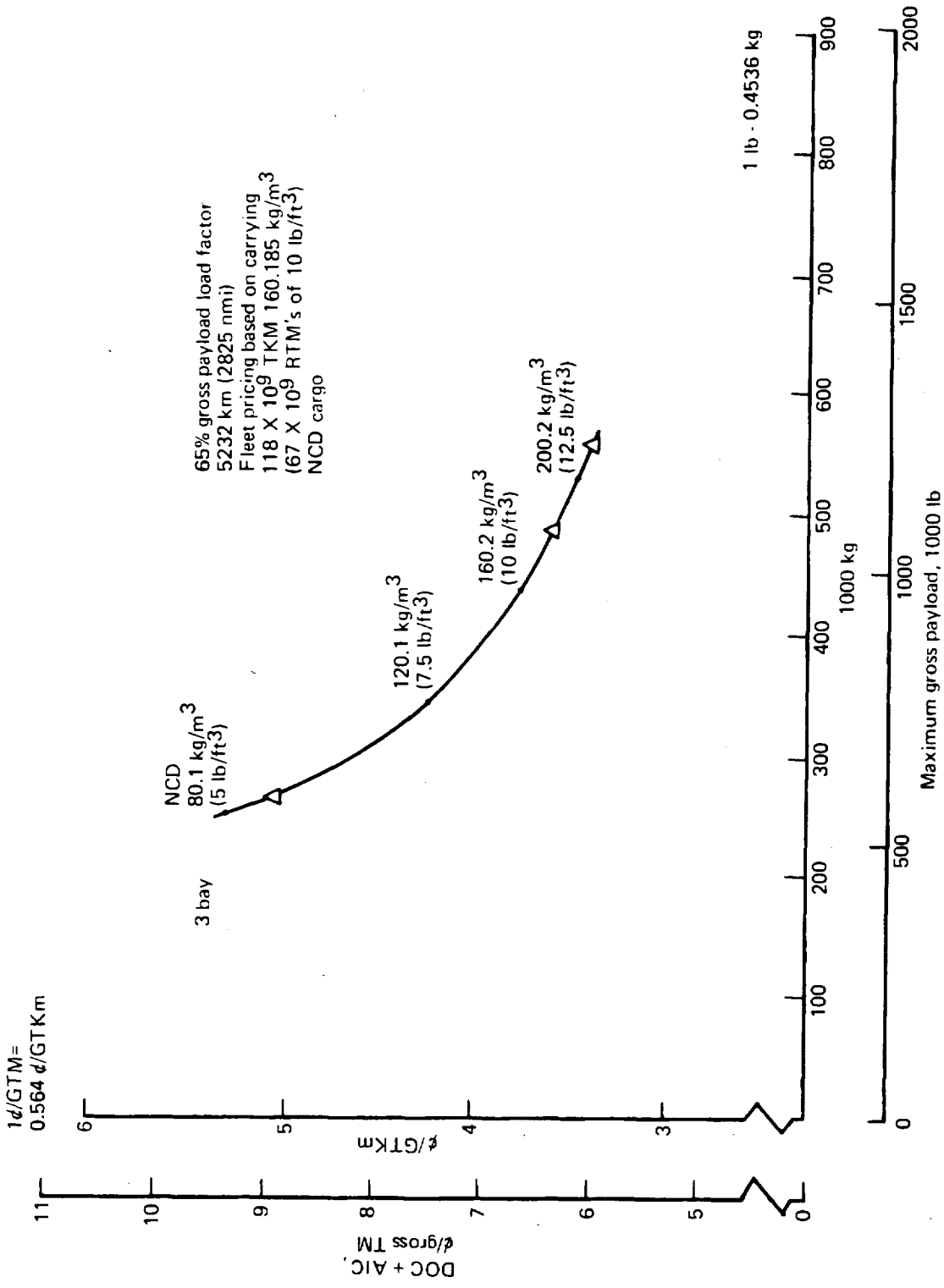


Figure 22.—Effect of Payload on Economics—121.9 m (400 ft) Span Parametric Configurations



65% gross payload load factor  
 5232 km (2825 nmi)  
 Fleet pricing based on carrying  
 118 X 10<sup>9</sup> TKM 160.185 kg/m<sup>3</sup>  
 (67 X 10<sup>9</sup> RTM's of 10 lb/ft<sup>3</sup>)  
 NCD cargo

Figure 23.—Effect of Payload and Payload Density on Economics—152.4 m (500 ft) Span Parametric Configurations

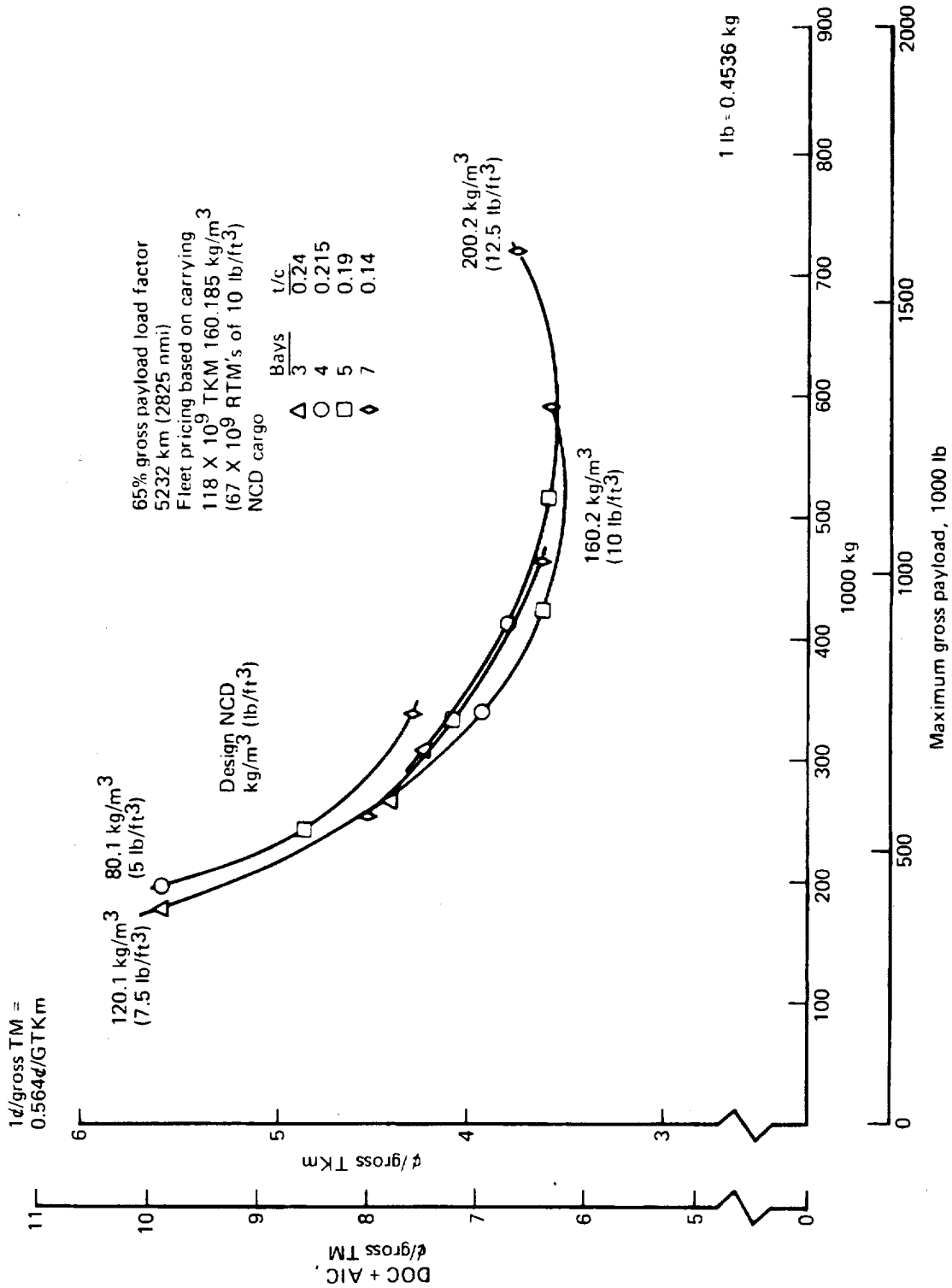


Figure 24.—Effect of Payload Density on Economics 89.9 m (295 ft.) Span Parametric Configurations



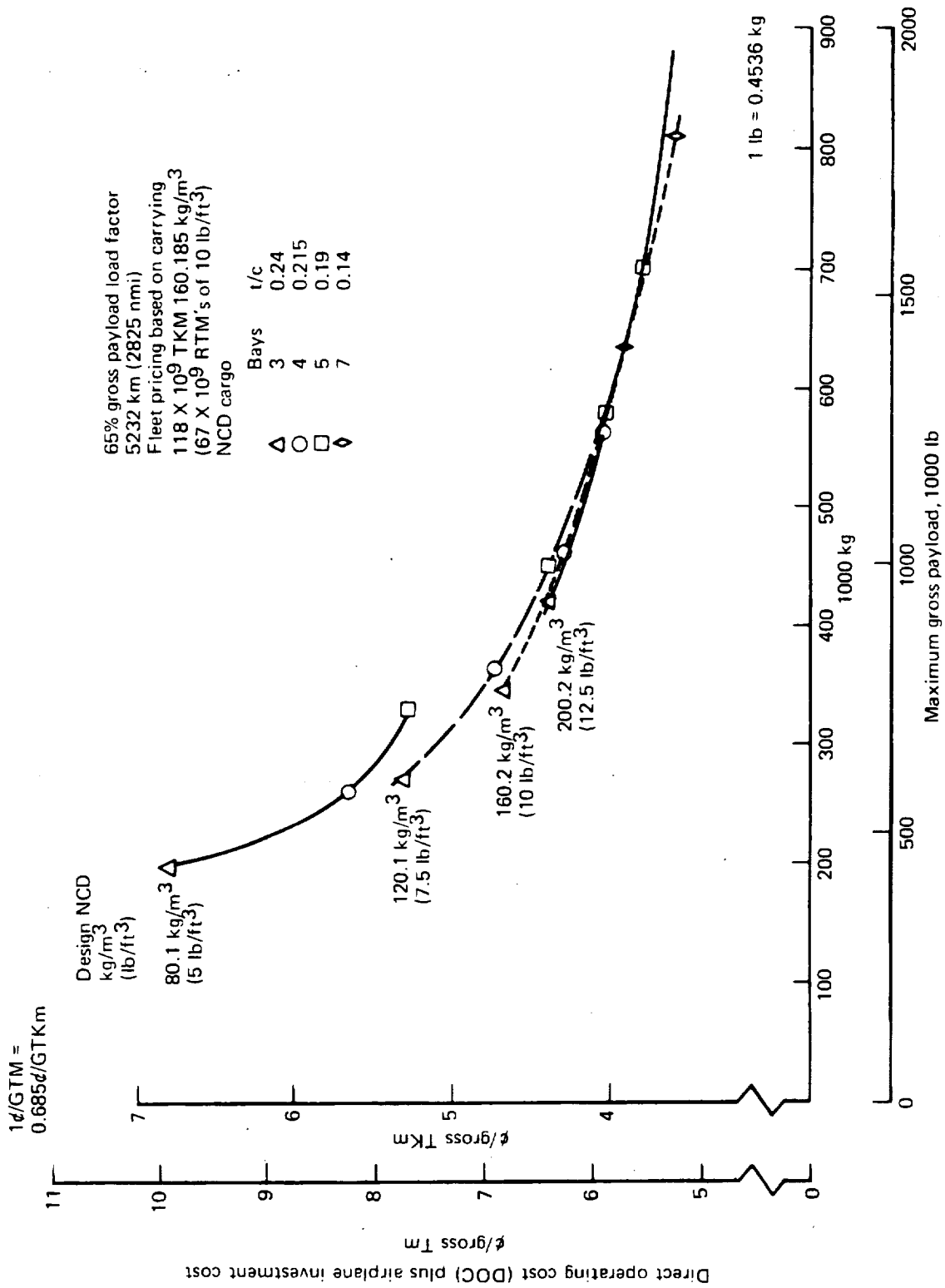


Figure 25.—Effect of Payload Density on Economics—121.9 m (400 ft) Span Parametric Configurations

1980 Technology

65% gross payload load factor  
 5232 km (2825 nmi)  
 Fleet pricing based on carrying  
 67 X 10<sup>9</sup> RTMs of 10 lb/ft<sup>3</sup>  
 NCD cargo  
 118 X 10<sup>9</sup> TKM 160.185 kg/m<sup>3</sup>

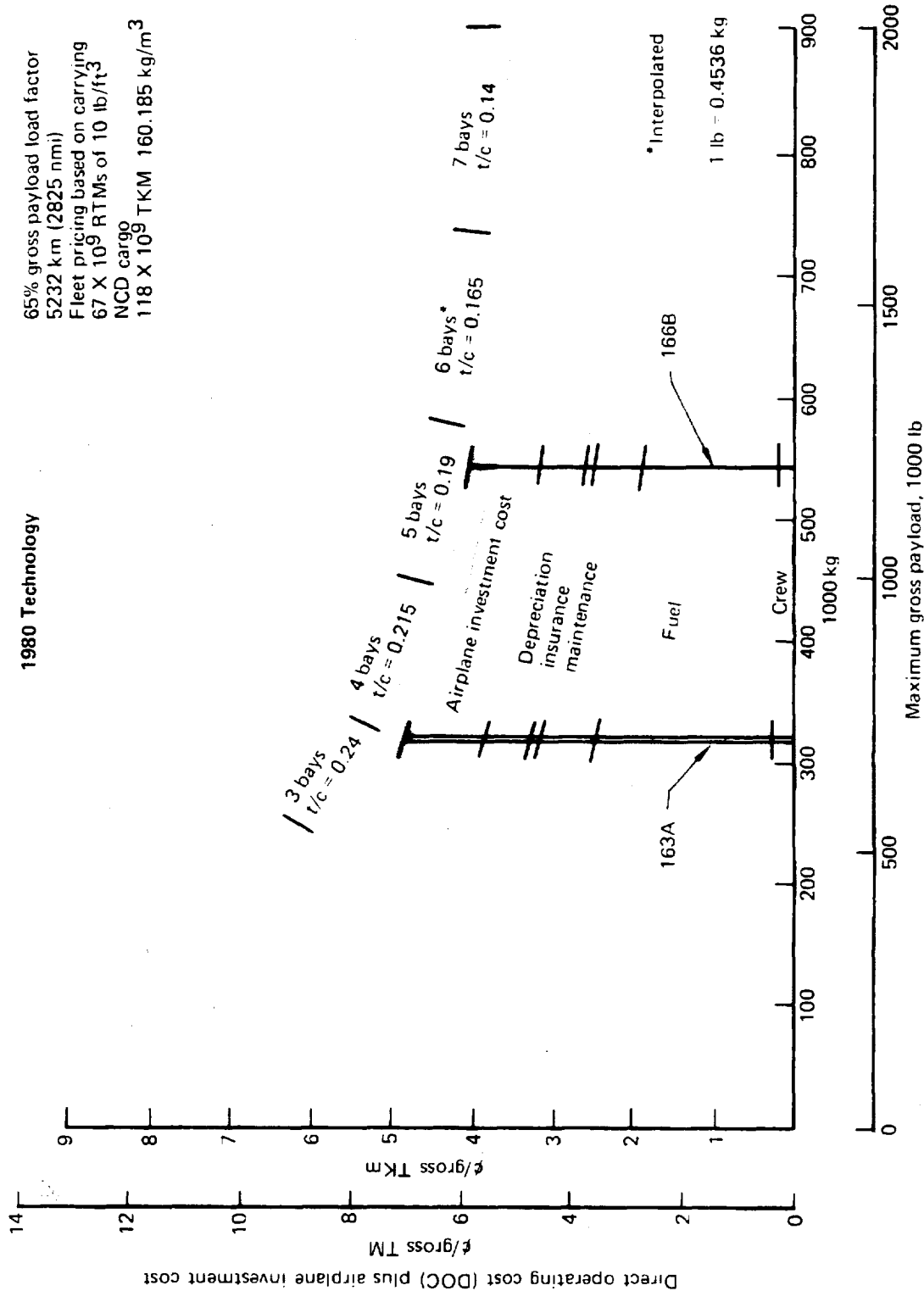


Figure 26.—Effects of Airplane Size on Economics—Parametric Study Trends

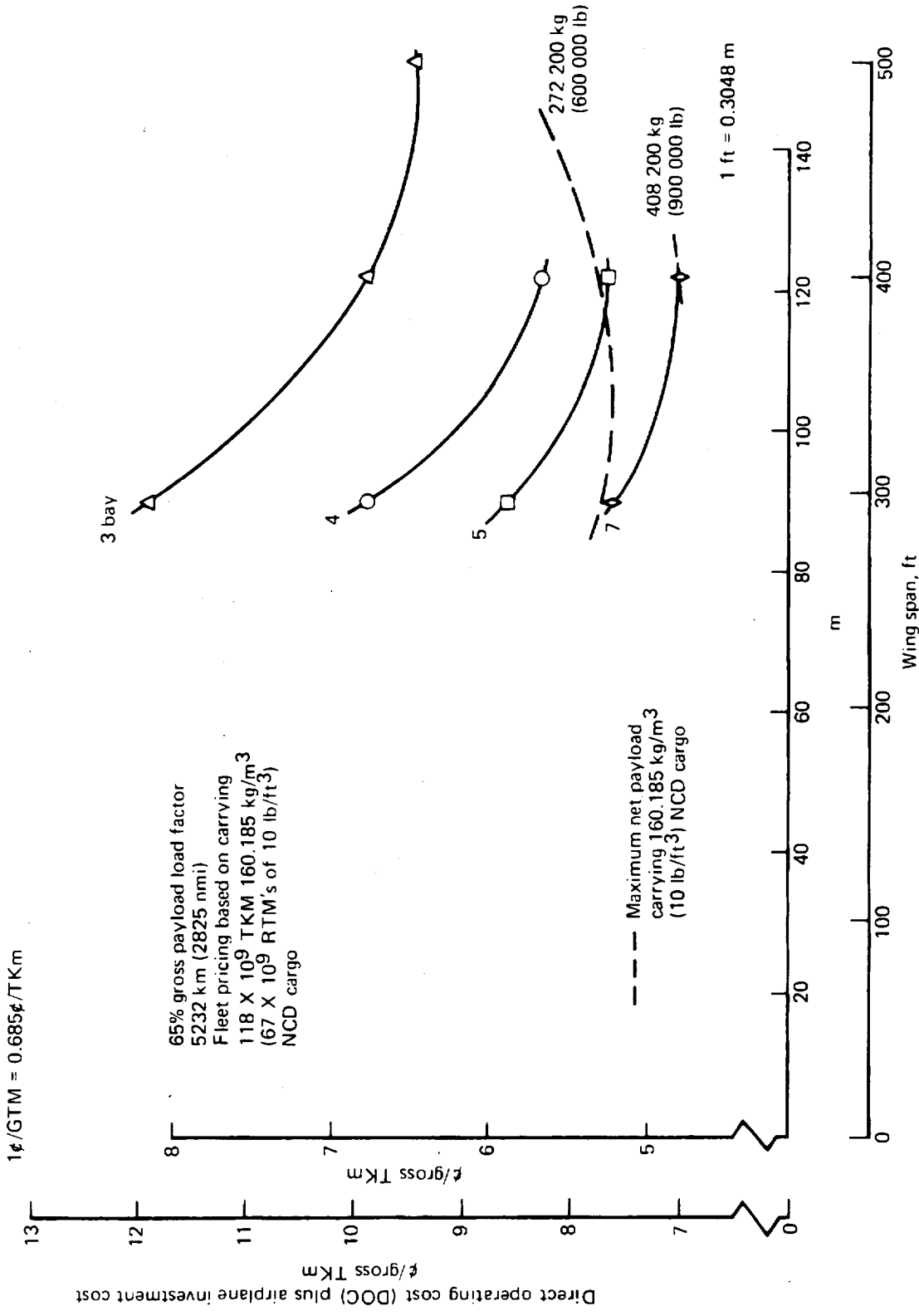


Figure 27.—Effect of Airplane Size and Geometry on Economics—Constant Design Net Containerized Density = 80.1 kg/m<sup>3</sup> (5 lb/ft<sup>3</sup>)

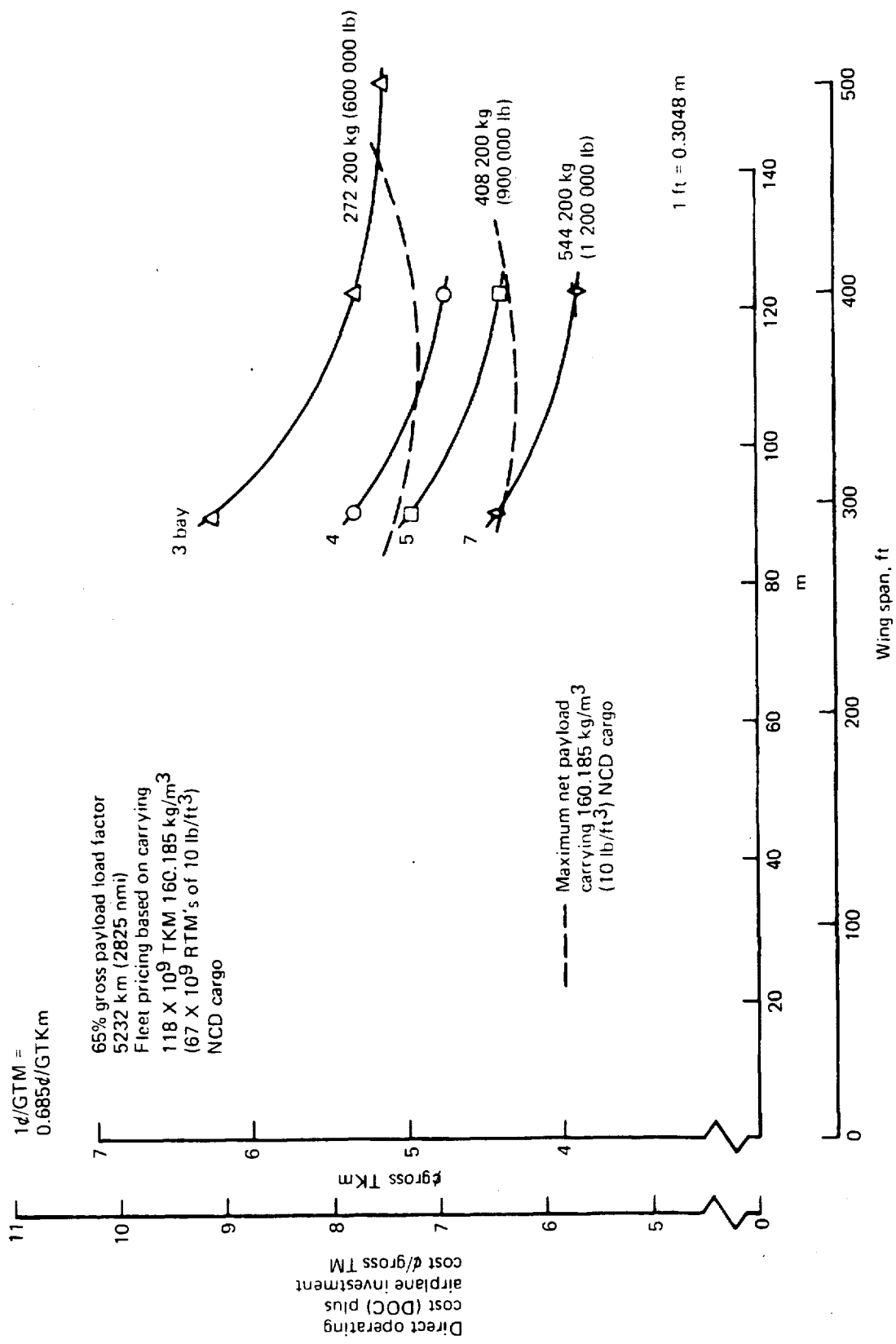


Figure 28.—Effect of Airplane Size and Geometry on Economics—Constant Design Net Containerized Density =  $120.1 kg/m^3$  ( $7.5 lb/ft^3$ )

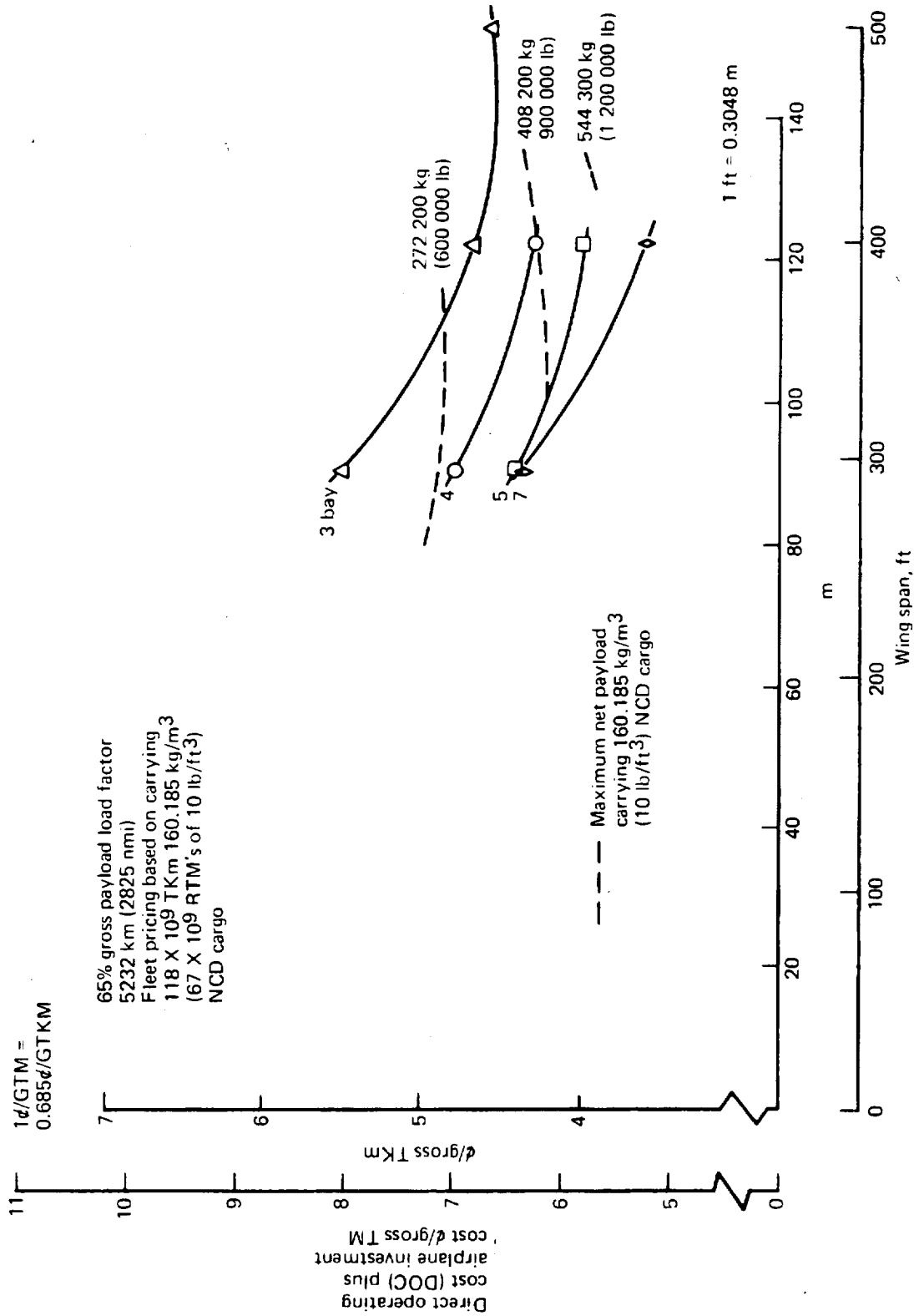


Figure 29.—Effect of Airplane Size and Geometry on Economics—Constant Design Net Containerized Density = 160.185 kg/m<sup>3</sup> (10 lb/ft<sup>3</sup>)

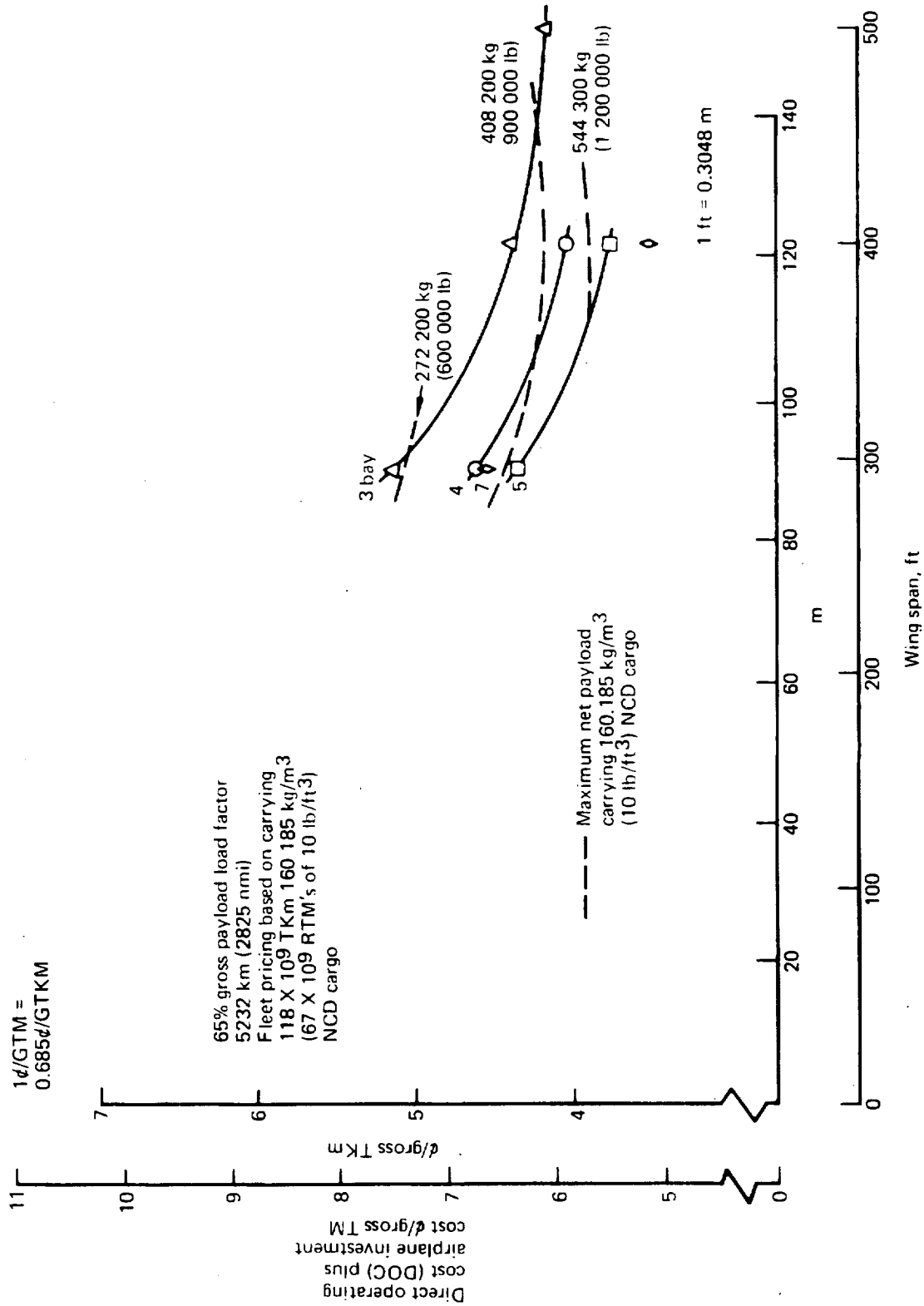


Figure 30.—Effect of Airplane Size and Geometry on Economics—Constant Design Net Containerized Density = 200.2 kg/m<sup>3</sup> (12.5 lb/ft<sup>3</sup>)

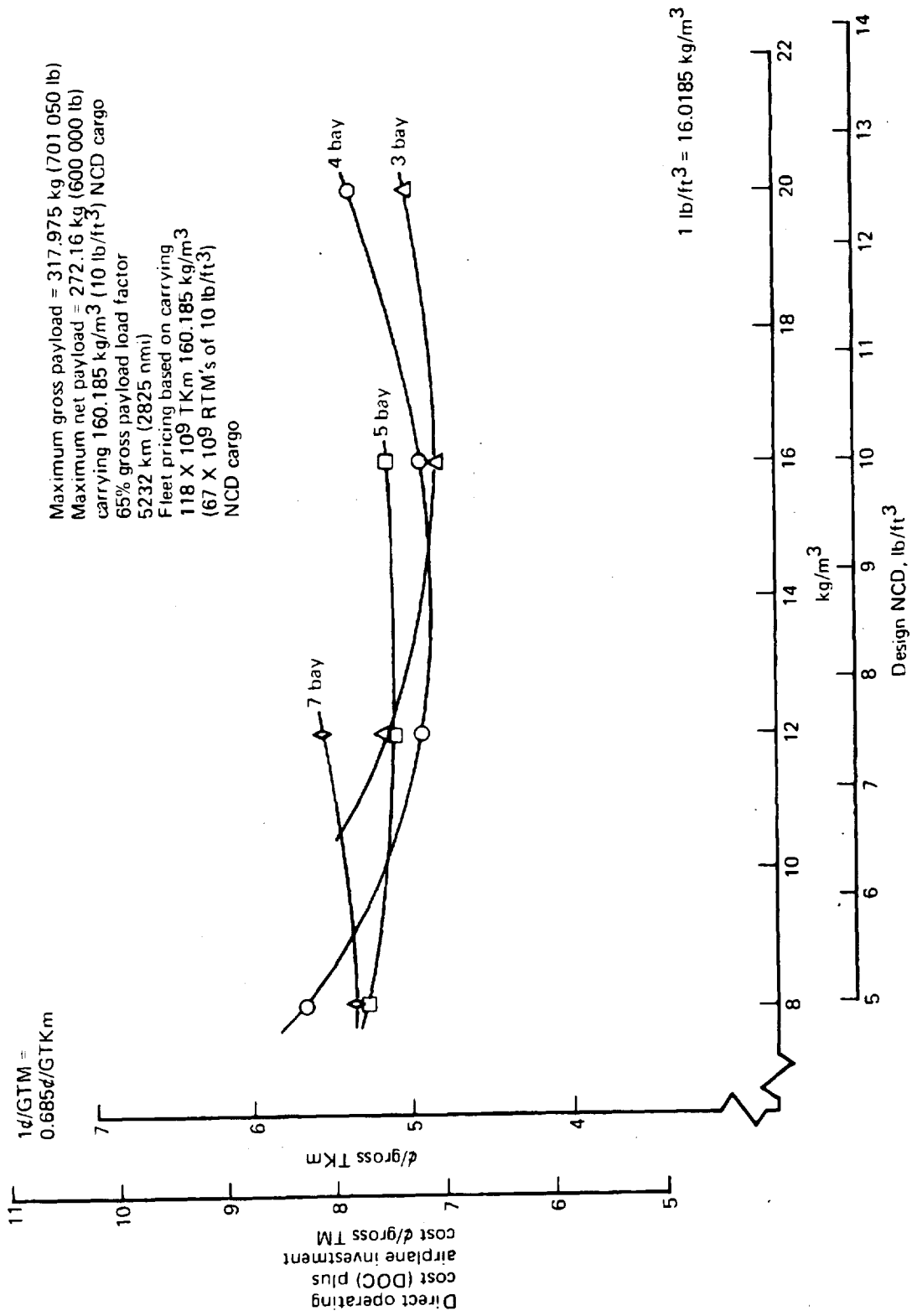


Figure 31.—Design NCD Versus DOC + A/C

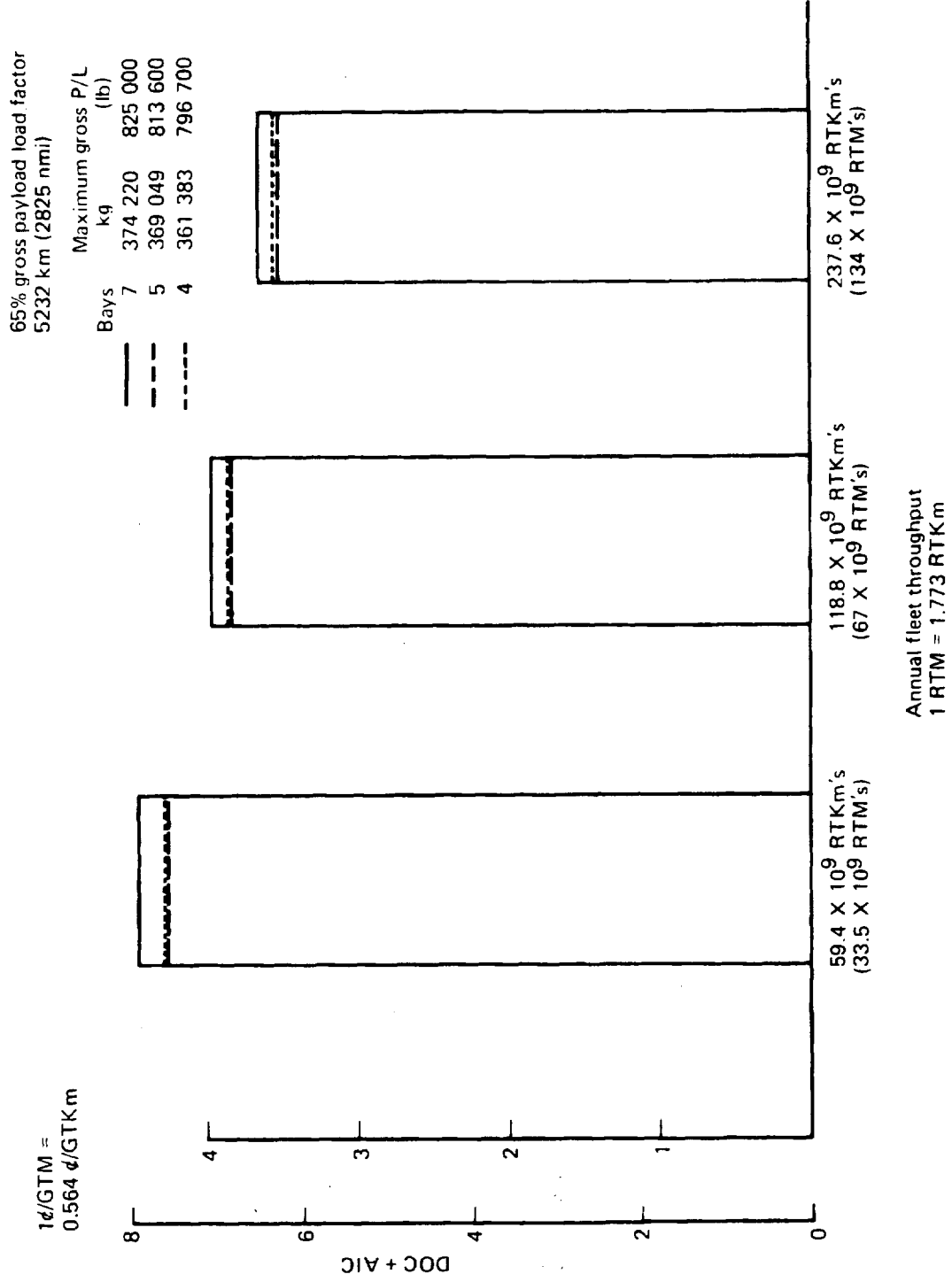


Figure 32.—Effect of Throughput



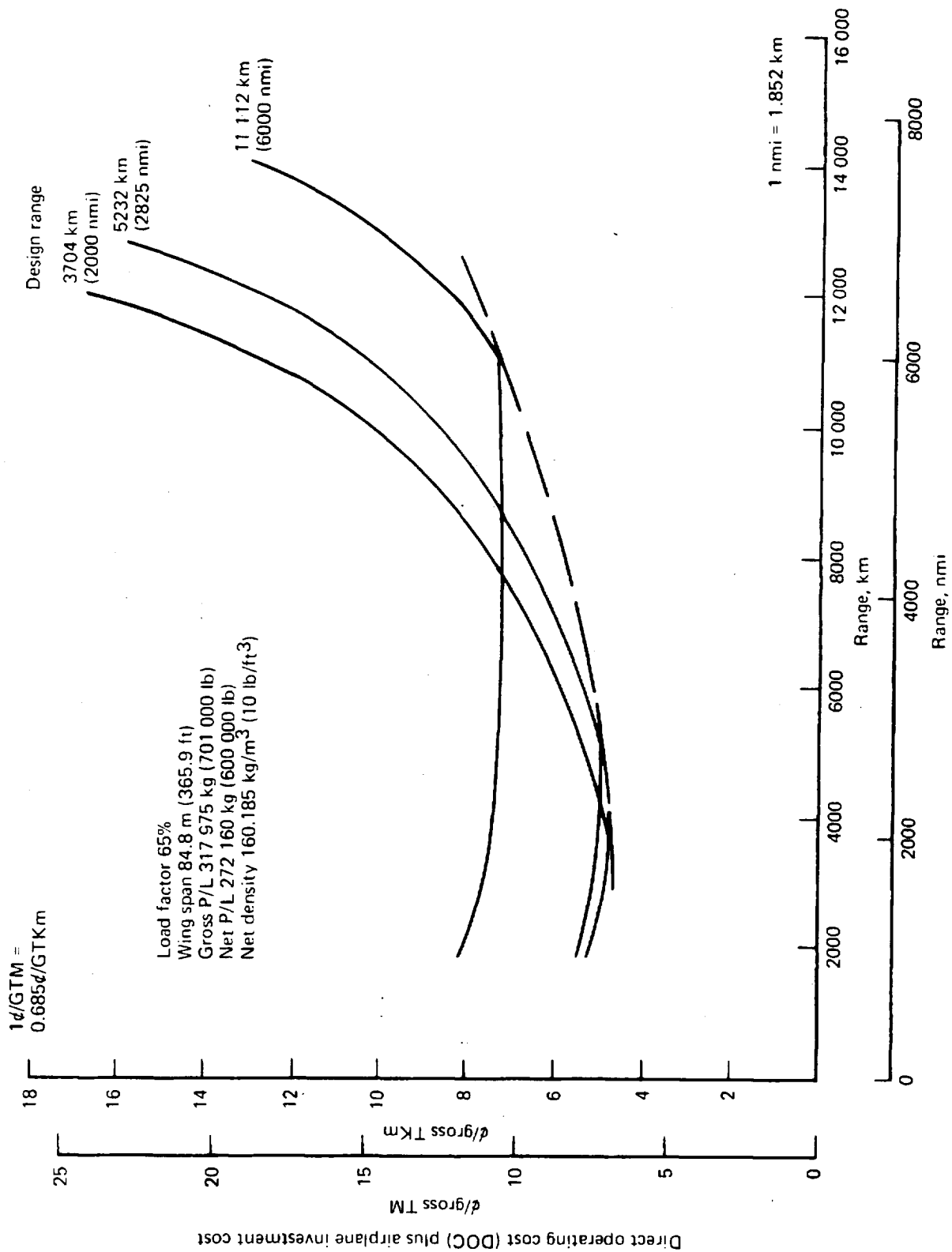


Figure 33.—Design Range Sensitivity—3 Bays

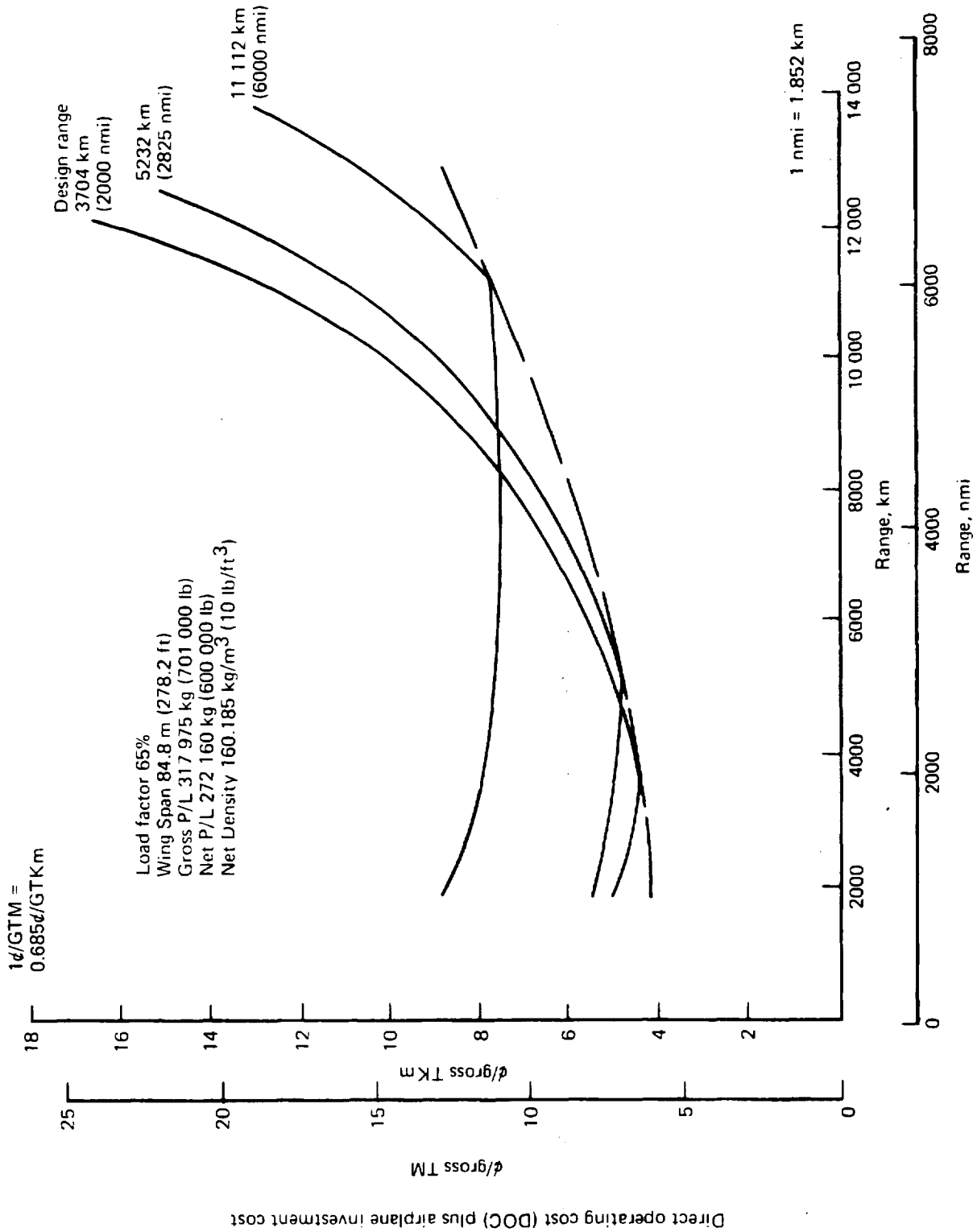


Figure 34.—Design Range Sensitivity—4 Bays

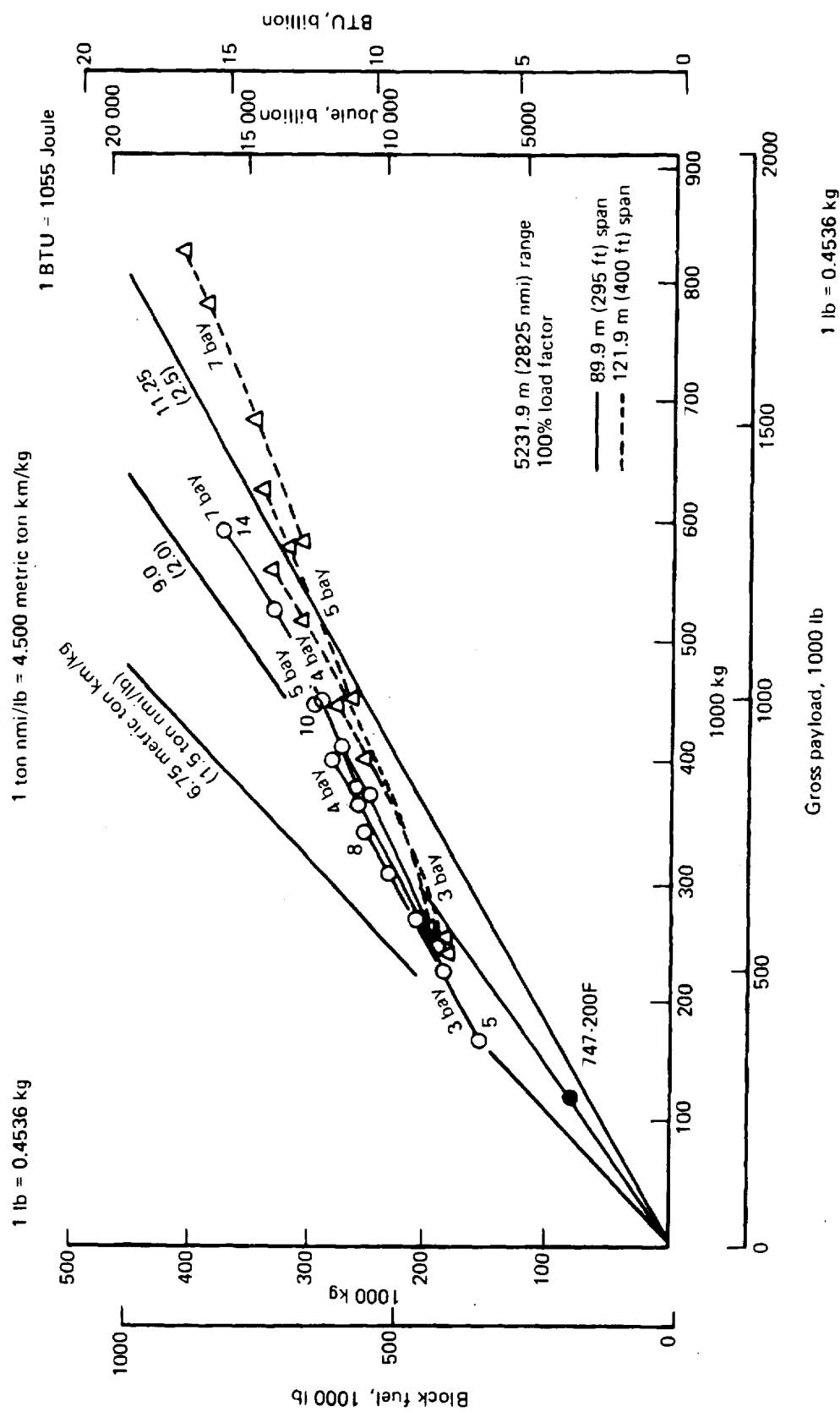
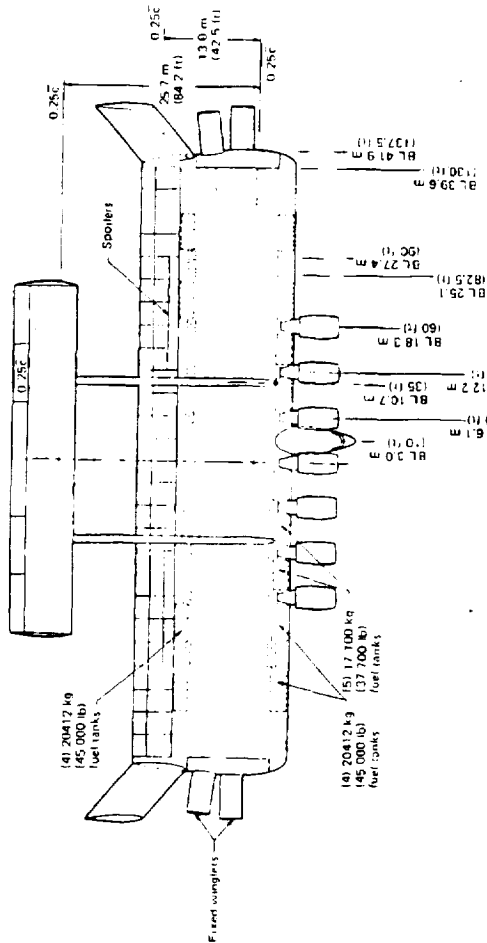
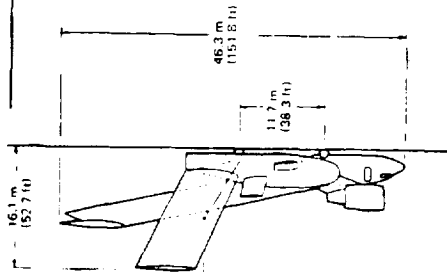
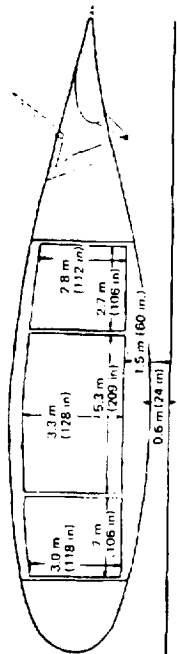


Figure 35.—Block Fuel Versus Gross Payload





Total wing span, 95.7 m (314 ft)  
 Area, 1891 m<sup>2</sup> (20 358 ft<sup>2</sup>)  
 Aspect ratio, 4.84

Total fuel mass, 248 794 kg (548 500 lb)

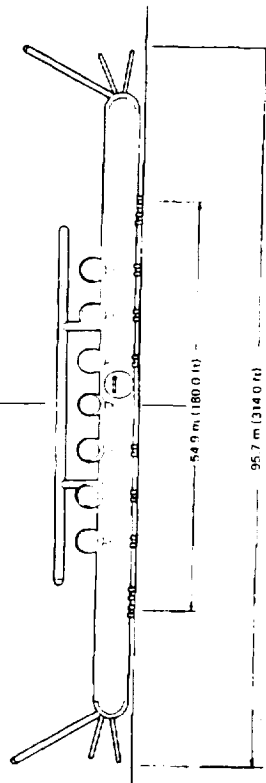
Gross containerized volume 1885 m<sup>3</sup> (66 560 ft<sup>3</sup>) or 52 standard containers  
 (7) 241 760 N (54 350 lb) SLST engines

Landing gear (40) 50 X 20-20 tires, 20 posts

Maximum T.O. gross mass = 759 190 kg (1 673 700 lb)

	Wing	ft. tail (ea)	V. tail (ea)	Boom (ea)	Winglet (ea)
Area, m <sup>2</sup> (ft <sup>2</sup> )	1730 (18 620)*	392 (4217)	109 (1170)	76.6 (825)	18.1 (195)
Span, m (ft)	83.8 (275)*	46.9 (153.8)	1.4 (4.6)	—	5.9 (19.5)
Aspect ratio	4.06*	5.61	1.81	—	1.95
Sweep, deg	0	0	22.0	78.0	—
MAC, m (in)	20.7 (81.6)*	8.4 (32.9)	7.6 (30.0)	—	3.0 (12.0)
t/c, %	21.5*	16.0	16.0	—	10.0
Vol. coef. V	—	0.28	0.0097	—	—

\* Basic wing only



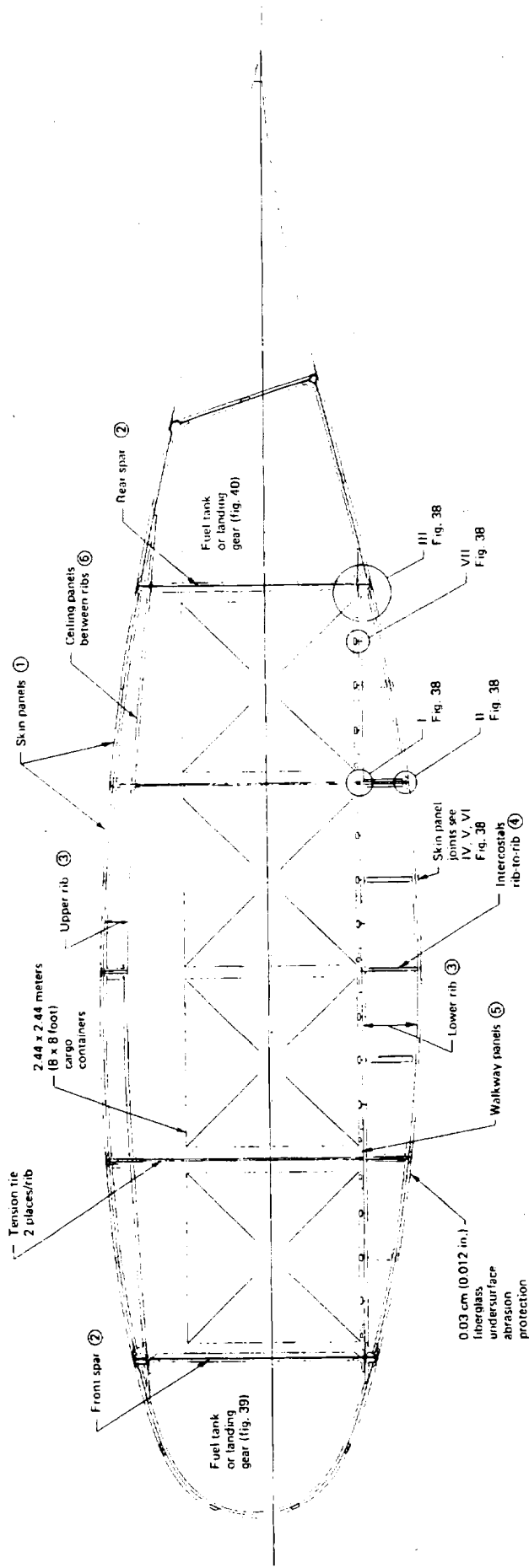
ORIGINAL PAGE IS  
 OF POOR QUALITY

PRECEDING PAGE BLANK NOT FILMED

FOLDOUT FRAME

Figure 36.—Distributed Load Freighter,  
 Selected Configuration





- ① Honeycomb sandwich 3.81 cm (1.50 in.) thick aluminum faces 0.081 cm (0.032 in.) outer, 0.03 cm (0.012 in.) inner, 147 cm (58 in.) maximum width
- ② Honeycomb sandwich plus stiff's, 10.16 cm (4.00 in.) thick, 0.05 cm (0.02 in.) aluminum faces
- ③ Honeycomb sandwich web 3.81 cm (1.50 in.) thick aluminum angle chords
- ④ Honeycomb sandwich web 3.81 cm (1.50 in.) thick aluminum channel chords
- ⑤ Honeycomb sandwich 3.81 cm (1.50 in.) thick aluminum faces upper, 0.03 cm (0.012 in.) lower
- ⑥ Honeycomb sandwich 2.54 cm (1.00 in.) thick, 0.03 cm (0.012 in.) aluminum faces

Figure 37 - Wing Cross Section

PRECEDING PAGE BLANK NOT FILMED





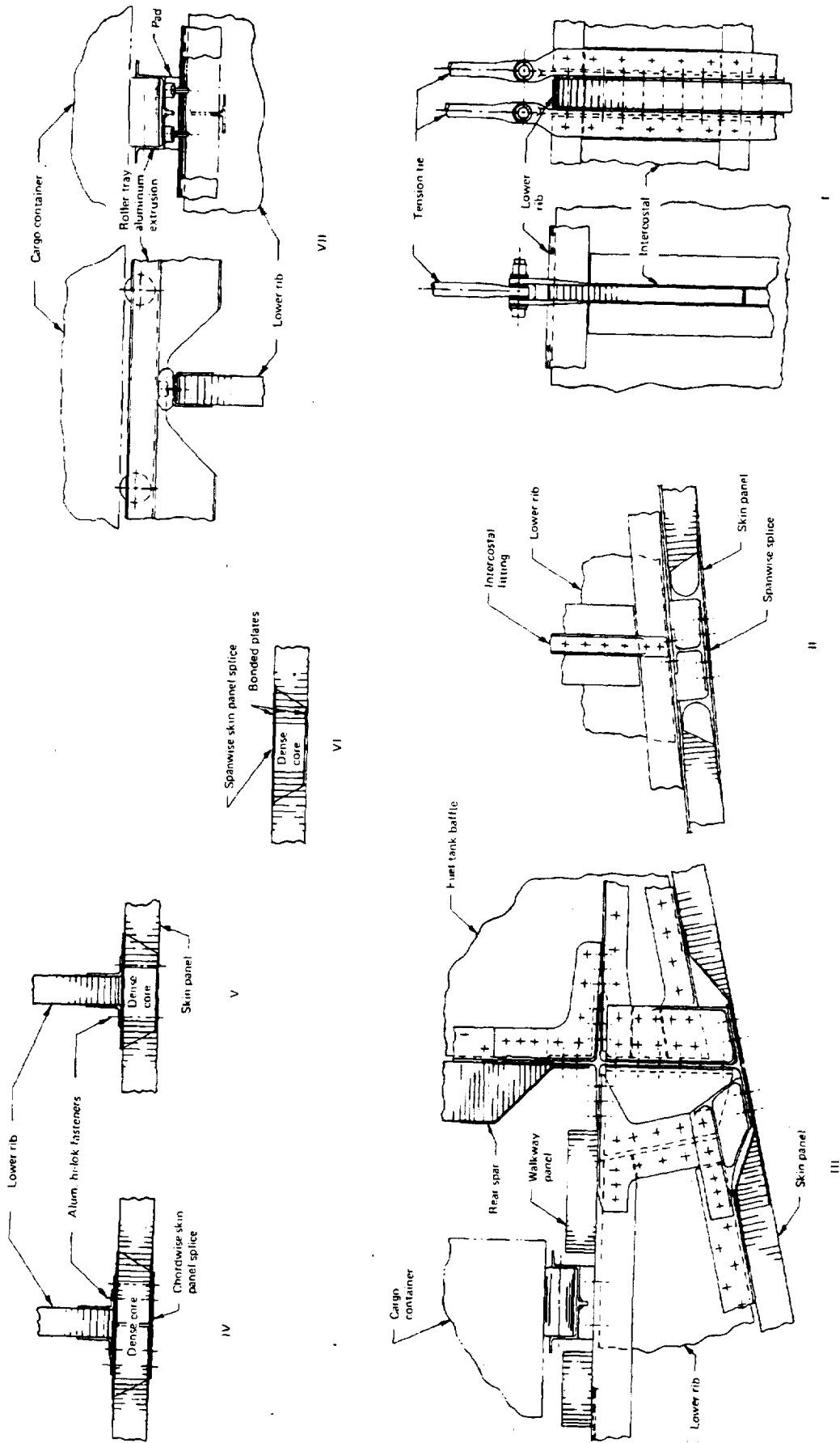


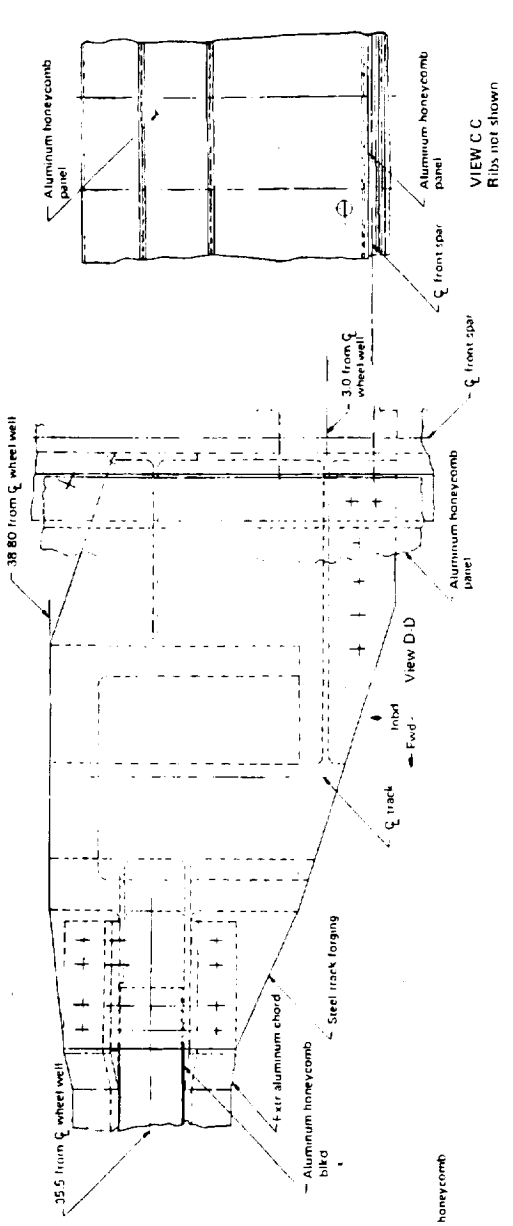
Figure 38. Wing Structural Details

PRECEDING PAGE BLANK NOT FILMED

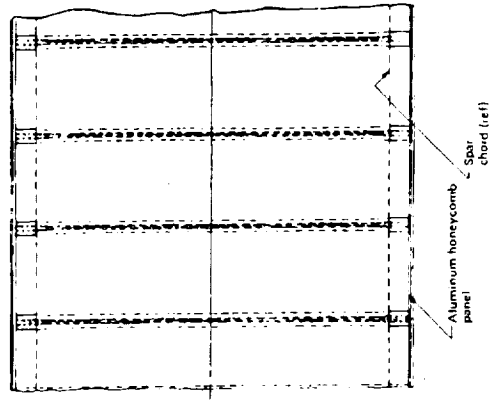
100-100000-1

100-100000-1





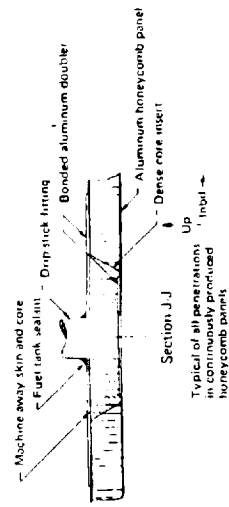
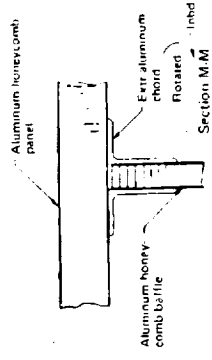
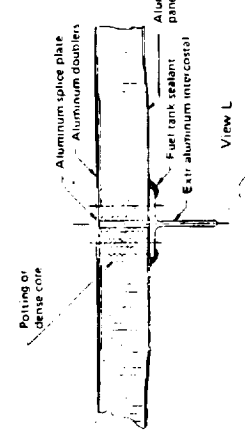
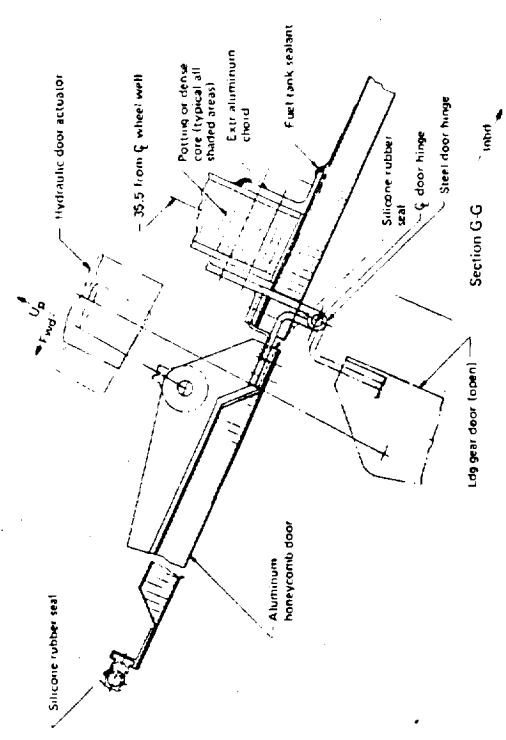
VIEW C C  
 Ribs not shown



View E E

Figure 39 - Leading Edge Box Installation  
 (Sheet 1)

FOLDOUT FRAME 2-



C.2  
 PREPARE PAGE BLANK NOT FILMED

FOLDOUT FRAME 1



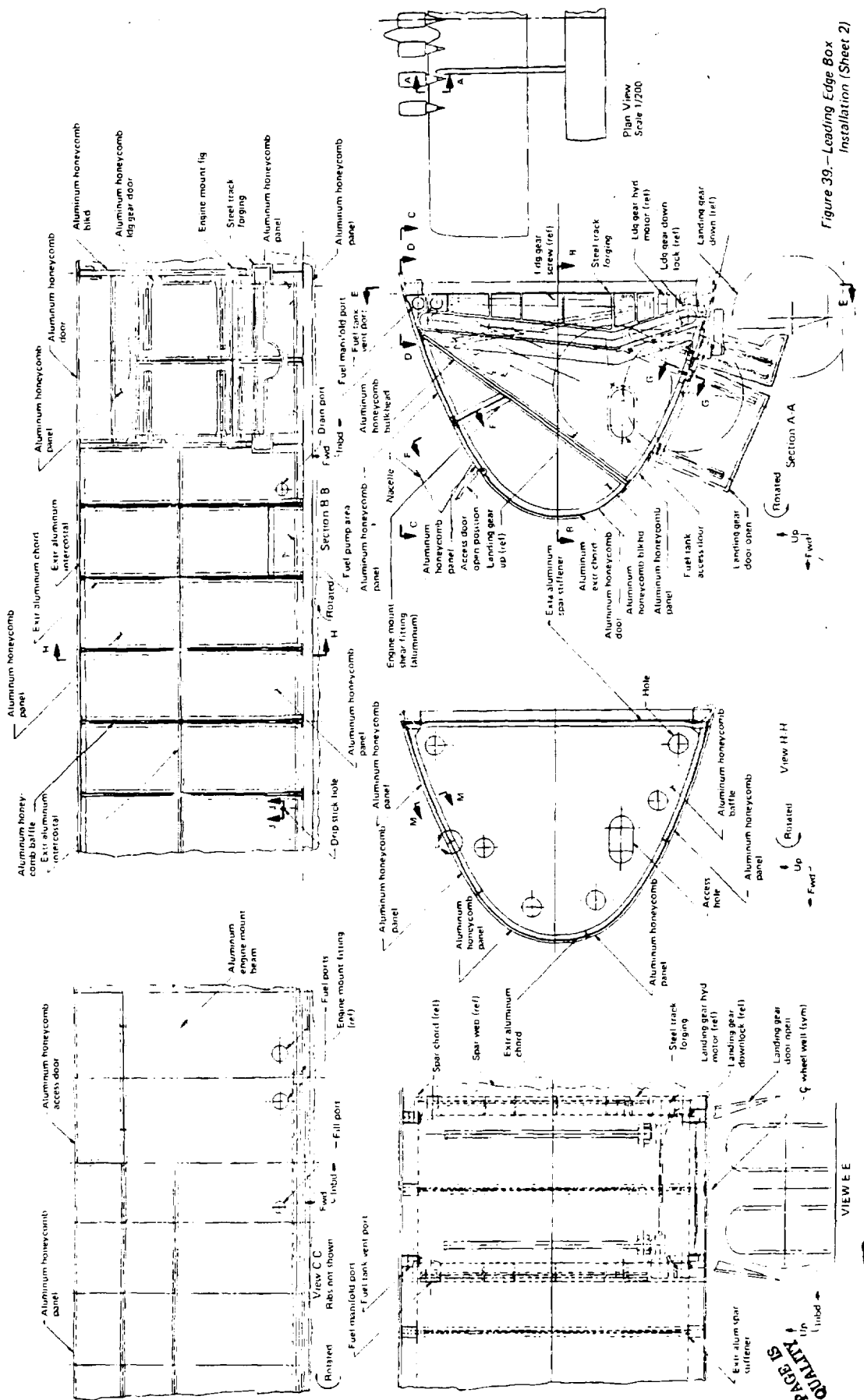


Figure 39.—Leading Edge Box Installation (Sheet 2)

PREVIOUS PAGE IS REPRODUCED FROM QUALITY CONTROL

PRECEDING PAGE BLANK NOT FILMED



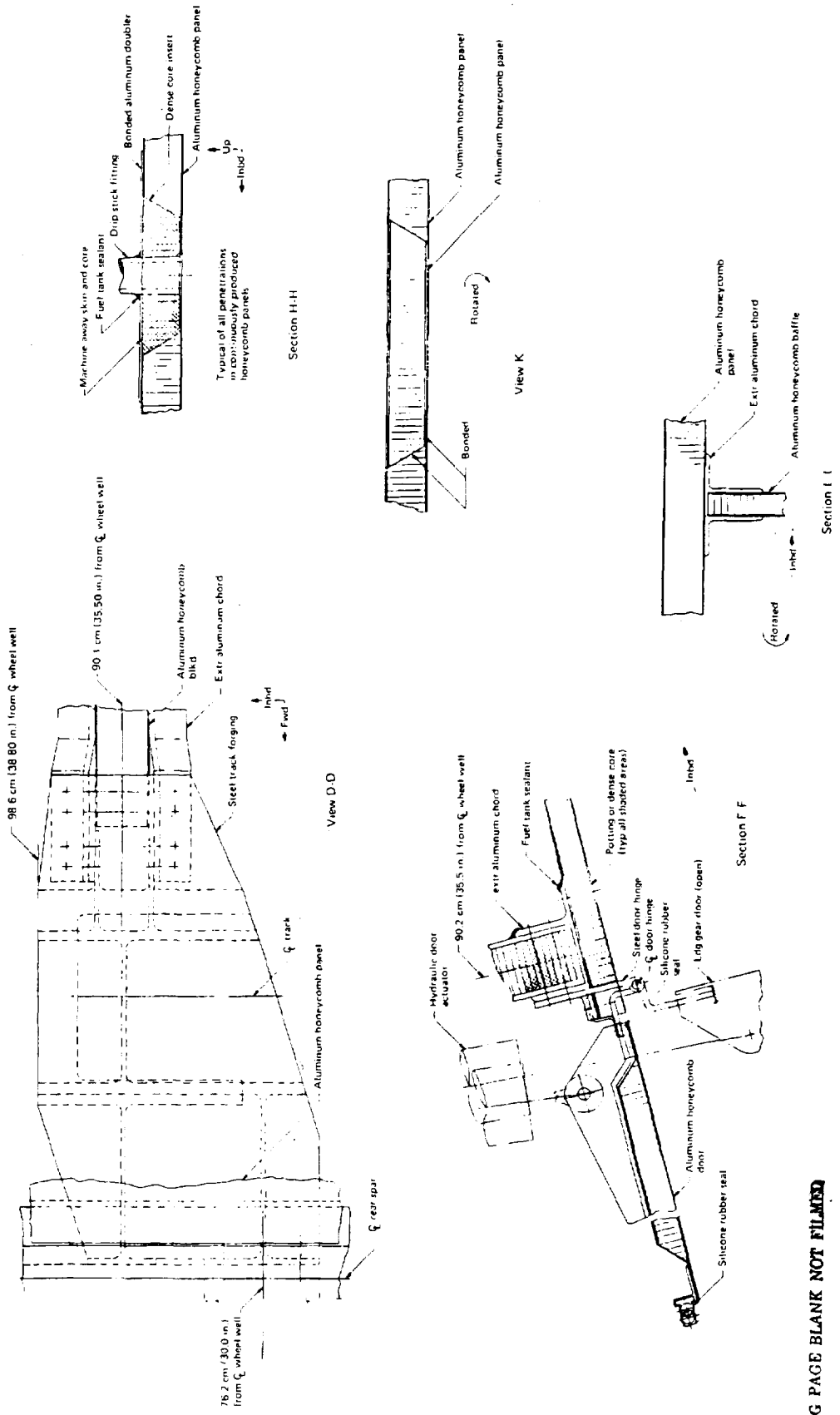


Figure 40 - Trailing Edge Box Installation (Sheet 1)

PRECEDING PAGE BLANK NOT FILMED

FOLDOUT FRAME 1

FOLDOUT FRAME 2





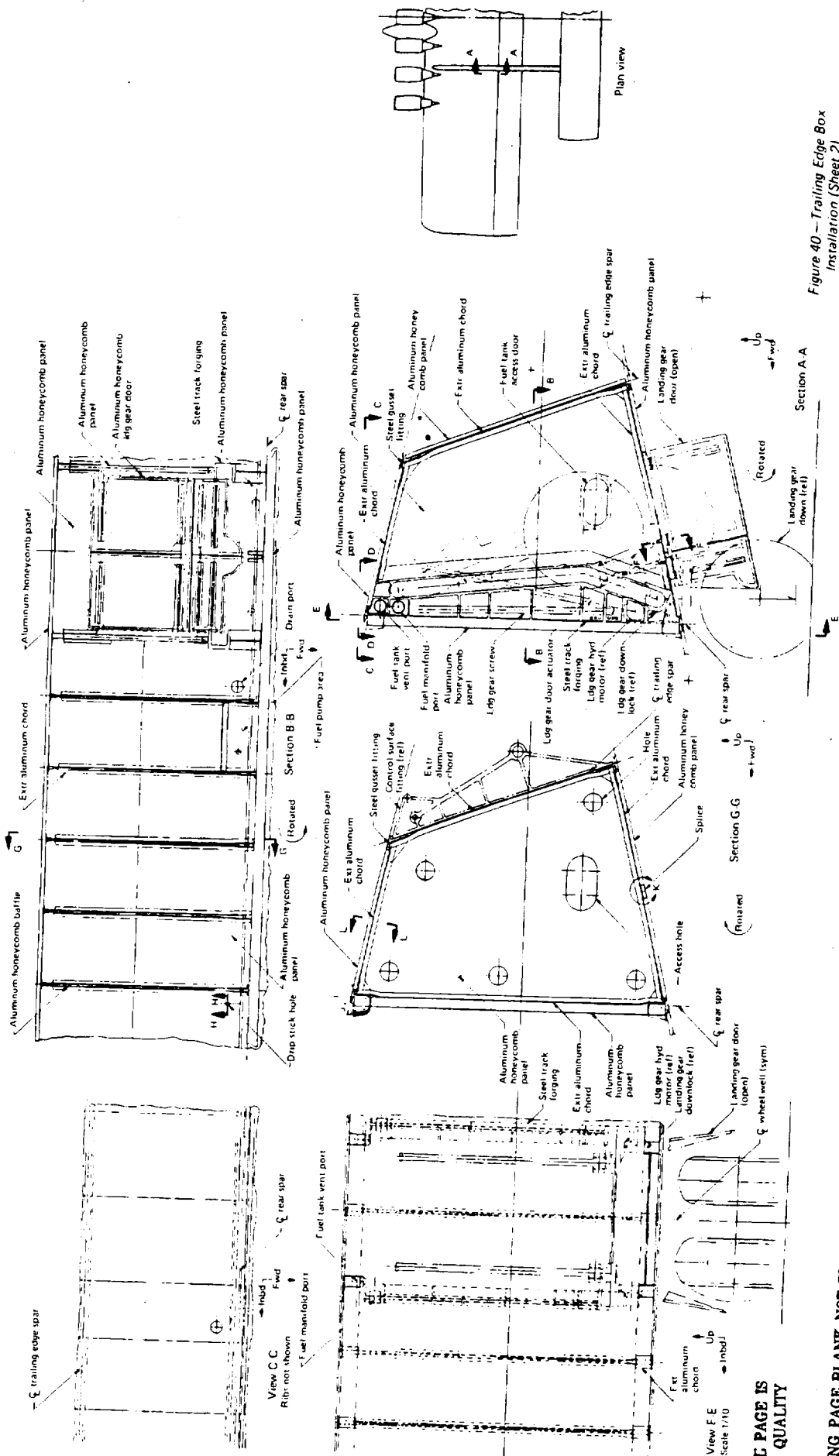


Figure 40—Trailing Edge Box Installation (Sheet 2)

ORIGINAL PAGE IS OF POOR QUALITY

PRECEDING PAGE BLANK NOT FILMED

FOLDOUT FRAME



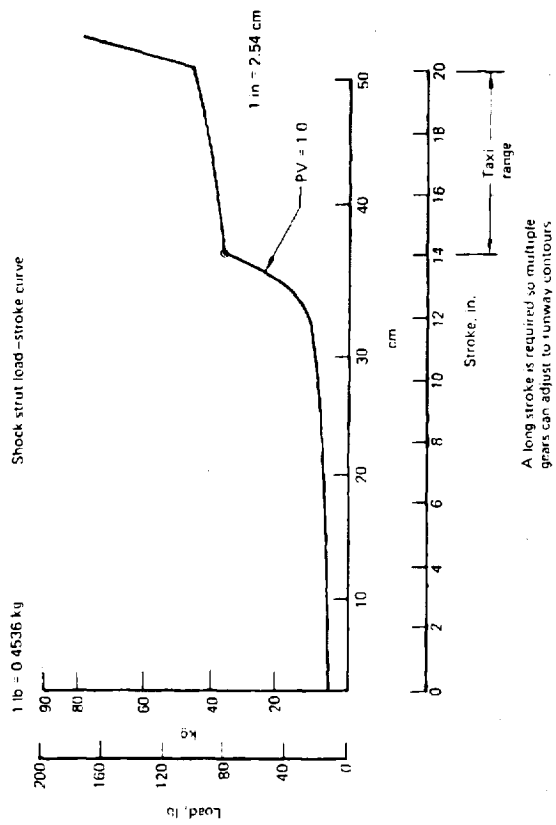
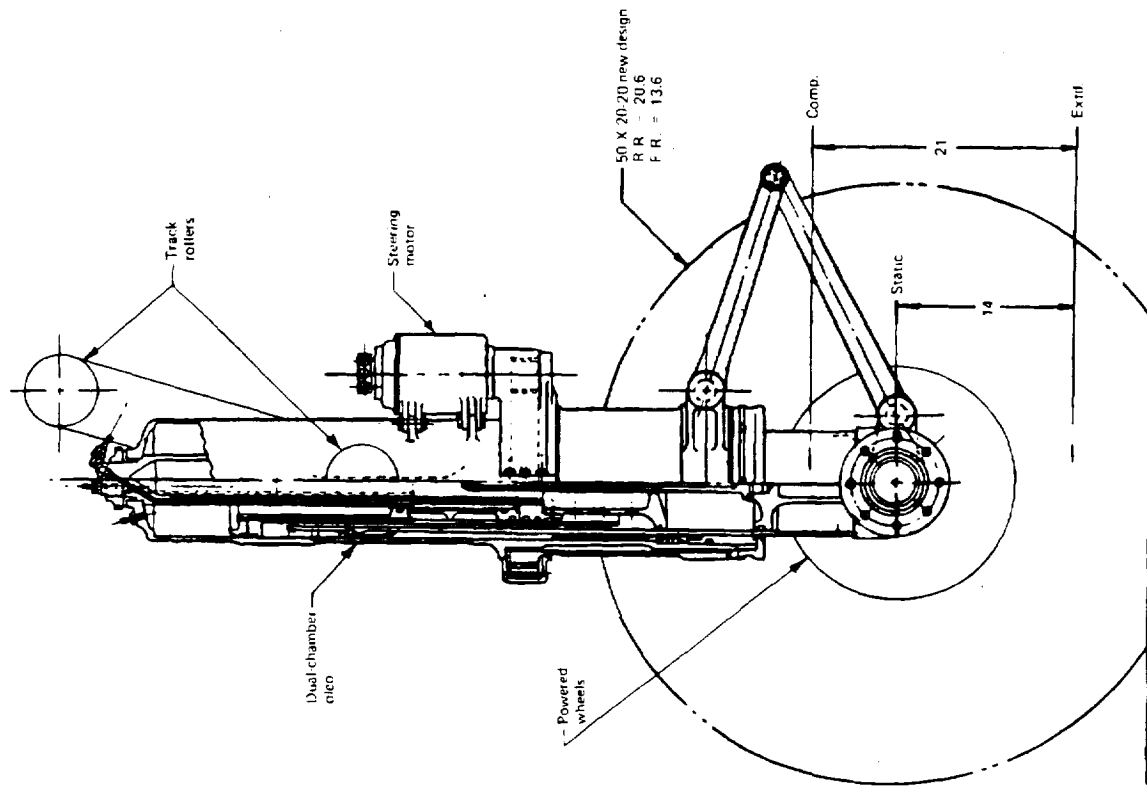


Figure 41. - Shock Strut Assembly—Alt and Forward Landing Gears

FOLDOUT FRAME /

PRECEDING PAGE BLANK NOT FILMED



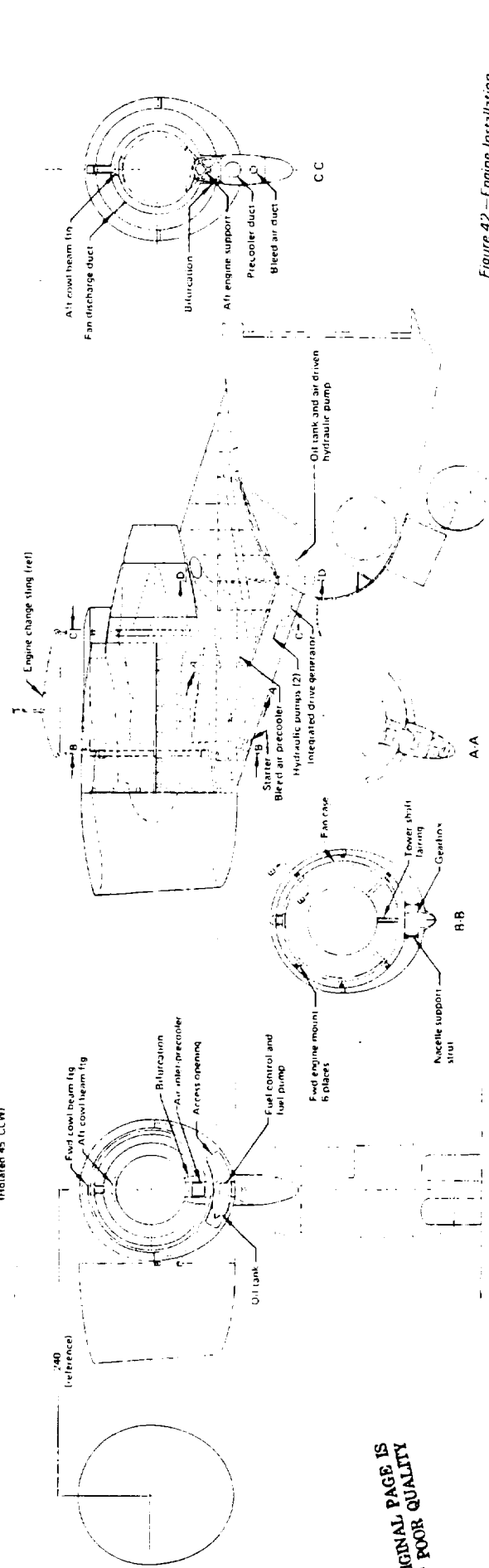
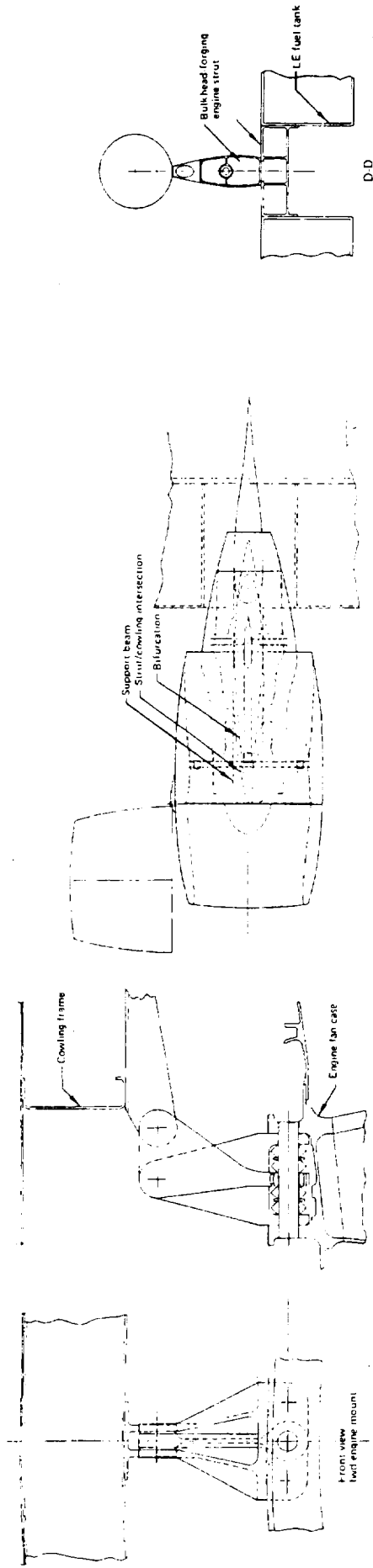


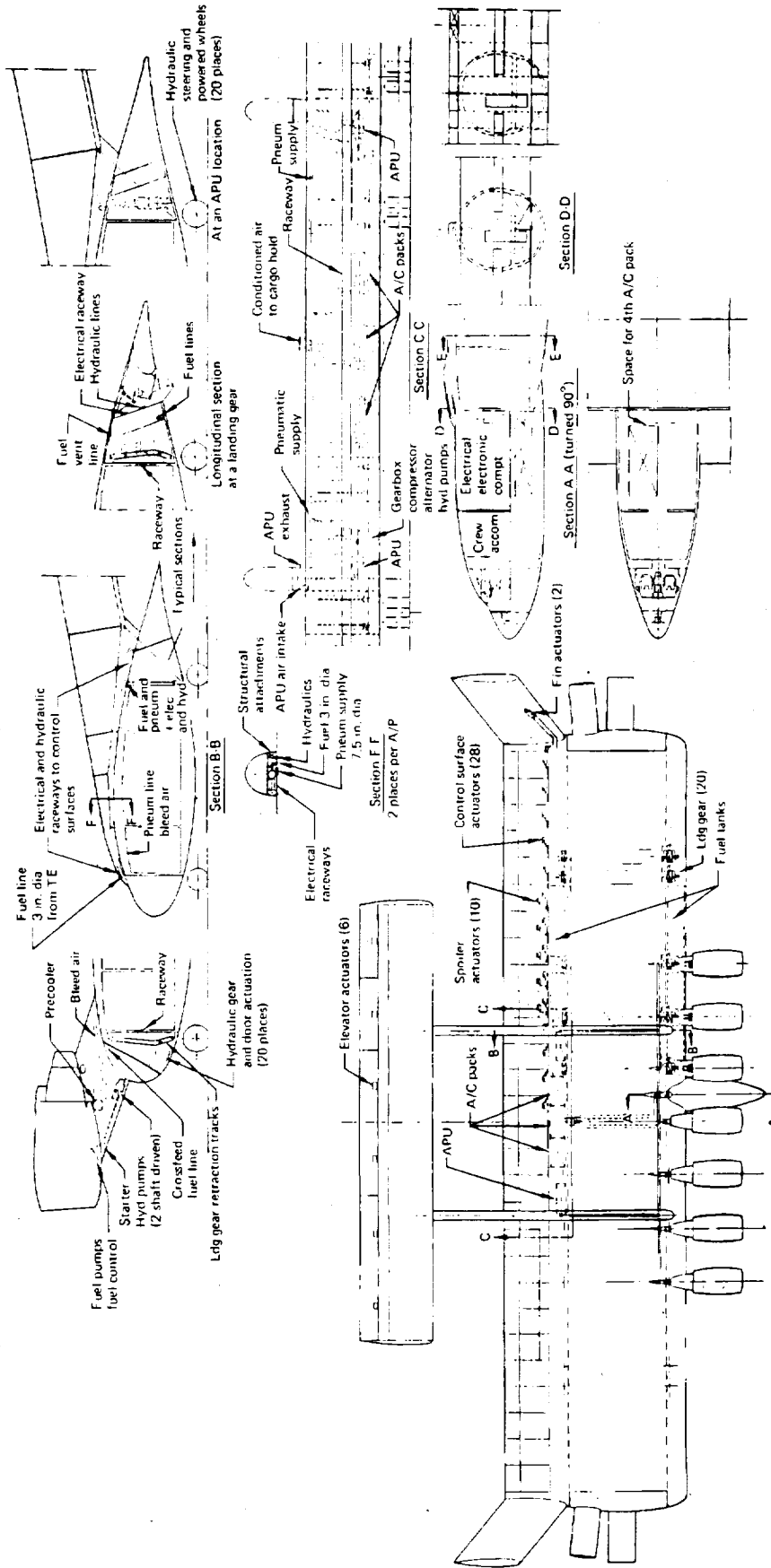
Figure 42 - Engine Installation

ORIGINAL PAGE IS  
OF POOR QUALITY

PRECEDING PAGE BLANK NOT FILLED

FOLDOUT FRAME



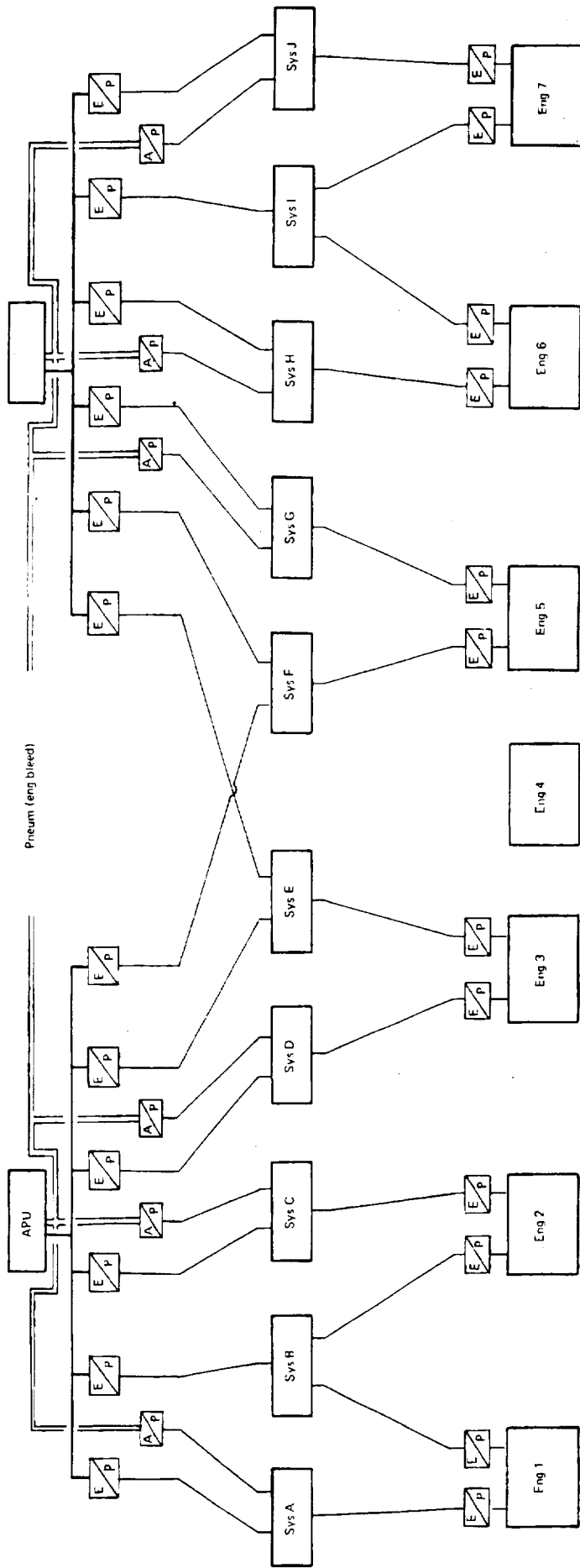



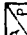
PRECEDING PAGE BLANK NOT FILMED

Figure 4.3.—Preliminary System Arrangement







 Shaft-driven pump  
 Air-driven pump

**Pumps**  
 24 shaft driven pumps  
 6 air driven pumps  
 30 pumps total

**Hydraulic systems**  
 10 subsystems  
 3 pumps per subsystem

PRECEDING PAGE BLANK NOT FILMED

Figure 44.—Hydraulic Power Supply System



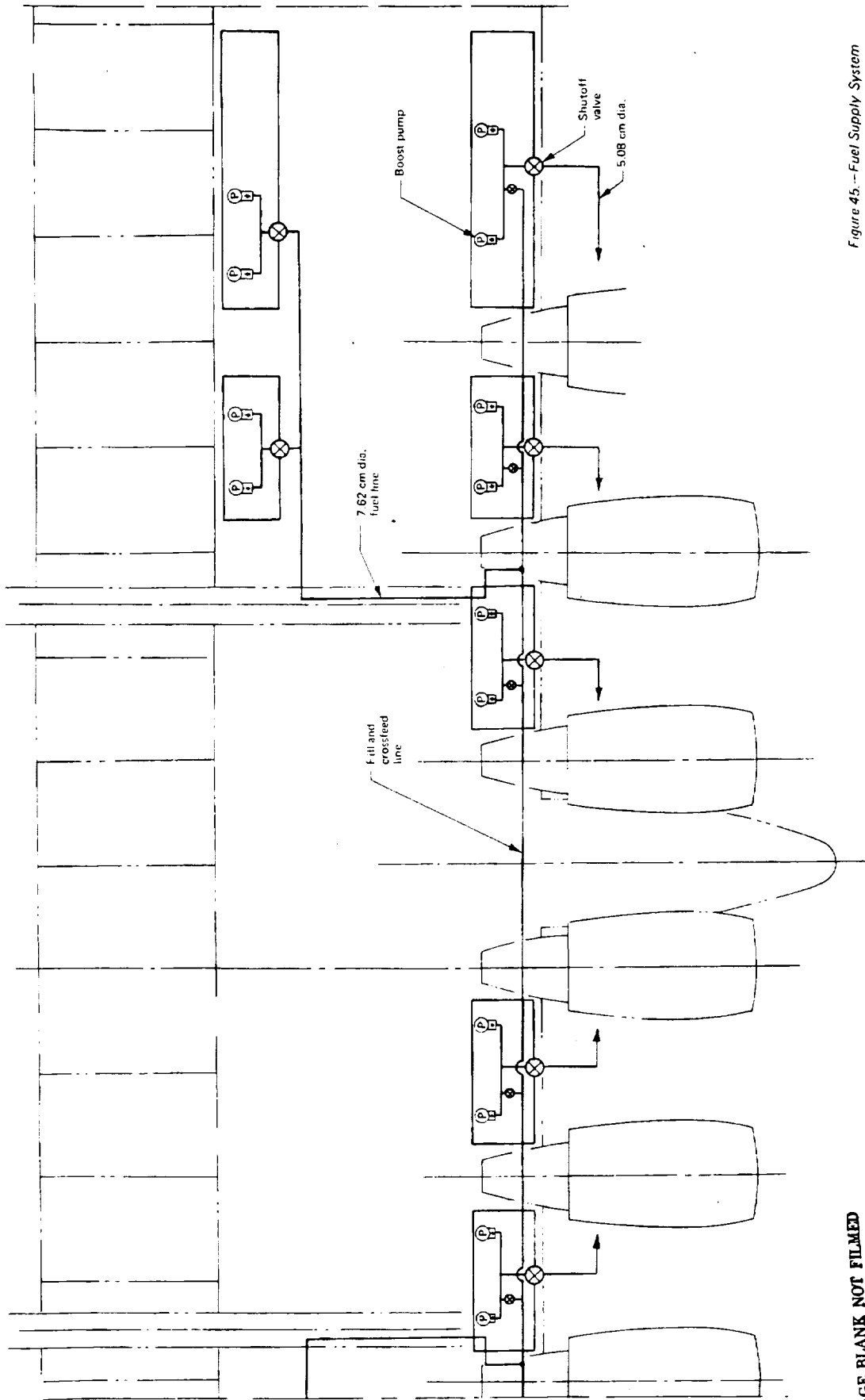


Figure 45.-- Fuel Supply System

PRECEDING PAGE BLANK NOT FILMED

FOLDOUT FRAME /



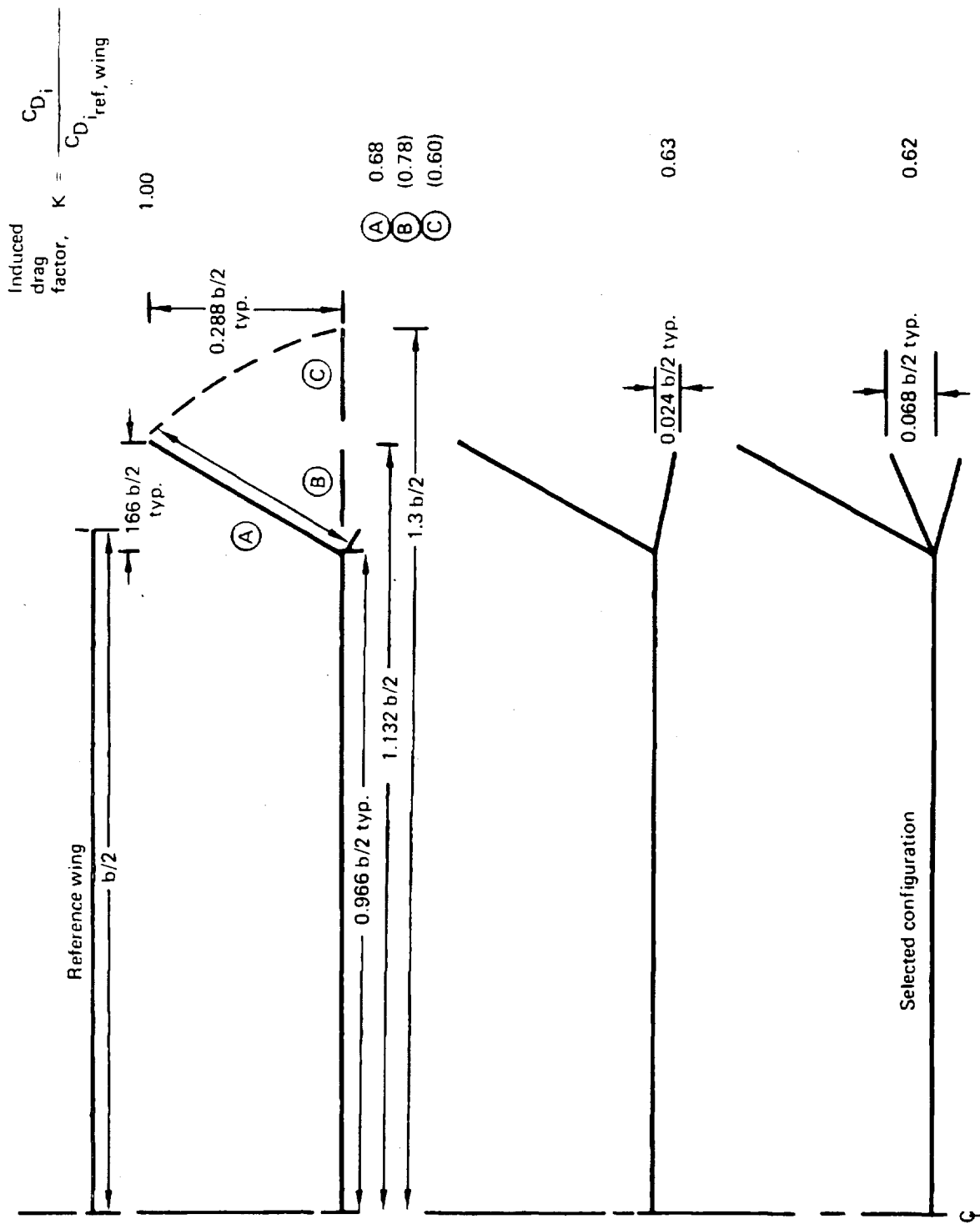


Figure 46.—Induced Drag Factors for Optimum Loaded Wings With Tip Fins

PRECEDING PAGE BLANK NOT FILMED

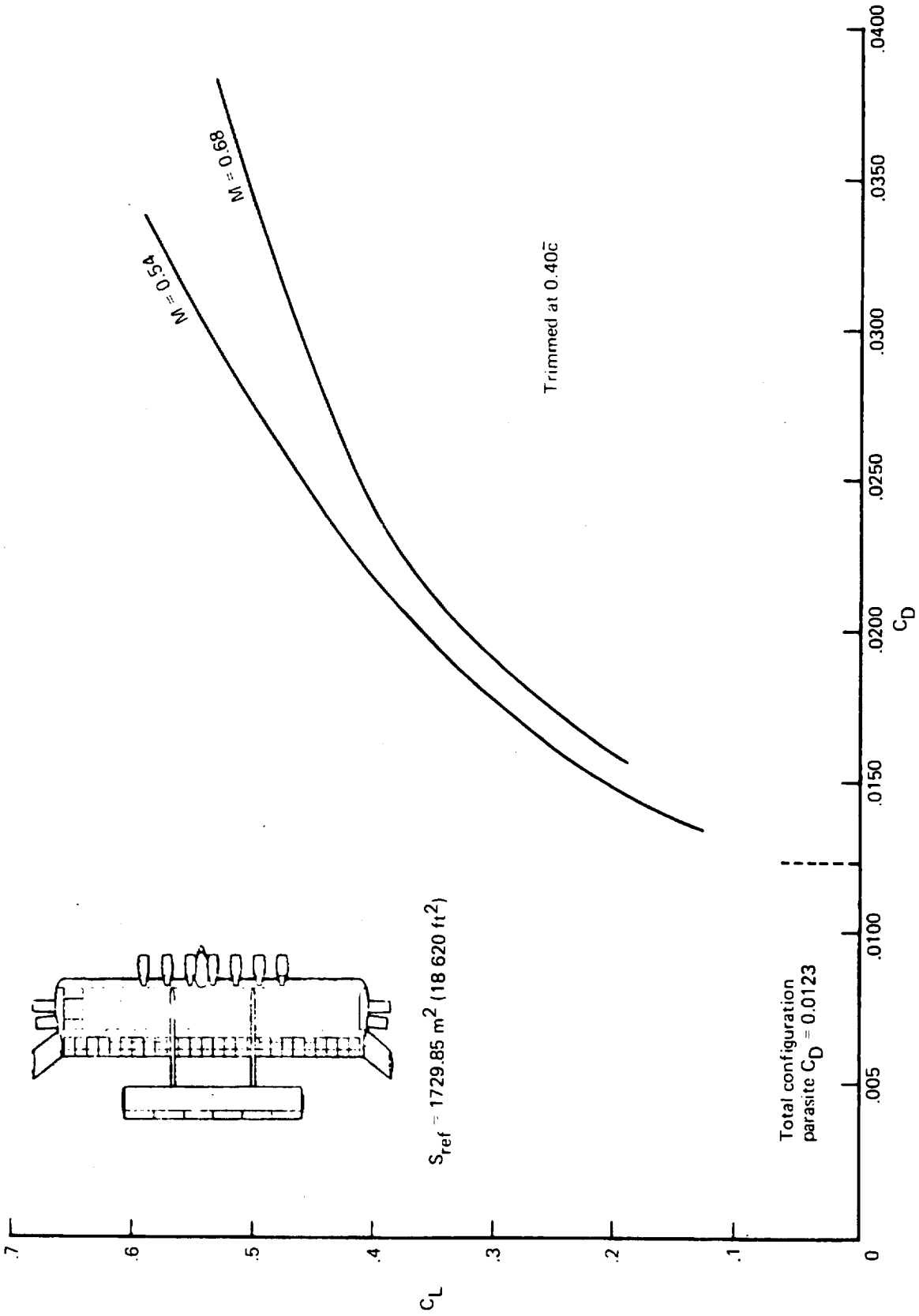


Figure 47.—High-Speed Drag Polar, Distributed-Load Freighter—Selected Configuration

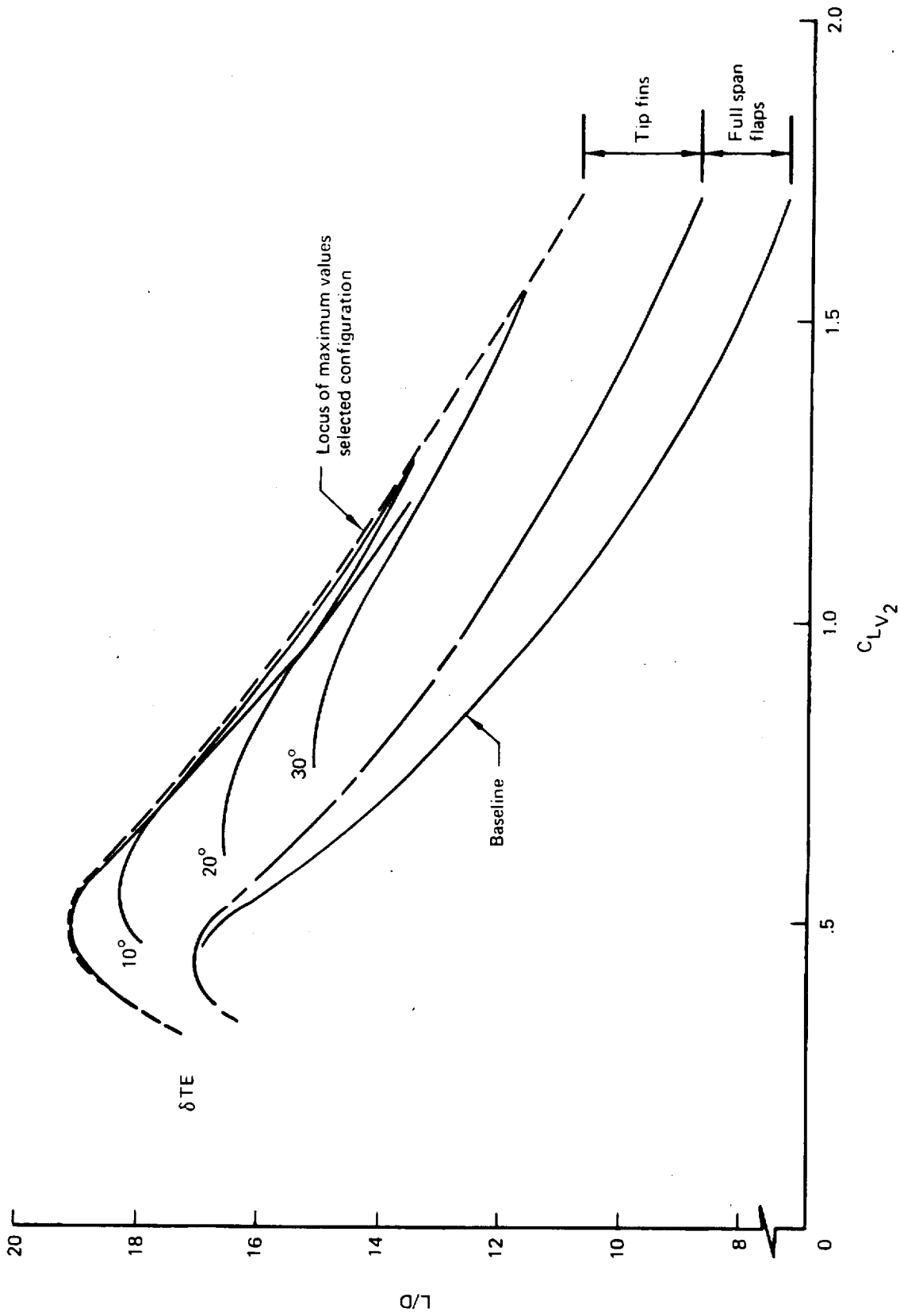


Figure 48.—Low Speed Drag Polar, Selected Configuration

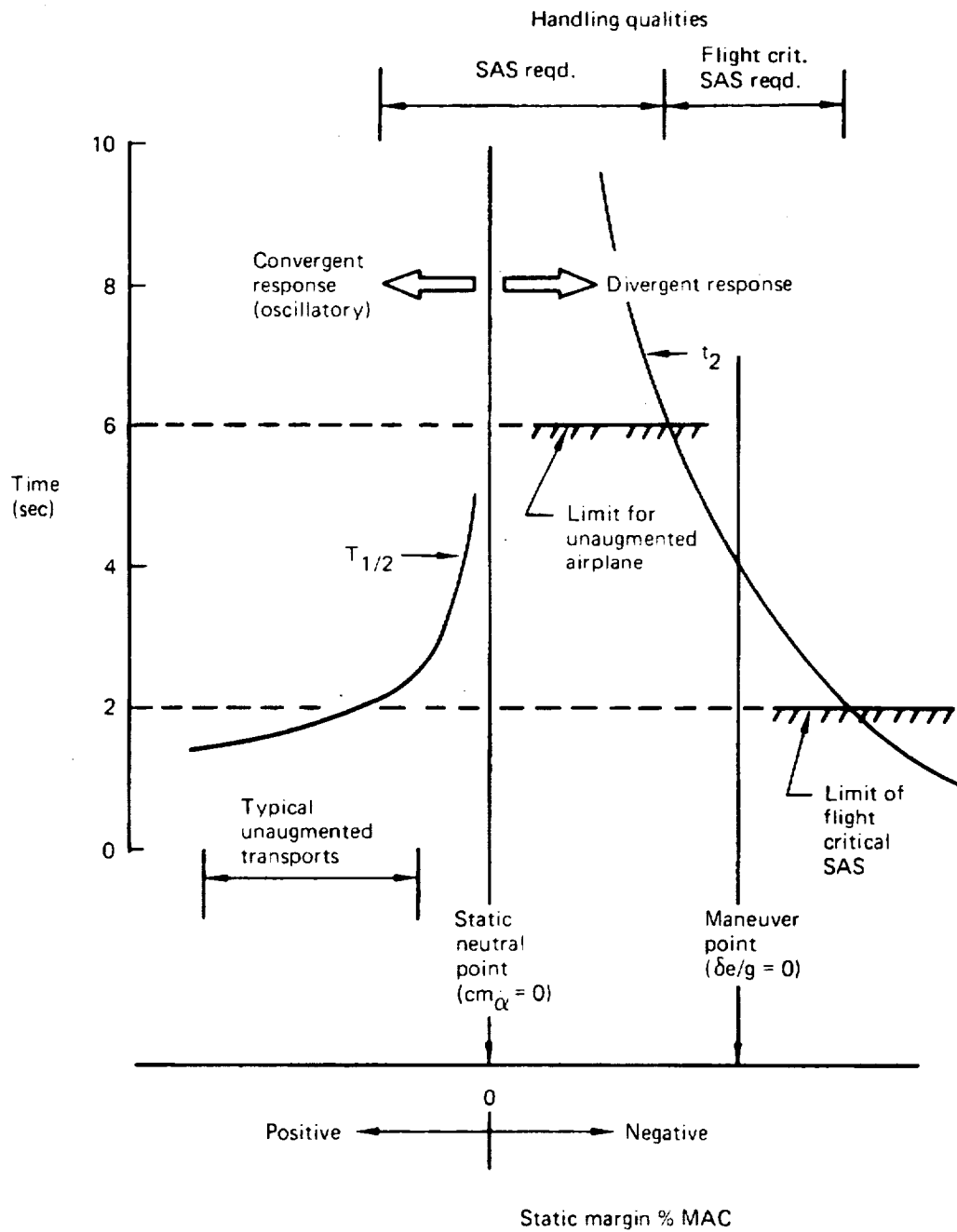


Figure 49.—Longitudinal Balance Philosophy



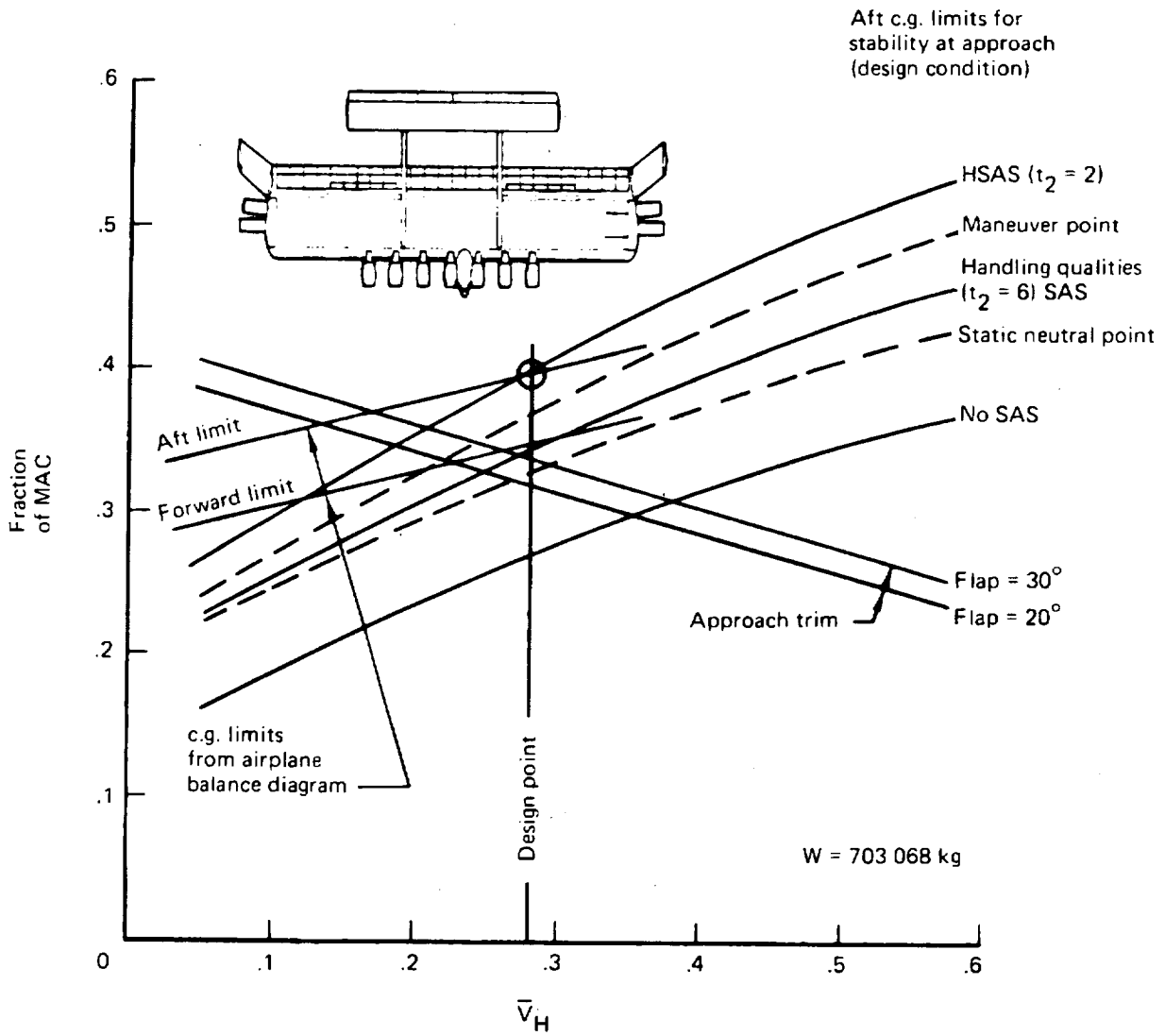


Figure 50.—Balance Philosophy Application

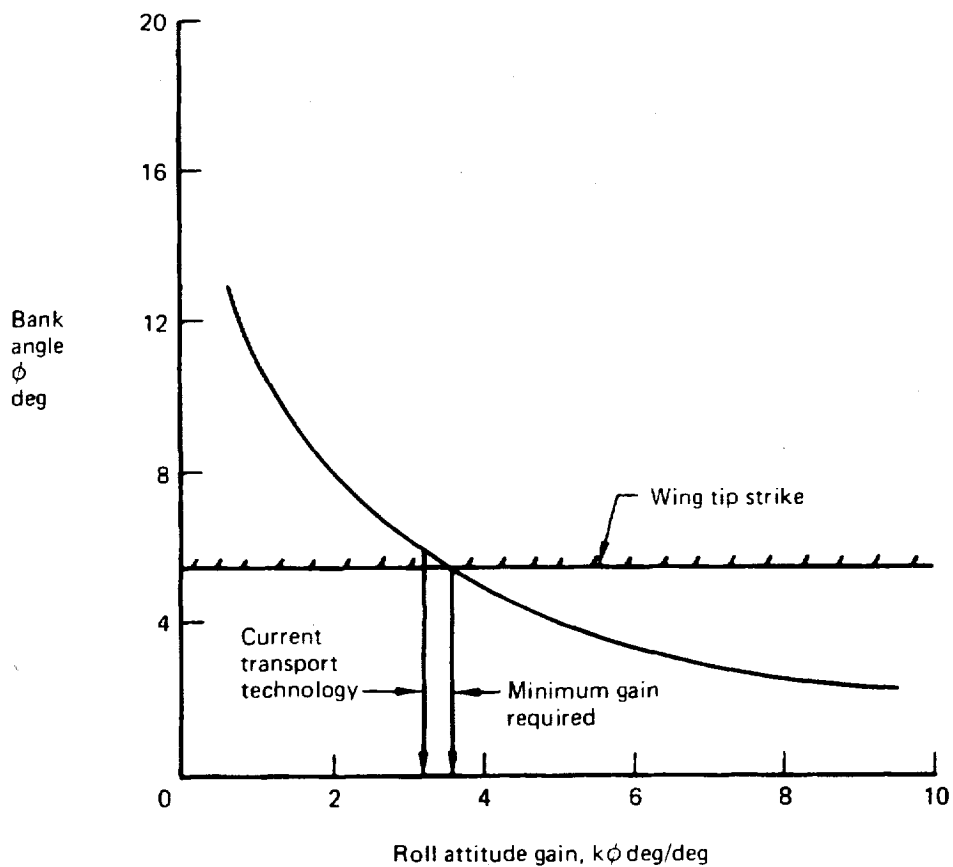
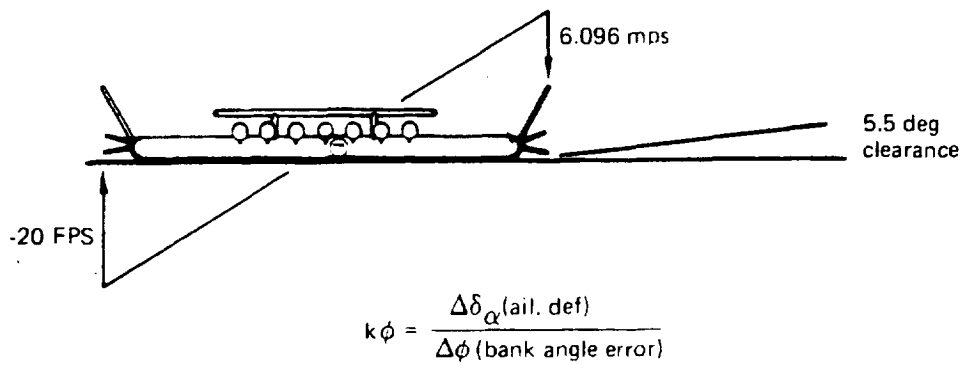
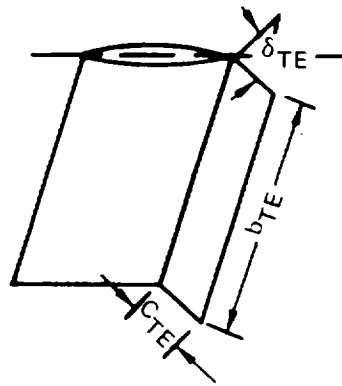


Figure 51.—Roll Response Due to 20 FPS Asymmetric Gust



$$C_{D_{TE}} = \frac{\Delta D_{TE}}{q S_{TE_{proj}}} = 1.0$$

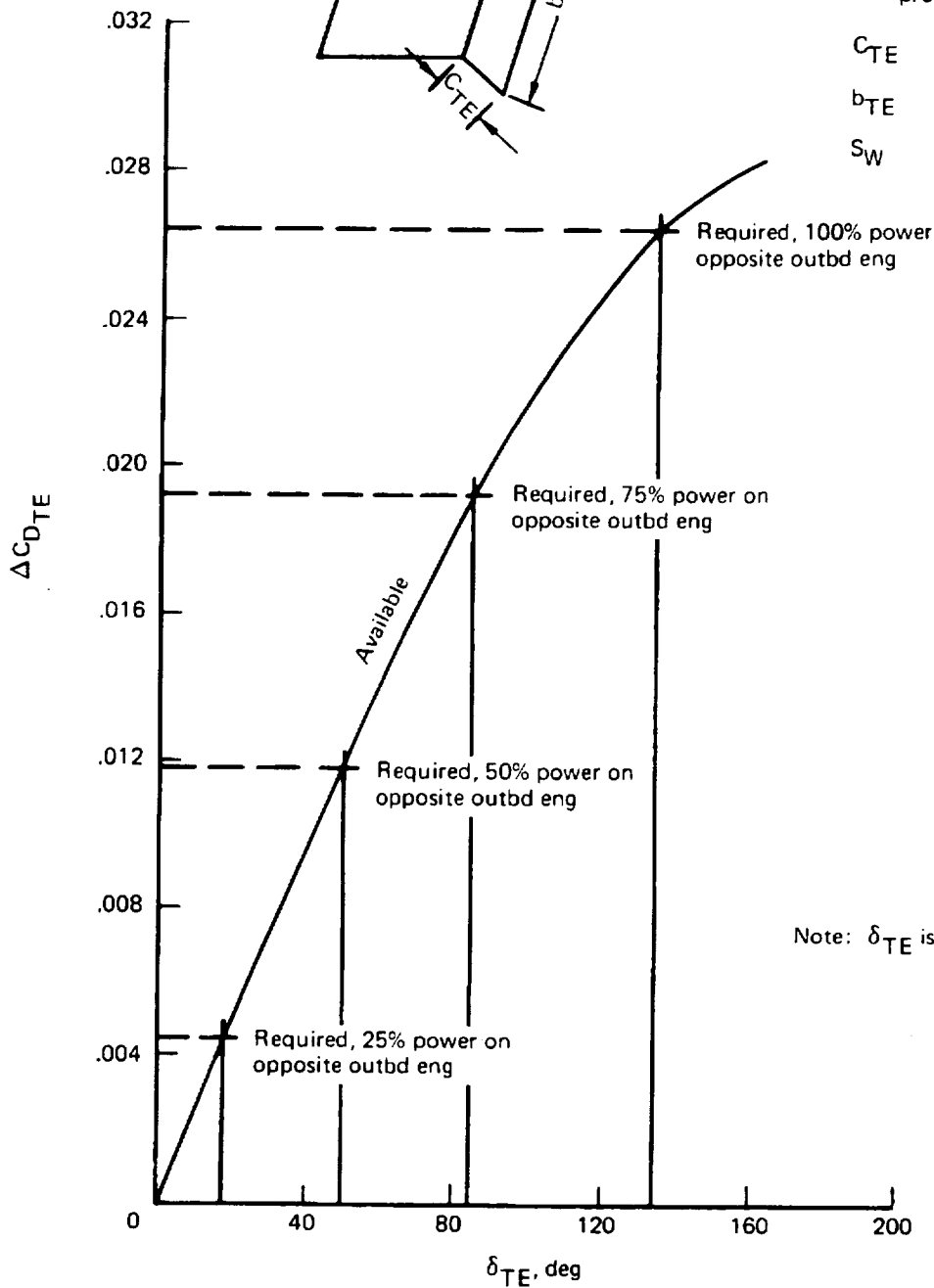
$$\Delta C_{D_{TE}} = \frac{\Delta D_{TE}}{q S_W}$$

$$S_{TE_{proj}} = 2 b_{TE} C_{TE} \sin \frac{\delta_{TE}}{2}$$

$$C_{TE} = 0.32 C_V = 2.44 \text{ m}$$

$$b_{TE} = b_V = 14.02 \text{ m}$$

$$S_W = 1729.85 \text{ m}^2$$



Note:  $\delta_{TE}$  is total included angle

0% power on remaining outbd eng

Figure 52.—Vertical Fin Trailing Edge Deflection Required for Takeoff Engine Out Trim

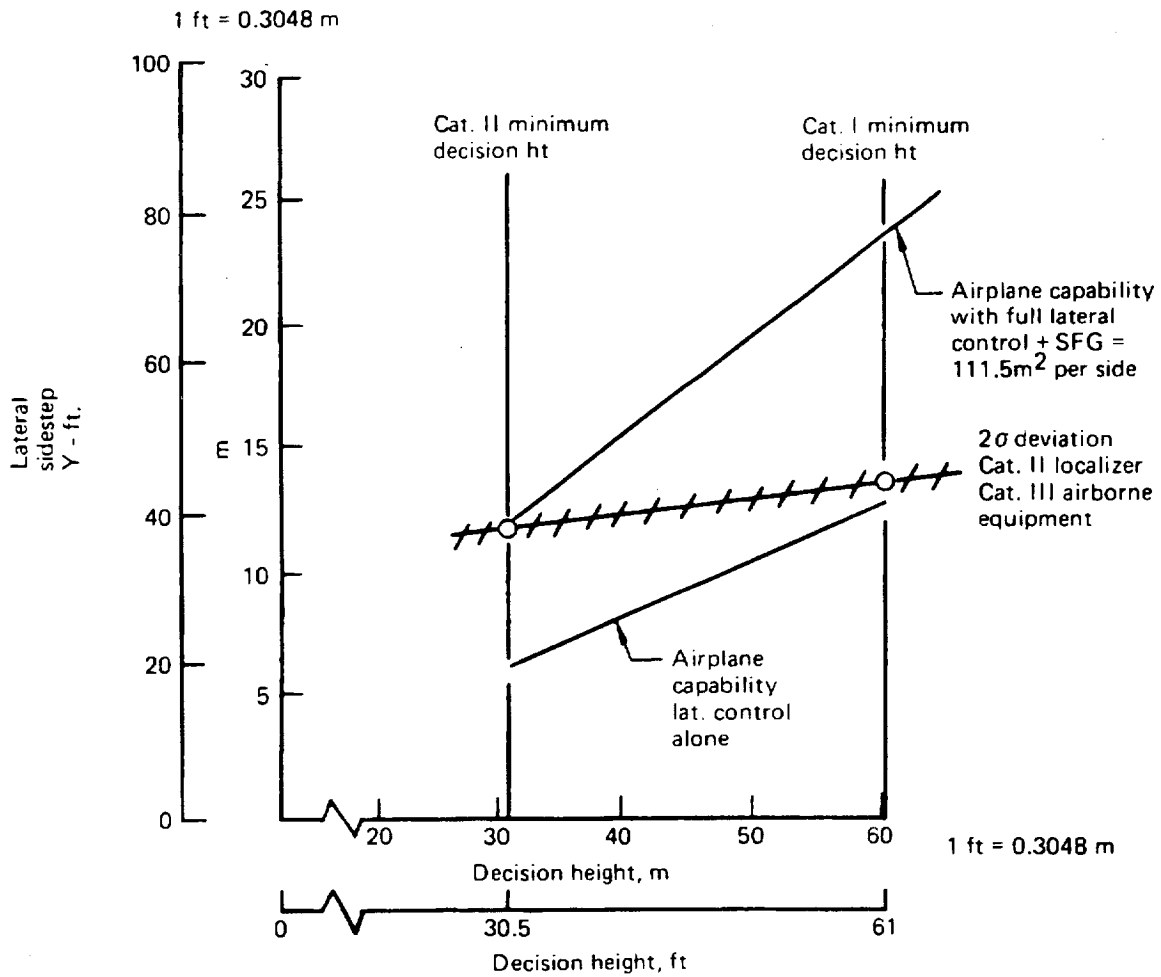
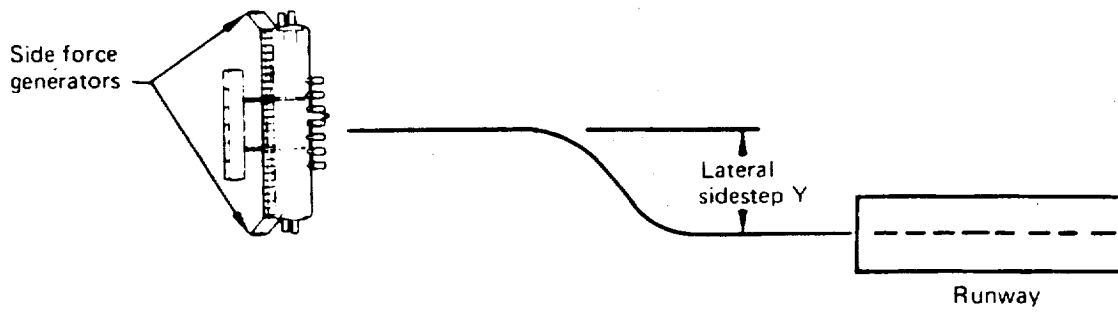


Figure 53.—Side Force Generators in Landing Approach

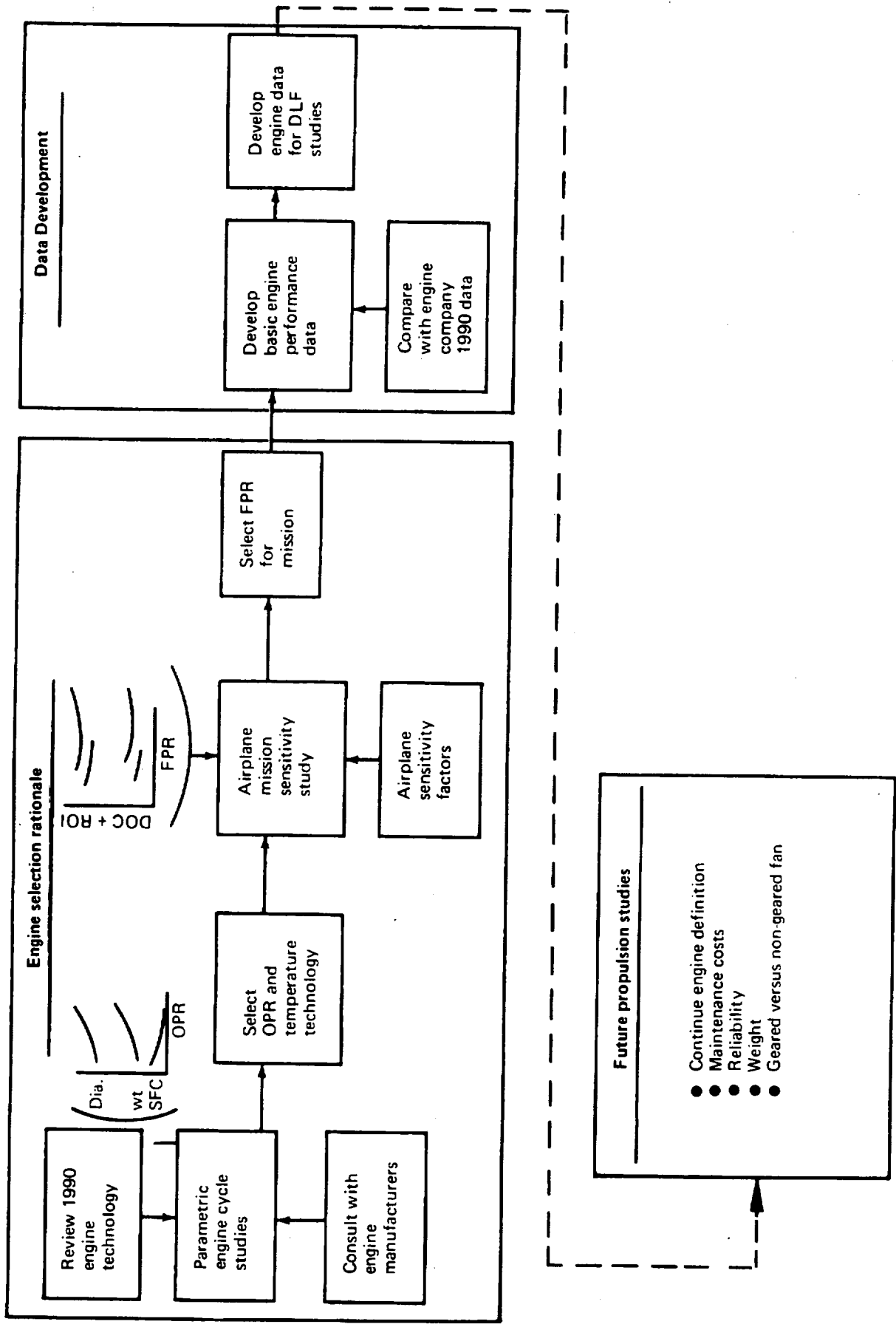


Figure 54.—Propulsion Technology Study

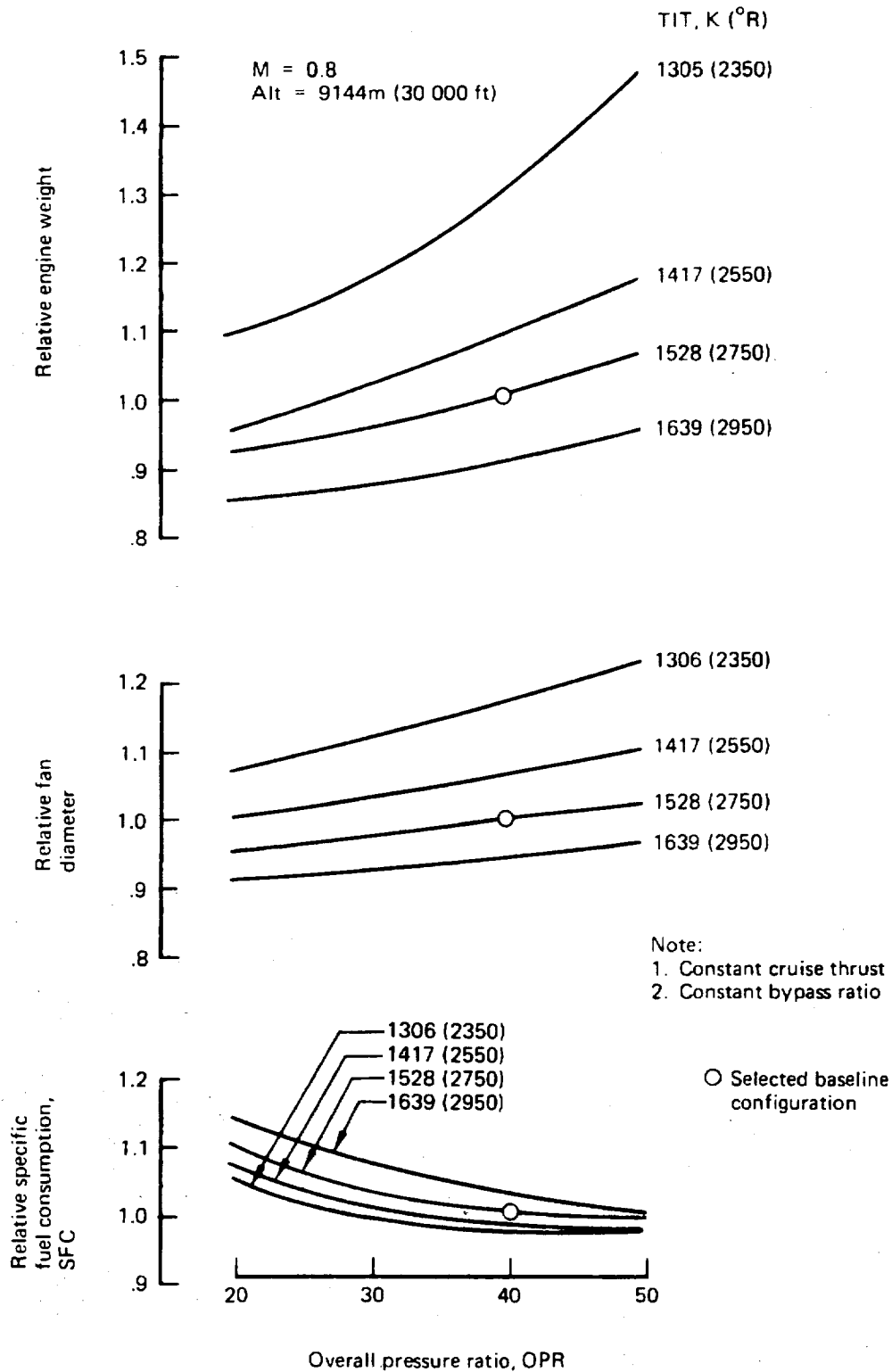


Figure 55.—1990 Technology Engine, Effects of Varying Overall Pressure Ratio and Turbine Inlet Temperature

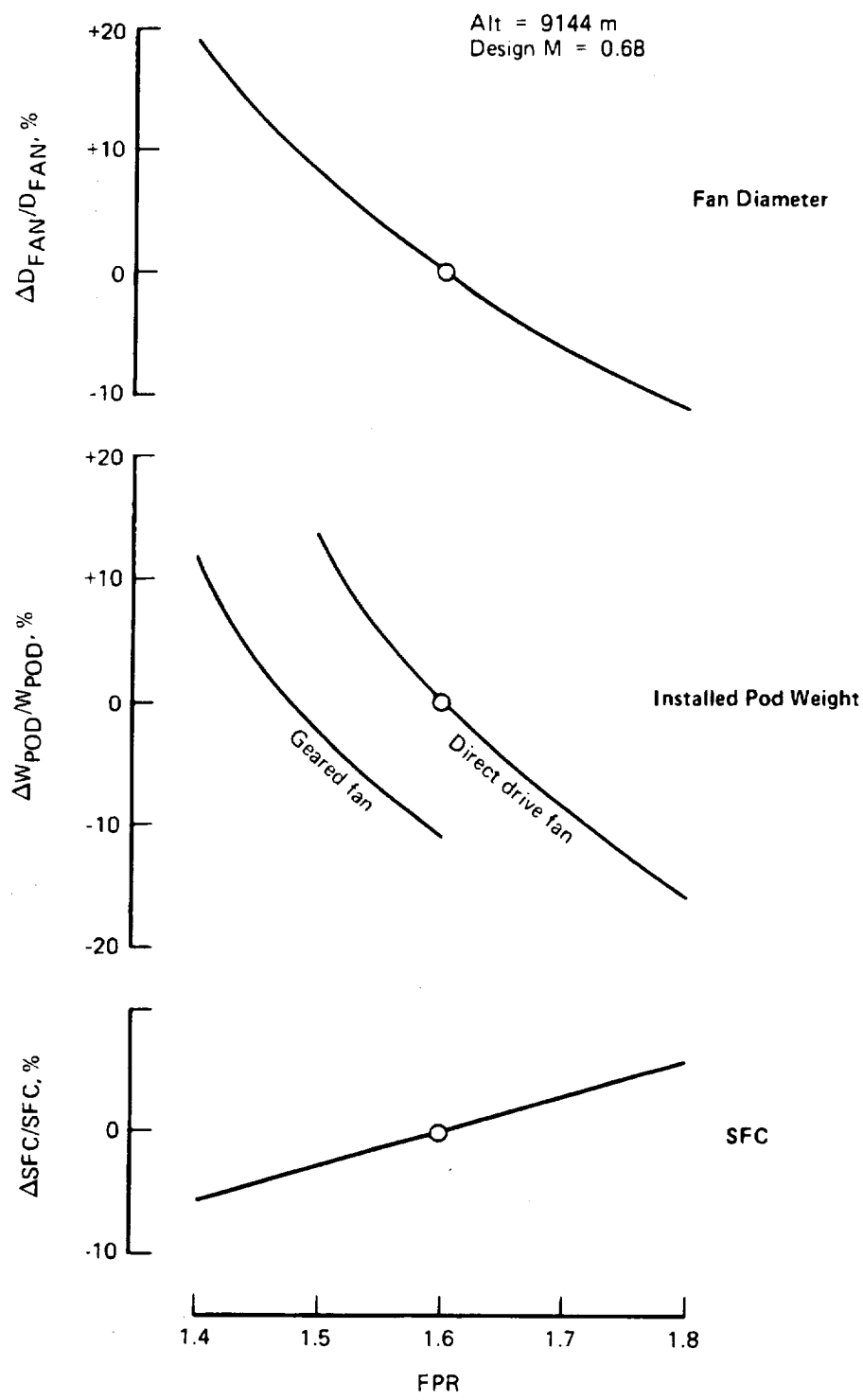
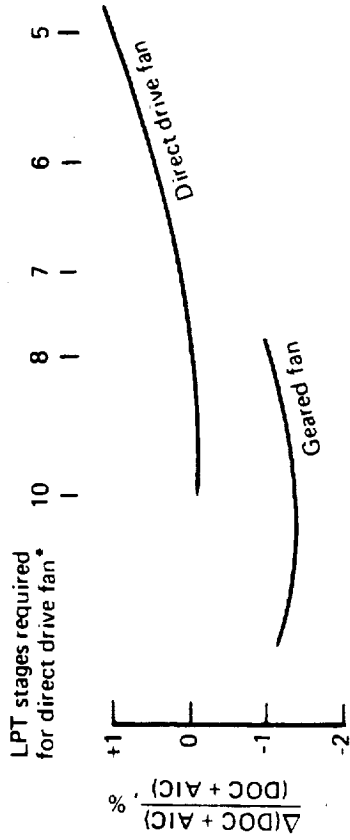


Figure 56.—1990 Turbofan Engines, Fan Pressure Ratio Impact

Design Mach 0.68



Alt = 9144 m (30 000 ft)  
 TIT (cruise) = 1528 K  
 OPR = 40

\*Gearing required 2 LPT stages at all fan pressure ratios

Design Mach 0.78

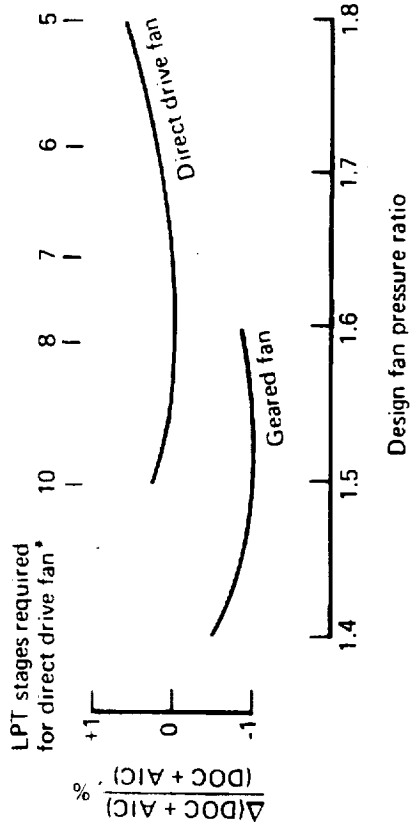


Figure 57.—1990 Technology Engines, Effect of Design Cruise Mach on Optimum Cycle Selection



TSLS = 226 858 N (51 000 lb)

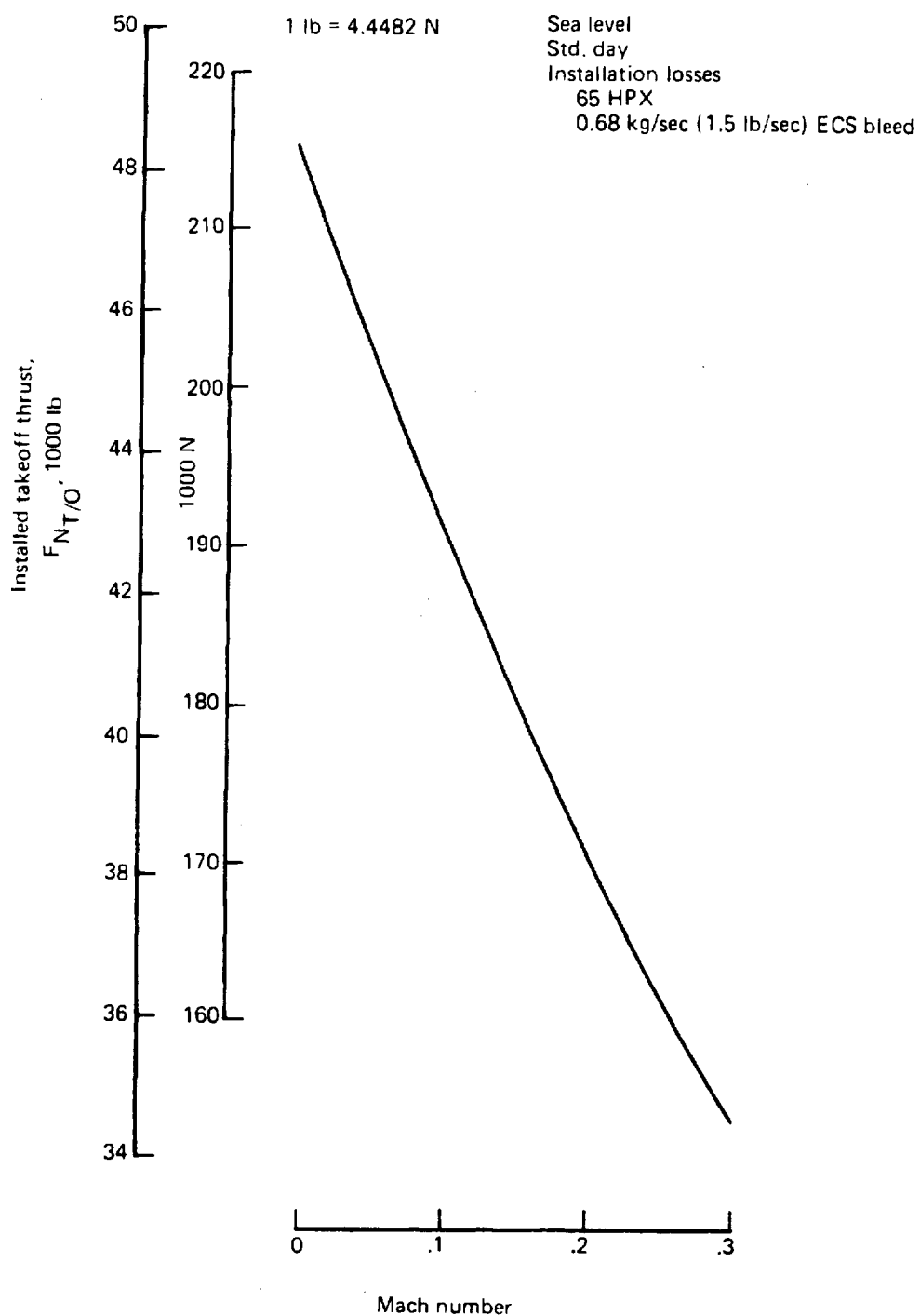


Figure 58.—1990 Technology Engine, Installed Takeoff Performance

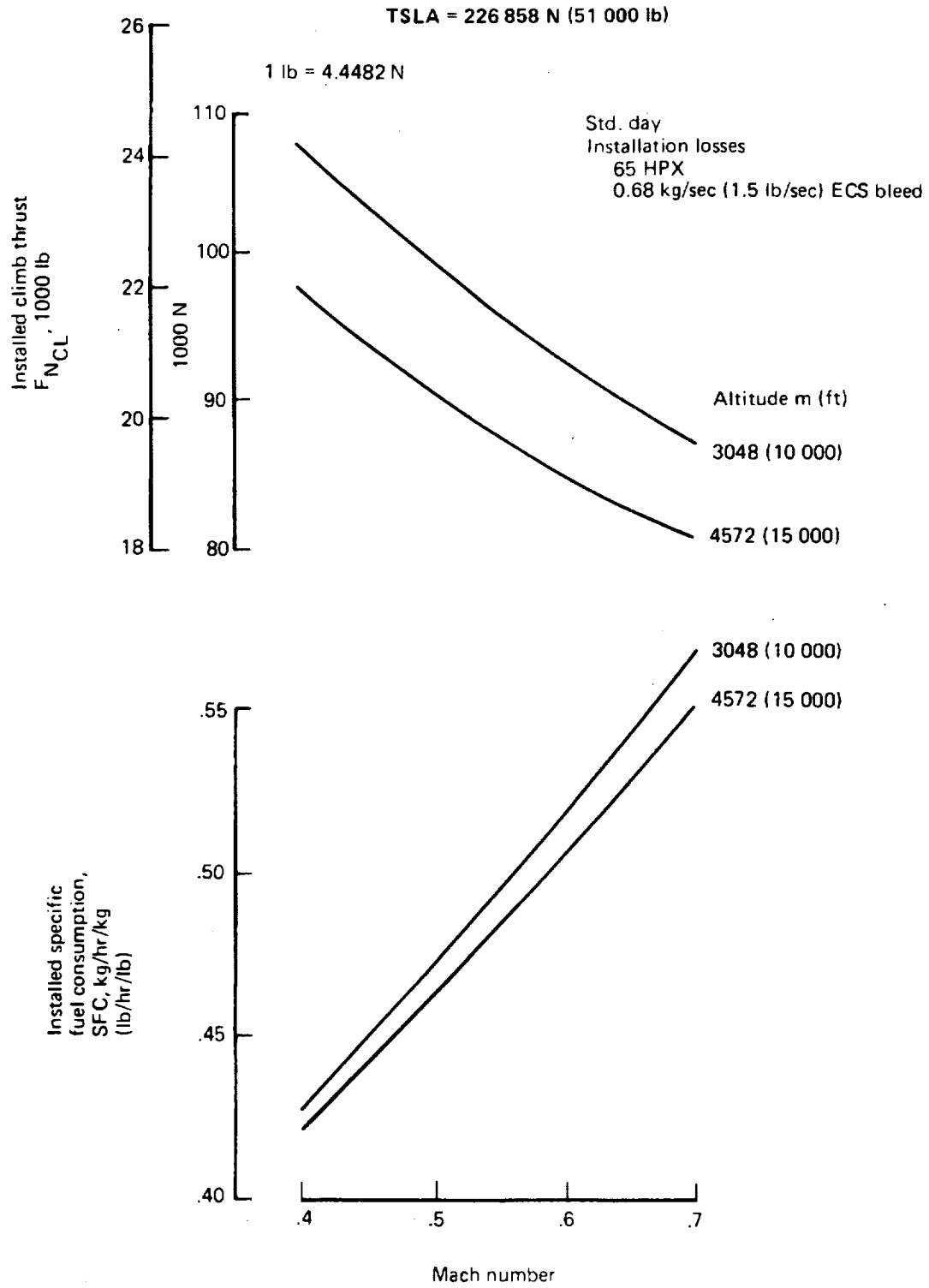


Figure 59.—1990 Technology Engine, Installed Climb Performance

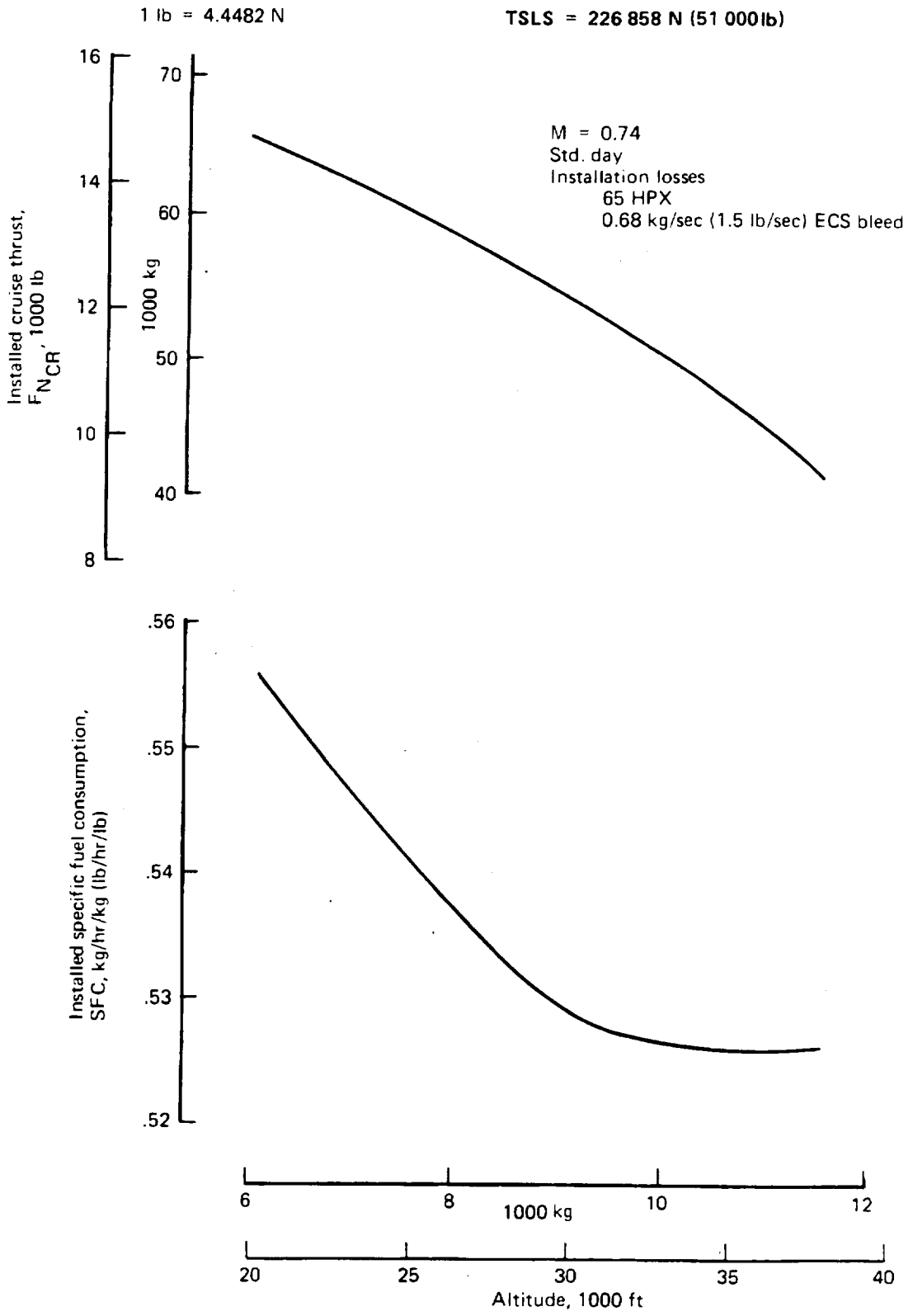


Figure 60.—1900 Technology Engine, Installed Cruise Performance

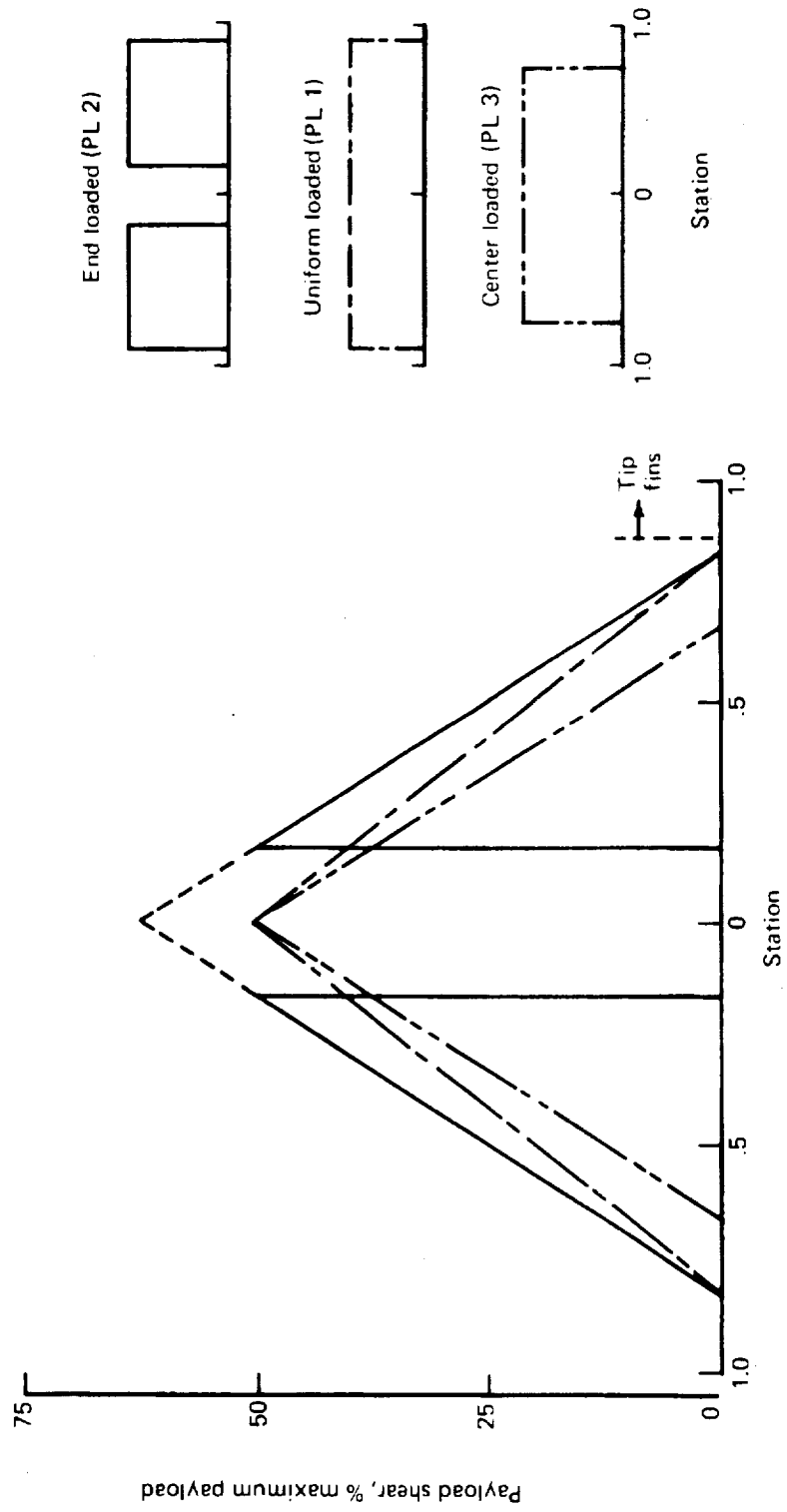


Figure 61.—Design Payload Distribution Variation

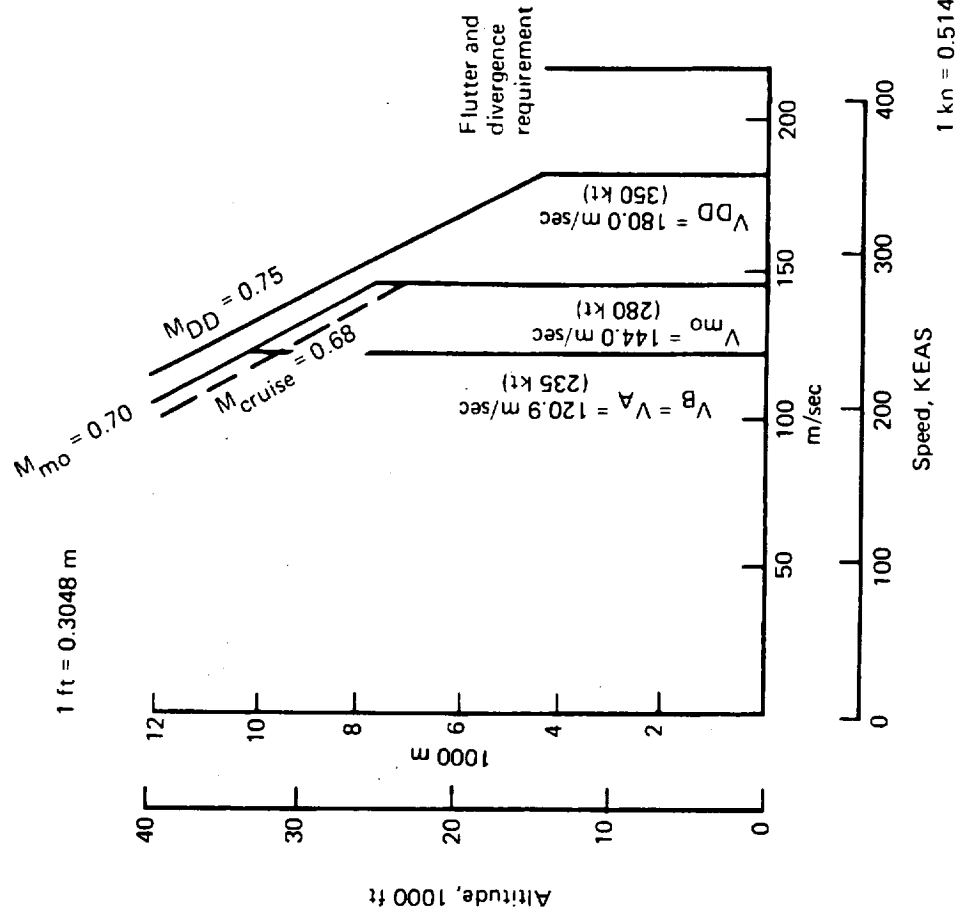


Figure 62.—Structural Design Speeds

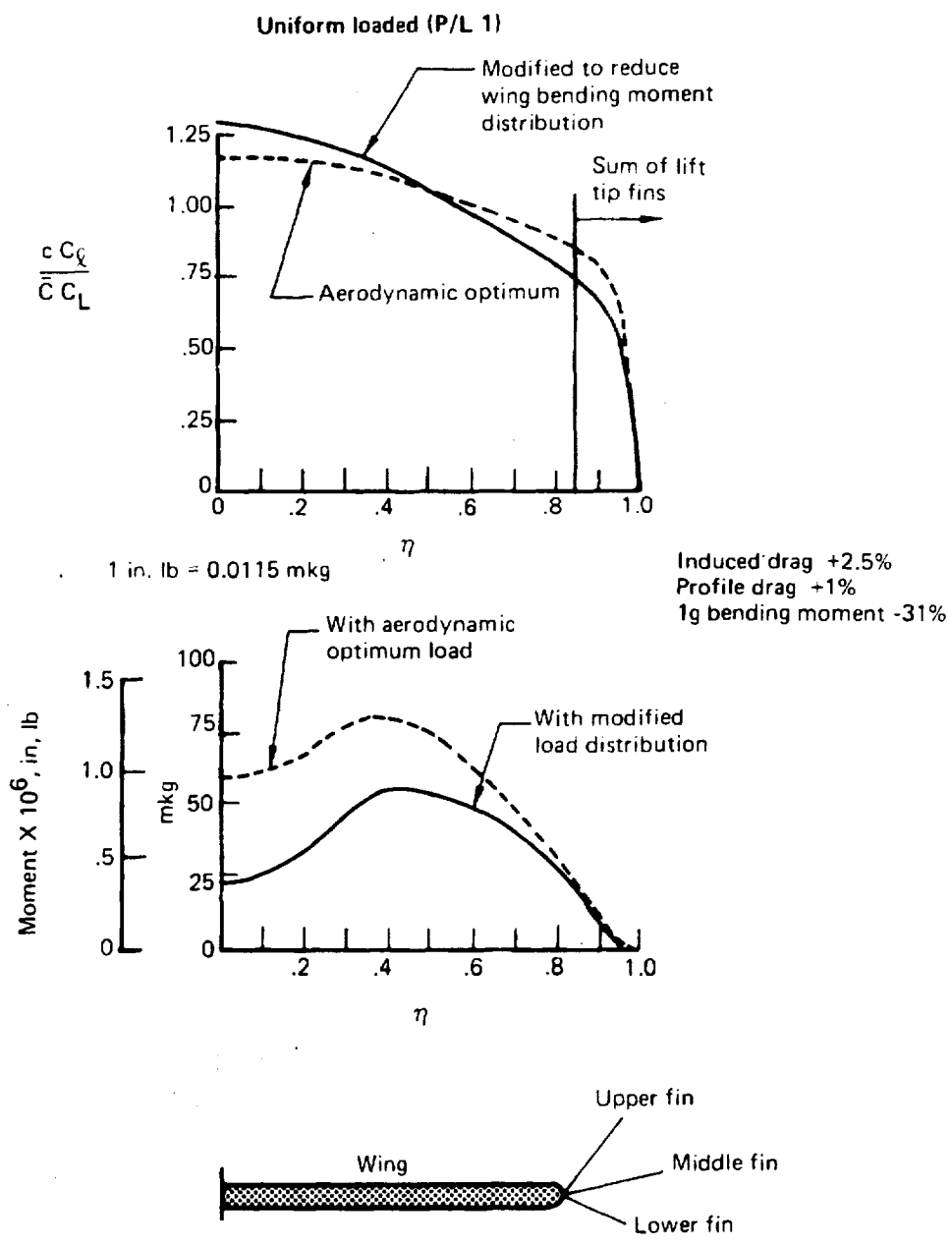


Figure 63.—Effect of Lift Distribution on Bending Moment

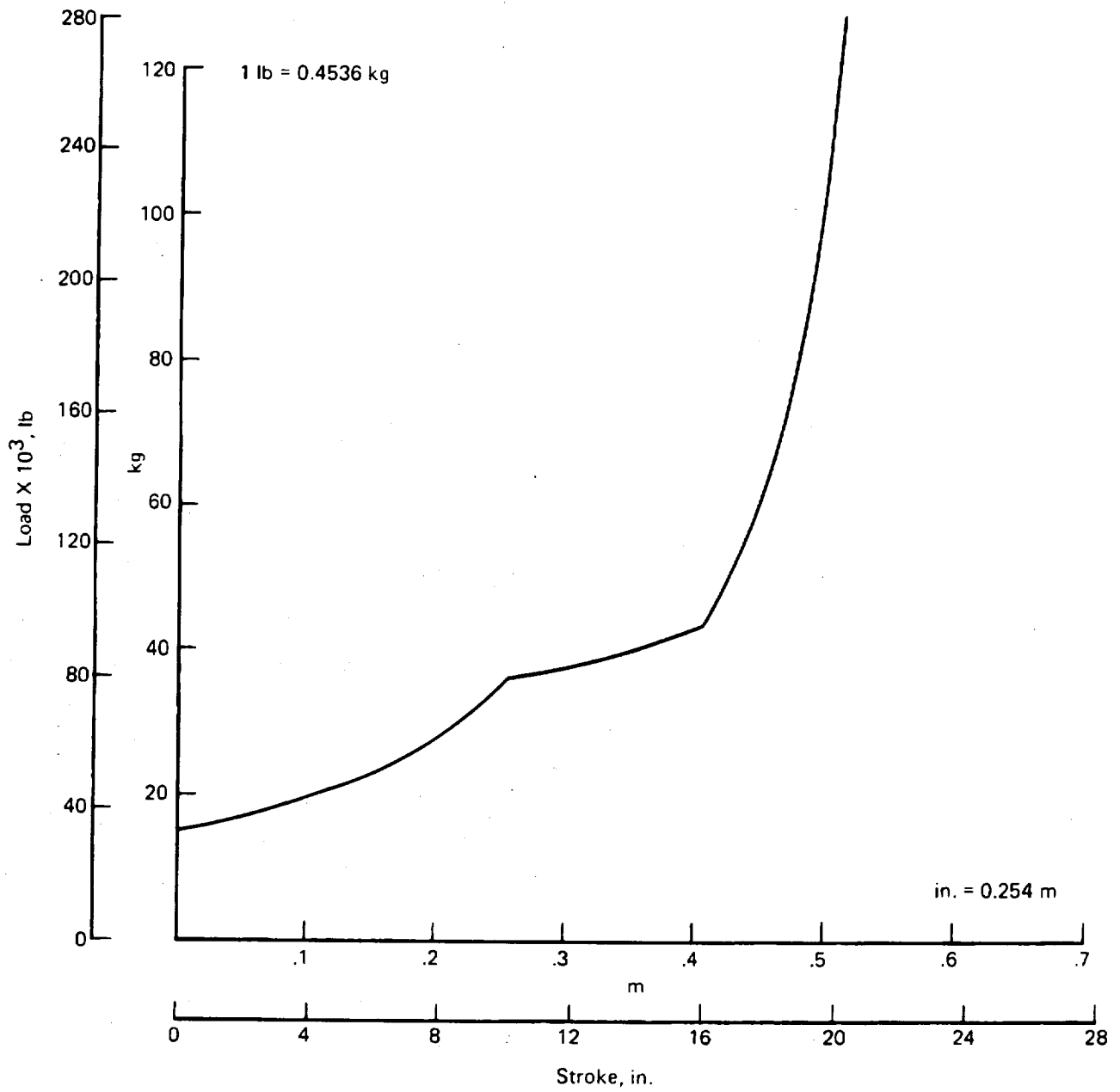
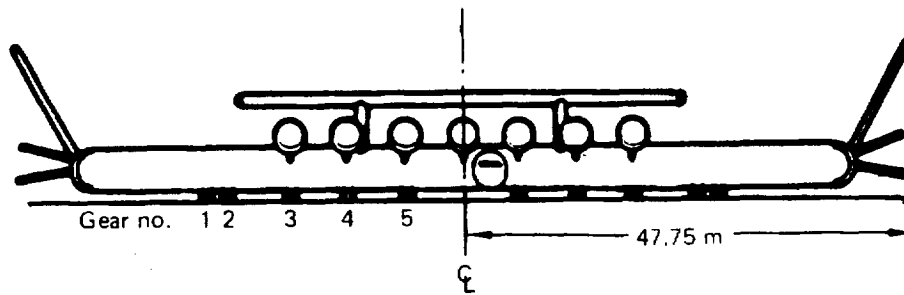


Figure 64.—Air Curve for Gear



Limit gear loads, 1000 N/strut

Gear no.	Station percent semispan	1g flat	1.0g crown	1.67g flat	1.67g crown
1	0.575	498	436	1143	1081
2	0.527	418	409	823	778
3	0.383	378	378	480	498
4	0.255	356	365	418	440
5	0.128	302	365	405	467

End loaded payload (P/L 2)

Figure 65.—Taxi Gear Loads



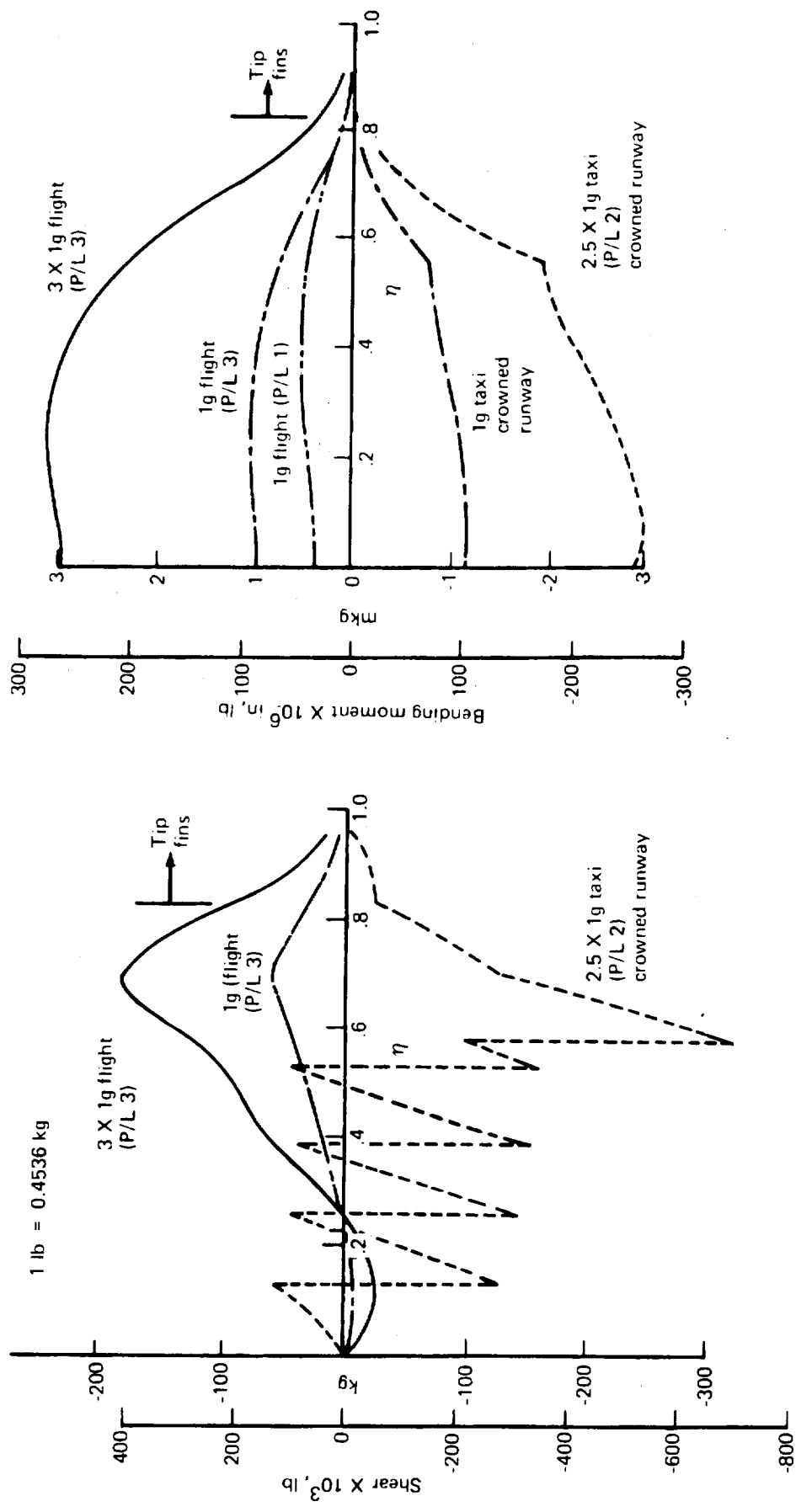


Figure 66.—Wing Design Loads Envelope

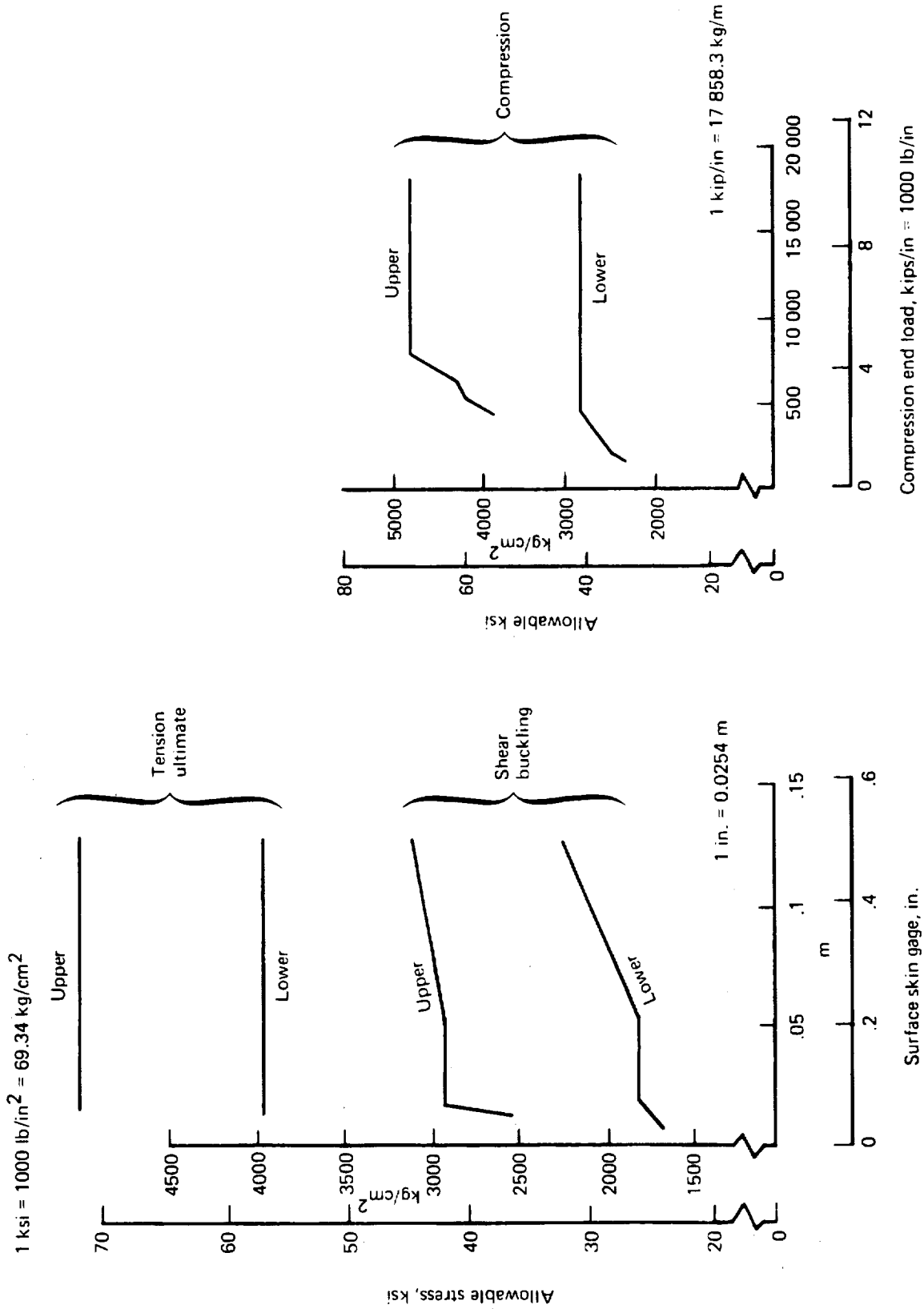
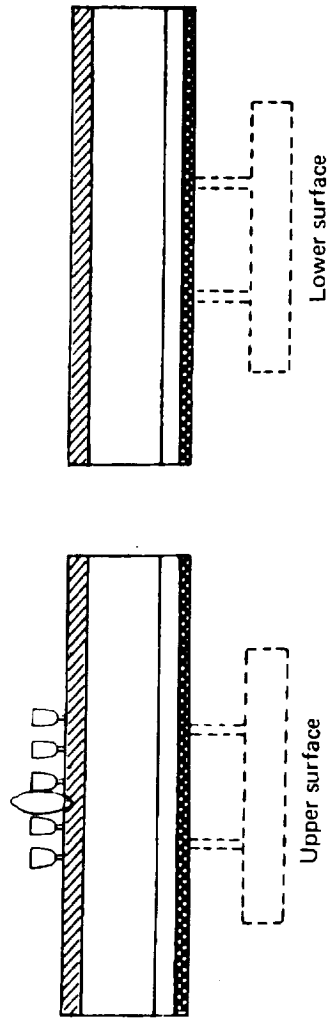
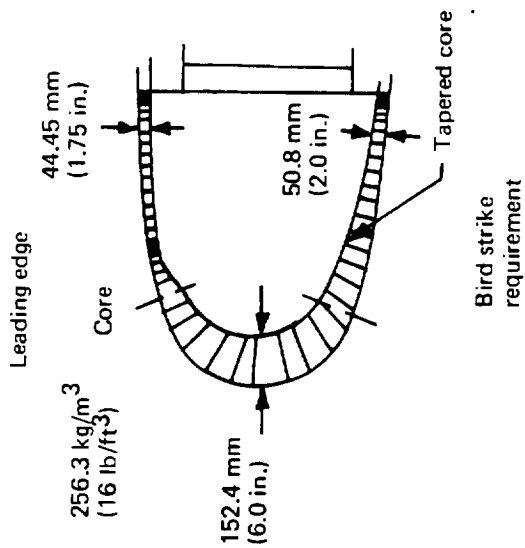





Figure 67.—Structural Allowables



Spars min. face sheets = 0.3048 mm (0.012 in.)  
 Ribs min. face sheets = 0.3048 mm (0.012 in.)

	Hail	0.9144 mm (0.036 in.) outer face sheet 0.3048 mm (0.012 in.) inner face sheet	0.9144 mm (0.036 in. outer face sheet) 0.3048 mm (0.012 in. inner face sheet)
	Maintenance	0.8128 mm (0.032 in.) outer face sheet 0.3048 mm (0.012 in.) inner face sheet	0.4064 mm (0.016 in. outer face sheet)* 0.3048 mm (0.012 in. outer face sheet)
	Control surfaces	0.4064 mm (0.016 in.) outer face sheet 0.3048 mm (0.012 in.) inner face sheet	0.4064 mm (0.016 in. outer face sheet)* 0.3048 mm (0.012 in. inner face sheet)

\* Add 2 layers of fiberglass 181 in areas exposed to damage from tires in the lower surface.

Figure 68.—Wing Minimum Gauge Preliminary Requirements, Honeycomb

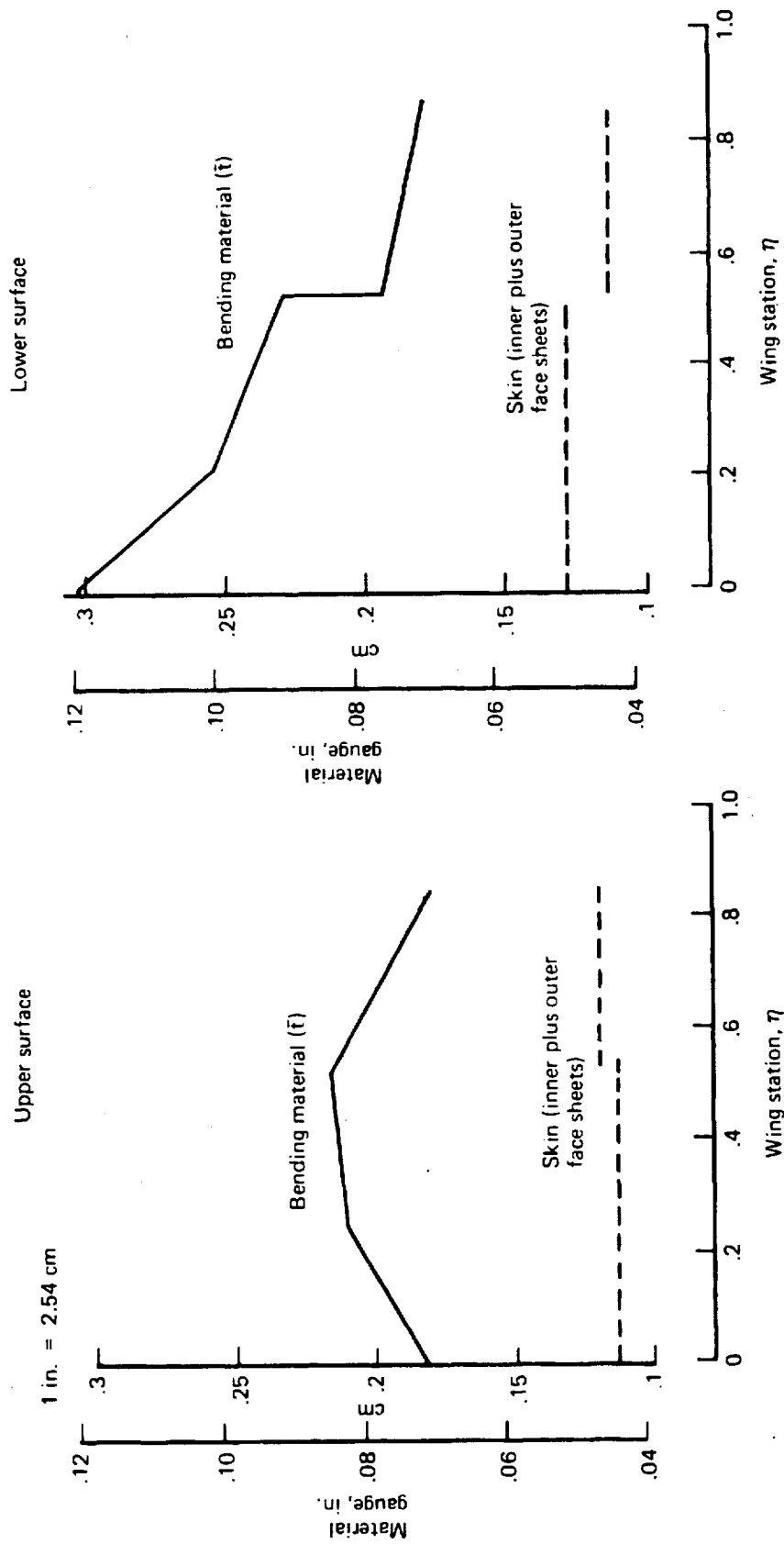
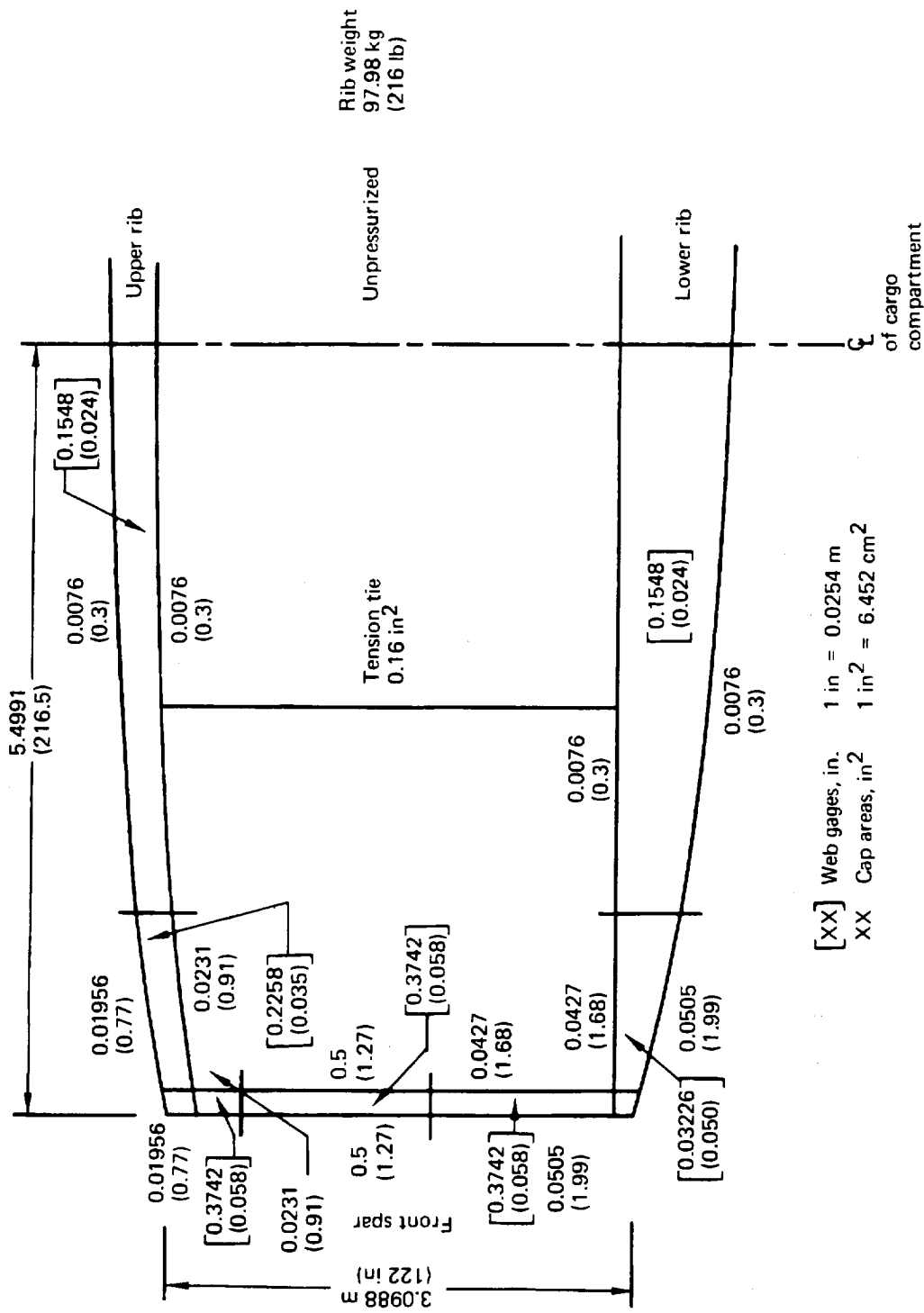


Figure 69.—Surface Bending Material



[XX] Web gages, in. 1 in = 0.0254 m  
 XX Cap areas, in<sup>2</sup> 1 in<sup>2</sup> = 6.452 cm<sup>2</sup>

Figure 70.—Typical Rib Structure

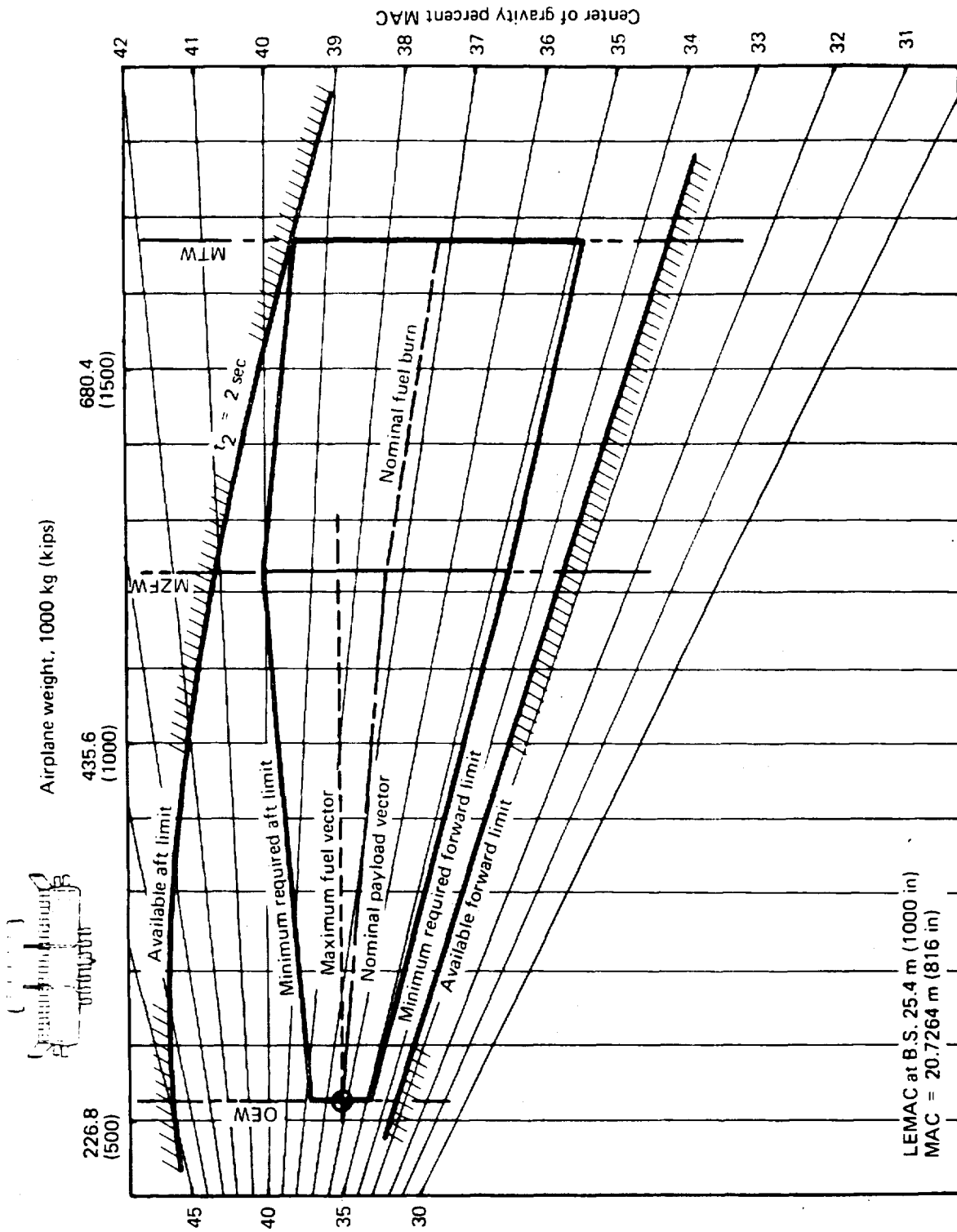
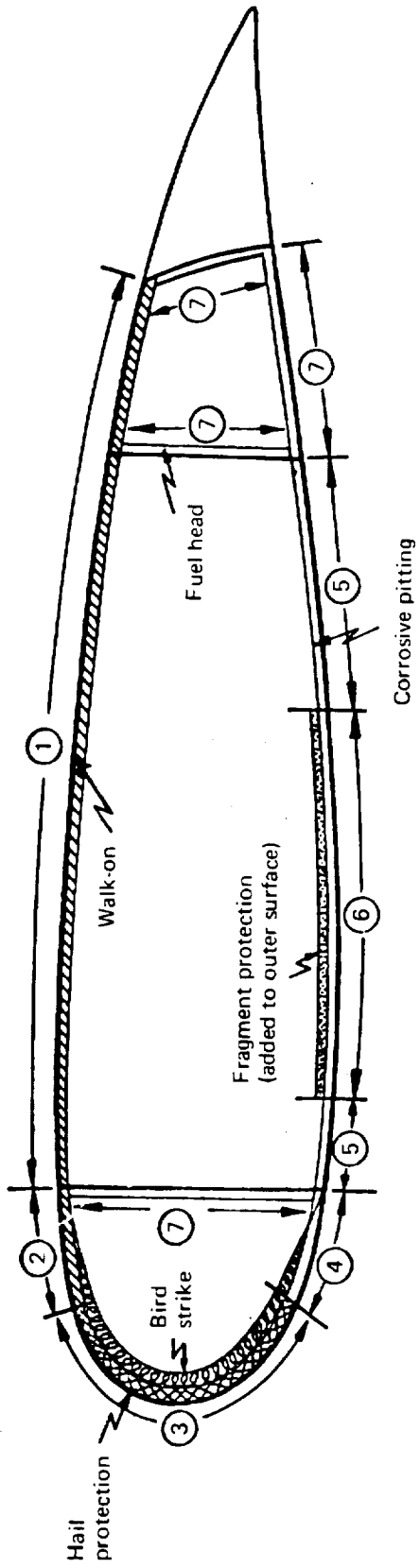


Figure 71.—Selected Configuration, Loading Diagram



Criteria Zone	Basic honeycomb panel	Weight increments to basic panel						Zone total wt, kg/m <sup>2</sup> (lb/ft <sup>2</sup> )
		Corrosive pitting	Fuel head	Walk-on kg/m <sup>2</sup> (lb/ft <sup>2</sup> )	Hail protection	Fragment protection	Bird strike protection	
1	4.307 (0.882)	-	-	1.416 (0.290)	-	-	-	5.723 (1.172)
2	4.307 (0.882)	-	-	1.416 (0.290)	-	-	3.213 (0.658)	8.936 (1.830)
3	4.307 (0.882)	-	-	-	1.704 (0.349)	-	38.659 (7.917)	44.67 (9.148)
4	4.307 (0.882)	0.283 (0.058)	-	-	-	-	17.745 (3.634)	22.33 (4.574)
5	4.307 (0.882)	0.283 (0.058)	-	-	-	-	-	4.59 (0.94)
6	4.307 (0.882)	0.283 (0.058)	-	-	-	0.869 (0.178)	-	5.459 (1.118)
7	4.307 (0.882)	-	1.133 (0.232)	-	-	-	-	5.44 (1.114)

Note:

For example zone 3 design condition is bird strike protection 44.67 (9.148 psf)

Figure 72.—Zone Unit Weight Requirements, Selected Configuration

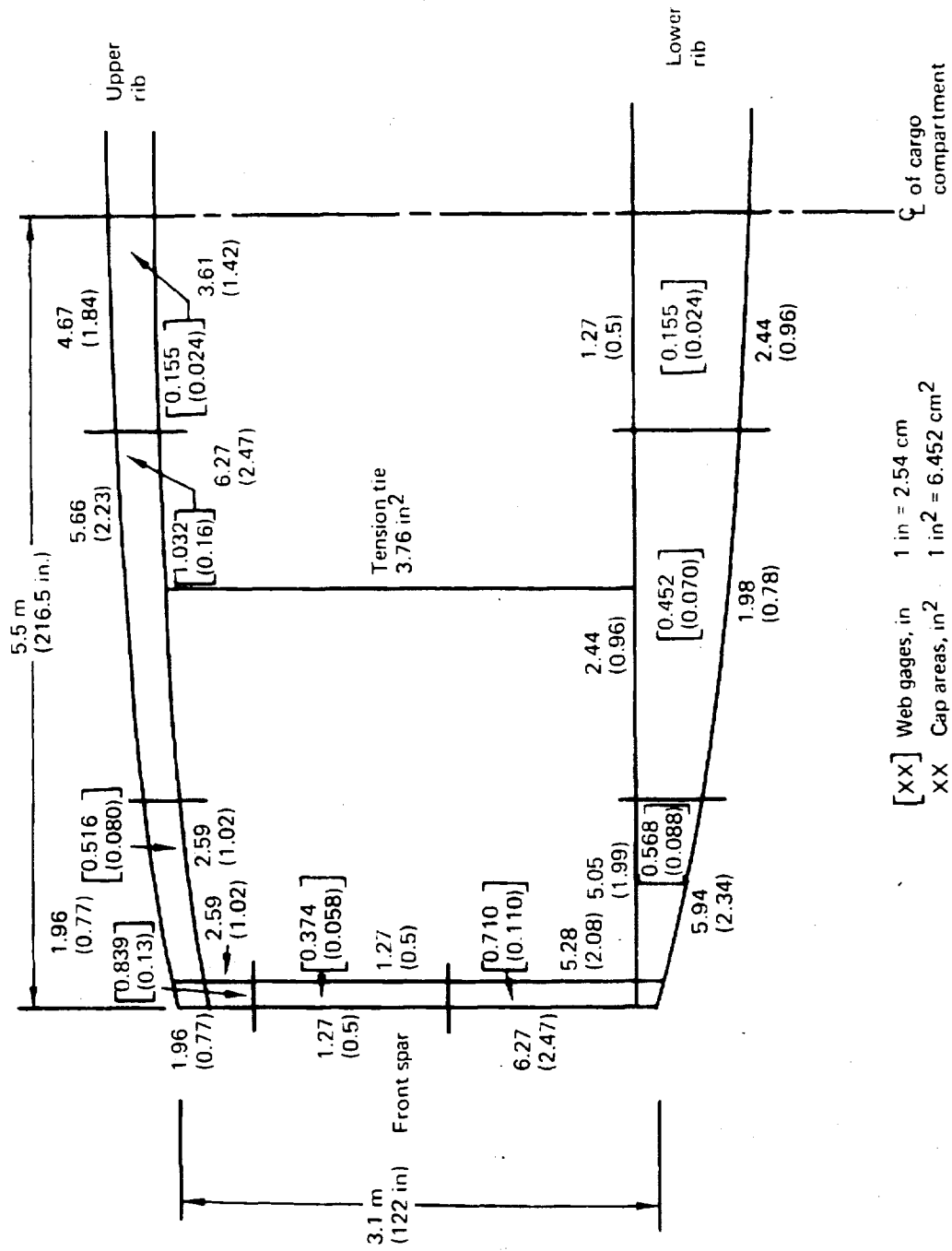


Figure 73.—Typical Rib Structure, Pressurized to 10 psia



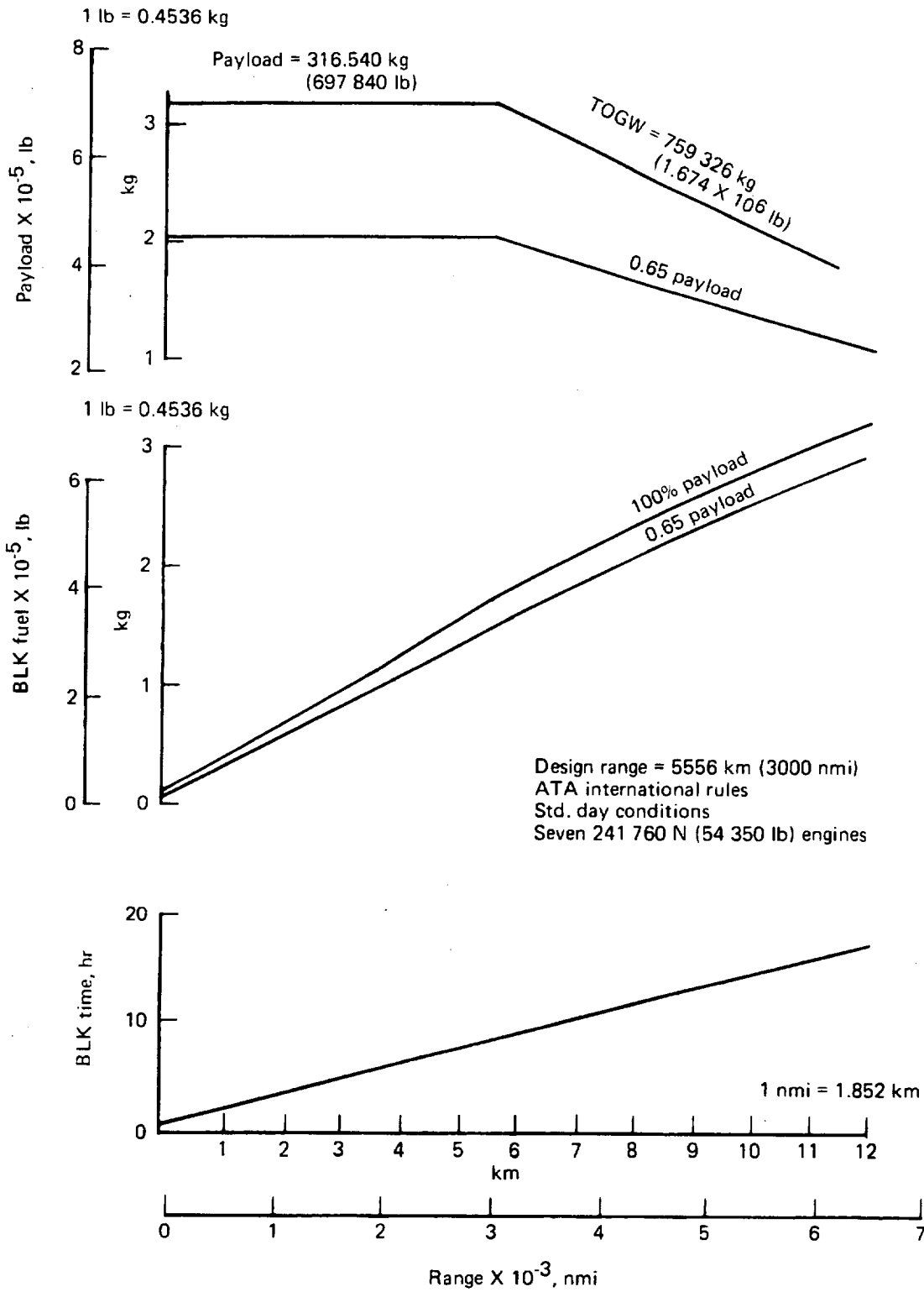


Figure 74.—Distributed Load Freighter Selected Configuration Performance

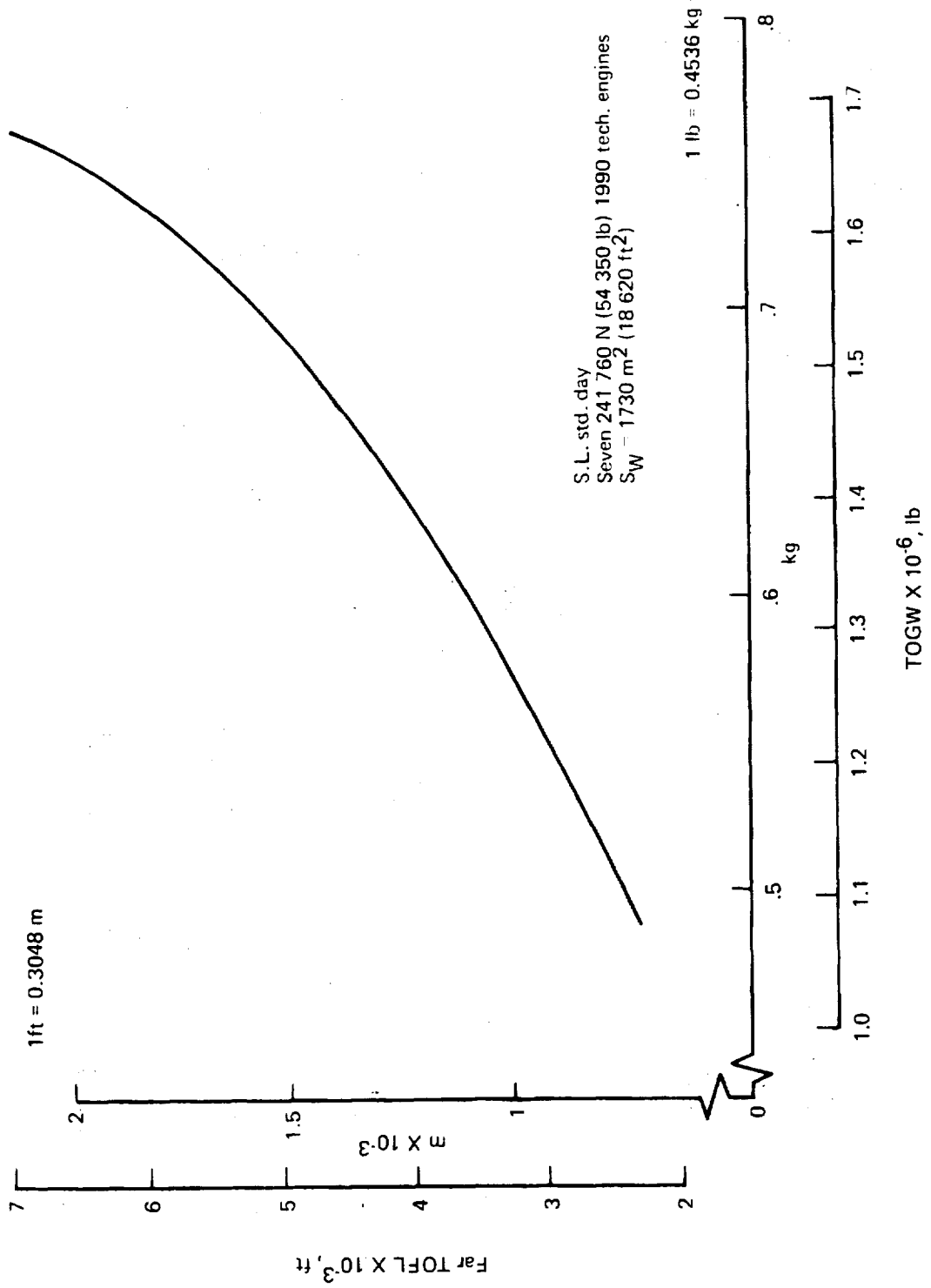
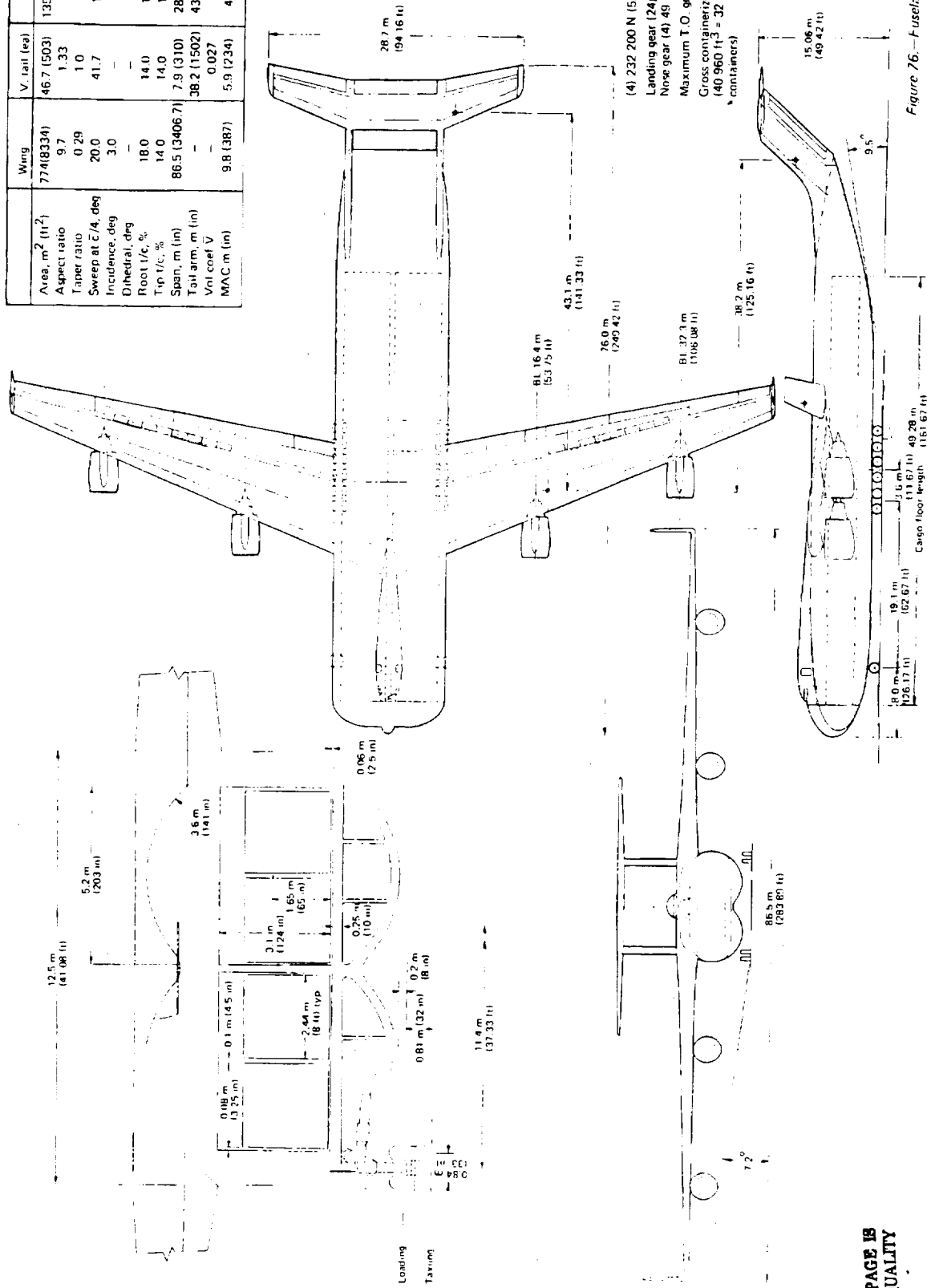


Figure 75.—Distributed Load Freighter, Selected Configuration Takeoff Performance

	Wing	V. tail (ea)	H. tail	Winglet (ea)
Area, m <sup>2</sup> (ft <sup>2</sup> )	774(8334)	46.7 (503)	135.4 (1457)	15.3 (165)
Aspect ratio	9.7	1.33	6.09	1.21
Taper ratio	0.29	1.0	0.62	0.74
Sweep at $\bar{c}/4$ , deg	20.0	41.7	17.8	20
Incidence, deg	3.0	—	0	—
Dihedral, deg	18.0	14.0	11.0	14.0
Root $t/c$ , %	14.0	14.0	11.0	14.0
Tip $t/c$ , %	86.5 (3406.7)	7.9 (310)	28.7 (1130)	4.3 (170)
Span, m (in)	—	38.2 (1502)	43.1 (1696)	10.3 (405)
Tail arm, m (in)	—	0.027	0.76	0.002
MAC, m (in)	9.8 (387)	5.9 (234)	4.8 (189)	3.4 (135)



(4) 232 200 N (52 200 lb) SLS engines  
 Landing gear (24) 49 X 17-20 tires, 6 posts  
 Nose gear (4) 49 X 17-20 tires, 2 posts  
 Maximum T.O. gross weight  
 Gross containerized volume 1160 m<sup>3</sup>  
 (40 960 ft<sup>3</sup> = 32.8 ft X 8 ft X 20 ft containers)

Figure 76.—Fuselage Loaded Freighter, Reference Configuration

ORIGINAL PAGE IS OF POOR QUALITY





Airplane weight, 1000 kg (kips)

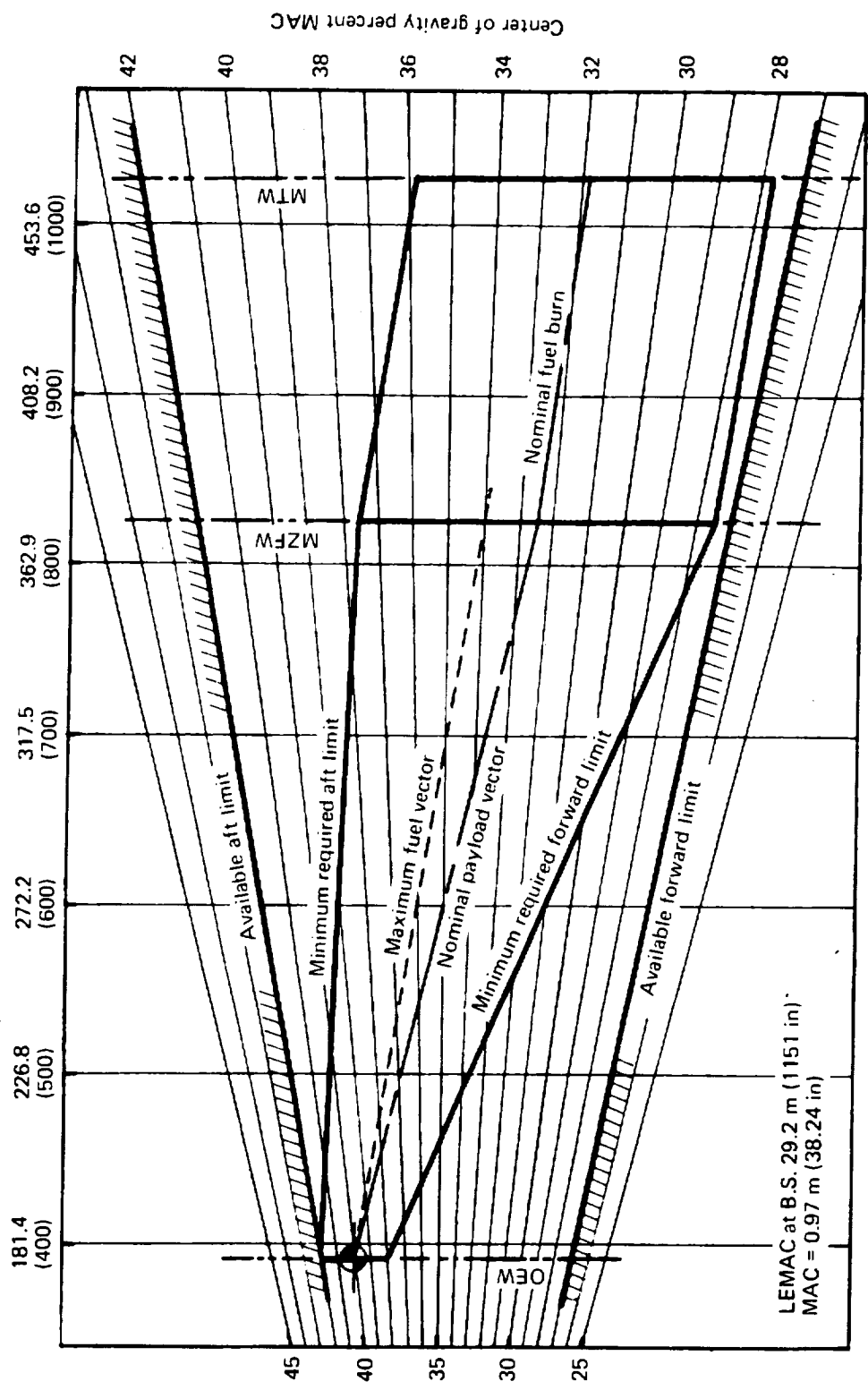


Figure 77.—Reference Configuration Loading Diagram

PRECEDING PAGE BLANK NOT FILMED

Model 759-182

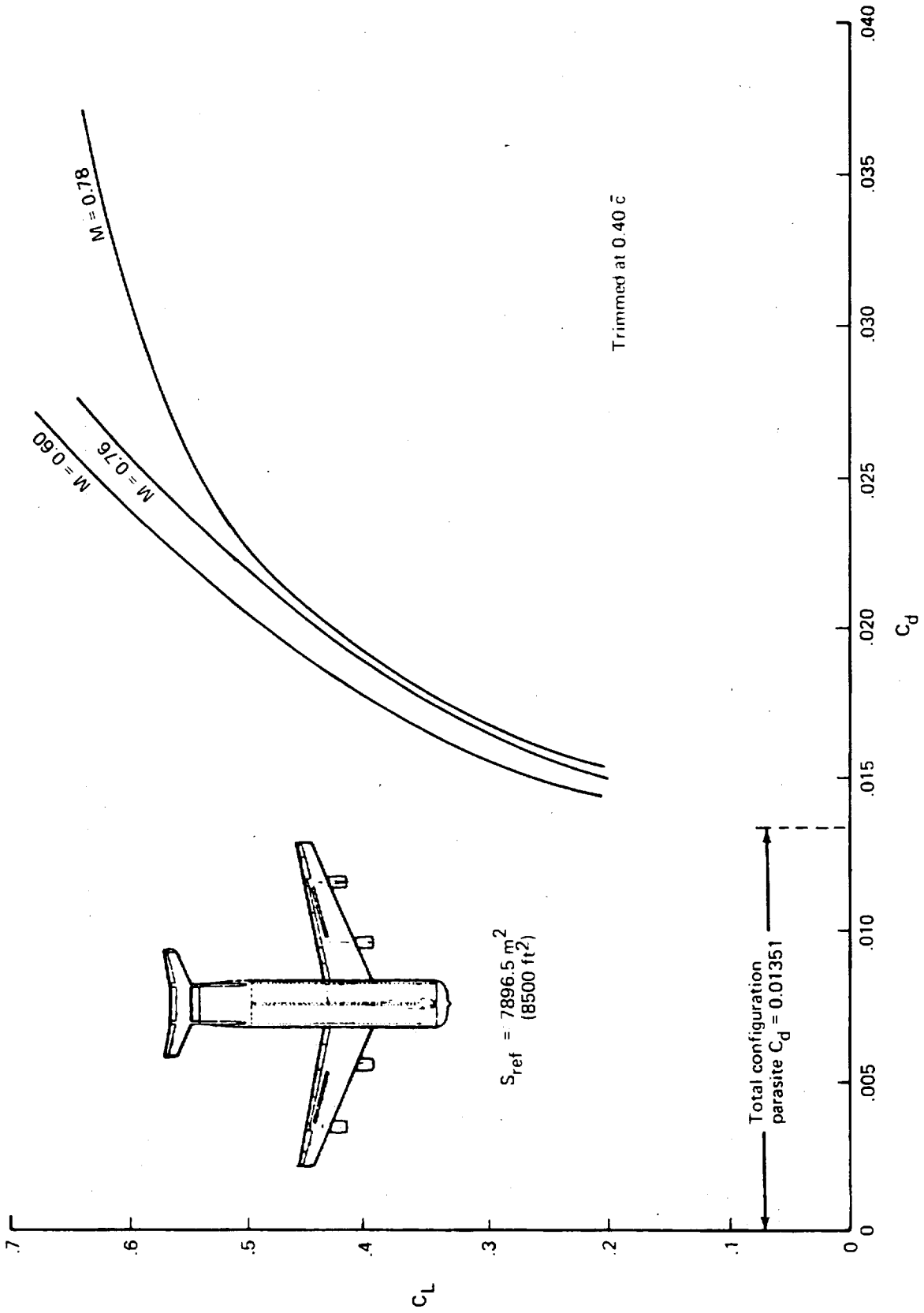


Figure 78.—Drag polar, reference configuration

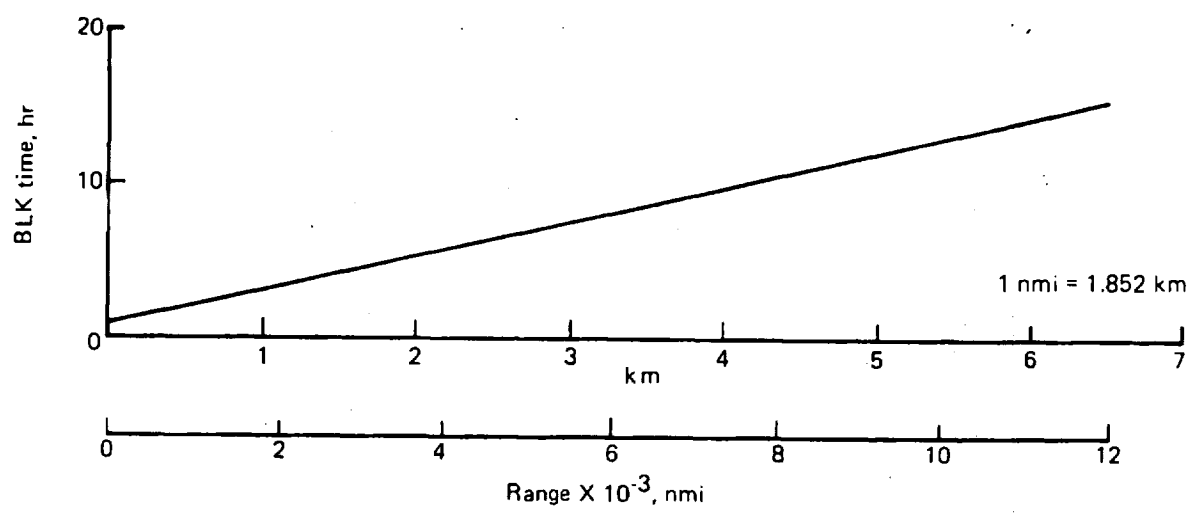
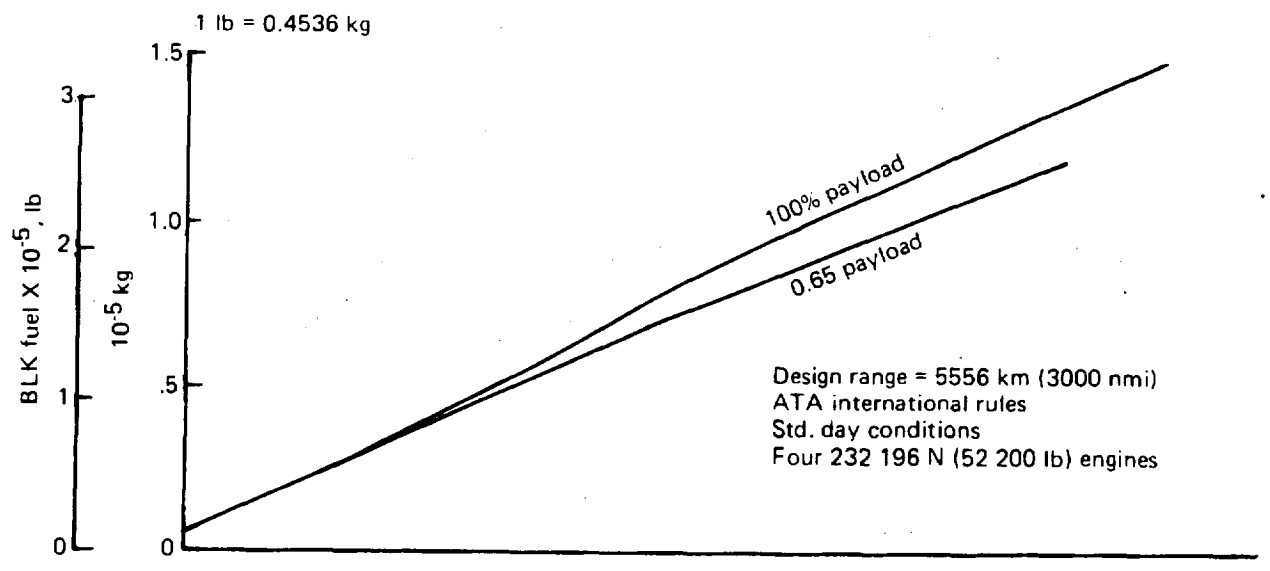
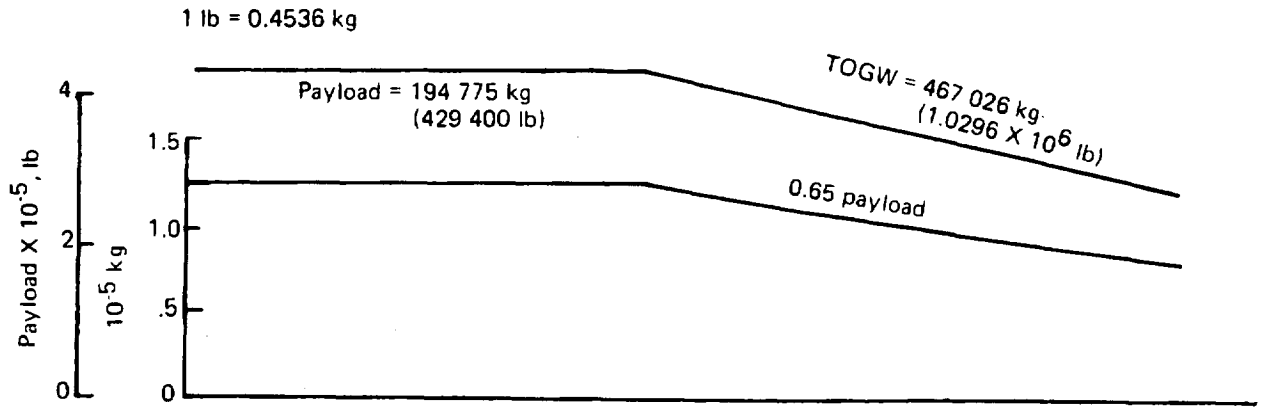
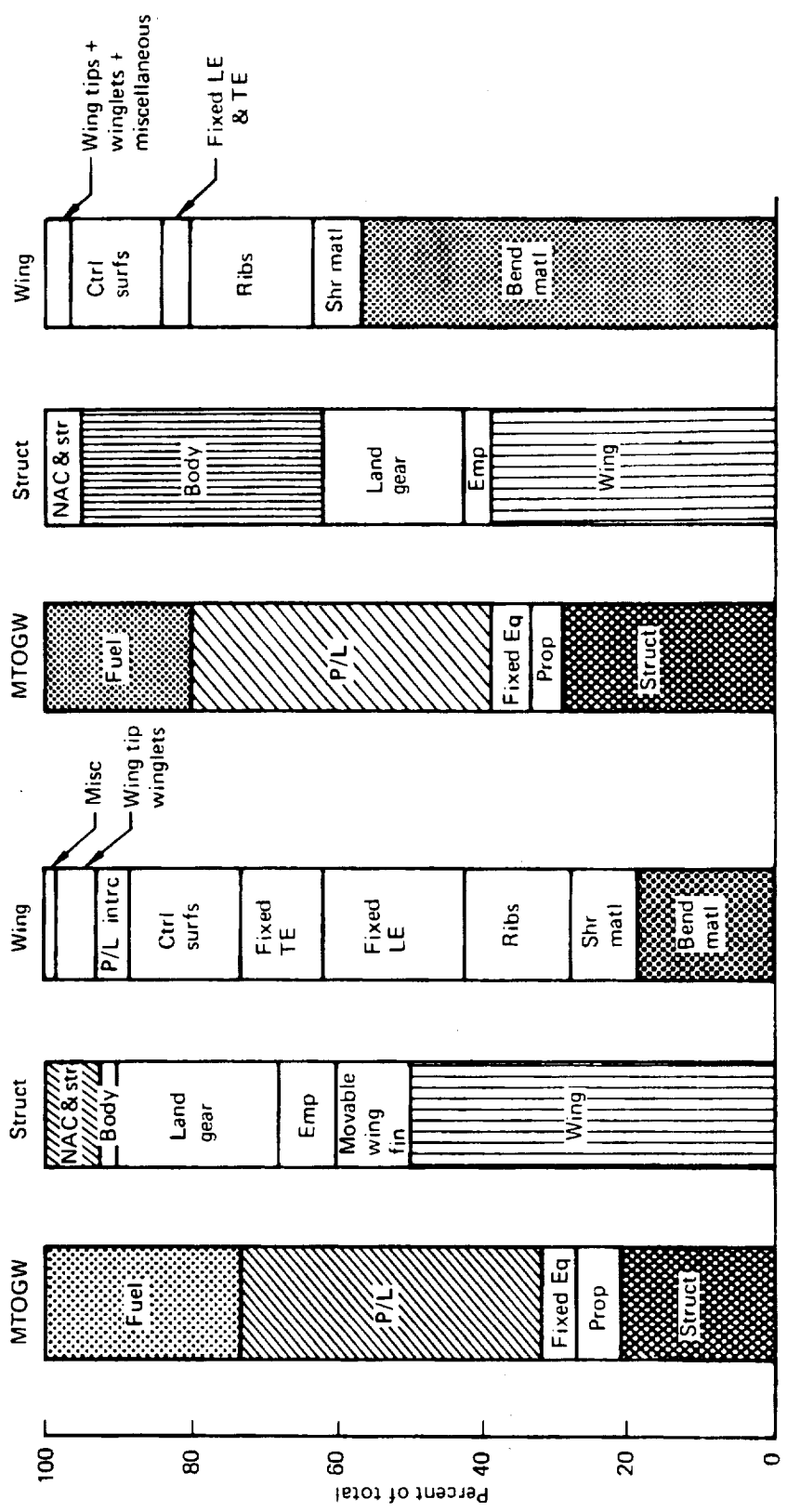


Figure 79.—Reference Configuration Performance



Reference configuration conventionally loaded  
 OEW = 179 713 kg  
 (396 200 lb)

Selected configuration distributed load  
 OEW = 238 753 kg  
 (526 360 lb)

Figure 80.--Weight Distribution Comparisons



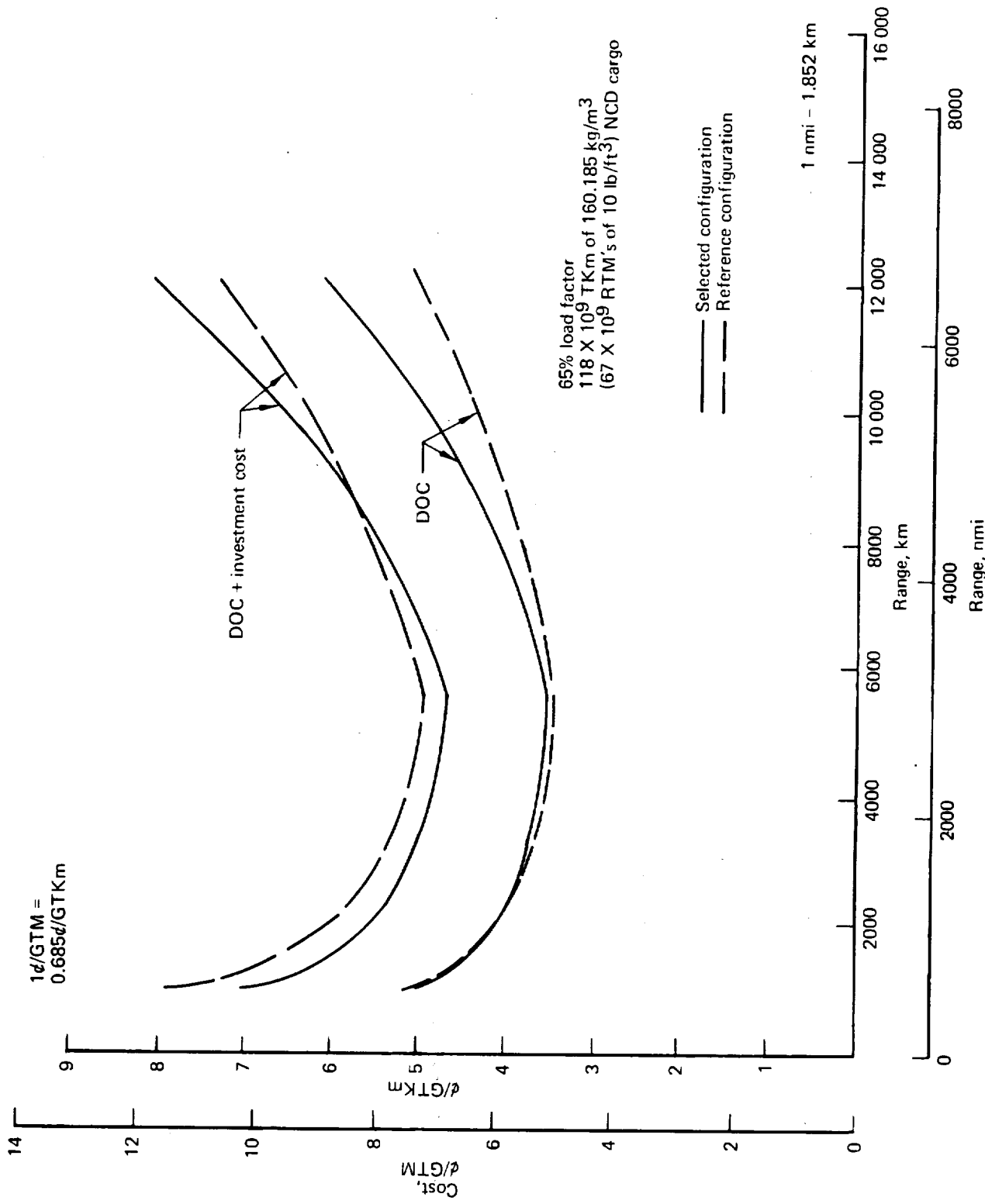


Figure 81.—Economic Comparison, Selected Versus Reference Configuration

1990 Technology

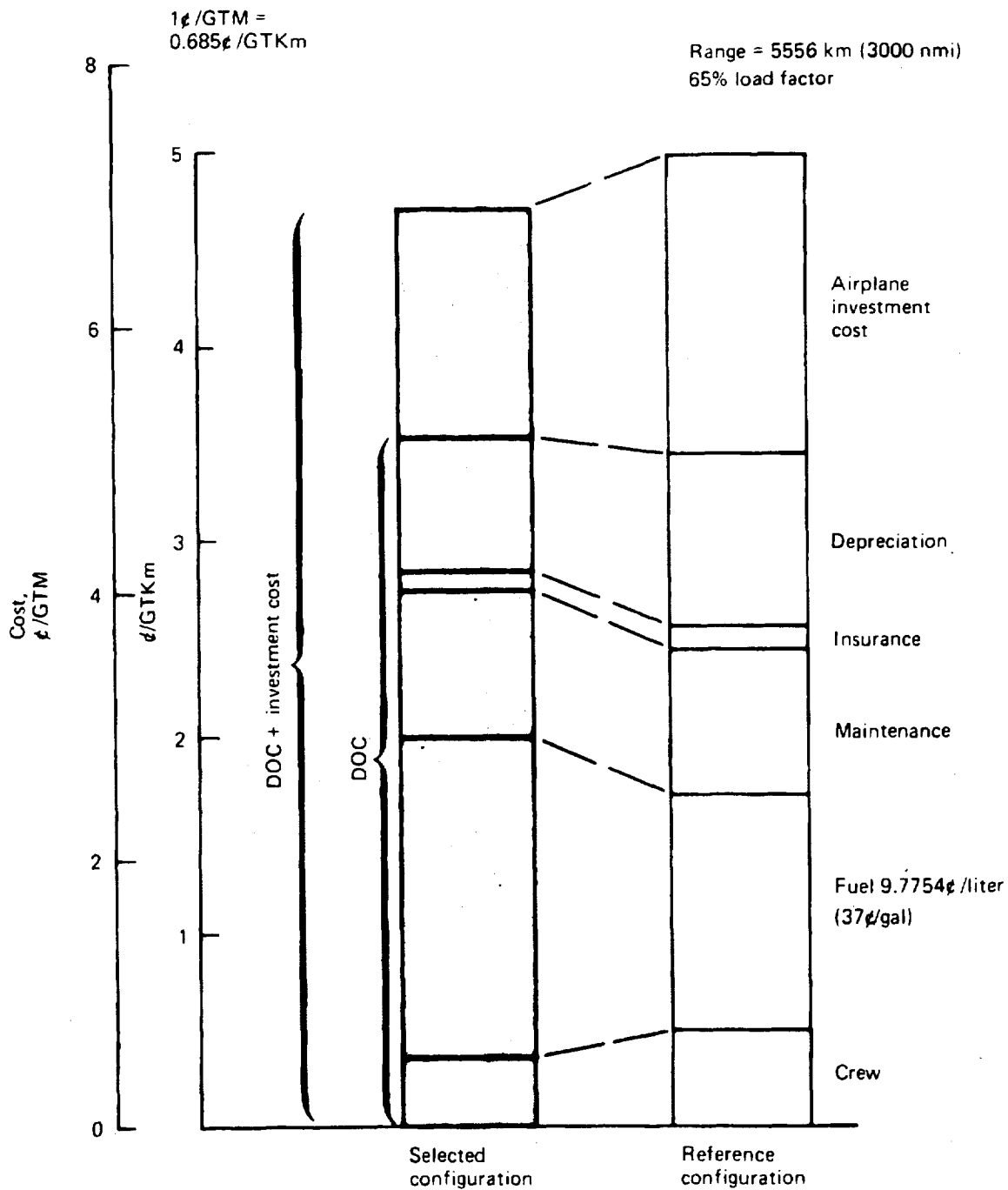


Figure 82.—Cost Breakdown Comparison, Selected Versus Reference Configurations

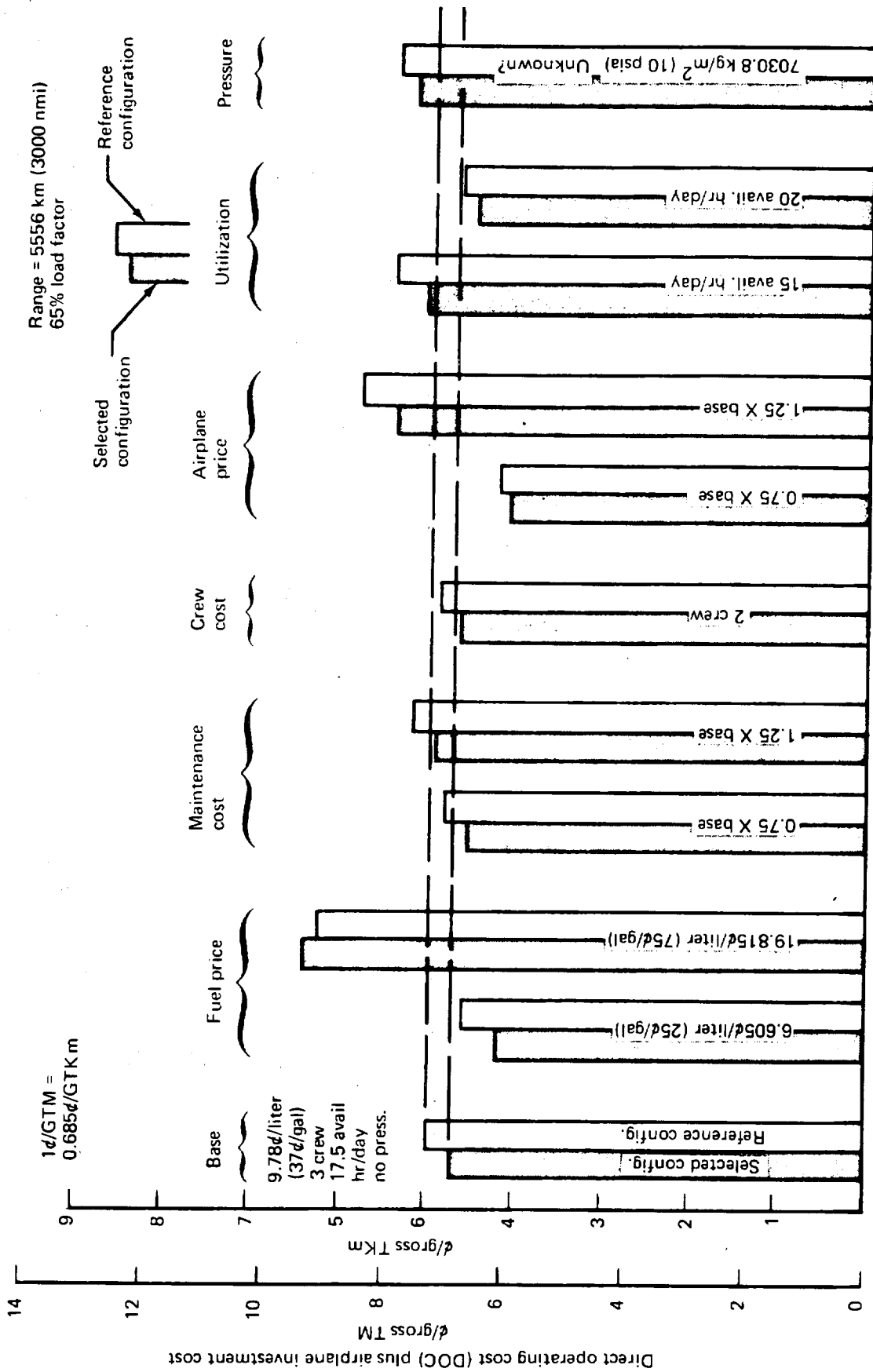


Figure 83.—Economic Sensitivity Comparisons, Selected Versus Reference Configurations

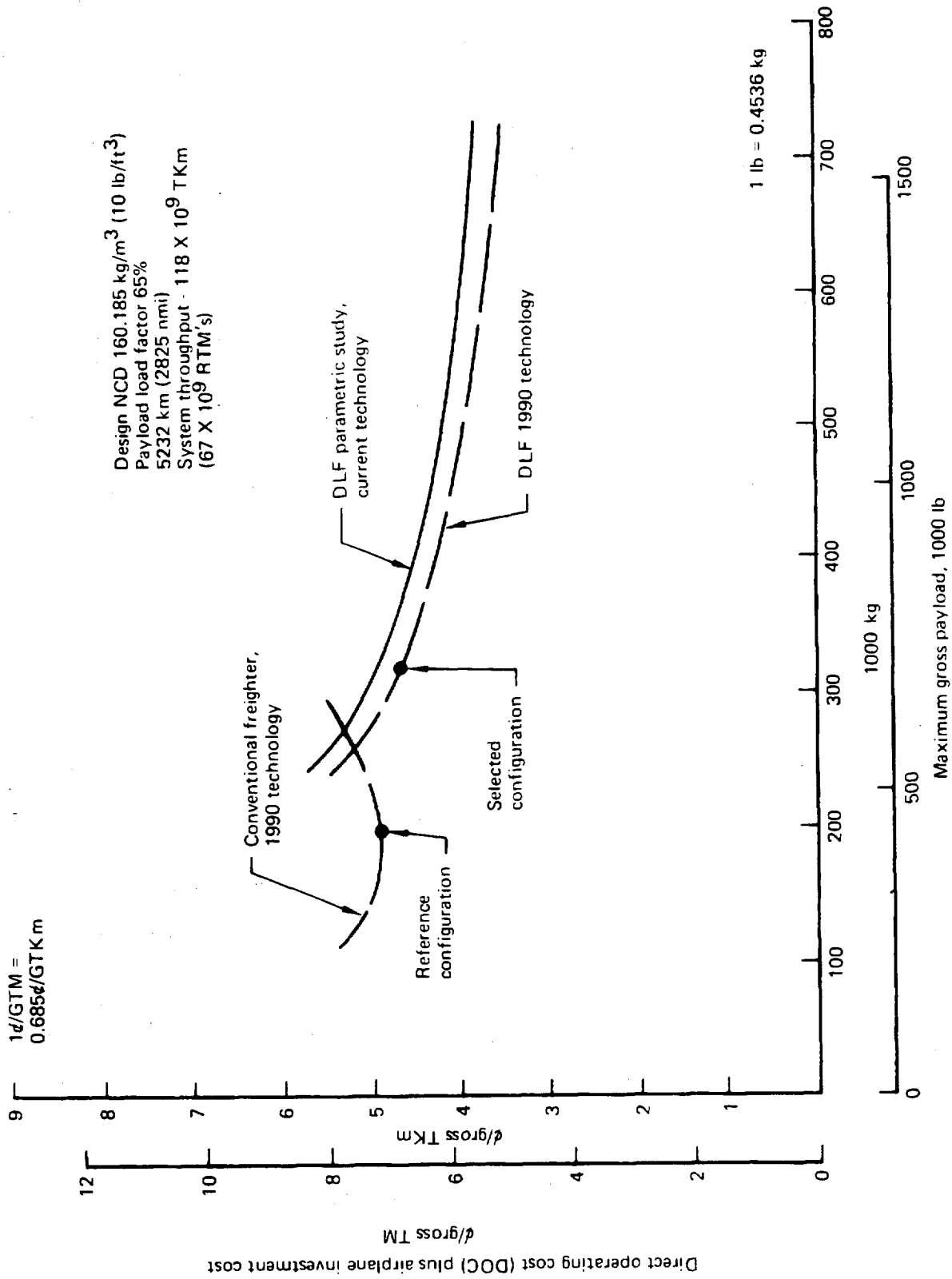


Figure 84.—Distributed Load and Conventional Freighter Comparative Economics

1d/GTM =  
0.685d/GTKm

Range = 5232 km (2825 nmi)  
65% load factor  
NCD = 148.97 kg/m<sup>3</sup>  
(9.3 lb/ft<sup>3</sup>)

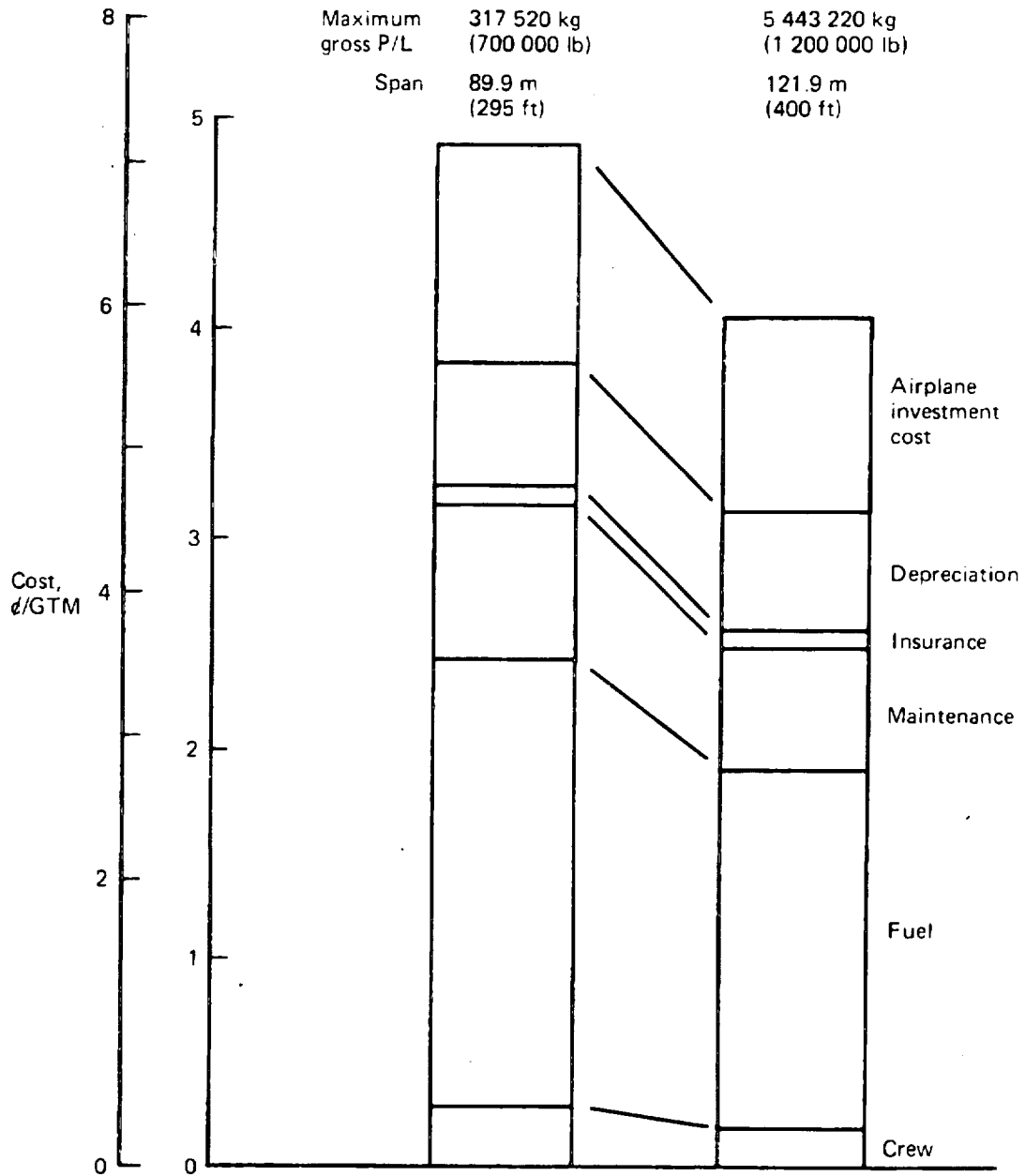
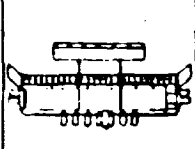
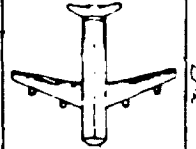
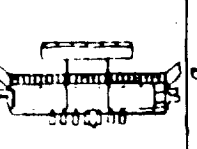
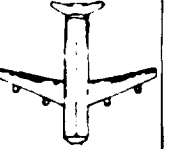


Figure 85.—Effect of Airplane Size on Economics—Parametric Study, 1980 Technology

Table 1.—Distributed Load Freighter Comparison With Reference Configuration

					
		DLF conf.	REF. conf.	DLF	REF.
TOGW—lbs	kg	1 673 700	1 029 600	759 190	467 027
Thrust—lbs	newtons	7x54 350	4x52 200	241 760	232 196
OEW—lbs	kg	526 400	396 200	238 775	179 716
OEW/TOGW		0.3145	0.3848		
Gross pl—lbs	kg	697 800	429 400	316 522	194 776
Cargo vol—ft <sup>3</sup>	m <sup>3</sup>	60 000	36 928	1 699	1 046
PL density—lbs/ft <sup>3</sup>	lb/m <sup>3</sup>	10	10	160.185	160.185
PL/TOGW		0.4169	0.4171		
TOFL—ft	m	7 000	11 700	2133.6	3 566
Cruise: mach		0.68	0.78		
alt.—ft	m	28 000	33 000	8534.4	10 058
L/D		16.6	21.9		
RF (nmi)	km	13 000	18 800	24 076	34 817
Block fuel—lbs	kg	384 600	165 000	174 454	74 844
Block time—hrs		8.24	7.39		
BF/PL		0.5512	0.3843		
(PL/GW) mach	m ton km/kg	0.2836	0.3235		
(PLxR)/BF—ton st. mi/lb		3.13	4.50	12.24	17.60
Land wt—lbs	kg	1 290 000	861 400	585 144	390 731
Land fl—ft	m	6 200	6 100	1 890	1 859
V <sub>APP</sub> —kt	m/sec	131	130	67.4	66.9
Wing span—ft	m	314	284	95.7	86.6
S <sub>W</sub> —ft <sup>2</sup>	m <sup>2</sup>	18 620	8 500	1 730	790
W/S		90	121		
Λ—deg		0	20		
t/c—%		21.5	14		
Fleet size		153	226		
Price (millions)		72.6	63.9		
\$/lb of OEW	\$/kg	137.9	161.2	304.0	355.4
\$/lb of payload	\$/kg	104.0	148.8	229.3	328.0

Design range = 5556 km (3000 nmi)  
 Net PL density = 160.185 kg/m<sup>3</sup> (10 lb/ft<sup>3</sup>)  
 ATA international rules = std. day







Table 3.—Payload Characteristics—Parametric Study Airplanes

Span m (ft)	No. bays	No. engs	Maximum gross payload kg (lb)	Gross payload volume m <sup>3</sup> (ft <sup>3</sup> )	Maximum gross PL density kg/m <sup>3</sup> (lb/ft <sup>3</sup> )	Maximum net payload kg (lb)	Net containerized volume m <sup>3</sup> (ft <sup>3</sup> )	Maximum net PL density kg/m <sup>3</sup> (lb/ft <sup>3</sup> )	65% gross payload kg (lb)	Net PL at 65% gross payload kg (lb)	Volume load factor at 65% wt./LF 10 lb/ft <sup>3</sup>
89 9160 (295)	3	5	164 463 8144 (362 570)	1 522 4832 (53 760)	108 0287 (6 744)	127 887 5304 (281 939)	1 355 9616 (47 880)	94 3169 (5 808)	106 902 6336 (235 676)	91 492 9344 (201 704)	0.421
		6	266 399 7900 (587 300)		174 9860 (10 924)	279 870 9760 (613 660)		169 5077 (10 582)	173 159 5320 (381 745)	148 199 2848 (326 718)	0.682
		7	304 415 9496 (671 111)		199 9589 (12 483)	267 837 6456 (590 471)		197 5401 (12 337)	197 870 2992 (436 222)	169 348 3048 (373 343)	0.780
89 9160 (295)	4	8	222 820 5672 (491 227)	2 029 91776 (71 680)	222 7532 (13 906)	307 524 4376 (666 041)	1 807 9488 (63 840)	223 1216 (13 929)	220 416 9408 (485 928)	188 644 8824 (415 884)	0.869
		8	361 401 7176 (796 741)		109 7747 (6 853)	174 049 4952 (383 707)		96 2711 (6 010)	144 833 5728 (319 298)	173 956 6374 (387 273)	0.428
		9	399 127 1760 (879 910)		178 0456 (11 115)	312 630 6456 (689 221)		172 9307 (10 706)	234 911 2752 (517 882)	201 050 0352 (443 232)	0.694
89 9160 (295)	5	8	242 953 1496 (535 611)	2 537 4720 (89 600)	196 6431 (12 276)	350 356 1040 (772 390)	2 259 9360 (79 800)	193 8078 (12 099)	259 432 8912 (571 942)	222 037 2000 (489 500)	0.767
		8	369 963 0216 (813 631)		95 7585 (5 978)	181 989 3096 (401 211)		80 5410 (5 078)	157 919 4792 (348 147)	135 156 4704 (297 964)	0.373
		9	409 868 4240 (903 590)		145 4639 (9 081)	308 089 1816 (679 231)		136 3494 (8 512)	239 860 8960 (528 860)	205 311 6072 (452 627)	0.567
		10	447 218 5584 (986 044)		161 5465 (10 085)	348 904 5848 (769 190)		154 4023 (9 639)	266 414 2488 (587 333)	228 012 0192 (502 672)	0.630
89 9160 (295)	7	9	374 236 7832 (825 037)	3 552 4608 (125 440)	176 2835 (11 005)	386 305 7184 (851 644)	3 163 9104 (111 720)	169 3475 (10 572)	290 725 3944 (640 929)	248 818 6312 (548 542)	0.687
		10	446 773 3200 (984 350)		105 3586 (6 577)	288 887 4072 (636 877)		91 3214 (5 701)	243 253 8864 (536 274)	208 190 1528 (458 973)	0.411
		12	523 395 4320 (1 153 870)		125 7772 (7 852)	361 423 9440 (796 190)		114 2439 (7 132)	290 407 8848 (640 218)	245 821 2624 (541 934)	0.490
		14	592 028 2872 (1 305 177)		142 3541 (9 199)	438 046 0560 (965 710)		138 4639 (8 644)	340 209 5256 (750 021)	291 169 9274 (641 909)	0.575
121 9200 (400)	3	6	253 432 2168 (558 713)	2 093 4144 (73 920)	166 6724 (10 405)	530 719 7112 (1 170 017)	1 864 4472 (65 835)	109 9578 (6 802)	164 730 7368 (363 163)	140 983 6840 (310 815)	0.472
		7	309 614 7960 (680 985)		121 0678 (7 558)	203 137 0488 (447 833)		187 3844 (11 698)	258 749 5040 (572 640)	222 307 9992 (490 097)	0.744
		8	443 572 7184 (977 804)		190 9084 (11 918)	349 319 6280 (770 105)		210 9476 (13 169)	288 322 2216 (635 631)	246 762 0288 (544 008)	0.826
121 9200 (400)	4	7	262 095 5232 (577 812)	2 781 2192 (98 560)	211 9087 (13 229)	393 277 5504 (867 014)	2 485 9796 (87 780)	78 4586 (4 898)	170 362 1808 (375 578)	145 805 1840 (321 440)	0.366
		9	514 472 2128 (1 134 198)		93 9164 (5 863)	195 035 2992 (429 972)		198 1488 (12 370)	334 407 0744 (737 279)	286 203 8096 (630 961)	0.719
		10	559 614 4848 (1 233 718)		184 1646 (11 497)	447 411 9888 (986 358)		49 4971 (3 090)	354 462 1400 (780 525)	312 197 1840 (691 440)	0.266
121 9200 (400)	4	8	237 634 2360 (523 885)	3 489 0240 (123 200)	200 5035 (12 517)	492 554 2608 (1 085 878)	3 107 4120 (109 725)	179 9838 (11 236)	334 407 0744 (737 279)	286 203 8096 (630 961)	0.782
		9	448 877 5704 (989 589)		68 1106 (4 252)	153 808 9560 (339 085)		49 4971 (3 090)	354 462 1400 (780 525)	312 197 1840 (691 440)	0.502
		10	578 009 7792 (1 274 272)		128 6605 (8 032)	385 052 2904 (804 789)		117 4956 (7 335)	291 770 4888 (643 233)	249 713 1504 (550 514)	0.646
121 9200 (400)	7	11	624 823 3816 (1 377 481)	4 884 6336 (172 480)	165 6793 (10 343)	494 184 4992 (1 089 472)	4 350 3768 (153 615)	174 1210 (10 870)	406 136 6568 (895 363)	347 594 5872 (766 327)	0.698
		11	590 811 2128 (1 290 448)		179 1028 (11 181)	541 000 1010 (1 192 681)		106 5300 (6 651)	377 527 1976 (832 291)	323 108 8056 (712 321)	0.463
		12	686 794 3992 (1 514 097)		118 9213 (7 474)	463 455 8708 (1 021 728)		130 9031 (8 172)	446 416 3368 (984 163)	382 057 7336 (842 301)	0.548
		14	782 512 6176 (1 725 116)		140 6103 (8 728)	569 439 0072 (1 255 377)		152 9126 (9 546)	508 633 0200 (1 121 325)	435 316 2912 (959 692)	0.625
152 4000 (500)	3	7	267 457 8824 (589 634)	2 637 1584 (93 120)	169 3796 (10 574)	709 919 3808 (1 565 078)	2 348 7192 (82 935)	163 1964 (10 088)	537 728 7384 (1 185 468)	460 218 0240 (1 014 590)	0.660
		8	490 542 5448 (1 081 443)		101 4291 (6 332)	204 099 1344 (449 954)		86 9003 (5 425)	173 847 6437 (383 262)	143 788 5112 (328 017)	0.396
		9	561 322 2888 (1 237 483)		186 0228 (11 613)	477 183 8968 (941 763)		181 8000 (11 356)	318 849 5016 (702 931)	272 888 9352 (601 607)	0.775
					212 8698 (13 288)	497 963 4408 (1 097 803)		212 0368 (13 237)	364 859 5104 (804 364)	312 266 8584 (688 419)	0.830

\* Thrust - 266 892 newtons (60 000 lb) per engine

ORIGINAL PAGE IS  
OF POOR QUALITY

PRECEDING PAGE BLANK NOT FILMED

FOUNDED



Table 4.—Economic Characteristics—Parametric Study Airplanes

No. engines	No. Bays	Span m. (ft)	t/c	Cruise M	Range km (nmi)	Block time hrs	Maximum gross payload kg (lb)	65% maximum gross payload kg (lb)	Fleet size	Airplane price 10 <sup>6</sup> \$	Block fuel at 66% payload kg (lb)	DOC \$/GTkm (¢/GTm)	DOC + airplane investment cost \$/GTkm (¢/GTm)
5	3	89.9160 (295)	0.24	0.58	5232 (2825)	9.03	164 465.8344 (362 579)	106 902.6336 (235 676)	338	39.1	143 068.6152 (315 407)	5.7656 (8.417)	7 1651 (10 460)
6	7					8.88	266 399.2800 (587 300)	173 159.6320 (381 745)	205	49.7	177 567.1632 (391 462)	4.3113 (6.294)	5.3923 (7.872)
7	6					8.81	304 415.9496 (671 111)	197 870.2992 (436 272)	178	56.3	189 331.7328 (417 398)	4.0935 (5.976)	5.1566 (7.528)
8	8					8.75	339 102.7416 (747 581)	220 416.9408 (485 978)	159	61.5	204 507.8280 (450 855)	3.9784 (5.808)	5.0148 (7.321)
8	4	89.9160 (295)	0.215	0.64		8.78	272 870.5672 (597 227)	144 833.5728 (319 298)	227	49.5	167 226.8976 (368 666)	4.8354 (7.059)	6.0403 (8.818)
8	8					8.12	361 401.7176 (796 441)	234 911.2752 (517 882)	139	66.2	209 650.2912 (462 197)	3.7325 (5.449)	4.7080 (6.873)
9	5					8.06	399 127.1760 (879 910)	259 432.8912 (571 947)	125	73.5	224 222.6448 (494 318)	3.6435 (5.319)	4.6169 (6.740)
7	8			0.68		7.96	242 953.1496 (535 611)	157 919.4792 (348 147)	205	56.3	172 421.5248 (380 118)	4.6675 (6.814)	5.8779 (8.581)
8	9					7.83	369 063.0216 (813 631)	239 890.8960 (528 860)	131	70.3	214 579.1088 (473 058)	3.7024 (5.405)	4.6826 (6.836)
9	9					7.79	409 868.4240 (903 590)	266 414.2488 (587 333)	118	77.9	226 376.3376 (499 068)	3.4613 (5.053)	4.4346 (6.474)
10	10					7.75	447 269.5584 (986 044)	290 725.3944 (640 929)	107	85.3	235 671.5088 (519 558)	3.4434 (5.027)	4.8463 (7.075)
10	7	80.9160 (295)	0.14	0.75		7.27	374 236.7832 (825 037)	243 253.8864 (536 244)	121	83.5	217 515.2616 (479 531)	3.3573 (4.902)	4.4422 (6.488)
10	10					7.25	446 773.3200 (984 950)	290 402.8848 (640 218)	101	124.7	304 295.7456 (670 846)	3.3510 (4.892)	4.3545 (6.357)
12	14					7.18	523 395.4320 (1 153 870)	340 209.5256 (750 021)	85	109.8	267 975.0964 (590 744)	3.4013 (4.926)	4.3422 (6.339)
14	14					7.12	592 028.2872 (1 305 177)	384 795.6840 (848 315)	75	51.0	163 183.5072 (359 752)	4.4013 (6.426)	5.5973 (8.172)
6	3	121.9200 (400)	0.24	0.58		9.12	253 432.2168 (558 713)	164 947.1040 (363 163)	221	66.9	188 031.2616 (414 531)	3.4736 (5.071)	4.4504 (6.497)
7	7					8.95	399 614.7960 (880 985)	259 749.5040 (572 640)	138	74.9	221 662.0728 (488 673)	3.3565 (4.900)	4.3339 (6.327)
8	8					8.88	443 572.7184 (977 894)	286 372.2216 (635 631)	123	90.8	252 838.9080 (557 405)	3.2037 (4.677)	4.1504 (6.059)
7	4	121.9200 (400)	0.215	0.64		8.46	262 095.5232 (577 817)	170 362.1808 (375 578)	199	58.3	173 338.7040 (382 140)	4.4929 (6.559)	5.7238 (8.356)
9	9					8.18	514 472.2128 (1 134 198)	334 407.0744 (737 229)	98	98.1	264 675.6000 (583 500)	3.1167 (4.550)	4.0510 (5.914)
10	10					8.13	559 614.4848 (1 233 718)	363 749.5512 (801 917)	90	64.2	165 450.6000 (364 750)	4.9737 (7.261)	6.4205 (9.373)
8	5	121.9200 (400)	0.19	0.68		8.17	237 634.2360 (523 885)	154 462.1400 (340 525)	213	87.6	227 835.5688 (502 783)	3.3048 (4.956)	4.4134 (6.443)
9	9					7.95	448 877.4704 (989 589)	291 770.4888 (643 233)	110	87.6	227 835.5688 (502 783)	3.0208 (4.410)	3.9503 (5.788)
10	10					7.87	578 011.5936 (1 274 276)	375 706.4472 (832 331)	84	104.9	273 694.9824 (603 384)	2.9455 (4.300)	3.8825 (5.668)
11	11			0.75		7.83	624 825.3816 (1 377 481)	406 136.6568 (895 363)	78	113.8	263 493.0648 (580 893)	3.0875 (4.500)	4.0894 (5.970)
12	14					7.34	580 811.2128 (1 280 448)	377 527.1976 (832 291)	79	120.8	265 765.1472 (585 902)	2.7091 (3.955)	3.7729 (5.508)
13	14					7.30	686 794.3992 (1 514 097)	446 416.3368 (984 163)	66	133.6	239 968.3360 (529 260)	3.0875 (4.500)	4.0894 (5.970)
14	14					7.25	782 512.6176 (1 725 116)	508 633.0200 (1 121 325)	58	147.5	311 887.0592 (687 572)	2.7091 (3.955)	3.6113 (5.272)
15	15					7.22	827 274.7728 (1 823 798)	537 729 7384 (1 195 469)	54	151.1	318 439.4472 (702 027)	2.6578 (3.880)	3.5626 (5.201)
8	3	152.4000 (500)	0.24	0.58		9.24	267 457.9824 (589 634)	173 847.6432 (383 262)	213	60.9	180 483.8112 (397 892)	4.7312 (6.907)	6.1012 (8.907)
9	9					8.96	490 542.5448 (1 081 443)	318 849.5016 (702 931)	113	84.1	240 474.9472 (537 657)	3.3414 (4.878)	4.3435 (6.341)
9	9					8.93	561 322.2888 (1 237 483)	401 147.5104 (884 364)	98	93.5	261 381.1032 (576 237)	3.1290 (4.568)	4.0997 (5.985)

\*Thrust - 266 587 newtons (60 000 lb.) per engine



Table 5.—DLF Selected Configuration

1990 Aerodynamic Technology Development

Item	1980 Base			1990 %	
	f(ft <sup>2</sup> )	C <sub>D</sub> item	% of total Cruise drag	Drag reduct. of item, %	Increase M(L/D)
Roughness excrescence interference	15.83	0.00079	3.4	33	1
Improved airfoil					
Form	58.5	0.00292	12.5	4	0.5
Δ M <sub>crit</sub> = 0.04	—	—	—	—	6
Tip fins	—	—	—	*	16
Total					23.5

S<sub>ref</sub> = 19 980 ft<sup>2</sup>

\*Induced drag is reduced 34.5%, but profile drag at zero lift is increased 9.5% and profile drag variation with lift is assumed to be unchanged.

Table 6. — Parasite Drag Summary Selected Configuration

$S_{ref} = 1730 \text{ m}^2$  (18 620  $\text{ft}^2$ );  $Re/ft = 1.46 \times 10^6$   $M = 0.51/9144 \text{ m}$  (0.51/30 000 ft)

Item	Flat plate friction drag				Form drag		Pressure and interference drag		Rough & excr. $f$ $\text{m}^2$	Total $f_{total}$ $\text{m}^2$ (ft $^2$ )
	$A_{wet}$ $\text{m}^2$ (ft $^2$ )	$L_{ref}$ m (ft)	$Re \times 10^{-6}$	$C_{f, avg}$	$f_{PL}$ $\text{m}^2$ (ft $^2$ )	Form factor	$f$ form $\text{m}^2$ (ft $^2$ )	A $\text{m}^2$		
Wing	3 602 (38 768)	21.67 (71.1)	(103.8)	(0.00201)	7.24 (77.92)	(0.72)	5.2051 (56.03)		0.565 (6.08)	13.01 (140.03)
Body	90.1 (970)	9.14 (30.0)	(43.8)	(0.00228)	0.205 (2.21)	(0.31)	0.064 (0.69)		0.014 (0.15)	0.283 (3.05)
Horizontal tail	859.3 (9 250)	8.60 (28.2)	(41.1)	(0.00230)	1.977 (21.28)	(0.53)	1.048 (11.28)		11.39 (1.50)	3.164 (34.06)
Tail booms	353.0 (3 800)	18.29 (60.0)	(87.6)	(0.00208)	0.734 (7.90)	(0.02)	0.015 (0.16)		0.038 (0.41)	0.807 (8.69)
Nacelles (7)	448.7 (4 830)	8.14 (26.7)	(39.0)	(0.00232)	1.041 (11.21)	(0.37)	0.386 (4.15)		0.061 (0.66)	1.488 (16.02)
Nacelle struts	97.5 (1 050)	4.05 (13.3)	(19.5)	(0.00258)	0.252 (2.71)				0.013 (0.14)	0.265 (2.85)
Cab									0.252 (2.71)	0.252 (2.71)
Large tip fins	426.4 (4 590)	7.22 (23.7)	(34.6)	(0.00238)	1.014 (10.92)	(0.23)	0.233 (2.51)		0.069 (0.74)	1.32 (14.17)
Small tip fins	150.5 (1 620)	3.08 (10.1)	(14.8)	(0.00270)	0.4059 (4.37)	(0.23)	0.094 (1.01)		0.024 (0.26)	0.524 (5.64)
Wing-nac-strut interference							73.48 (791)	(0.0022)	1.59 (1.71)	1.59 (1.71)
Total	6027.166 (64 878)				138.52		7.045 (75.83)		0.449 (4.83)	21.268 (228.93)

$C_{Dp, min} = 0.01229$

Table 7.—1990 Engine Technology Gains

Item	Gain	$\Delta$ SFC*, %	$\Delta$ WT*, %
● Engine improvements			
Improved sealing/clear control	}	-12.6	-20.6**
Increased cooling EFF			
Higher comp. EFF			
Cycle change			
FPR = 1.6 OPR = 40 BPR = 9.5 CR. TIT = 1528°K			
Advanced electronic control		-1.0	N/A
Advanced materials/composites		N/A	-7.0
Advanced design concepts		N/A	-3.0
● Installation improvements			
Improved inlet shape	}	-1.0	N/A
Better nozzle design			
Reduced leakage (fan T/R)			
*Relative to current turbofans	**Geared fan		





Table 8. Selected Configuration Weight Statement  
 1 in. = 0.254 m

Configuration technology level	1 lb = 0.4536 kg		1 in. = 0.254 m	
	1980 technology kg (lb)	Δ W kg (lb)	Uncycled 1990 W kg (lb)	Cycled 1990 W kg (lb)
Wing and fixed tip fins	81 811.2960 (180 360)	2 630.0800 (-5 800)	79 180.4160 (174 560)	73 209.7120 (172 420)
Horizontal tail	8 196.5520 (18 070)	2 109.2400 (-4 650)	6 087.3120 (13 420)	6 087.3120 (13 420)
Vertical tail	7 756.5600 (17 100)	571.5360 (-1 260)	7 185.0240 (15 840)	7 185.0240 (15 840)
Body	3 220.5600 (7 100)	1 088.6400 (-2 400)	18 189.3600 (40 100)	17 463.6000 (38 500)
Main landing gear - fwd	19 278.0000 (42 500)	1 088.6400 (-2 400)	18 189.3600 (40 100)	17 463.6000 (38 500)
Noise landing gear aft	17 091.6480 (37 680)	5 071.2480 (-11 180)	12 020.4000 (26 500)	12 809.6640 (28 240)
Nacelle and strut	15 916.8240 (35 090)	240.7000 (-750)	15 576.6240 (34 340)	15 576.6240 (34 340)
Wing tip fins - movable	172 549.4400 (380 400)	6 223.3920 (-13 720)	159 649.0560 (351 960)	158 016.0960 (348 360)
Total structure	29 973.8880 (66 080)	635.0400 (1 400)	23 750.4960 (52 360)	25 511.2880 (56 330)
Engine	235.3720 (520)	235.3720 (520)	635.0400 (1 400)	635.0400 (1 400)
Engine accessories	2 984.6880 (6 580)	2 984.6880 (6 580)	153.7600 (350)	158.7600 (350)
Engine controls	5 715.3600 (12 600)	6 631.6320 (+14 620)	2 984.6880 (6 580)	2 984.6880 (6 580)
Engine control system	39 703.6080 (87 530)	5 715.3600 (12 600)	6 631.6320 (14 620)	7 067.0880 (15 580)
Fuel system	417.3120 (920)	417.3120 (920)	417.3120 (920)	417.3120 (920)
Thrust reverser	5 561.1360 (12 260)	5 561.1360 (12 260)	417.3120 (920)	417.3120 (920)
Engine burst protection	3 098.0880 (6 830)	3 098.0880 (6 830)	5 561.1360 (12 260)	5 561.1360 (12 260)
Total propulsion system	802.8720 (1 770)	802.8720 (1 770)	3 098.0880 (6 830)	3 098.0880 (6 830)
Instruments	1 515.0240 (3 340)	1 515.0240 (3 340)	802.8720 (1 770)	802.8720 (1 770)
Surface controls	1 809.8640 (3 990)	1 809.8640 (3 990)	1 515.0240 (3 340)	1 515.0240 (3 340)
Hydraulics	358.3440 (790)	358.3440 (790)	1 809.8640 (3 990)	1 809.8640 (3 990)
Pneumatics	10 568.8800 (23 300)	10 568.8800 (23 300)	358.3440 (790)	358.3440 (790)
Electrical	512.5680 (1 130)	512.5680 (1 130)	10 568.8800 (23 300)	10 568.8800 (23 300)
Electronics	1 587.6000 (3 500)	1 587.6000 (3 500)	512.5680 (1 130)	512.5680 (1 130)
Flight provisions	589.6800 (1 300)	589.6800 (1 300)	1 587.6000 (3 500)	1 587.6000 (3 500)
Passenger accommodations	1 052.3520 (2 320)	1 052.3520 (2 320)	589.6800 (1 300)	589.6800 (1 300)
Cargo handling	6 708.7440 (14 790)	6 708.7440 (14 790)	1 052.3520 (2 320)	1 052.3520 (2 320)
Emergency equipment	34 582.4640 (76 240)	34 582.4640 (76 240)	6 708.7440 (14 790)	6 708.7440 (14 790)
Air conditioning	272.1600 (600)	272.1600 (600)	34 582.4640 (76 240)	34 582.4640 (76 240)
Insulation - cargo	680.4000 (1 500)	680.4000 (1 500)	272.1600 (600)	272.1600 (600)
Total fixed equipment	247 988.0720 (546 270)	247 988.0720 (546 270)	680.4000 (1 500)	680.4000 (1 500)
Exterior paint	2 481.1920 (5 470)	2 481.1920 (5 470)	235 295.9280 (518 730)	236 275.7040 (520 890)
Options	250 269.2640 (551 740)	250 269.2640 (551 740)	2 481.1920 (5 470)	2 481.1920 (5 470)
Manufacturer's empty weight	(7) J190 70	(7) J190 70	237 777.1200 (524 200)	238 756.8960 (526 360)
Standard and operational items	60 000 ea	60 000 ea	237 777.1200 (524 200)	238 756.8960 (526 360)
Operational empty weight	266 892 N	266 892 N	51 000 ea	(1) ADVBPR = 9.5
Engines (qty/designation)	509 846.4000 (1 124 000)	509 846.4000 (1 124 000)	226 959 N	54 350 ea
Engine thrust (SLS) lb newtons	816 480 0000 (1 800 000)	816 480 0000 (1 800 000)	509 346.4000 (1 124 000)	241 760 N
Cargo containers (qty/type)	814 665 6000 (1 796 000)	814 665 6000 (1 796 000)	816 480 0000 (1 800 000)	555 297 1200 (1 224 200)
Maximum zero fuel weight			814 665 6000 (1 796 000)	759 125 7760 (1 674 660)
Maximum landing weight				759 172 1760 (1 673 660)
Maximum flight weight				
Maximum taxi weight				
Maximum takeoff weight				

PRECEDING PAGE BLANK NOT FILMED

FOLDOUT FRAME /

FOLDOUT FRAME



Table 9.—1990 Technology Items Utilized

<u>Item</u>	<u>Selected configuration weight lb</u>	<u>Kg</u>
Improved aluminum alloys:		
Wing	(Incl. in base)	
Bonded aluminum:		
Horizontal tail	-3820	-1732.752
Vertical tail	-1260	-571.536
Wingtip fins	-1000	-453.6
Composite control surfaces:		
Wing	-4800	-2177.28
Horizontal tail	-830	-376.488
Movable wing tip fin	-750	-340.2
Improved titanium alloys:		
Nacelle	-440	-199.584
Advanced carbon brakes:		
Main gear	-4800	-2177.28
Maneuver load alleviation:		
Wing	(Incl. in base)	
Reduced longitudinal stability:		
Horizontal tail	(Incl. in base)	
Advanced engine and installation:	-6900*	-3129.84

\*Based on 226,858.2 n (51 000 lb) engines

**ORIGINAL PAGE IS  
OF POOR QUALITY**

Table 10.—Selected Configuration  
Minimum Structural Requirements

Criteria	Weight kg/m <sup>2</sup> (lb/ft <sup>2</sup> )	Skin gage		Core	
		Outside cm (in.)	Inside cm (in.)	Density kg/m <sup>3</sup> (lb/ft <sup>3</sup> )	Thickness cm (in.)
Basic honeycomb panel	4.307 (0.882)	0.03048 (0.012)	0.03048 (0.012)	55.424 (3.46)	3.81 (1.50)
Corrosive pitting	4.590 (0.940)	0.04064 (0.016)	0.03048 (0.012)	55.424 (3.46)	3.81 (1.50)
Fuel head	5.44 (1.114)	0.0508 (0.020)	0.0508 (0.020)	55.424 (3.46)	3.81 (1.50)
Walk on	5.723 (1.172)	0.08128 (0.032)	0.03048 (0.012)	55.424 (3.46)	3.81 (1.50)
Hail	6.011 (1.231)	0.09144 (0.036)	0.03048 (0.012)	55.424 (3.46)	3.81 (1.50)
Bird strike	44.67 (9.148)	0.09144 (0.036)	0.09144 (0.036)	256.296 (16.00)	15.24 (6.00)
Fragment protect	0.869 (0.178)	2 plies fiberglass			

Table 11.—Pressurization Impact—Selected Configuration  
(Incremental Weight Required to Maintain 68,948 nm<sup>2</sup> (10 psia) Cargo Hold Pressure,  
48,263.6 nm<sup>2</sup> (7 psig) Operating Pressure)

	Kg	Lb
Cover material		
● Honeycomb face sheets	1,673.8	3 690
● Honeycomb core	1,378.9	3 040
● Doors	167.8	370
Spars		
● Honeycomb face sheets	362.9	800
● Tension ties	1,088.6	2 400
● Doors	90.7	200
Ribs and bulkheads		
● Face sheets and chords	13,444.7	29 640
● Sill bulkheads	136.1	300
Cargo door, strengthen	816.5	1 800
Seals and sealant	362.9	800
Miscellaneous	208.7	460
Total pressurization penalty	19,731.6	43 500 (8.3% OEW)

Table 12.—Performance Summary—Selected Configuration

Design range = 5556 km (3000 nmi)  
 Net P/L density = 160.185 kg/m<sup>3</sup> (10 lb/ft<sup>3</sup>)  
 ATA international rules

TOGW—kg	lb	759 190	167.37x10 <sup>4</sup>
OEW—kg	lb	238 775	526 400
OEW/TOGW			0.3145
Gross PL—kg	lb	316 522	697 800
Cargo vol.—m <sup>3</sup>	ft <sup>3</sup>	1 699	60 000
PL density—kg/m <sup>3</sup>	lb/ft <sup>3</sup>	160.185	10
PL/TOGW			0.4169
TOFL—m	ft	2133.6	7 000
Cruise: mach			0.68
Alt.—m	ft	9534.4	28 000
L/D			16.6
RF (km)	nmi	24 076	13 000
Block fuel—kg	lb	174 454	384 600
Block time	hr		8.24
BF/PL			0.5512
(PL/GW) mach			0.2836
(PLxR)/BF—m ton km/kg ton st. mi/lb		12.1	3.13
Land wt—kg	lb	385 144	129x10 <sup>4</sup>
Land fl—m	ft	6 200	6 200
V <sub>app</sub> —m/sec	kt	67.4	131
S <sub>w</sub> —m <sup>2</sup>	ft <sup>2</sup>	1 730	18 620
W/S	lb/ft <sup>2</sup>		90
Λ	deg		0
t/c	%		21.5



Table 13.—Reference Configuration Weight Statement

1 lb = 0.4536 kg

1 in = 0.0254 m

Configuration technology level	Baseline 1980 Technology W, kg (lb)	$\Delta W$ , kg (lb)	Uncycled 1990 W, kg (lb)	Cycled 1990 W, kg (lb)	C <sub>d</sub> X, B.S. m (in.)
Wing	59 008 8240 (130 090)	6 853 8960 (-15 110)	52 154 9280 (114 980)	52 404 4080 (115 530)	32 8168 (1292)
Horizontal tail	3 783 0240 (8 340)	843 6960 (-1 860)	2 939 3280 (6 480)	3 138 9120 (6 920)	75 9460 (2990)
Vertical tail	2 884 8360 (6 360)	349 2720 (-770)	2 535 6240 (5 590)	2 417 6880 (5 330)	70 3580 (2770)
Body	49 143 0240 (108 340)	4 422 6000 (-9 750)	44 720 4240 (98 590)	44 797 5360 (98 760)	34 2138 (1347)
Main landing gear	22 262 6880 (49 080)		22 262 6880 (49 080)	22 380 6240 (49 340)	34 0360 (1340)
Nose landing gear	3 861 0640 (8 490)		3 861 0640 (8 490)	3 873 7440 (8 540)	11 5570 (455)
Nacelle and strut	12 991 1040 (28 640)	6 395 7600 (-14 100)	6 595 3440 (14 540)	6 749 5680 (14 880)	29 3370 (1155)
Total structure	153 974 6240 (339 340)		135 059 4000 (297 750)	135 767 4800 (299 300)	34 3662 (1353)
Engine	15 363 4320 (33 870)	1 787 1840 (-3 940)	13 576 2480 (29 930)	13 943 6640 (30 740)	27 6860 (1090)
Engine accessories	303 9120 (670)		303 9120 (670)	303 9120 (670)	27 6860 (1090)
Engine controls	149 6880 (330)		149 6880 (330)	149 6880 (330)	20 5740 (810)
Starting system	90 7200 (200)		90 7200 (200)	90 7200 (200)	27 6860 (1090)
Fuel system	1 369 8720 (3 020)		1 369 8720 (3 020)	1 369 8720 (3 020)	29 3370 (1155)
Thrust Reverser	1 088 6400 (2 400)	2 703 4560 (+5 960)	3 792 0960 (8 360)	3 878 2800 (8 550)	27 4066 (1079)
Total propulsion system	18 366 2640 (40 490)		19 282 5360 (42 510)	19 736 1360 (43 510)	27 6860 (1090)
Instruments	421 3480 (930)		421 3480 (930)	421 3480 (930)	3 5090 (335)
Surface controls	4 377 2400 (9 650)		4 377 2400 (9 650)	4 431 6720 (9 770)	41 5798 (1637)
Hydraulics	1 533 1680 (3 380)		1 533 1680 (3 380)	1 546 7760 (3 410)	30 9610 (1215)
Pneumatics	861 8400 (1 900)		861 8400 (1 900)	860 3760 (1 910)	29 7180 (1170)
Electrical	1 279 1520 (2 820)		1 279 1520 (2 820)	1 279 1520 (2 820)	25 4000 (1000)
Electronics	1 406 1600 (3 100)		1 406 1600 (3 100)	1 406 1600 (3 100)	13 9700 (580)
Flight provisions	607 8240 (1 340)		607 8240 (1 340)	607 8240 (1 340)	10 9220 (430)
Passenger accommodations					
Cargo handling 1	6 676 9920 (14 720)		6 676 9920 (14 720)	6 676 9920 (14 720)	31 7500 (1250)
Emergency equipment	240 4080 (530)		240 4080 (530)	240 4080 (530)	25 3497 (998)
Air conditioning	957 0960 (2 110)		957 0960 (2 110)	957 0960 (2 110)	25 9080 (1020)
Anti icing	235 8720 (520)		235 8720 (520)	235 8720 (520)	25 4762 (1003)
Auxiliary power unit	36 2880 (80)		36 2880 (80)	36 2880 (80)	53 9280 (2320)
Hull insulation	3 125 3040 (6 890)		3 125 3040 (6 890)	3 125 3040 (6 890)	32 9946 (1299)
Total fixed equipment	21 759 1920 (47 970)		21 759 1920 (47 970)	21 831 7680 (48 130)	30 8864 (1216)
Exterior paint	331 1280 (730)		331 1280 (730)	331 1280 (730)	33 1978 (1307)
Options	680 4000 (1 500)		680 4000 (1 500)	680 4000 (1 500)	35 8140 (1410)
Manufacturer's empty weight	195 061 6080 (430 030)		177 117 6580 (390 460)	178 341 9120 (393 170)	33 1978 (1307)
Standard and operational items	1 369 3720 (3 020)		1 369 3720 (3 020)	1 374 4080 (3 030)	23 2156 (914)
Operational empty weight	196 431 4800 (433 050)		178 482 5280 (393 480)	167 469 1200 (396 200)	33 1216 (1304)
Engines (qty/designation)	(4) CF-6-50C		(4) ADVBPR - 9 5	(4) ADVBPR - 9 5	5
Engine thrust (SLS) newtons	51 000 ea	276 858	51 000 ea	52 200 ea	232 196
Cargo containers (qty/type)	8 500	789.7	8 500	8 330	773.9
SW, ft <sup>2</sup>	1516/1054	126.7/97.9	1364/1054	1457/1005	135.4/83.4
SH/SV, ft <sup>2</sup> per APL m <sup>2</sup>	140.8/97.9				
Maximum zero fuel weight	371 180 8800 (818 300)		371 180 8800 (818 300)	374 492 1600 (827 500)	
Maximum landing weight	387 192 9600 (853 600)		387 192 9600 (853 600)	390 731 0400 (861 400)	
Maximum flight weight flaps up					
Maximum taxi weight	462 989 5200 (1 020 700)		462 989 5200 (1 020 700)	467 480 1600 (1 030 600)	
Maximum takeoff weight	462 535 9200 (1 019 700)		462 535 9200 (1 019 700)	467 026 5600 (1 029 600)	

PROCEEDING PAGE BLANK NOT FILMED

FOLDOUT FRAME 1







Table 14.—1990 Technology Items Utilized

<u>Item</u>	<u>Reference configuration weight kg (lb)</u>
Improved aluminum alloys:	
Wing	-4,803.6 (-10 590)
Bonded aluminum:	
Body	-4,227.5 ( -9 320)
Horizontal tail	-308.4 ( -680)
Vertical tail	-258.6 ( -570)
Wing tip fins	-54.4 ( -120)
Composite control surfaces:	
Wing	-952.6 ( -2 100)
Horizontal tail	-158.8 ( -350)
Vertical tail	-90.7 ( -200)
Improved titanium alloys:	
Nacelle	-113.4 ( -250)
Advanced carbon brakes:	
Main gear	(Incl. in base)
Maneuver load alleviation:	
Wing	-1,043.3 ( -2 300)
Reduced longitudinal stability:	
Horizontal tail	-376.5 ( -830)
Advanced engine and installation:	-1,787.2 ( -3 940)

\*Based on 226,858.2 n (51 000 lb) SLST engines

**PRECEDING PAGE BLANK NOT FILMED**

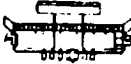



Table 15.—1990 Advanced Aerodynamic Technology

*Percent increase in M(L/D)	Reference Configuration 	Selected Configuration 
Roughness, excrescence, and interference	2	1
Improved airfoil parasite	0.5	0.5
High speed $M_{crit} = 0.04$	5.5	6
Tip fins	4	16
Active controls (longitudinal SAS)	2	**
Total	14	23.5

\*Relative to 1975 technology levels

\*\*These items included in original performance

Table 16.—Distributed Load Freighter Comparison With Reference Configuration

					
		DLF conf.	REF. conf.	DLF	REF.
TOGW—lb	kg	1 673 700	1 029 000	759 190	467 027
Thrust—lb	newtons	7x54 350	4x52 200	241 760	232 196
OEW—lb	kg	520 400	396 200	238 775	179 716
OEW/TOGW		0.3145	0.3848		
Gross PL—lb	kg	697 800	429 400	16 522	194 776
Cargo vol—ft <sup>3</sup>	m <sup>3</sup>	60 000	36 928	1 699	1 046
PL density—lb/ft <sup>3</sup>	lb/m <sup>3</sup>	10	10	160.185	160.185
PL/TOGW		0.4169	0.4171		
TOFL—ft	m	7 000	11 700	2133.6	3 566
Cruise: mach		0.68	0.78		
Alt.—ft.	m	28 000	33 000	5534.4	0.0058
L/D		16.6	21.9		
RF (nmi)	km	13 000	18 800	24 076	34 517
Block fuel—lb	kg	384 600	165 000	174 454	74 844
Block time—hr		8.24	7.39		
BF/PL		0.5512	0.3843		
(PL/GW) mach — m ton	km/kg	0.2836	0.3235		
(PLxR)/BF—ton st. mi/lb		3.13	4.50	12.24	17.60
Land wt—lb	kg	1 290 000	861 400	585 144	390 731
Land fl—ft	m	6 200	6 100	1 890	1 859
V <sub>app</sub> = kt	m/sec	131	130	67.4	66.9
Wing span—ft	m	314	284	95.7	86.6
S <sub>w</sub> = ft <sup>2</sup>	m <sup>2</sup>	18 620	8 500	1 730	790
W/S		90	121		
Λ—deg		0	20		
t/c—%		21.5	14		
Fleet size		153	226		
Price (millions)		72.6	63.9		
S/lb of OEW	\$/kg	137.9	161.2	304.0	355.4
S/lb of payload	\$/kg	104.0	148.8	229.3	328.0

Design range = 5556 km (3000 nmi)

Net PL density = 160.185 kg/m<sup>3</sup> (10 lb/ft<sup>3</sup>)

ATA international rules - std day



# APPENDIX A

## PARAMETRIC DATA BASE

### AERODYNAMICS

#### PERFORMANCE METHODS--THUMBPRINT COMPUTER PROGRAM

The airplane performance produced during the course of this study was calculated using the Boeing developed computer program "TEI-004, Computer Application to Airplane Design Selection (Thumbprint Program)." This program is a tool for the sizing of aircraft performing given transport missions. It parametrically adjusts base-point design input data to generate large numbers of sized variants, analyzes their characteristics, and permits optimum point selection. The program internally calculates variations in field length, direct operating costs and community noise levels, thus permitting selection within chosen constraints on these parameters. These tasks are accomplished using aerodynamic, weight, propulsion, and noise preliminary design procedures. A conceptual flow chart of the Thumbprint program is shown in figure 86.

Inputs to the program include: (1) a base-point airplane geometry, aerodynamics, weights, and propulsion and (2) scaling relationships for adjusting the base-point values for changes in wing area, engine size, payload, and range.

Output of the program as utilized in this study defines the performance weight and aerodynamic characteristics of point design airplanes. Also, off-design data for the specific point designs provide the variation of performance for off-loaded conditions. An example chart of the airplane matching technique is shown in figure 87.

#### AERODYNAMIC PREDICTION TECHNIQUES

Early studies indicated that the aerodynamic areas of concern in the design of the payload-in-wing, distributed-load airplane could be divided into three categories:

1. Wing-thickness-dependent items that would strongly influence the choice of configuration and regarding which further information was desired. Such items included thick-wing drag level and drag rise characteristics, flap effectiveness, and ground effects.
2. Items unaffected or only marginally affected by wing thickness deemed calculable with a high degree of confidence. These items included induced drag (of planar and nonplanar systems) and trim drag.
3. Items that are thickness-dependent but deemed to be of relatively small magnitude or noncritical to the choice of configuration. Such items included engine nacelle interference drag and the choice of nacelle installation.

In order to provide needed thick-wing experimental data and improve confidence in prediction techniques, two exploratory wind tunnel tests were conducted in 1974. These tests provided drag data over a range of Mach numbers and indicated that high-lift device characteristics were predictable and that ground effects were noncritical.

### **Aerodynamic Data Base**

Early studies, plus the results of the above-mentioned wind tunnel tests, indicated that three thickness-dependent aerodynamic parameters would be of primary importance in the selection of wing thickness ratio (and hence chord, area, aspect ratio, and payload volume for given span). These three parameters were:

1. Subcritical form drag factor
2. Drag divergence Mach number
3. Degree of drag "creep"

These three parameters, together with calculable drag items, were used to describe the cruise drag characteristics of payload-in-wing airplanes in the manner shown in figure 88.

In order to provide aerodynamic inputs for a study in which wing thickness ratio was to be one of the main independent variables, parametric trends of these three variables as a function of thickness ratio were generated, making use of the above wind tunnel results and other pertinent airfoil data. These parametric trends are shown by the heavy lines in figure 89, 90, and 91, respectively.

### **Cruise Drag Buildup**

The parametric trends shown above in figures 89, 90, and 91, together with established subsonic drag prediction techniques and secondary data obtained from the above-mentioned wind tunnel tests, were used to construct cruise drag characteristics in the manner described below.

*Parasite Drag.*—The parasite drag for each configuration component was built up in the manner shown in table 17 for the sample Model 759-165A using four items:

- Flat-plate skin friction drag
- Viscous-related form drag
- Pressure and interference drag
- Roughness and excrescence drag

All items in this buildup with the exception of lifting surface form drag (which was computed using the parametric form drag factor trends shown in figure 89) were computed using internal Boeing methods. No interference drag was charged to the nacelles, since applicable data

for nacelles mounted on thick wings were not available and the expected magnitude of this term was small compared with the total configuration parasite drag.

*Induced Drag.*—Induced drag of the medium-to-low-aspect-ratio rectangular wings was computed by multiplying elliptic induced drag ( $CL^2/\pi AR$ ) by a factor of 1.03. This factor was held constant for all aspect ratios, although it is realized that a slow variation with aspect ratio is predicted theoretically.

*Profile Drag Due to Lift.*—Profile drag due to lift was extracted from applicable wind tunnel data by subtracting calculated induced drag from total lift-dependent drag.

*Compressibility Drag.*—The drag-rise curve for a lift coefficient of 0.4 was constructed from the parametric drag divergence Mach number and drag creep data in figures 90 and 91, using the drag-rise shapes obtained in the wind tunnel tests as a guide. The drag-rise curves for the other lift coefficients were obtained by applying wind-tunnel-determined increments to the  $C_L = 0.4$  curve.

*Untrimmed Cruise Polars.*—Untrimmed cruise polars were constructed by adding items 1 through 4 above. A typical set of untrimmed polars for the Model 759-165A is shown in figure 92.

*Trim Drag.*—Trim drag was calculated by a Boeing-developed minicomputer program that uses configuration geometric data, tail-off drag polars, tail-off pitching moment curves, and tail downwash data as inputs. A typical set of curves, showing trim drag plotted against airplane center-of-gravity location with lift coefficient as parameter, is shown for the 759-165A airplane at Mach 0.58 in figure 93. Subsequent parametric inputs assumed a c.g. location of 0.40 MAC for all airplanes.

*Thumbprint Inputs.*—As stated previously, cruise drag inputs to the "Thumbprint" matching and sizing program consist of a parasite drag breakdown such as that shown in table 17, a curve of subcritical "polar shape" versus  $C_L$ , and curves of "compressibility drag" versus  $C_L$  and Mach number.

"Polar shape" is defined as all lift-dependent drag items in excess of minimum elliptic induced drag and includes nonelliptic induced drag, profile drag due to lift, and trim drag. "Compressibility drag" consists of increments to be applied to the subcritical drag polar to yield compressible polars and includes drag creep and trim drag increments. Typical polar shape and compressibility drag inputs are shown in figure 94.

The Thumbprint method also accepts parasite drag scalars in order to calculate drag increments due to changes in the sizes of wing, empennage, body and propulsion system away from the baseline input (uncycled) configuration. Since only propulsion system scaling was performed in this study, the only scalars input were a value of  $0.00352 \text{ m}^2$  ( $0.0379 \text{ ft}^2$ ) of equivalent flat-plate friction area per 4448 N of installed sea-level static thrust for the engine nacelles plus a corresponding figure of  $0.00065 \text{ m}^2$  ( $0.00697 \text{ ft}^2$ ) per 4448 N (1000 lb) of thrust for nacelle struts.

## Low-Speed Predictions

A wind tunnel test, coupled with potential flow analyses, indicated that the "suckdown" ground effect on a thick wing would be severe only with low trailing edge flap deflections at low angles of attack and at very low ground height values. Furthermore, the theoretically predicted reductions in induced drag at low ground heights were observed in the test. Generally theoretical estimates of flap effectiveness were confirmed by the results, allowing for the very low Reynolds numbers at which the tests were conducted.

Given these results, the following assumptions were made:

1. Incremental flap lift, drag, and pitching moments could be predicted with reasonable confidence using contractor estimating methods.
2. Ground effects would be noncritical to takeoff and landing performance, provided a reasonable amount of trailing-edge flap deflection was used during ground roll.

Other assumptions made as a result of technology integration studies were:

1. Ailerons would be required for critical low-speed phases of flight. The studies were therefore conducted assuming a fixed flap span-to-wingspan ratio of 0.61.
2. The optimum takeoff procedure would consist of:
  - a. Ground roll with flaps and ailerons drooped and spoiler panels closed to yield a full-span, plain-flap configuration.
  - b. Transition or flare during which ailerons would be retracted and spoiler panels slightly raised in order to open flap slots.
  - c. Free-air climbout with ailerons retracted and single-slotted flap configuration.

The low-speed drag predictions embodies the following:

1. Parasite drag level computed for the cruise drag buildup
2. Incremental flap lift and pitching moments computed using contractor methods
3. Induced drag of flapped systems from contractor methods
4. Flap parasite drag
5. Trim drag using a Boeing-developed minicomputer program
6. A constant gear drag of 0.0086



7. An asymmetric engine-out drag due to rudder given by:

$$C_{D4} = \frac{1}{2AR_V} \cdot \frac{S_{ref}}{S_V} \frac{b^2}{\ell_v} \cdot C_n^2$$

Low-speed inputs to the Thumbprint method were submitted in the form shown in figures 95 and 96, which show all-engine, free-air lift-to-drag ratio versus lift coefficient with flap deflection as parameters for the Model 759-165A in climbout (gear-up) and approach (gear-down) conditions, respectively. Only the envelope of best L/D (heavy line), coupled with asymmetric engine-out drag, is used by the Thumbprint method to determine the thrust required to meet second segment gradient with an engine out for a given takeoff weight.

### STABILITY AND CONTROL

Ground rules are chosen for sizing the flight control surfaces in the parametric study in order to provide consistent inputs without having to perform detailed and lengthy stability and control analyses for each configuration. The ground rules following are chosen with experience gained in the Boeing Arctic Resources Airplane (ARA) and the present DLF program. The technology assumed is advanced and appropriate to the 1980 design period.

#### GROUND RULES LONGITUDINAL AXIS

1. Tail size and aft c.g. are chosen to balance the airplane no more than 5% MAC aft of the maneuver point. This design requires a flight-critical stability augmentation system for safety of flight and a command augmentation system for good handling qualities. From previous studies on the baseline parametric four-bay, 89.92-m (295-ft) span configuration (Model 759-163A), it is expected that the unaugmented configurations for this study will experience a short period divergent response time of not less than 2 seconds ( $t_2 \geq 2.0$ ). This criterion is based on the SST hard-SAS analysis.
2. Trim capability is provided at all wing flap settings and design approach speeds for a range from 0.5  $CL_{app}$  to 1.3  $CL_{app}$  in free air, and at  $CL_{app}$  in ground effect with sufficient control remaining to provide a pitch flare capability of 3 deg/sec<sup>2</sup>.
3. No takeoff rotation is required (airplane lifts off in taxi attitude).
4. Recovery from stall or high angles of attack does not size the horizontal tail. An alpha limiter system will be used if required.

#### LATERAL AND DIRECTIONAL AXIS

1. The vertical tails are sized to balance (with 30% chord rudders) the yawing moment produced by a critical engine failure at takeoff.

The critical speeds used are:

$$V_{\text{balance speed}} = V_1 + 5.15 \text{ mps (10 kn)}$$

$$\text{where } V_{\text{mcg}} \leq V_1$$

$$\text{and } V_1 = V_R$$

2. No directional stability requirement is used for vertical tail size. The lateral-directional modes will be stabilized when required by the stability augmentation system.
3. Lateral controls follow the design of the 759-163A parametric baseline configuration using the wing outboard trailing edge surfaces as ailerons supplemented by spoilers ahead of the inboard trailing edge flap panels.

### GEOMETRIC RELATIONSHIPS

It is found that a simple set of geometric relationships for the horizontal tail will reduce the amount of analysis required for establishing the horizontal tail size and aft c.g. limit. The intent of using these relationships is to maintain the horizontal tail in a constant downwash field, thus making the tail contribution to longitudinal stability dependent only on  $\bar{V}_H =$

$$\frac{S_H}{S_W} \frac{C_H}{\bar{c}_W}$$

$$\frac{H}{C_W} = \text{constant}$$

$$\frac{Z_H}{b_W} = \text{constant}$$

$$\frac{b_H}{b_W} = \text{constant}$$

### LONGITUDINAL STABILITY

The design longitudinal stability criteria of the DLF concept are based on Boeing SST experience. The airplanes are geometrically configured for a static longitudinal stability level corresponding to a time-to-double-amplitude of 2 seconds. To simplify the parametric analysis, the DLF configurations were configured with horizontal tails maintained in a constant downwash field. This permitted the tail sizing to be achieved for the unaugmented longitudinal response time of  $t_2 \geq 2$  without having to perform dynamic analyses for each configuration.

The geometric relationships of figure 97 were maintained constant using the values developed for the 759-163A configuration.

A hard stability augmentation system will provide an augmented time-to-double-amplitude equal to or greater than 6 seconds. A handling qualities SAS will satisfy the following Reference Class III, Level 1, longitudinal handling qualities criteria:

$$\text{Category B } 0.30 \leq 3_{SP} \leq 2.00$$

$$\text{Category C } 0.35 \leq 3_{SP} \leq 1.30$$

$$3_p \geq 0.04$$

Short period frequency shall also meet reference 5 requirements. The above unaugmented time-to-double-amplitude of 2 seconds represents the projected capability of flight controls technology in the 1980-1990 operational time period. Military handling qualities criteria are used here rather than civil criteria because of the more detailed guidelines of the former.

### LATERAL-DIRECTIONAL STABILITY

Reference level 3 Dutch roll and spiral stability criteria shall be met by a hard SAS. The following Class III, Level 1 criteria will be satisfied, as required, by a handling-qualities SAS.

$$t_{2S} \geq 20 \text{ sec}$$

$$3_D \geq 0.08, w_{nD} \geq 0.4 \text{ rad/sec}^*$$

The Reference Class III, Level 1, minimum-roll-mode time constant of 1.4 may be reduced to the extent compatible with the operational DLF flight regime.

### STRUCTURES AND WEIGHTS

Airplane performance analysis methodology discussed in the PERFORMANCE METHODS section of this PARAMETRIC DATA BASE describes the use of the Thumbprint program for airplane sizing. The conceptual flow chart for the program shows a requirement for structures and weights as input for preliminary airplane definition and as scaling rules for airplane sizing. This section describes the structures, weight, and balance methodology used in the airplane parametric analysis and some of the results when applied to the development of a "mission sized" configuration.

### ANALYSIS TECHNIQUES

Weight estimating techniques used are shown in table 18 and would be applied to the initially drawn configuration and its variations in the parameters. The percent of operational empty weight that each technique represents is a variable dependent on design selection; however, the percentages shown are very representative of the span-loaded design. These techniques are in the order of increasing confidence, from the bottom to the top, and show that nearly 50% of this calculated weight is the result of actual weight or structural sizing.

\*May be reduced subject to customer approval and provided that other lateral-directional response requirements are met

Examples of actual weights in addition to engine weight would include the production 737-200 body sections 41 and 43 selected for the airplane and modified by the incorporation of a constant section 43 body plug and aft pressure bulkhead. Wing structural sizing was accomplished both through the use of an integrated aeroelastic beam analysis computer program for bending and shear material and by hand stress sizing selected structural members.

Evaluation of many design load conditions in this program on the selection section geometry and with suitable stress allowables resulted in the definition of theoretical material requirements to carry critical loads. Estimated weights have been developed after application of non-optimum factors to account for joints, splices, fasteners, etc.

The interspar ribs were sized assuming end-supported beams and uniform loading across the beam in direct relationship to cargo container cross sectional area. With this assumed loading, payload densities of 80, 160, and 240 kg/m<sup>3</sup> (5, 10, and 15 lb/ft<sup>3</sup>) were used with the appropriate load factor to size rib chords (flange material) as a function of shear flow. In a similar manner, the horizontal stabilizer and vertical tail booms were hand-sized using the ultimate tail load from the computer analysis and assuming a uniform load distribution on the horizontal stabilizer and an end-loaded, cantilevered beam for the tail booms.

Weight calculations based on related studies are typically data derived from stress-sized design layout work on similar designs of a different geometry or size. Statistical weight technique results are based on a selected population of airplanes and the usefulness of the equations depends on the quality of the base data and the significance of the selected independent variables.

## PARAMETRIC WEIGHT RESULTS

Application of these methods to the parametric study configurations resulted in the group weight statements shown in table 19. Each of these nine configurations had to be scaled to different gross weights and thrust levels to clearly reveal the impact of payload density. Model 759-163A, which was scaled in this manner, is typical of all the configurations and its weight scalars were developed by the following procedure:

1. A matrix of potential configurations was generated about the base (759-163A) with wing area, aspect ratio, thickness ratio, design range, and containerized volume being held constant. Maximum taxi weights were varied, giving a range of wing and thrust loadings. Similarly, the number of engines (total airplane thrust) was varied, resulting in a wide range of thrust loading for each of the new wing loadings. This matrix for Model 759-163A is shown in table 20.
2. The mission fuel and reserve (design fuel) was estimated for each airplane in the matrix. This was used to calculate the weight of fuel tankage required, a major OEW variable. The design fuel weights ranged from 138 000 kg (305 kips) to 821 000 kg (1810 kips) for this set.
3. The weight of design fuel was subtracted from maximum taxi weight to obtain maximum taxi weight to obtain maximum zero fuel weight (MZFW) for each configuration.

4. Based on the design gross weights and fuel weights calculated above, a first estimate of OEW was made.
5. MZFW-OEW = maximum payload (gross)
6. 
$$\frac{\text{gross maximum payload} - \text{tare weight}}{\text{gross volume} - \text{tare volume}} = \text{net containerized density (NCD)}$$
7. The completed matrix was tabulated (table 20). Unacceptable alternates were rejected on the basis of the NCD being less than  $80 \text{ kg/m}^3$  ( $5 \text{ lb/ft}^3$ ) or of airplane thrust-to-weight ratio being less than 0.15.
8. OEW's for the remaining alternate configurations were calculated using the analysis techniques of section 1 of this discussion. This final array, with corrected OEW's, was used to plot weight-scaling curves. OEW was separated into propulsion items versus total airplane thrust (fig. 98) and OEW-less-propulsion items versus maximum taxi weight (fig. 99) for this purpose.

These two curves allow: (a) performance-sizing to the best combination of wing-loading/thrust-loading and (b) sensitivity studies to a wide range of parameters, including payload density. The propulsion items in figure 98 are defined as total propulsion group plus nacelle and strut.

## BALANCE AND LOADABILITY

Airplane balance and loadability are now checked on the baseline configuration. The convergent grid is used, since a moment vector is true at any gross weight. The center of gravity is calculated and expressed as a percent of MAC or reference chord for the configuration in the OEW, MZFW, and MTW conditions. The required loading range is established by considering the degree of the uncertainty in various parameters. These parameters and the selected uncertainties are:

1. OEW tolerance (1% to 2% MAC):
  - Due to customer options, manufacturing options, crew variation and movement, etc.
  - Increase for unorthodox designs or short MAC
  - DLF use:  $\pm 1.5\%$
2. Cargo centroid variation:
  - Use 10% cargo container width/length
  - DLF use: 10% of 2.44 m (96 in.)

3. Cargo weight variation:
  - Due to difference in containerized cargo density
  - Use 5% weight increase in forward/aft bay for maximum variation (corresponding decrease in opposite bay)
  - DLF use: 5% tank width or 0.152 m (6 in.)
4. Fuel distribution error (10%):
  - Due to tank over/underfill if tanks are located at different BS
  - Assumes excess tank volume exists
  - DLF use: 10% weight increase in forward/aft tanks
  - Required void due to expansion (3%)
5. Fuel weight variation:
  - Due to different density of JP-5 and other jet fuels
  - Density variations due to temperature
  - DLF use: 2% weight
6. Cargo loading error:
  - Assume an offload of one standard container or loading one empty container
  - DLF use: one standard size container of 5443 kg (12 000 lb)
7. Moment changes:
  - Moment from gear down to gear up
  - Moment from flaps down to flaps up
  - DLF use: zero
8. Loading restrictions:
  - Loading procedures and/or landing gear arrangements must preclude aircraft tipping.
  - Maximum allowable static nose gear load must not be exceeded.
  - DLF use: (not applicable)

9. Ice accretion:

- Maximum DLF = 5.08-cm (2-in.) over 55.88-cm (22-in.) width center section  
= 7.62 cm (8 in.) over 55.88-cm (22-in.) outer swept tips

These tolerances are accumulative and, when plotted, provide the required forward and aft limits. These limits, as well as the static neutral point, are established by stability and control requirements.

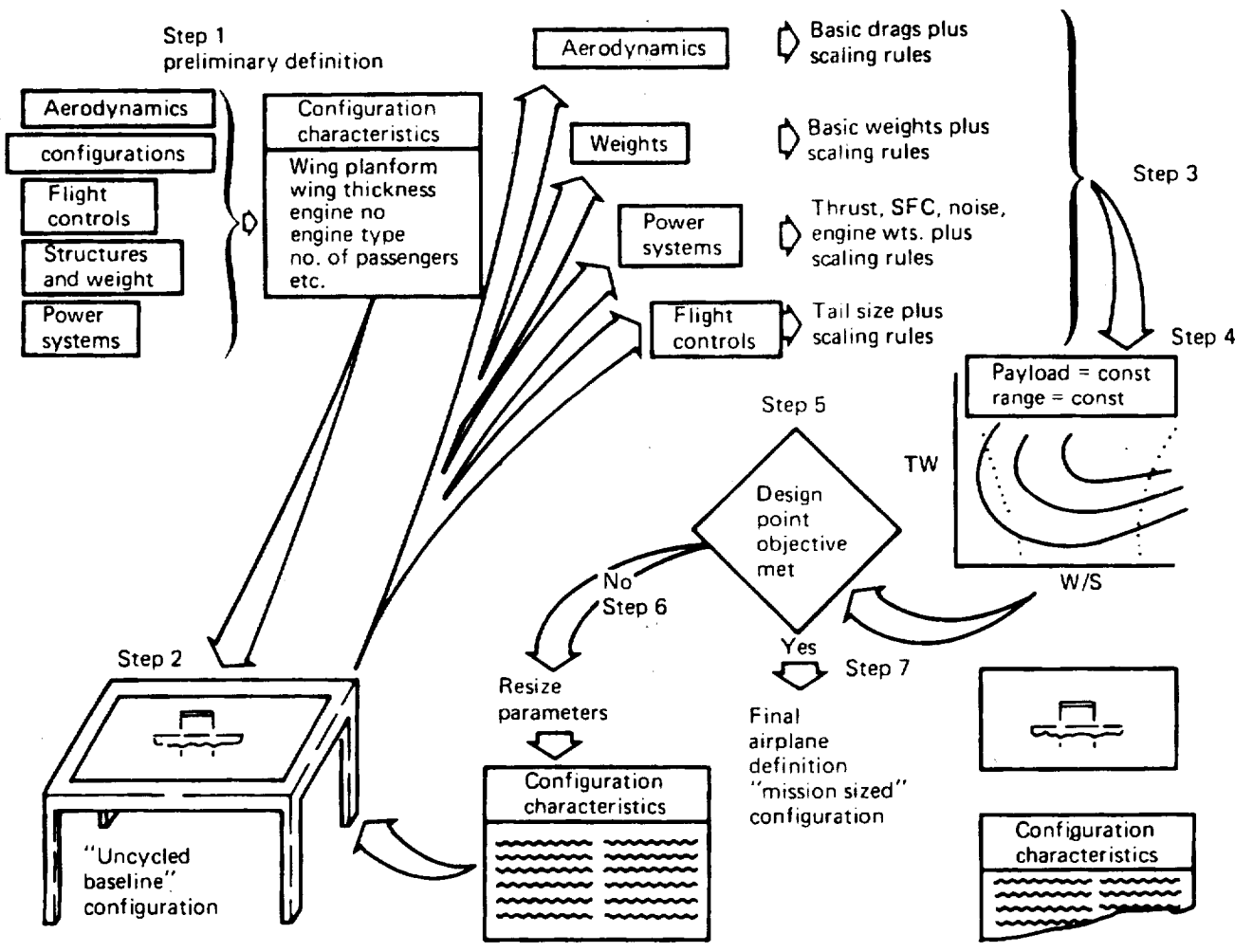


Figure 86.—Aerodynamic Thumbprint Program Flow Chart

ORIGINAL PAGE IS  
OF POOR QUALITY



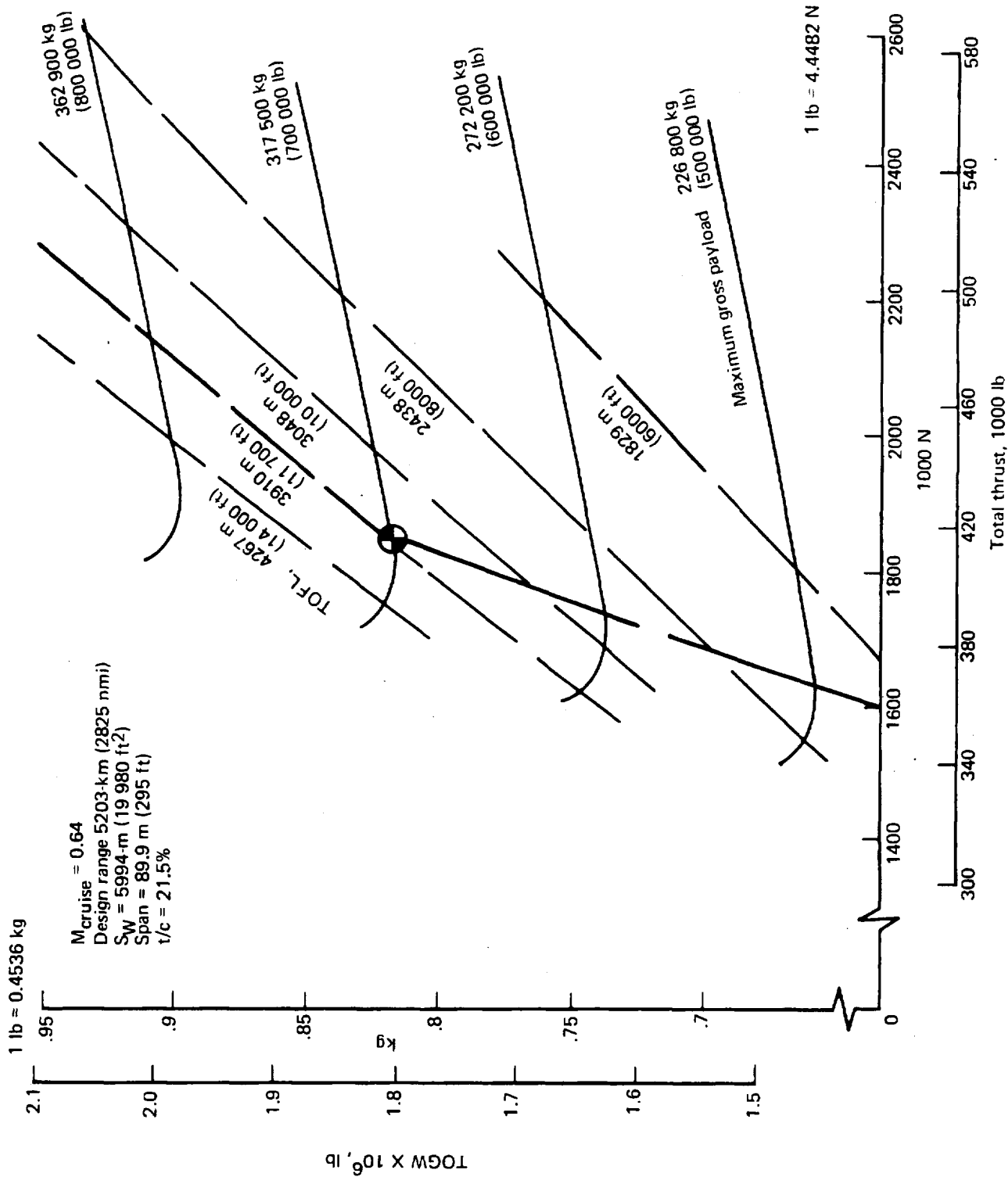


Figure 87.—Airplane Matching Technique 759-163A Baseline

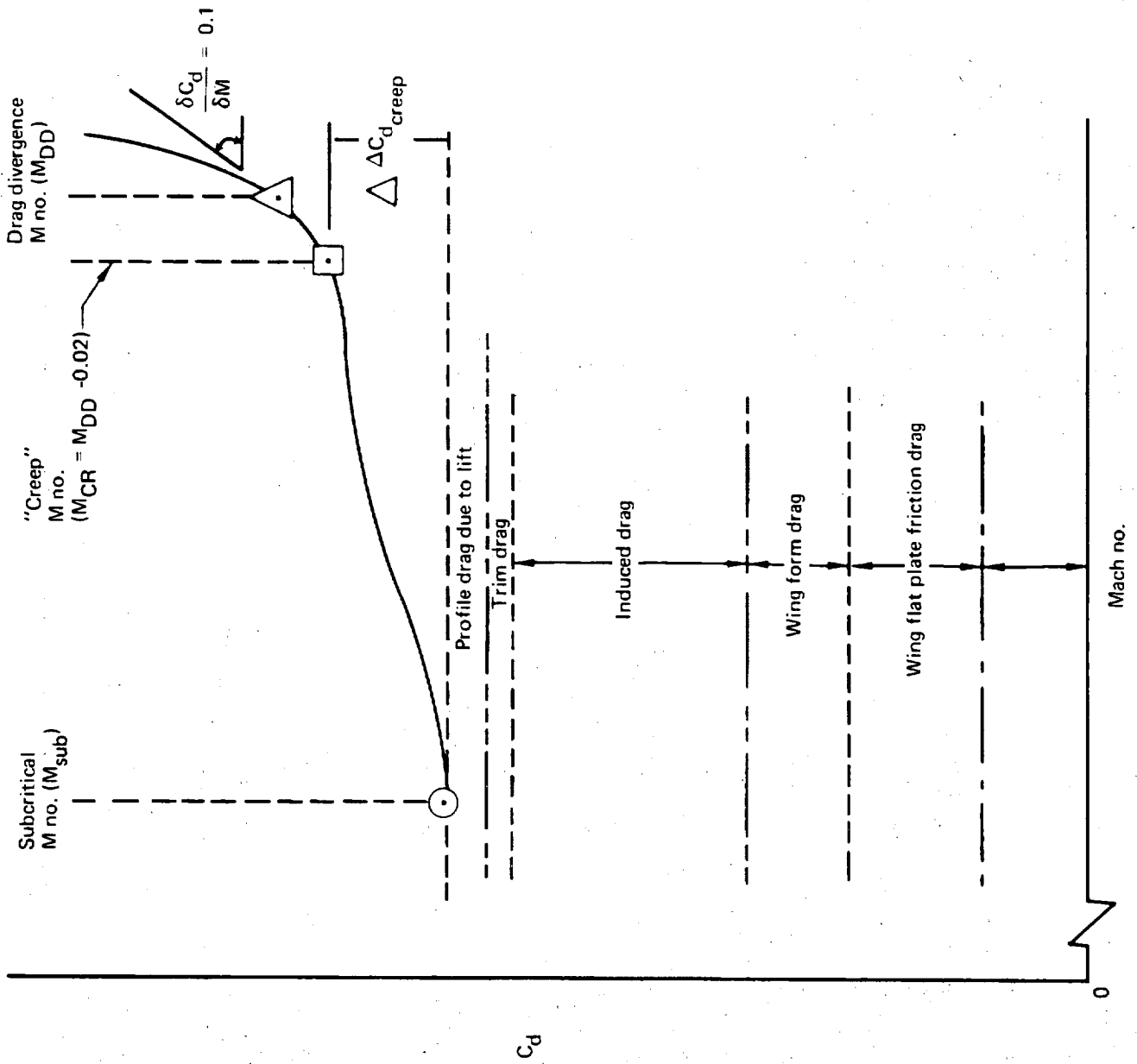


Figure 88.—Cruise Drag Characteristics

$$\text{* Form drag factor} = \frac{C_{d \text{ min}} - C_{d \text{ flat plate}}}{C_{d \text{ flat plate}}}$$

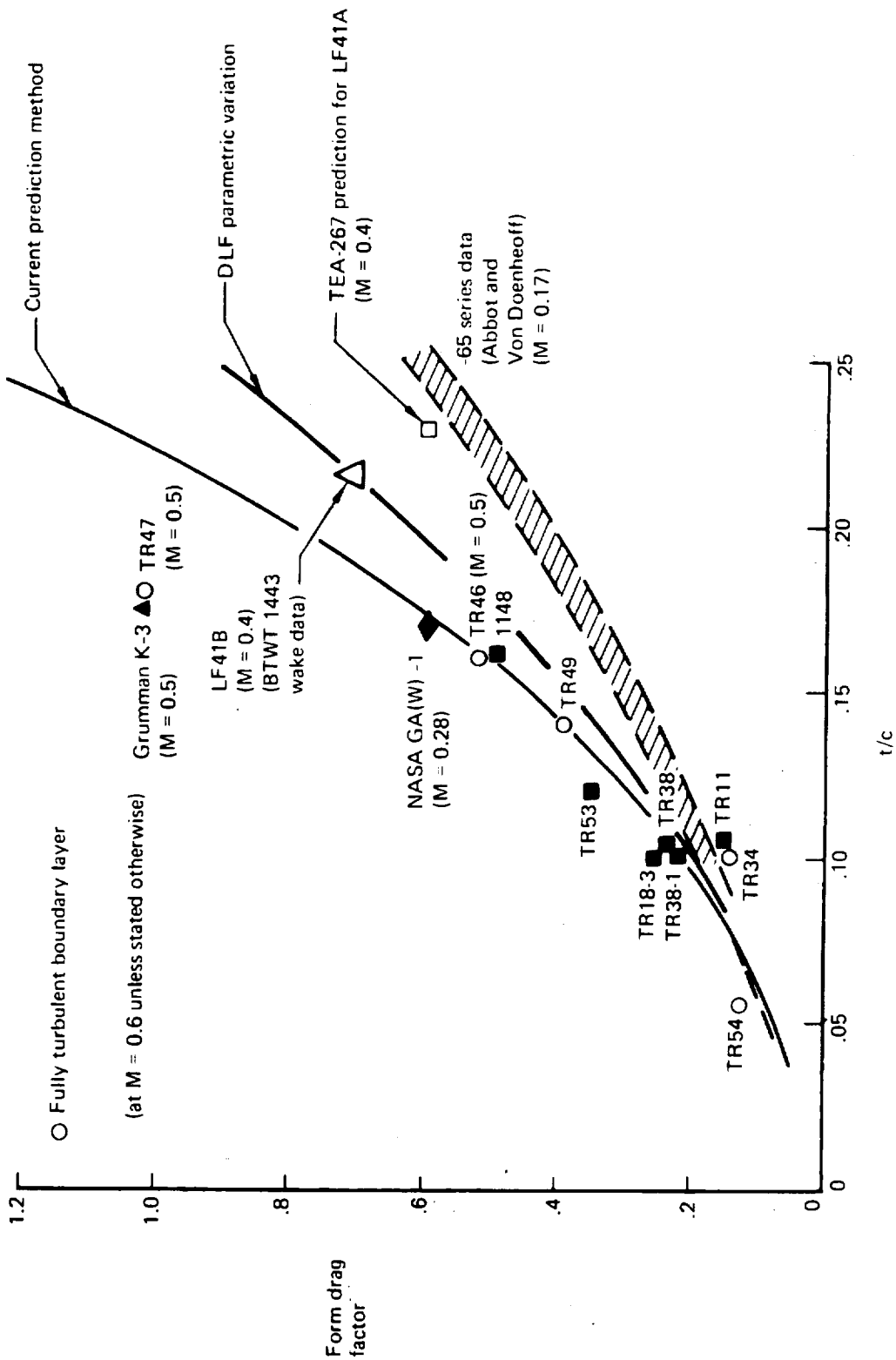


Figure 89.—Form Drag Characteristics

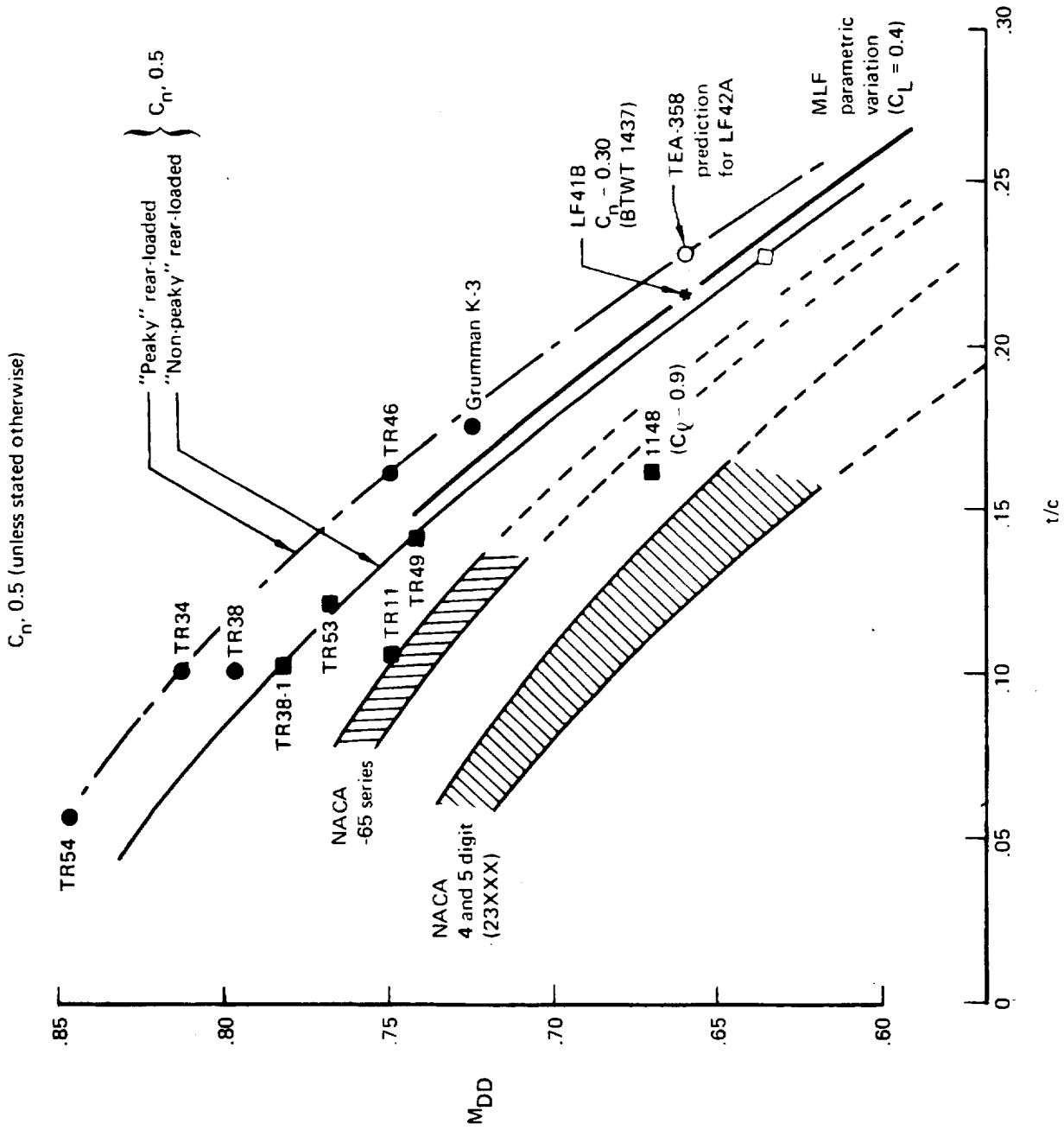


Figure 90.—Drag Divergence Mach Number Versus Thickness Ratio

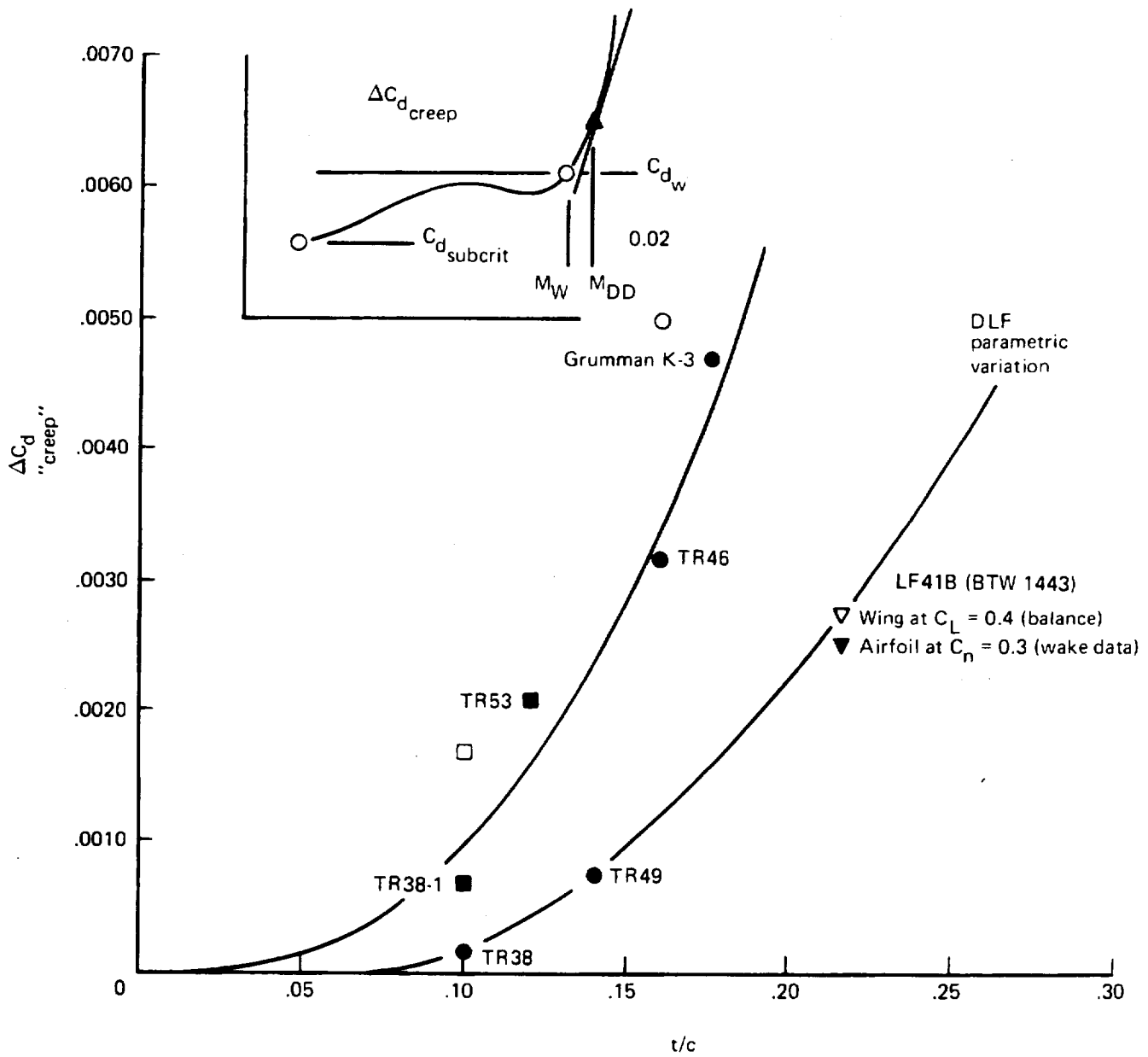


Figure 91.—Drag Creep Characteristics

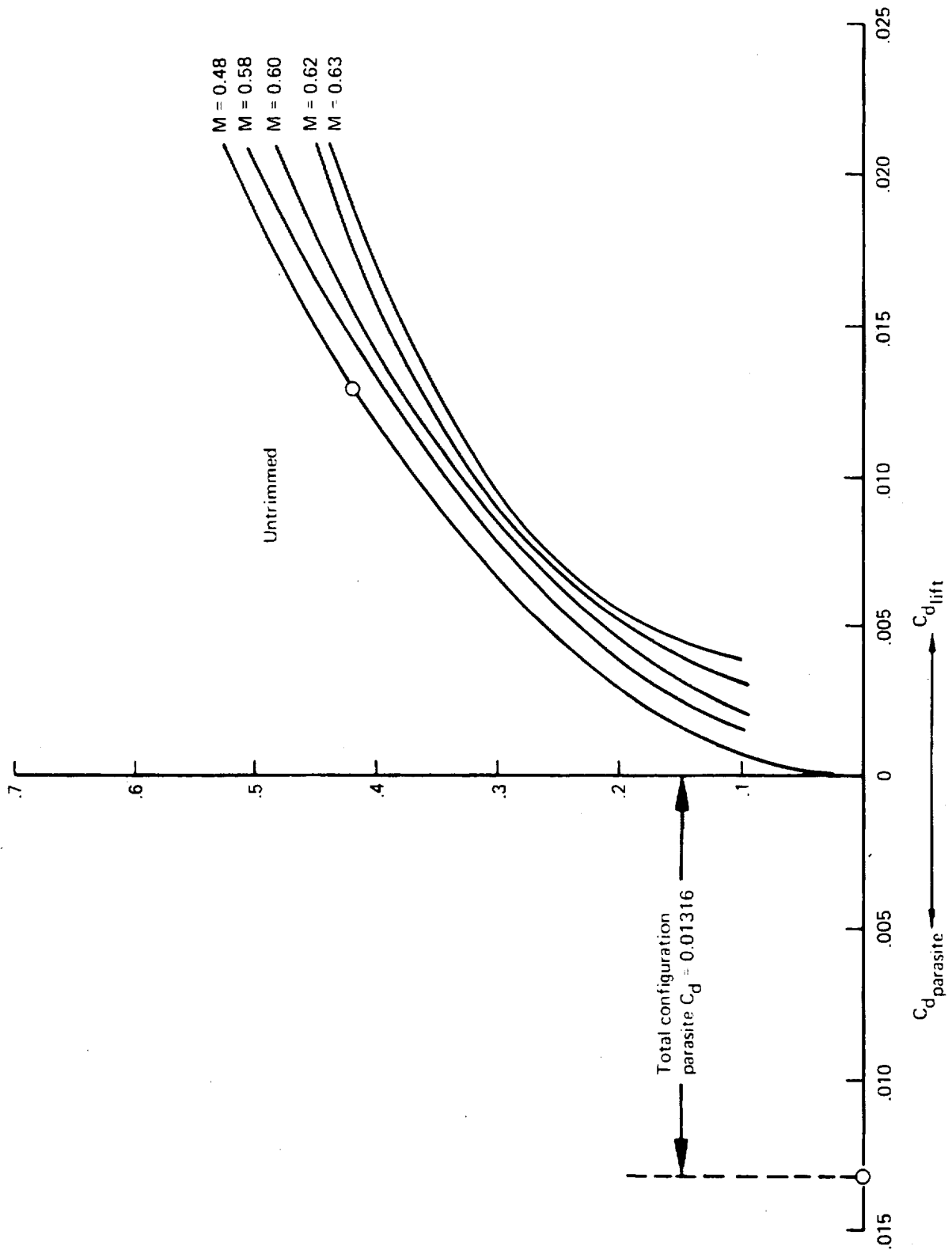


Figure 92.—Untrimmed Cruise Polars, Model 759-165A

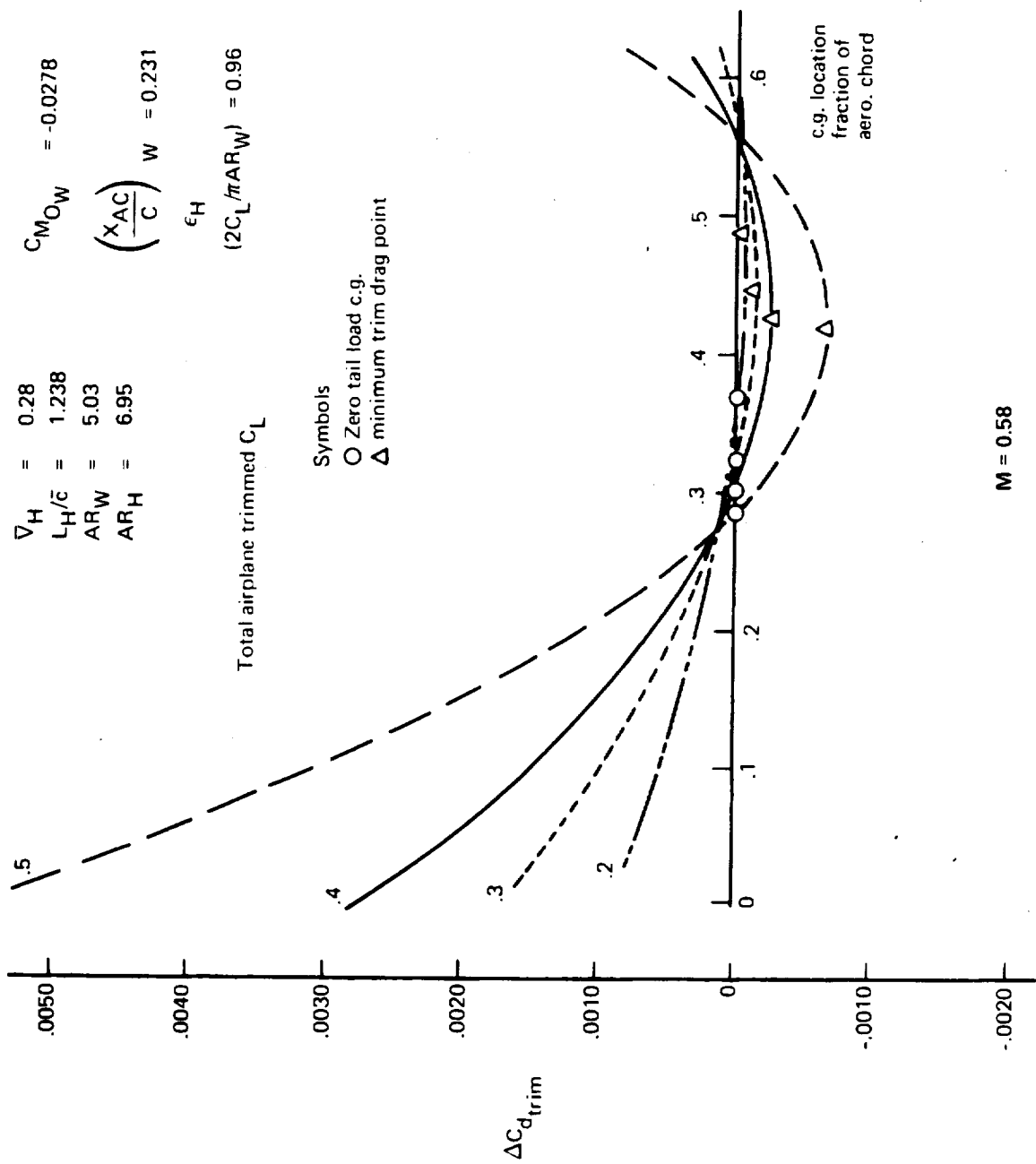


Figure 93.—Cruise Trim Drag Versus C.G. Location and  $C_L$  Model 759-165A

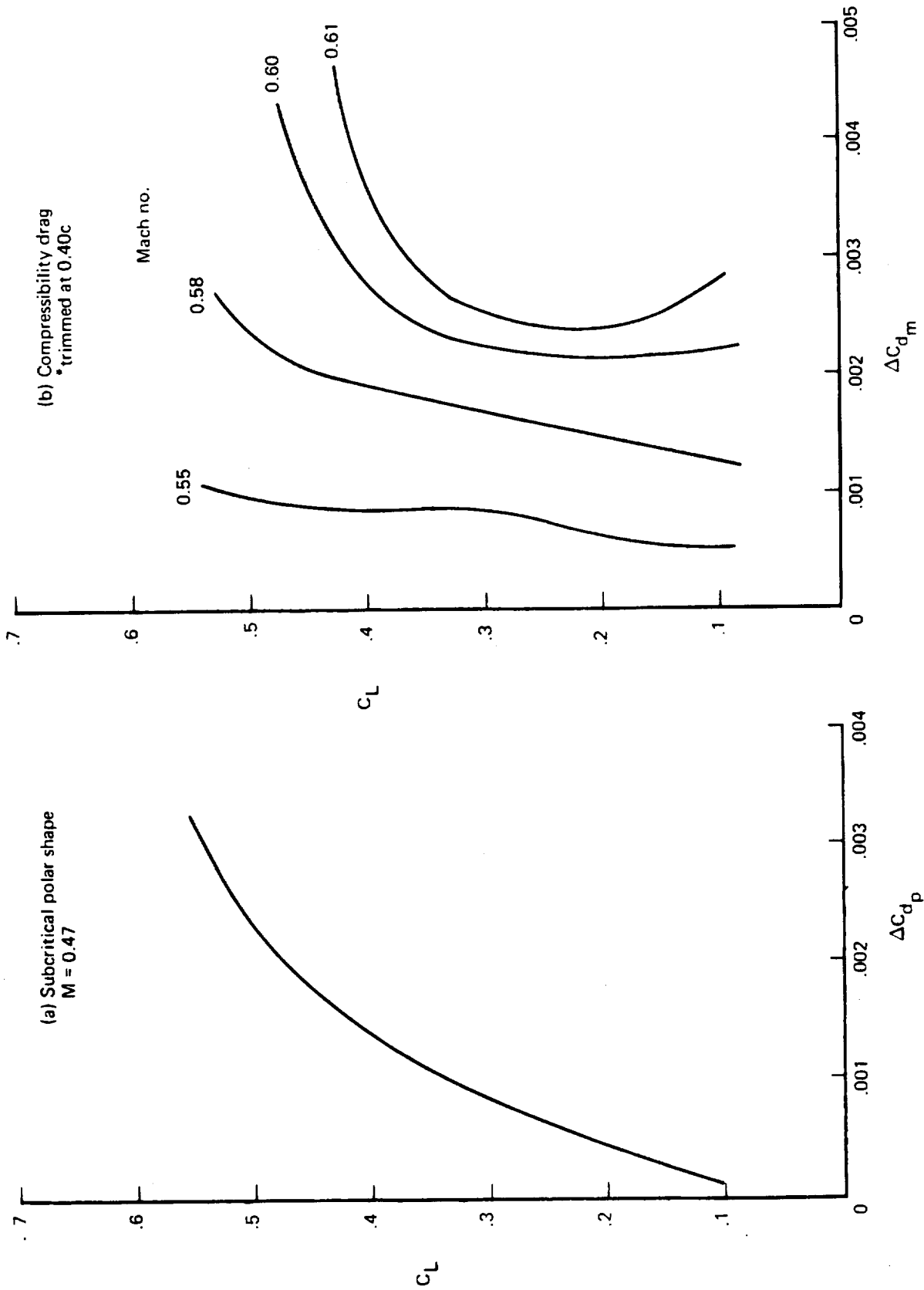


Figure 94.—Cruise Polar Shape and Compressibility Drag, Model 759-165A



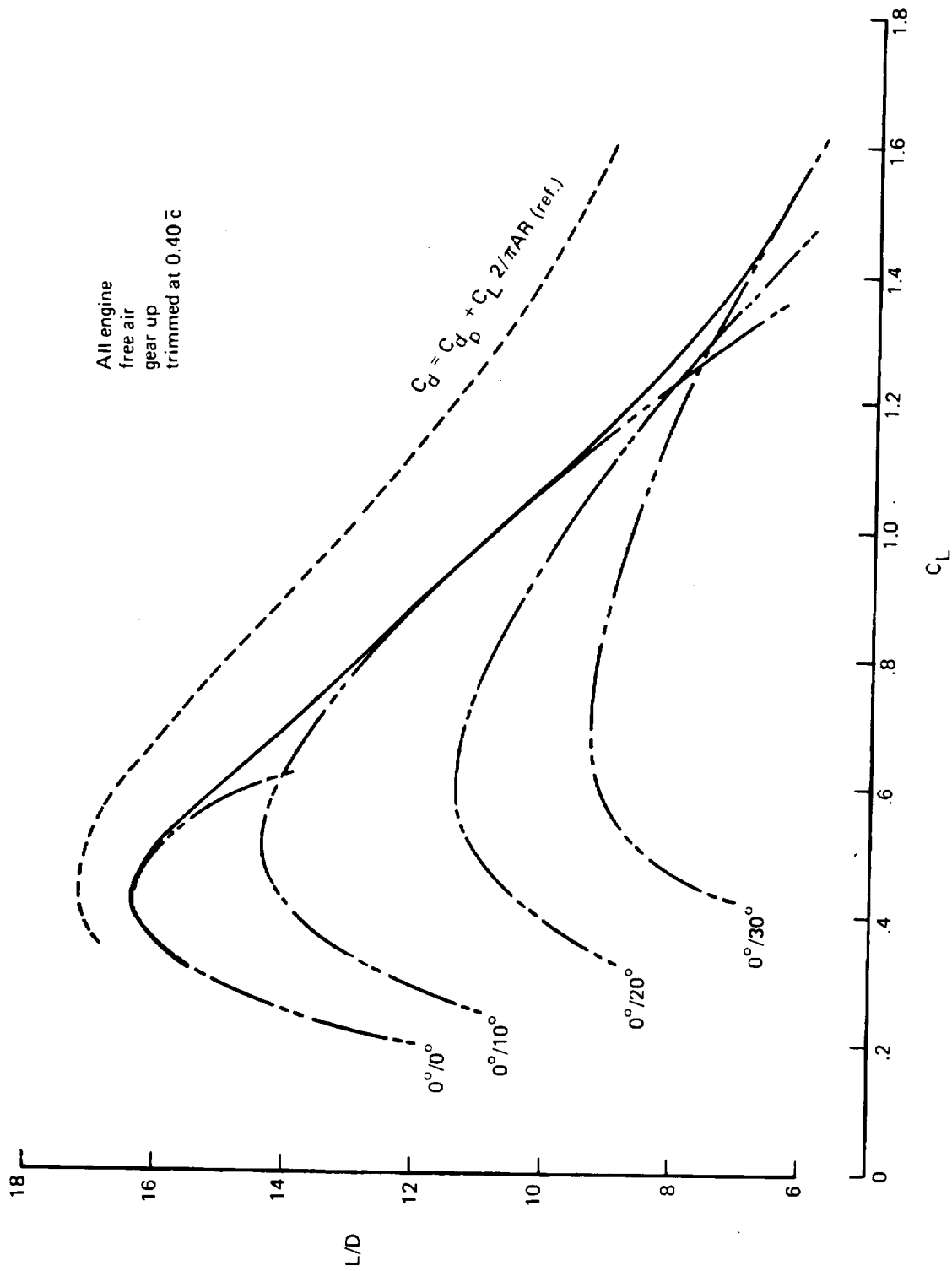


Figure 95.—Climbout L/D Versus  $C_L$ , Model 759-165A

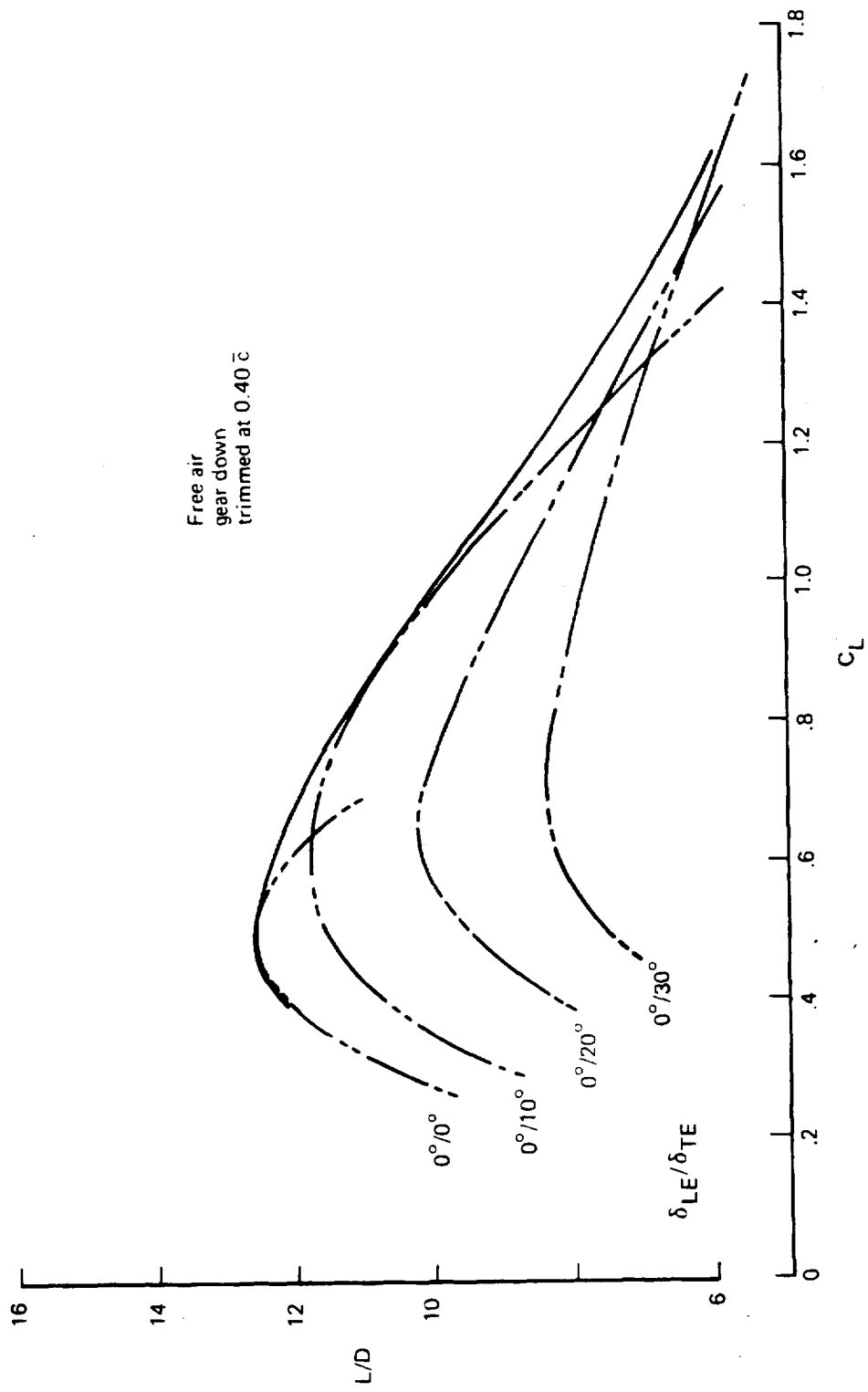


Figure 96.—Approach  $L/D$  Versus  $C_L$ , Model 759-165A

$$\frac{\xi_H}{C_W} = 1.2377$$

$$\frac{Z_H}{b_w} = 0.0861$$

$$\frac{b_H}{b_w} = 0.5593$$

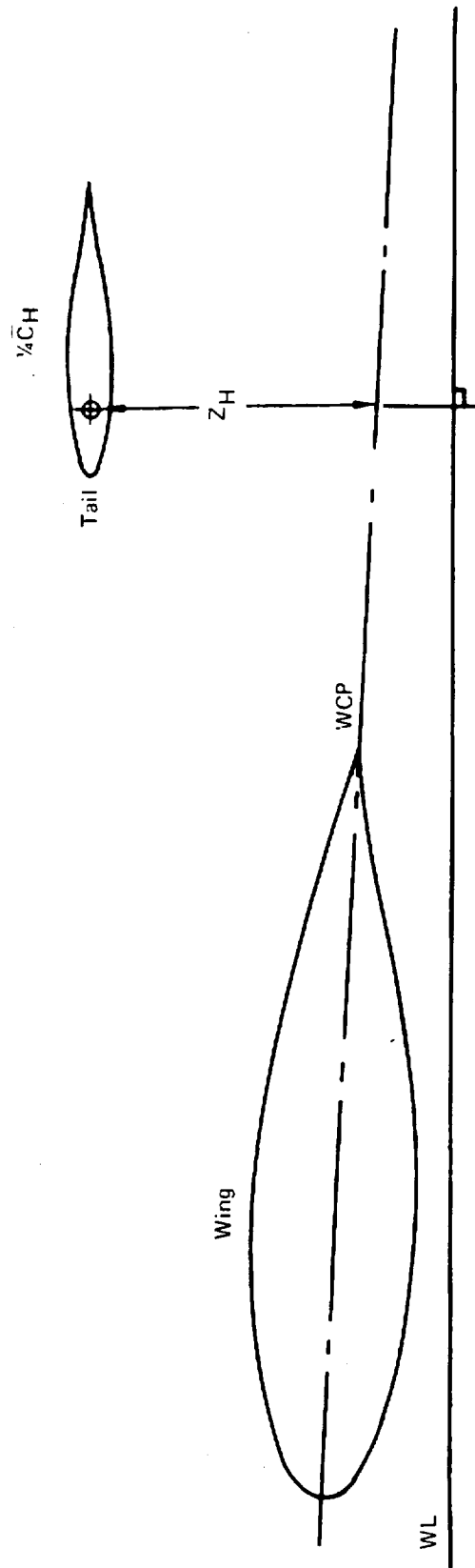
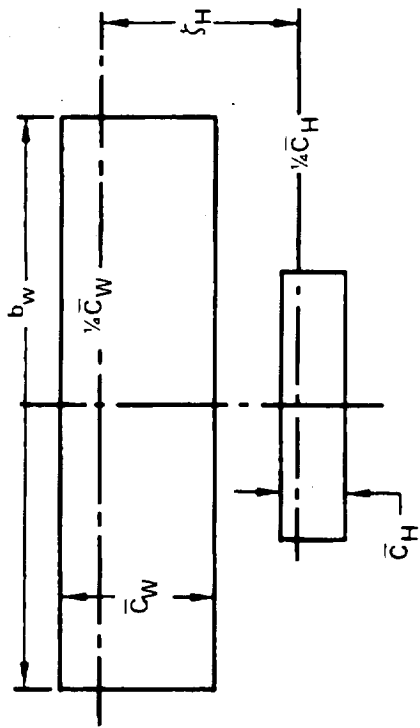


Figure 97.—Geometric Relationships

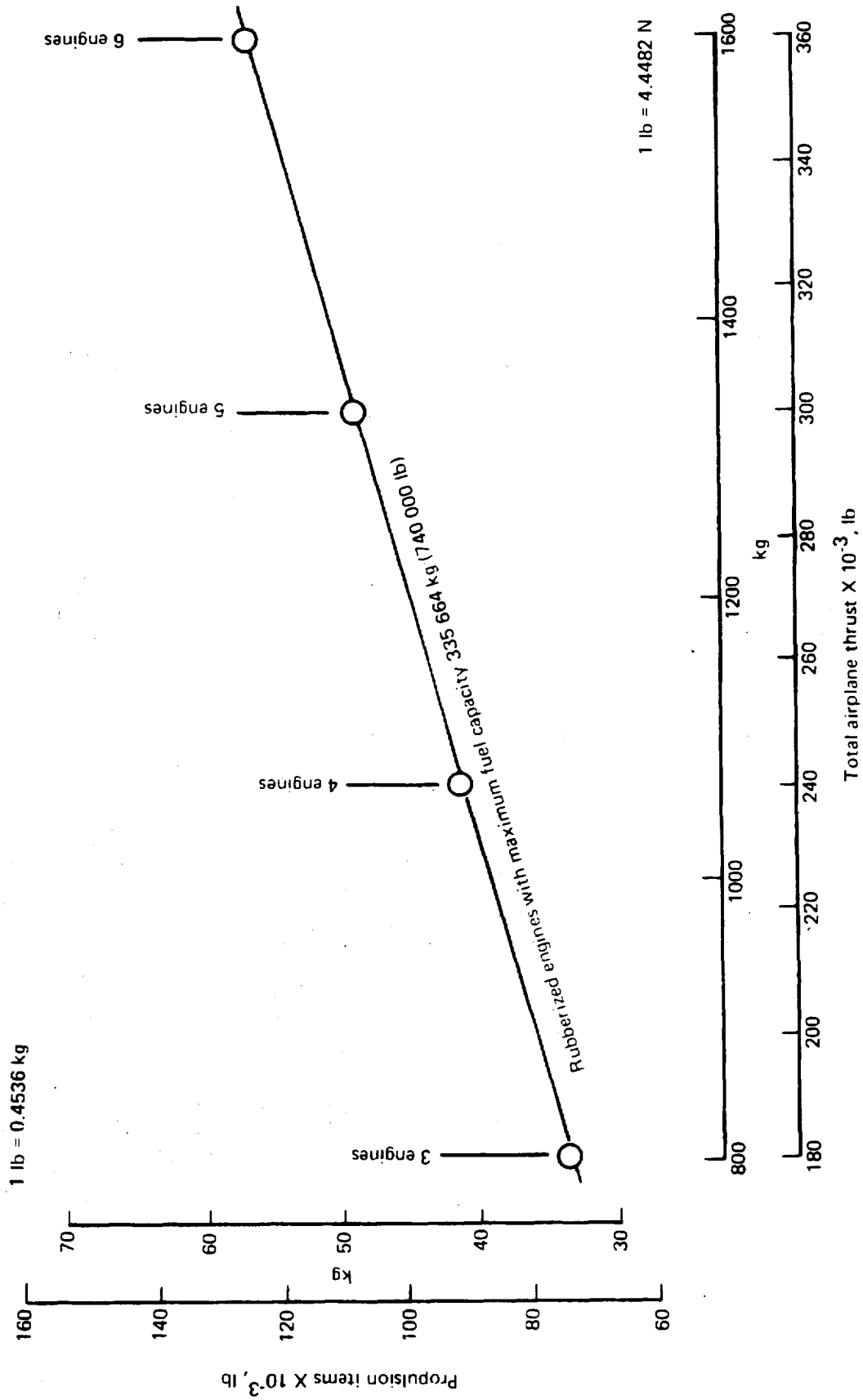


Figure 98.—Weight Scalars, Model 759-163A Propulsion Items

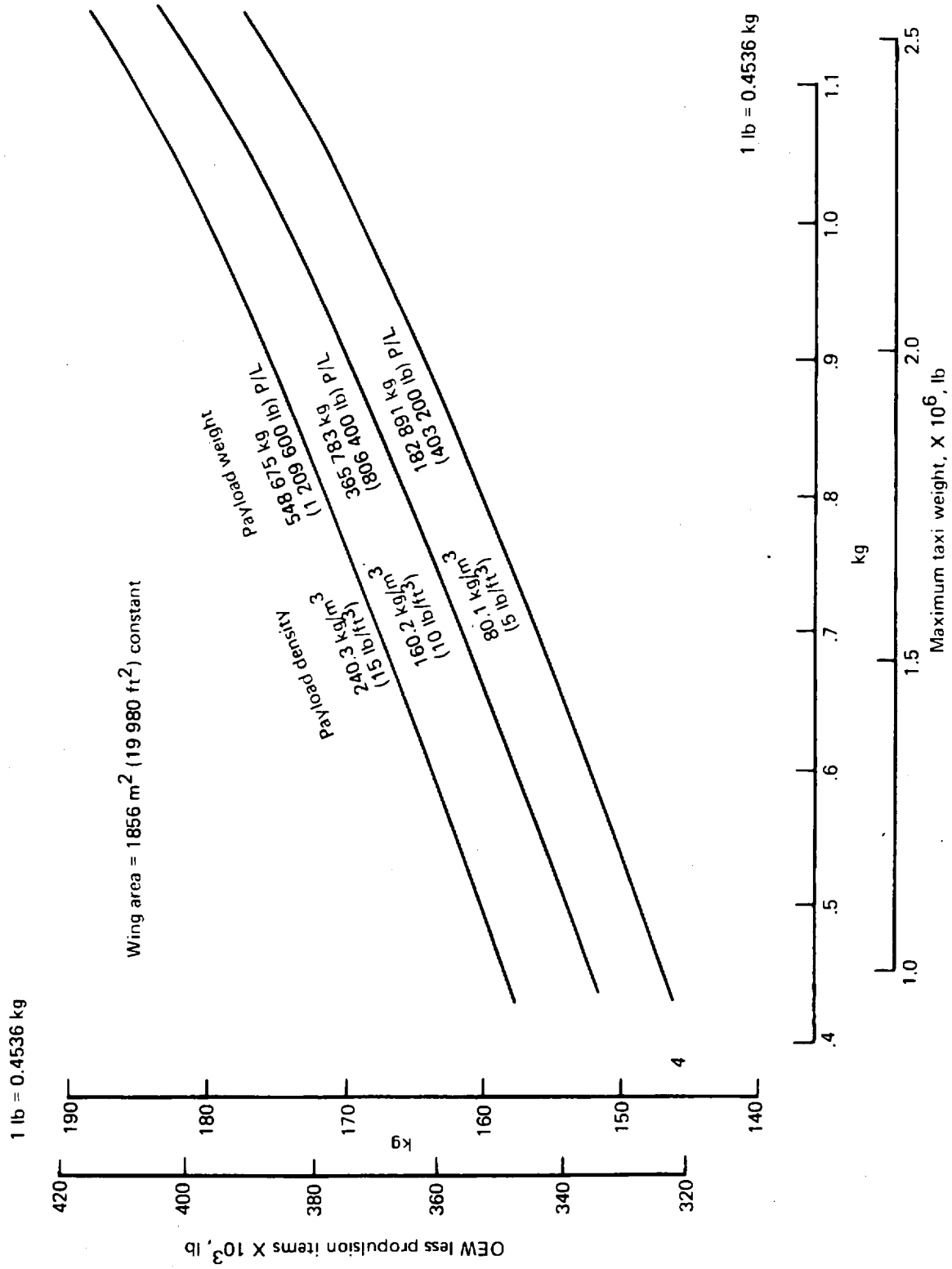


Figure 99.—Weight Scalars, Model 759-163A

Table 17.—Parasite Drag Summary—Model 759-165A

$S_{ref} = 1603 \text{ m}^2 (17\ 260 \text{ ft}^2)$ ;  $Re/ft = 1.41 \times 10^6 (M = 0.49/9144 \text{ m } (0.49/30\ 000 \text{ ft}))$  BTWT 1437—Based Form Factor

Item	Flat plate friction drag						Form drag		Pressure and interference drag		Rough and excres.	Total
	$A_{wet}$ $\text{m}^2 (\text{ft}^2)$	$L_{ref}$ $\text{m} (\text{ft})$	$Re \cdot 6$ $\times 10$	$C_{f, avg}$	PL $\text{m}^2 (\text{ft}^2)$	Form Form $\text{m}^2 (\text{ft}^2)$	Form Form $\text{m}^2 (\text{ft}^2)$	Pressure and interference drag				
								A	C	Press & int	Total $\text{m}^2 (\text{ft}^2)$	
Wing	3 382 (36 400)	18.8 (61.6)	(86.8)	(0.00210)	7.107 (76.50)	6.039 (65.00)				0.678 (7.30)	13.824 (148.80)	
Wing tips	106.8 (1 150)	18.8 (61.6)	(86.8)	(0.00210)	0.225 (2.42)					0.021 (0.23)	0.246 (2.65)	
Body Top and bottom sides	90.1 (970)	9.1 (30.0)	(43.8)	(0.00229)	0.206 (2.22)	0.509 (0.64)				0.016 (0.17)	0.281 (3.03)	
Vertical tail	454.3 (4 890)	7.4 (24.4)	(34.4)	(0.00239)	1.087 (11.70)	0.543 (5.85)				0.091 (0.98)	1.721 (18.53)	
Horiz. Center section	748.8 (8 060)	7.4 (24.4)	(34.4)	(0.00239)	1.789 (19.26)	0.895 (9.63)				0.150 (1.62)	2.834 (30.51)	
Outboard section												
Tail booms	269.4 (2 900)	12.2 (40.0)	(56.4)	(0.00222)	0.598 (6.44)	0.021 (0.226)				0.054 (0.58)	0.674 (7.25)	
Nacelles (5)	320.5 (3 450)	8.1 (27.7)		(0.00231)	0.739 (7.95)	0.259 (2.79)				0.058 (0.62)	1.055 (11.36)	
Nacelle struts Wing (5)												
Other	69.7 (750)	4.1 (13.3)		(0.00257)	0.181 (1.95)					0.013 (0.14)	0.194 (2.09)	
Cab									0.279 (3.00)		0.279 (3.00)	
Fairings Main gear												
Nose gear												
Flap tracks												
Misc.												
Total	5 441 (58 570)			(0.00219)	11.932 (128.44)	7.817 (84.14)				0.279 (3.00)	1.081 (11.64)	21.109 (227.22)

b/  $A_{wet} = 1.22$

$C_{Dp, min} = 0.1316$

*Table 18.—Weight Estimating Techniques*

<u>Technique</u>	<u>Component</u>	<u>% OEW</u>
Actual	Bare engines, body, landing gear units, APU, flight provisions	26
High AR beam analysis	Bending material, shear material	11
Hand sized structure	Interspar ribs, intercostals, horizontal tail, vertical tail, vertical booms	11
Related studies	Burst protection, engine cowling, shear material, dirt pan, trailing edge flaps, wing misc. and manufacturing variation, landing gear units, cargo handling, insulation, engine equipment, electrical emergency equipment, anti-icing	26
Statistical	Engine struts, interspar ribs, intercostals, fixed leading edge, fixed trailing edge, spoilers, access doors, tip installation, tip fence, horizontal tail, vertical tail, vertical booms, fuel systems, surface controls, hydraulic, pneumatic, electronics, air conditioning, paint, standard and operational items, airplane miscellaneous	26
	Operating empty weight	100









Table 20.—Model 759-163A, Potential Configurations

Number engines Total thrust	Constant: Wing area = 1856 m <sup>2</sup> (19 980 ft <sup>2</sup> ) Range = 5232 km (2825 nmil) Containerized volume = 112 (8 x 9 x 10 ft) = 2284 m <sup>3</sup> (80 640 ft <sup>3</sup> ) Aspect ratio = 4.356, t/c = 21.5%	Variable: MTW Thrust Payload density											
		Wing loading (W/S) - kg/m <sup>2</sup> (lb/ft <sup>2</sup> )	MTW - 1000 kg	kips	(50)	(1000)	567	(1250)	(1500)	(1778)	(89)	488.3	(100)
6 (360 000 lb) 1 601 352 N	Wing loading (W/S) - kg/m <sup>2</sup> (lb/ft <sup>2</sup> )	244.2	(50)	305.2	(62.5)	366.2	(75)	434.6	(89)	488.3	(100)	610.4	(125)
	MTW - 1000 kg	453.6	(1000)	567	(1250)	680.4	(1500)	806.5	(1778)	907.2	(2000)	1134	(2500)
	OEW - 1000 kg	201.9	(445)	209.6	(462)	216.8	(478)	225.0	(496)	231.3	(510)	246.3	(543)
	Maximum payload - 1000 kg	113.4	(250)	190.5	(420)	267.2	(589)	354.7	(782)	424.1	(935)	574.7	(1267)
	MZFW - 1000 kg	315.3	(695)	400.1	(882)	484.0	(1067)	519.7	(1278)	655.5	(1445)	821.0	(1810)
5 (300 000 lb) 1 334 460 N	Design fuel - 1000 kg	138.3	(305)	166.9	(368)	196.4	(433)	226.8	(500)	251.7	(555)	313.0	(690)
	Thrust/MTW - ND		(0.36)	(0.29)	(0.24)	(0.20)	(0.20)	(0.20)	(0.20)	(0.18)	(0.18)	(0.14)	(0.14)
	*Payload density - kg/m <sup>3</sup> (lb/ft <sup>3</sup> )	29.31	(1.83)	67.12	(4.19)	104.92	(6.55)	147.85	(9.23)	182.13	(11.37)	256.30	(16.00)
	OEW - 1000 kg	192.8	(425)	200.5	(442)	207.7	(458)	215.9	(476)	222.3	(490)	237.2	(523)
	Maximum payload - 1000 kg	122.5	(270)	199.6	(440)	276.2	(609)	363.8	(802)	433.2	(955)	583.8	(1287)
4 (240 000 lb) 1 067 568 N	MZFW - 1000 kg	315.3	(695)	400.1	(882)	484.0	(1067)	579.7	(1278)	655.5	(1445)	821.0	(1810)
	Design fuel - 1000 kg	138.3	(305)	166.9	(368)	196.4	(433)	226.8	(500)	251.7	(555)	313.0	(690)
	Thrust/MTW - ND		(0.300)	(0.240)	(0.20)	(0.20)	(0.20)	(0.20)	(0.160)	(0.160)	(0.150)	(0.120)	(0.120)
	Payload density - kg/m <sup>3</sup> (lb/ft <sup>3</sup> )	33.64	(2.10)	71.60	(4.47)	109.41	(6.83)	152.34	(9.51)	186.67	(11.65)	260.62	(16.27)
	OEW - 1000 kg	183.7	(405)	191.4	(422)	198.7	(438)	206.8	(456)	213.2	(470)	228.2	(503)
3 (180 000 lb) 800 676 N	Maximum payload - 1000 kg	131.5	(290)	208.7	(460)	285.3	(629)	372.9	(822)	442.3	(975)	592.9	(1307)
	MZFW - 1000 kg	315.3	(695)	400.1	(882)	484.0	(1067)	579.7	(1278)	655.5	(1445)	821.0	(1810)
	Design fuel - 1000 kg	138.3	(305)	166.9	(368)	196.4	(433)	226.8	(500)	251.7	(555)	313.0	(690)
	Thrust/MTW - ND		(0.240)	(0.192)	(0.160)	(0.160)	(0.160)	(0.160)	(0.134)	(0.134)	(0.120)	(0.096)	(0.096)
	Payload density - kg/m <sup>3</sup> (lb/ft <sup>3</sup> )	38.12	(2.38)	76.09	(4.75)	113.89	(7.11)	156.98	(9.80)	191.10	(11.93)	265.11	(16.55)
3 (180 000 lb) 800 676 N	OEW - 1000 kg	174.6	(385)	182.3	(402)	189.6	(418)	197.8	(436)	204.1	(450)	219.1	(483)
	Maximum payload - 1000 kg	140.6	(310)	217.7	(480)	294.4	(649)	381.9	(842)	451.3	(995)	601.9	(1327)
	MZFW - 1000 kg	315.3	(695)	400.1	(882)	484.0	(1067)	579.7	(1278)	655.5	(1445)	821.0	(1810)
	Design fuel - 1000 kg	138.3	(305)	166.9	(368)	196.4	(433)	226.8	(500)	251.7	(555)	313.0	(690)
	Thrust/MTW - ND		(0.180)	(0.144)	(0.120)	(0.120)	(0.120)	(0.120)	(0.101)	(0.101)	(0.090)	(0.072)	(0.072)
Payload density - kg/m <sup>3</sup> (lb/ft <sup>3</sup> )	42.61	(2.66)	80.57	(5.03)	118.22	(7.38)	161.31	(10.07)	195.43	(12.20)	269.59	(16.83)	

\*Net containerized density = maximum payload/71 700 = 1.658

## APPENDIX B

### PRICING AND COSTING METHODOLOGY

#### BASIC REQUIREMENTS AND ASSUMPTIONS

The basic requirements and assumptions needed for airplane costing and pricing are listed on table 21. Utilizing the description of the airplane, a part card and commonality assessment are required. Also needed is an assessment of common and peculiar weights by airplane major component parts or sections (e.g., wing, body, empennage) for estimating the major cost elements, such as engineering, tooling, and production material.

Figure 100 shows the relative-structure part card releases for distributed-load configurations as compared to conventional aircraft. There has been an attempt to minimize the structural part card releases because of the impact of this parameter in every area of airplane cost. Figure 101 shows the cost savings attributed to part commonality in the selected configuration. The savings are most pronounced in the nonrecurring costs, although they are significant in the recurring portion as well.

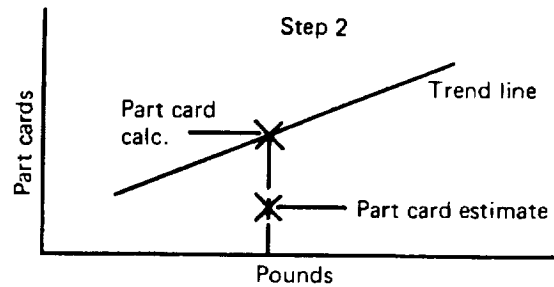
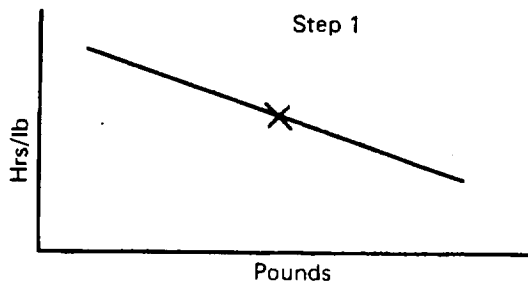
The program length for development and production for all configurations and quantities in the study is 10 years. Each program was determined individually and differs in timing within the 10-year period and in rate of production. A sample program schedule for a four-bay, 295-foot-span airplane is shown in figure 102.

The airplane fleet sizes or quantities were calculated to provide a constant annual fleet productivity (at 5232 km (2825 nmi) for the parametric study airplanes and 5556 km (3000 nmi) for the selected and reference configurations) of 118 billion Tkm (67 billion RTM's) carrying cargo at the design net containerized density and 65% gross payload load factor.

The assumption is made that the required facilities and technology are available. All costs/ prices are computed in 1975 dollars. Prices are calculated to yield a 20% return on investment to the manufacturer with the condition that the break-even quantity should be no more than 50% of the contractor's market quantity.

#### COST ESTIMATING METHODOLOGY

The basic estimating approach utilizes hours per pound of design weight for major components of the airplane. Design weight is the weight that the engineering designs rather than the total weight. Examples are the design of landing gear, engine nacelles, and struts. If all are identical, the weight to be considered is the weight of one end item. Adjustment to the base hours is made based on the part card deviation from historical part card versus weight relationship. This particularly affects components of the airframe that have a high degree of commonality within that component.



Formula for a major component of the airplane:

Engineering hours = hrs/lbs X pounds X part card estimate/part card calculations

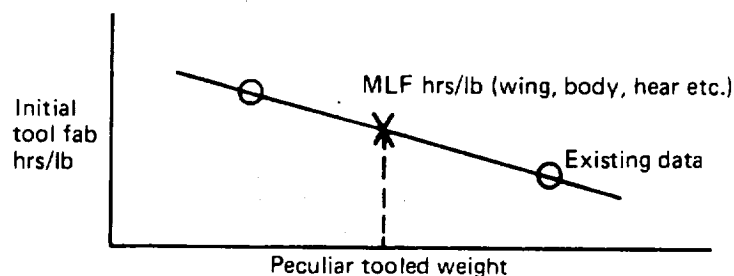
### Developmental Labor

Developmental labor estimate is composed of tests in support of engineering and the fabrication of mockups. Developmental test labor is estimated as a factor of engineering labor and developmental mockup is estimated upon weight as a parameter.

### Tool Labor

The basic estimating approach utilizes an initial hour-per-pound of peculiar tooled weight, extrapolating from existing airplane data. For example, if the nacelles and struts are identical for all locations, the weight of one determines the initial set of tools. Similarly, the wing may have multiple common parts due to nontapered configuration. The initial tooling requirements are based on only the determined peculiar tooled weight. Adjustments, however, are considered for final assembly or major tools that are not necessarily affected by common parts.

Airplane sectional estimates are made from peculiar weight as follows:

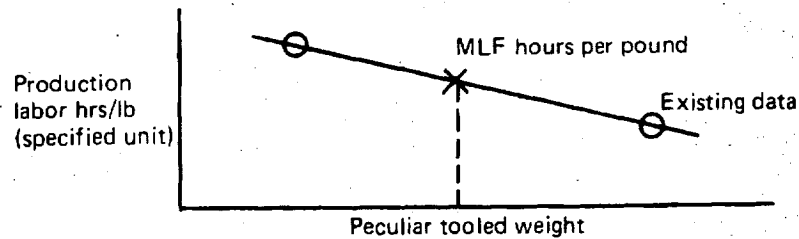


Design and coordination requirements are added as factors of initial fabrication.

Duplication and/or rate tool hours are determined from the production schedule as well as the commonality assessment and are factored from initial tooling. Recurring tooling is estimated as a factor of basic tooling or production labor.

## Production Labor

As in the case of the tool estimating approach, hours per pound of peculiar weight are used.



As an example, identical nacelles are estimated by unit from historical data and extrapolated to total program requirements (e.g., six per airplane X 350 airplanes = 2100 units) on an improvement curve.

Because of multiple common parts in the wing, the peculiar portion (by weight) is estimated as a unit and extrapolated on an improvement curve to total airplane and program requirements. For example, if the wing is determined to be 40% peculiar by weight, each airplane includes 2.5 equivalent units of peculiar construction with cost reductions reflected due to the improvement curve application.

Planning requirements are added as a factor of labor hours. Nonrecurring planning is calculated from part card estimates.

## Quality Control

Quality control is based on a factor of operations labor.

## Material

Tool material and developmental material are estimated from historical data as a dollar rate per tool or developmental hour. Production material is calculated as a cost per pound of structure and nonstructure weights.

## Purchased Equipment

Requirements are assessed from existing airplane cost data.

## Engines

Engines are based on the engine manufacturer's latest available data within The Boeing Company for either existing or study engines.

## **Flight Test**

Flight test is estimated as a rate per flight hour.

## **PARAMETRIC VERSUS POINT DESIGN COSTING**

The selected and reference point design configurations were costed the priced using the methodology discussed above. The techniques used for the parametric study differed, however, from the above methods. The parametric study required less detail, since the prime interest is the relative comparison of similar configurations. The parametric costing was based on data from previous Boeing studies of distributed-load aircraft. Recurring costs were estimated based on differences in airframe weight and engine quantities. The same learning curve was used for all configurations, since base data was insufficient to determine the effect of size and engine quantity per airplane on the learning curve for various quantities of airplanes.

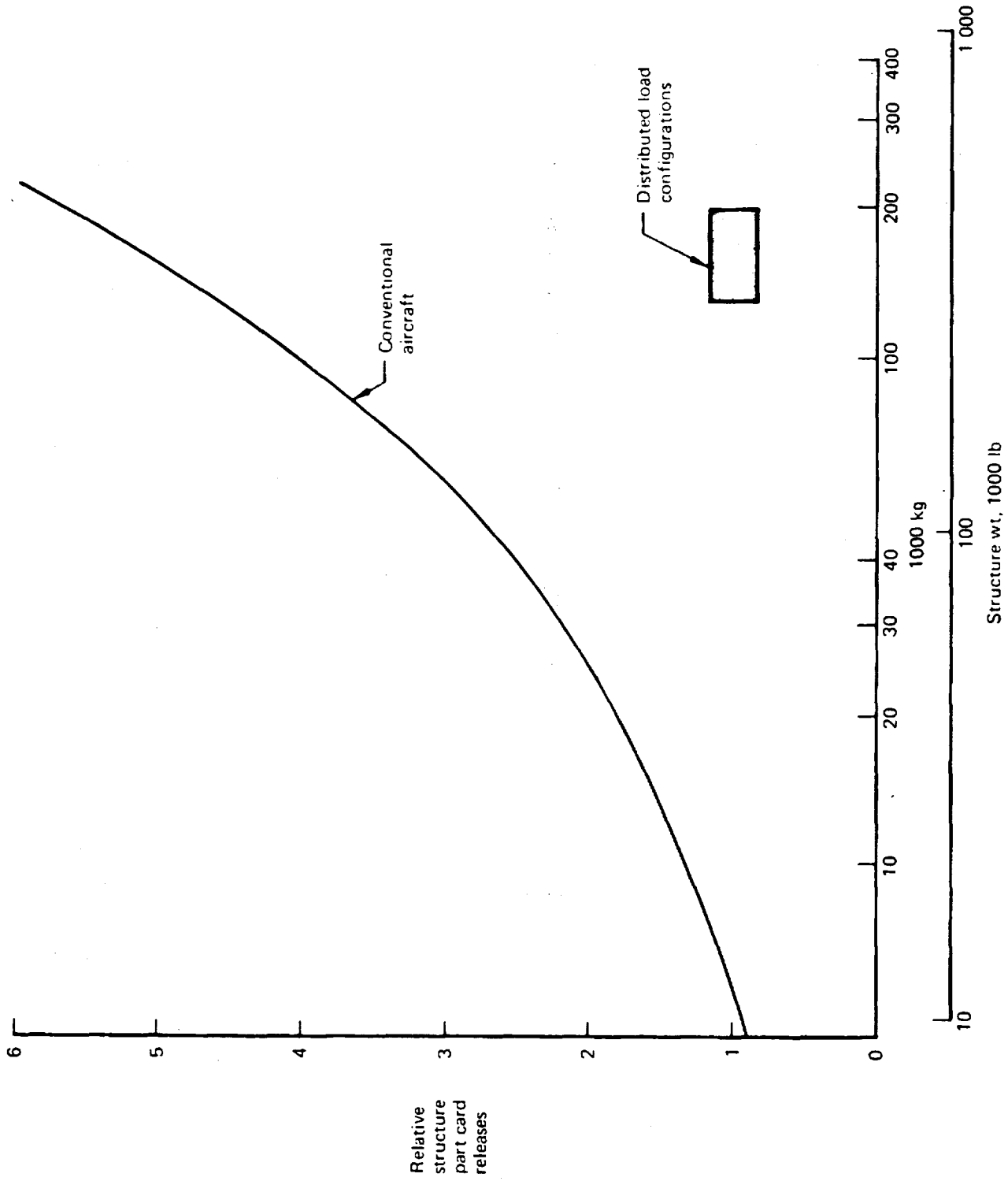


Figure 100.—Relative Structure Part Card Releases Versus Structure Weight



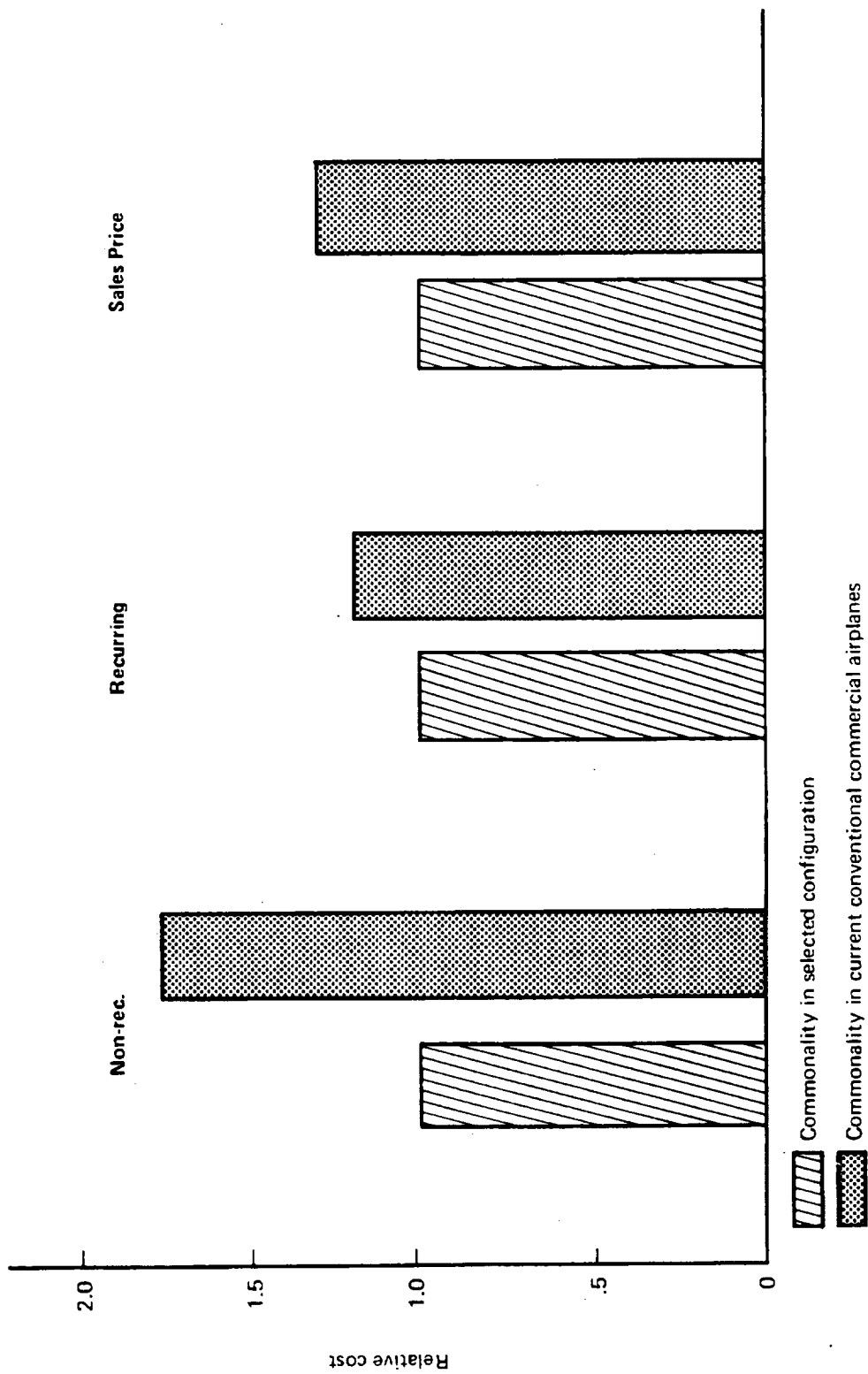


Figure 101.—Span-Distributed Loading Cargo Aircraft Study—Cost Savings Attributed to Part Commonality

759-163A-6 airplane  
 4 bays  
 89.92 m (295 ft) wing span  
 6 engines

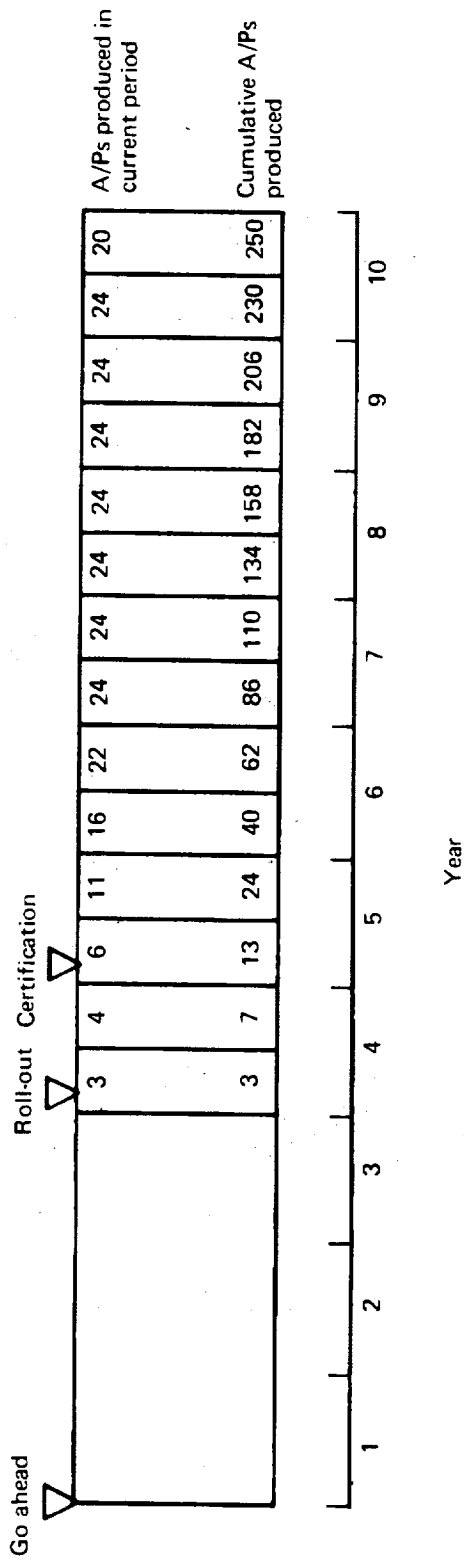


Figure 102.—Sample Program Schedule

*Table 21.—Distributed Load Freighter Price Analysis*

Basic requirements and assumptions

1. Description of airplane
  - A) 3 view drawing
  - B) Construction details (structural and systems)
  - C) Materials description
2. Part cards
  - A) Structural and systems PCR analysis
  - B) Commonality assessment
3. Weight (section and system)
  - A) Assess common and/or peculiar weights within sectional breakdown for estimating tooling, production, etc.
4. Program schedule
  - A) Development and production schedule
  - B) Airplane quantity
  - C) Production rate
  - D) Total program length is 10 years
5. Assume facilities and technology are available
6. Cost/price in 1975 dollars
7. 20% ROI to the manufacturer

## APPENDIX C

### ECONOMIC ANALYSIS METHODS

Direct operating costs (DOC) and airplane investment cost (AIC) are calculated in 1975 dollars. The DOC is calculated using the 1967 Air Transport Association (ATA) equations with coefficients updated to 1975 experience and corrected for expected differences between freight and passenger operations. The equations used are for international operations with a three-man crew and are presented in table 22.

The AIC required is assumed to be equal to 12% of the initial investment for the airplane and spares annually. This AIC is approximately equivalent to what would be allowable using current CAB rules.

The DOC and AIC are presented in cents per gross ton times statute mile ( $\text{¢/GTM}$ ). A load factor of 65% on gross payload weight, net payload weight, container internal volume, and container positions is used.

No alterations were made in the equations to reflect the effects of 1990 technology on DOC. In actual practice, differences would arise, especially in areas such as engine and airframe maintenance.

#### STANDARD CONTAINER CHARACTERISTICS

*Table 22.—Direct Operating Cost Formulas for Dedicated International Airfreighters*

Crew Pay (\$/blk hr)	ATA (1975 Coefficients)
3-Man Jet	$26.456 \left( V_c \times \frac{\text{TOGW}}{10^5} \right)^{.3} + 92.291$ (over 7 hrs/day A/P utilization)
Fuel (\$/gal)	\$0.37
Nonrevenue factor	1.02 on fuel and maintenance
Airframe maintenance—cycle	
Material (\$/CYC)	0.89 (1.9229 $Ca/10^6$ + 2.2504)
Direct labor (MH/CYC)	0.89 (0.21256( $\log_{10}(Wa/1000)$ ) <sup>3.7375</sup> )
Airframe maintenance—hourly	
Material (\$/RH)	0.89 (1.5994 $Ca/10^6$ + 3.4263)
Direct labor (MH/FH)	0.89 (4.9169( $\text{Log}_{10}(Wa/1000)$ ) - 6.425)
Engine maintenance—cycle	
Material (\$/CYC)	1.18 [(3.6698 $Ce/10^6$ + 1.3685) Ne]
Direct labor (MH/CYC)	1.13 (0.20 Ne)

Table 22.—Direct Operating Cost Formulas for Dedicated International Airfreighters  
(Concluded)

Fuel (\$/gal)		\$0.37
Engine maintenance—hourly		
Material (\$/FH)	1.18 [(28.2353 Ce/10 <sup>6</sup> - 6.5176) Ne]	
Direct labor (MH/FH)	1.13 [(T/10 <sup>3</sup> )/(0.82715 T/10 <sup>3</sup> + 13.639) Ne]	
Burden \$/direct maintenance (\$)	1.00	
Maintenance labor rate (\$/MH)	8.60	
Insurance (% price/yr)	1.0	
Investment spares ratio (%)		
Airframe	6	
Engine	30	
Depreciation schedule (years/% residual)		
Subsonic	14/10	
Utilization (hrs/yr)	$U + \frac{5683 t_b}{t_b + t_a}$ hrs per year	
	where $t_a$ = turnaround time hrs and	
	$t_b$ = block time (hrs)	

Airplane Investment Cost = 12%

Definition of Terms and Units:

TOGW = Maximum takeoff gross weight  
Ca = Airframe price  
Ce = Engine price (excluding reverser)  
Ne = Number of engines  
T = Sea level static thrust (pounds)  
V<sub>c</sub> = 715 X M - 75 X M<sup>4</sup>  
Wa = Airframe weight  
M = Mach no.  
FH = Flight hours  
MH = Manhours  
CYC = Cycle

Turnaround time = 0.5 hr

Note:

The DOC formula is indicated to the 1975 ATA international passenger formula except for utilization and maintenance cost corrections, as noted.

A nominal gross volume of  $36.25 \text{ m}^3$  ( $1280 \text{ ft}^3$ ) was used to determine gross payload density (actual gross container volume is  $36.02 \text{ m}^3$  ( $1272 \text{ ft}^3$ ), since the container is  $6.0579 \text{ m}$  ( $238.5 \text{ in.}$ ) in length instead of the nominal  $6.096 \text{ m}$  ( $240 \text{ in.}$ ).

A net container volume of  $32.28 \text{ m}^3$  ( $1140 \text{ ft}^3$ ) was used as the internal volume to compute net containerized density.

The number of container per bay was determined by subtracting  $4.572 \text{ m}$  ( $15 \text{ ft}$ ) from the wingspan and dividing by  $6.096$  ( $20$ ):

At  $89.92\text{-m}$  ( $295\text{-ft}$ ) span: no./bay =  $(89.92-4.572)/6.096$  (or  $295-15/20$ ) =  $14$

At  $121.92 \text{ m}$  ( $400 \text{ ft}$ ) span: no./bay =  $(121.92-4.572)/6.096$  (or  $400-15/20$ ) =  $19.25$

At  $152.4 \text{ m}$  ( $500 \text{ ft}$ ) span: no./bay =  $(152.4-4.572)/6.096$  (or  $500-15/20$ ) =  $24.25$

The tare weight of each standard container was  $870.9 \text{ kg}$  ( $1920 \text{ lb}$ ).

The net cargo weight when loaded with  $160 \text{ kg/m}^3$  ( $10 \text{ lb/ft}^3$ ) containerized cargo was  $5170.95 \text{ kg}$  ( $11\,400 \text{ lb}$ ).

The loaded container weight was  $6041.85 \text{ kg}$  ( $13\,320 \text{ lb}$ ) when loaded with  $160 \text{ kg/m}^3$  ( $10 \text{ lb/ft}^3$ ) containerized cargo (i.e.,  $5170.95 \text{ kg} + 870.90 \text{ kg}$  ( $11\,400 \text{ lb} + 1920 \text{ lb}$ ) =  $6041.85 \text{ kg}$  ( $13\,320 \text{ lb}$ ))

## REFERENCES

1. R. M. Kulfan and W. M. Howard, *Application of Advanced Aerodynamic Concepts to Large Subsonic Transport Airplanes*, AFFDL-TR-112, November 1975.
2. *Fuel Conservation Possibilities for Terminal Area Compatible Aircraft*, NASA CR 132609, March 1975.
3. P. K. Pierpont, "Bring Wings of Change; NASA's Airfoil Research Program," *Astronautics and Aeronautics*, October 1975.
4. Abbot and Von Doenhoff, *Theory of Wing Sections*, Dover Publications, 1958.
5. *Military Specification—Flying Qualities of Piloted Airplanes*, MIL-F-8785B (ASG), August 1969.

